UNIVERSIDAD DE MÁLAGA

IHSM La Mayora
Instituto de Hortofruticultura Subtropical y Mediterránea
CSIC
Consejo Superior de Investigaciones Científicas

Tesis Doctoral

Organisation and control of the ascorbate biosynthesis pathway in plants

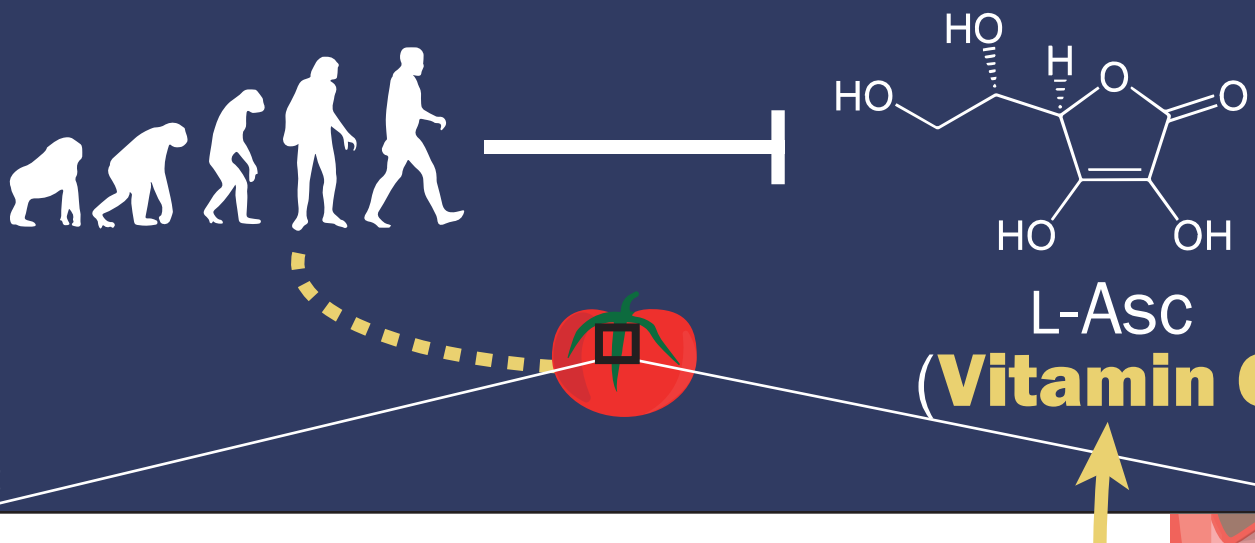

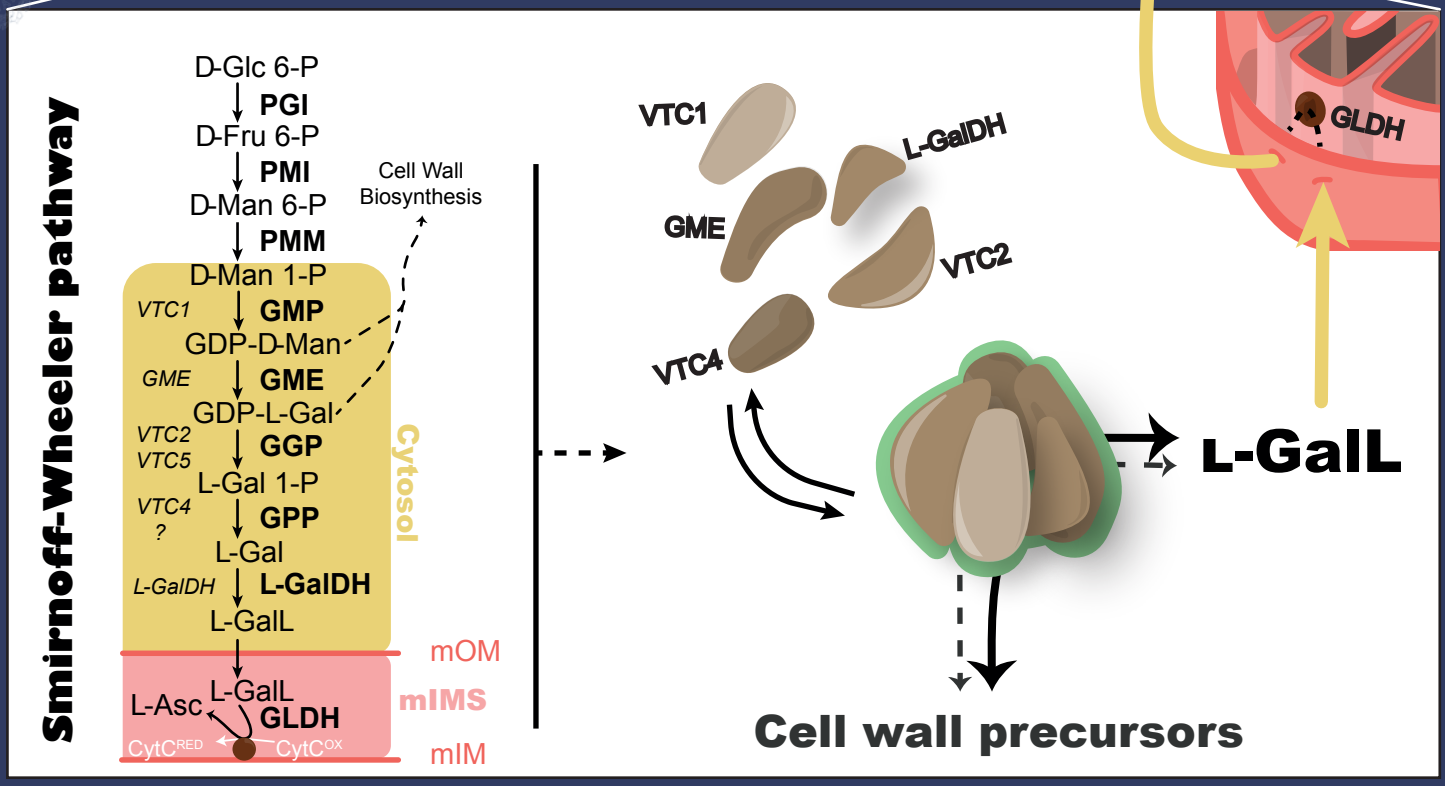

Mario Fenech Torres

Dirigido por Miguel Ángel Botella Mesa

Instituto de Hortofruticultura Subtropical y Mediterránea (IHSM-UMA-CSIC)

Programa de doctorado en Biotecnología Avanzada.
Facultad de Ciencias. Universida de Málaga, 2020.

UNIVERSIDAD
DE MÁLAGA

AUTOR: Mario Fenech Torres

http://orcid.org/0000-0001-9879-3456

EDITA: Publicaciones y Divulgación Científica. Universidad de Málaga

UNIVERSIDAD DE MÁLAGA

Instituto de Hortofruticultura Subtropical y Mediterránea

CSIC
Consejo Superior de Investigaciones Científicas

Facultad de Ciencias
Departamento de Biología Molecular y Bioquímica

Dr. MIGUEL ÁNGEL BOTELLA MESA, Catedrático de Bioquímica y Biología Molecular de la Universidad de Málaga,

INFORMA:

Que D. MARIO FENECH TORRES ha realizado bajo mi dirección y supervisión el trabajo de investigación correspondiente a su Tesis Doctoral titulada “Organization and control of the ascorbate biosynthesis pathway in plants” con la cual aspira a la obtención del grado de Doctor en Biología.

Y para que así conste, y tenga los efectos oportunos, en cumplimiento de la legislación vigente, se extiende el presente informe en Málaga, a 19 de junio de 2019.

Dr. Miguel Ángel Botella Mesa

DECLARACIÓN DE AUTORÍA Y ORIGINALIDAD DE LA TESIS PRESENTADA PARA OBTENER EL TÍTULO DE DOCTOR

D./Dña MARIO FENECH TORRES
Estudiante del programa de doctorado BIOTECNOLOGÍA AVANZADA de la Universidad de Málaga, autor/a de la tesis, presentada para la obtención del título de doctor por la Universidad de Málaga, titulada: GDP-L-GALACTOSE PHOSPHORYLASE ACTIVITY ORCHESTRATES ASCORBATE (VITAMIN C) BIOSYNTHESIS IN HIGHER PANTS (PROVISIONAL)

Realizada bajo la tutorización de MIGUEL ÁNGEL BOTELLA MESA y dirección de MIGUEL ÁNGEL BOTELLA MESA (si tuviera varios directores deberá hacer constar el nombre de todos)

DECLARO QUE:

La tesis presentada es una obra original que no infringe los derechos de propiedad intelectual ni los derechos de propiedad industrial u otros, conforme al ordenamiento jurídico vigente (Real Decreto Legislativo 1/1996, de 12 de abril, por el que se aprueba el texto refundido de la Ley de Propiedad Intelectual, regularizando, aclarando y armonizando las disposiciones legales vigentes sobre la materia), modificado por la Ley 2/2019, de 1 de marzo.

Igualmente asumo, ante a la Universidad de Málaga y ante cualquier otra instancia, la responsabilidad que pudiera derivarse en caso de plagio de contenidos en la tesis presentada, conforme al ordenamiento jurídico vigente.

En Málaga, a 19 de JUNIO de 2020

Fdo.: MARIO FENECH TORRES

Edificio Pabellón de Gobierno. Campus El Ejido. 29071
Tel.: 952 13 10 28 / 952 13 14 61 / 952 13 71 10
E-mail: doctorado@uma.es

This thesis has been carried out at the Department of Molecular Biology and Biochemistry, University of Malaga and at the Institute of Subtropical and Mediterranean Horticulture (IHSM) "La Mayora"-CSIC. It has been financed by the grant Formación del Profesorado Universitario (FPU14/01974) from the Spanish Ministerio de Educación, Cultura y Deporte as well as by the Spanish Ministerio de Economía, Industria y Competitividad (BIO2016-81957-REDT, BIO2017-82609-R).

Esta tesis ha sido realizada en el Departamento de Biología Molecular y Bioquímica, Universidad de Málaga y en el Instituto de Hortofruticultura Subtropical y Mediterránea (IHSM) “La Mayora” CSIC. Ha sido financiada con la beca para la Formación del Profesorado Universitario (FPU14/01974) del Ministerio de Educación, Cultura y Deporte y por el Ministerio de Economía, Industria y Competitividad cofinanciado por el Fondo Europeo para el Desarrollo Rural (BIO2016-81957-REDT, BIO2017-82609-R).

Agradecimientos

Después de casi cinco años, nadie se cree que esta tesis me la haya ganado yo solito. A lo largo del camino me han acompañado muchas personas que me han ayudado y enseñado a mejorar el proyecto de científico y de persona que poco a poco voy esculpiendo y que, por tanto, al final son las que han determinado que esté escribiendo estas palabras ahora mismo a modo de colofón.

A mi director, Miguel Ángel Botella, por abrirme las puertas de tu laboratorio a pesar de mi falta de experiencia y de conocimientos. Por dirigirme y redirigirme, por acotar mis elucubraciones cósmicas y enseñarme a discutir ciencia. Por tu trabajo conmigo.

To Nick Smirnoff, *for sharing all your experience and knowledges regarding vitamin C with me and raise this thesis one step higher with your suggestions and for providing me with all technical media necessary to accomplish my proposals. For so many useful discussions and for your work.*

A Carmen Beuzón, Javier Ruíz, Eduardo, Sonia, David, Iraida, Vicky y Victoriano por vuestras aportaciones y sugerencias en cada *lab meeting* o *journal club*. Me han ayudado mucho a explicar las cosas un poquito mejor y me han enseñado cómo mejorar gráficamente mis exposiciones. A Araceli, por tus continuas aportaciones y tu ayuda con el doble híbrido desde la cercanía. A David Navas, Lucía y Javi por todo vuestro soporte técnico.

A la vieja guardia de la Asociación Gastronómica de la Torre: Eli, Eva, Jessi que ya disfrutan de una mejor vida sin haberse muerto ni na. Gracias por hacerme parte desde el principio del grupo tan bonito que formabais. Especialmente a Eva y a Jessi, que se han tragado muchísimas inseguridades laborales al inicio de esta tesis e incluso alguna personal. Gracias por la terapia y por vuestra amistad. A Amalia, por zarandearme y enseñarme a ser un mejor compañero en el laboratorio. A los veteranos que siguen o que ya han tomado puerto, pero que han remado a la par durante la mayor parte de esta tesis: a Álvaro Piedra, por velar siempre por el bien del laboratorio con disciplina; a Noemí, por tus consejos, tu ayuda y tu apoyo; a Vítor, por tu compañerismo, por tu ayuda y tus consejos, por enseñarme gran parte de lo que sé; a Ali, por tantísima ayuda prestada, por escucharme y por ser una grandísima compañera; a Carmen, por los consejos y los *beer meetings*, por el cachondeo y por hacerlo más ameno. A Bego, por ser la mejor organizadora y promotora de eventos multitudinarios de toda Málaga de forma desinteresada. Sin ti, los viernes hubieran sido de hambruna y la familia que formamos al inicio hubiera estado menos unida; a Blanca, por sacar siempre un rato para una charla que ayude a evadirse un ratito. Por tus tontás y tu humor negro que acoge al mío como un amigo de toda la vida. A Pepaso, por tu humor absurdo-inteligente, primo hermano del mío, y por las conversaciones en las que, junto a Jessi, habéis compartido vuestra tan admirable sapiencia conmigo sin juzgarme cuando hablaba como un cuñao-cateto. A mi admiradísimo Miguelín, que no puede albergar más conocimiento en menos carne, siempre dispuesto a compartirlo (y a hacerte proposiciones indecentes). Estoy seguro de que, si Aristóteles viviera hoy día, su dirección de email sería *miguelín_ermalaguita@agora.gr*. A Delphine, por tu temple y tranquilidad, siempre lista para una cerveza. Por tu compañerismo ("¿me dejas la

cucharita?") y tu capacidad de organización que, junto con la de Bego, ha dejado patente el problema de memoria y organización que tengo, pero me ha salvado de ello en alguna ocasión. A Vito Meco, por las conversaciones, la cultura cinéfila y de deportes. Por tu actitud de currante y de disfrutón, que se contagia. A Sara, por tu compañerismo y tus ganas de ayudar. A Lidia, por aguantarme en el despachito horas y horas de sinsentidos y hacerme reír. Por ir siempre de frente y estar dispuesta a ayudar a pesar de todo. A Karen, a quien tanto admiro. Por tantísima ayuda y aportaciones científicas. Por tus innumerables consejos personales que me han ayudado a tomar decisiones importantes. Por preguntarme, considerar mi opinión científica y hacerme sentir un igual. Por tu amistad. Ojalá algún día podamos trabajar en el mismo equipo.

A las nuevas generaciones de la torre: a Carolina y a Gemma, por vuestro compañerismo y buen hacer; a Fran Percio, por tu paciencia y tolerancia con mi falta de organización en tus principios y ayudarme a ser mejor docente. Por tu gran compañerismo. A Fran Benítez, por tantísima ayuda prestada en todos los campos. Por "entrar al trapo" y forzarme a exprimirme el cerebro para poder replicarte. Por los planes propuestos que nos han unido más y por las buenas discusiones. Y, por supuesto, por tu amistad. A Carlos, por preguntarme si te odio y dar pie a conocerte, por no juzgarme cuando yo lo hice y darme a conocer una forma diferente de pensar. Por escucharme en algunas etapas complicadas. Por hacerme reír a carcajadas con tus *performances* y tu lenguaje *millenial* ininteligible. Por tus abrazos y tu amistad. A Selene, por darme el placer de ser tu amigo. Por tu cariño, reflejado en cada corazón o notita por la mañana y tu serenidad, que ayudan a calmar los ánimos en los momentos estresantes de todos nosotros y hacer de pegamento del grupo. Por hacerme vivir los mejores planes de estos años. Y por los años que están por venir, gracias. A mis dos hermanos de distinta sangre: A José, por ser mi compañero, mi enfermero, mi psicólogo y mi amigo. Por haber estado dispuesto a traspasar barreras por mi propio bien que muchas amistades ni siquiera se plantearían, sin importar ni cómo, ni dónde ni cuándo. Por animarme en muchas etapas complicadas, me has enseñado, me has hecho reír y me has escuchado. Siempre estaré en deuda contigo. Gracias de corazón. A Álvaro, el otro remo de mi barca. Por regalarme tu confianza desde el principio. Por las conversaciones serias y por las absurdas. Por animarme cuando lo he necesitado. Por ser mi compañero de atracones y de vomiteras. Por tu sentido del humor, que coge de la manita al mío de camino a la misma celda de la cárcel. Por hacerlo todo mucho más divertido. Gracias por ser parte de esta tesis. Gracias por tu amistad.

A quienes me han acompañado en mis primeros pasos como docente: a Noemí, a Karen y a Fernando de la Torre, que me han hecho sentir un igual y un compañero, no solo un aprendiz.

Al equipazo de genéticos, Javi, Diego, Nieves, Carla, Adri, Alba, Bea, Ana y Tábata, por vuestro compañerismo y los buenos ratos fuera del laboratorio.

A Almu, Mariem, Anika y Jennifer, que han pasado por el lab brevemente o llevan poquito pero que han hecho esos días mucho más agradables y divertidos.

A mis amigos siempre presentes: Gustavo, Javi, Juanje, Medi, Sonia, Carmen, Irene y Cristi, por estar. Por siempre apoyarme y preocuparos por mí. Por hacerme cargar pilas fuera del laboratorio para avanzar con más fuerza. Por todos los años que sé que nos quedan por compartir.

A Ángela, por la música, que calma y apacigua a las bestias malhumoradas en los momentos más complicados y motiva en los buenos.

A Miriam, porque tu disciplina, paciencia, calidez y cariño dentro y fuera del laboratorio me animaron a aventurarme en el mundo de la investigación (si, eso es algo positivo). Porque hiciste del tedio de una incubación larga una clase de baile del que ya no puedo escapar. Qué suerte tengo de haberte conocido y de tenerte como amiga.

A Cristina, por haberme acompañado durante parte de este camino sofocando pataletas y malos humores con tu dulzura. Por tu cariño y por creer en mí. Gracias.

A José y Gloria, por acogerme en su casa durante los seis meses que ha durado mi escarceo científico en Exeter. Por toda vuestra paciencia y vuestra implicación en mejorar mi estancia allí. Por vuestra amistad. Por supuesto, a la familia tan especial de Exetereños: Emilio, Ángela, Darío, Gabri, Paco, Claudia, Álex, Laura, Inma, Guille, Blas, Patri, Pepe y Concha, que me adoptaron desde el minuto uno y me hicieron sentir uno más del grupo.

To Johanna, for showing me a new way to face challenges. For teaching me how to respect myself. For making one of the best experiences in my life out of the time we have shared and for cheering me up to finish this project. For listening to me and being there despite circumstances. For all your love and patience. For turning my world upside down. Thanks.

A mi familia, a los que están y a los que se han marchado durante el transcurso de estos años. Por siempre apoyarme en las decisiones que he tomado e impulsarme a seguir adelante. Por hacerme sentir que siempre tengo un lugar donde estar protegido.

A mi padre, por enseñarme a siempre buscar la mejor versión de mí mismo y mantener la humildad de saber que siempre habrá alguien mejor que yo. Por ser el referente al que admirar. A mi hermana Paula, por enseñarme que el sacrificio, el esfuerzo y la constancia tienen su recompensa. Por todo cariño. A mi tía Carmina, porque es el pilar fundamental de la familia y es gracias a ella que muchos de nosotros hemos podido ir un paso más lejos. Por siempre apoyarnos y desvivirte por nosotros. Todos, incluido yo, estamos en deuda contigo. A mi madre, por su inconmensurable esfuerzo y amor, que son los que han hecho que yo haya llegado a donde estoy. Por siempre creer en mí. Sin ti no sería nada. Gracias, mamá.

INDEX

RESUMEN

¿Qué es el ácido ascórbico?

El ácido L-ascórbico (L-treo-hex-2-enono-1,4-lactona, ascorbato), también conocido como vitamina C, es un antioxidante esencial en el metabolismo de plantas y animales. El papel del ascorbato en los mamíferos ha sido ampliamente estudiado a lo largo del tiempo, particularmente desde el siglo XVIII con el descubrimiento de su papel en la prevención del escorbuto (Lind, 1753; Baron, 2009). Sin embargo, esto no era obvio en ese momento porque la falta de ascorbato en la dieta tarda aproximadamente un mes antes de que aparezcan los síntomas. Por lo tanto, esta enfermedad se manifestó típicamente durante largos viajes por mar con una dieta escasa en frutas y verduras frescas. A principios de la década de 1930, Albert Szent-Györgyi identificó y aisló la molécula responsable de esta actividad contra el escorbuto, lo que le llevó a ganar el Premio Nobel de Medicina en 1937. De esta manera, esa molécula anteriormente llamada ácido hexurónico, pasó a llamarse ácido ascórbico (de *a-*: anti + *scurvy*: escorbuto).

¿Por qué es importante incluirlo en la dieta?

Varios grupos de animales pueden sintetizar ascorbato en el hígado o en el riñón, sin embargo, algunos grupos como el de los conejillos de Indias, ciertos grupos de murciélagos, aves y los primates, en el que se incluyen los humanos, han perdido esta capacidad debido a la acumulación de mutaciones en la última enzima de la ruta de biosíntesis (L-gulono-1,4-lactona oxidasa, GULO; Chatterjee, 1973; Drouin et al., 2011; Nishikimi et al., 1994). Los cambios en la dieta que llevaron a incorporar abundantes frutas y verduras dieron como resultado la pérdida de presión selectiva que mantenía esta ruta funcional (Macknight et al., 2017). Por lo tanto, a raíz de incorporar esta molécula en la dieta, frutas y verduras se erigen como las principales fuentes de ascorbato.

Uno de los principales síntomas del mencionado escorbuto es el deterioro de la piel debido a la participación del ascorbato en la biosíntesis y la estabilidad del colágeno. El ascorbato funciona como cofactor en la hidroxilación enzimática catalizada por varios grupos de lisil y prolil hidroxilasas (Myllylä et al., 1984; Padayatty y Levine, 2016; Pekkala et al., 2003; Peterkofsky, 1991) mediante la reducción de Fe^{3+} al Fe^{2+} activo (de Jong et al., 1982; Gorres y Raines, 2010). La hidroxilación de prolina es una modificación postraduccional esencial que ocurre en los residuos de prolina permitiendo así la trimerización del colágeno, lo cual proporciona alta estabilidad térmica (Koide y Nagata, 2005). La hidroxilación catalizada por estas enzimas requiere un ion Fe^{2+} ubicado en el centro activo, que se oxida a Fe^{3+} en el ciclo catalítico y el ascorbato es responsable de mantener el hierro activo reduciéndolo a Fe^{2+}.

Además de prevenir el escorbuto, el ascorbato está involucrado en muchos otros procesos que también requieren la acción de otros miembros de

esta familia de mono- y dioxigenasas. Para estas enzimas, el ascorbato funciona como cofactor, manteniendo la actividad de los iones metálicos ubicados en los centros activos. Por ejemplo, el ascorbato es importante para la síntesis de carnitina, cuya falta está relacionada con la fatiga común que se encuentra en los pacientes con escorbuto. También se sabe que el ascorbato participa en la biosíntesis de dopamina (Rush y Geffen, 1980; Prigge et al, 1999). Más recientemente, se ha demostrado que la actividad de otras dioxigenasas dependientes de Fe^{2+}/αKG clave se ve reforzada por el ascorbato, como es el caso de las enzimas Translocaciones Diez-Once (Ten-Eleven Translocations, TET). Los TET están involucrados en la desmetilación del ADN a través de una cascada de oxidación de 5-metilcitosina a 5-hidroximetilcitosina, 5-formilcitosina, 5-carboxilcitosina y, finalmente, a citosina por el mecanismo de reparación de escisión de base (Blaschke et al., 2013; Hu et al., 2015; Minor et al., 2013). Es importante destacar que, además, el ascorbato funciona como cofactor de histona desmetilasas que albergan un dominio Jumonji C (JmjC) (JumonjiC Containing Histone Demethylases, JHDM), el mismo dominio catalítico presente en los TET (Young et al., 2015). Las lisinas tri-, di- y monometiladas en las histonas se pueden oxidar a hidroximetil lisinas por JHDM y ascorbato de forma similar a como ocurre con la desmetilación del ADN y los TET, con una eliminación espontánea de este grupo hidroximetilo (Young et al., 2015). En conjunto, estos hallazgos muestran que el ascorbato participa en la respuesta a los estímulos ambientales ejerciendo un control epigenético de la expresión génica.

¿Cuánto ascorbato es necesario ingerir?

La deficiencia de ascorbato en los países desarrollados ha registrado una disminución a lo largo del tiempo. A finales del siglo pasado, la deficiencia de ascorbato en EE. UU. fue de alrededor del 13% de la población (Hampl et al., 2004), pero se redujo al 7% en la última encuesta efectuada durante el período 2003-2004 (Schleicher et al., 2009). Según los primeros experimentos, se encontró que una dosis diaria de menos de 10 mg era suficiente para prevenir el escorbuto (Baker et al., 1969, 1971, Hodges et al., 1969, 1971; Johnstone et al., 1946; Peters et al., 1953). Sin embargo, se estableció un requisito promedio (RA) de 90 mg/día para hombres y 80 mg/día para mujeres, y una ingesta de referencia de población (PRI) de 110 mg/día para hombres y 95 mg/día para mujeres según la Autoridad Europea de Seguridad Alimentaria (Panel EFDA NDA, 2013). Esto se basa en mantener una concentración plasmática de alrededor de 50 µmol / L de ascorbato, indicativo de un estado adecuado (Kallner et al., 1979). Para entenderlo mejor, 100 g de naranja contienen 50 mg de ascorbato, y una naranja pesa entre 200-250 g. Es decir, una naranja nos aporta el requisito promedio de vitamina C de un día. No obstante, una dieta rica en ascorbato tiene varias ventajas para la salud (Carr y Maggini, 2017; Reczek y

Chandel, 2015; van Gorkom et al., 2018; Wintergerst et al., 2006). En los últimos años, el ascorbato se ha propuesto como un tratamiento contra diferentes tipos de cáncer a través de diversos mecanismos, como aumentar la actividad de TET, inducir el estrés oxidativo en las células cancerosas o mejorar la actividad de diversos tratamientos químicos (Agathocleous et al., 2017; Cimmino et al., 2017; Ko et al., 2015; Lu et al., 2018; Miura et al., 2018; Shenoy et al., 2017; Yun et al., 2015). La ingesta diaria de ascorbato proporcionada por las frutas depende de varios factores, pero claramente el contenido de ascorbato, así como la cantidad de fruta que se consume, son los factores más importantes. Es importante además tener en cuenta la forma en que se consume (cocinado o crudo), ya que esto tiene consecuencias importantes en la reducción y oxidación del ascorbato que puede alterar la biodisponibilidad del ascorbato debido a las interacciones con otros fitoquímicos como la vitamina E o los flavonoides (Carr y Vissers, 2013; Packer et al., 1979; Tanaka et al., 1997).

¿Cómo sintetizan las plantas el ascorbato?

La ruta predominante a través de la cual se sintetiza el ascorbato en las plantas es la ruta de Smirnoff-Wheeler (Wheeler et al., 1998). En esta ruta, una molécula de D-glucosa se transforma mediante sucesivas reacciones enzimáticas en GDP-D-manosa, GDP-L-galactosa, L-galactosa, L-galactono-1,4-lactona y, finalmente, en ascorbato. A diferencia de la ruta de biosíntesis en animales, en la ruta de la planta no hay inversión de carbono, es decir, que el carbono 1 en la molécula de D-glucosa permanece como carbono 1 en el ascorbato después de la conversión. El último sustrato de la ruta, la L-galactono-1,4-lactona, debe moverse del citosol al espacio intermembrana de las mitocondrias, donde se encuentra el sitio activo de la L-galactono-1,4-lactona deshidrogenasa (Imai et al., 1998; Mapson y Breslow, 1958; Pineau et al., 2008; Schertl et al., 2012; Schimmeyer et al., 2016). El hecho de que la oxidación de la L-galactono-1,4-lactona se lleve a cabo en las plantas mediante una deshidrogenasa en lugar de una oxidasa como ocurre en los animales, no es trivial. Contrariamente a la paradójica actividad de la oxidasa de animales, la deshidrogenasa de plantas no produce H_2O_2 como resultado de su actividad enzimática y, por lo tanto, la producción de ascorbato en plantas no tiene efectos secundarios sobre el estado redox de la célula (Wheeler et al., 2015). Existen otras rutas que pueden estar colaborando al contenido final de ascorbato que se describen en la introducción de esta tesis, pero los estudios con mutantes de los distintos componentes de la ruta de Smirnoff-Wheeler demuestran que esta es la predominante, especialmente en tejido fotosintético.

Por otro lado, en tejidos heterotróficos como son las frutas, la ruta de Smirnoff-Wheeler SW es funcional, como se demuestra en varias especies como acerola, kiwi, fresa, melocotón, tomate y manzana (Badejo et al., 2009, 2012; Bulley et al., 2009; Cruz-Rus et al., 2010; Imai et al., 2009; Ioannidi et al., 2009;

Mellidou et al., 2012a, 2012b). Sin embargo, dependiendo del estadio de maduración de la fruta, otras vías alternativas pueden resultar relevantes, especialmente la ruta del D-galacturonato (Mapson e Isherwood, 1956; Shigeoka et al., 1979), a través de la cual la degradación de las pectinas de pared celular puede proporcionar sustrato para la formación de ascorbato (Agius et al., 2003; Badejo et al., 2012; Cruz-Rus et al., 2010; Di Matteo et al., 2010). Mientras que la ruta del D-galacturonato es más activa a medida que la fruta madura, la ruta de Smirnoff-Wheeler y el transporte de ascorbato desde las hojas proporcionan la mayor parte del ascorbato en las frutas en la etapa verde inmadura.

¿Qué fruta resulta más interesante desde el punto de vista biotecnológico?

Según la Organización de las Naciones Unidas para la Alimentación y la Agricultura (FAO), el tomate ha sido la fruta más producida en el mundo en los últimos veinte años, una tendencia que ha aumentado durante los últimos años. En la Unión Europea en 2016, la producción de fruta estuvo dominada por la uva, seguida de tomate, manzana y naranja. Sin embargo, se procesa una gran proporción de tomate (61,5%), manzana (26,8%) y uva (96,5%), lo que conduce a una reducción del contenido de ascorbato y a una menor biodisponibilidad de otros nutrientes. que dependen del ascorbato (Hallberg et al., 1982, 1987). Por lo tanto, la ingesta de ascorbato a través de la naranja supera a la de la uva y de tomate. Las frutas de tomate y manzana, aunque podrían considerarse fuentes moderadas de ascorbato en base a su contenido relativamente bajo, se consumen ampliamente y, por lo tanto, proporcionan importantes fuentes dietéticas de ascorbato.

Los cultivos frutales tienen diferentes requisitos ambientales cuyo conocimiento nos permite optimizar el rendimiento y, además, afecta directamente al contenido de ascorbato de los frutos, ya que este se ve afectado por factores abióticos como la luz o la temperatura (Gautier et al., 2008; Suzuki et al., 2014; Zechmann et al., 2011). Por lo tanto, las pequeñas diferencias que podemos encontrar dentro de un mismo tipo de cultivo pueden venir dado por distinto grado de satisfacción de estos requisitos, por el tiempo de cosecha o por condiciones posteriores a la cosecha (Akhatou y Fernández-Recamales, 2014; Davey et al., 2007; Kevers et al., 2011; Oms-Oliu et al., 2011). Sin embargo, las grandes diferencias observadas en el contenido de ascorbato en especies estrechamente relacionadas probablemente tengan otras causas. Por ejemplo, se pueden encontrar grandes diferencias en la cantidad de ascorbato que tiene el tomate silvestre y el que tiene el tomate cultivado. Los cultivares de tomate domesticados típicamente contienen en torno a 15 mg/100 g de peso fresco, mientras que las variedades silvestres como *Solanum pimpinelifollium* o *Solanum pennellii* contienen alrededor de 40 mg/100 g de peso fresco (Lima-Silva et al., 2012) y hasta 70 mg/100 g de peso fresco (Stevens et al., 2007),

respectivamente. De hecho, los programas de mejora que cruzaron distintas líneas de tomate con *Solanum peruvianum*, otra especie silvestre (Atherton y Rudich, 1987), resultaron tener la mayor cantidad de ascorbato de entre las especies de *Solanum*: alrededor de 50 mg/100 g de peso fresco (Top et al., 2014), una cantidad similar a la de una naranja. Estas especies silvestres de tomate crecen naturalmente en áreas tropicales de Perú y México cuyos factores ambientales podrían haber favorecido la selección de un alto contenido de ascorbato a lo largo del tiempo. La evidencia actual sugiere que la domesticación de tomates se dirigió hacia la selección de un mayor tamaño de fruta y resistencia a enfermedades como el marchitamiento por *Fusarium* (Atherton y Rudich, 1987). Es probable que, durante los últimos 200 años de domesticación en Europa, el crecimiento en condiciones más controladas y menos duras haya disminuido la presión selectiva para mantener los alelos que confieren un alto contenido de ascorbato, particularmente porque se ha encontrado una aparente asociación de altos niveles de ascorbato con baja productividad en esta especie (Atherton y Rudich, 1987). Adicionalmente, el tamaño y el peso de la fruta se relacionan directamente con el contenido de agua, y han sido rasgos clave seleccionados durante los programas de reproducción que llevan a la dilución de la concentración de ascorbato en la fruta.

Todo junto, el gran consumo de tomate, su ascorbato relativamente bajo y su alta ingesta en crudo lo convierten en una diana biotecnológica excelente para aumentar su contenido de ascorbato desde un punto de vista de la mejora de la calidad nutricional de la población.

¿De qué maneras podemos incrementar el contenido de ascorbato en una especie de interés agronómico?

El aumento del contenido de ascorbato en frutas altamente consumidas claramente tendría un impacto en la nutrición humana. El incremento de ascorbato en tejidos u órganos sometidos a estrés oxidativo, es decir, tejidos fotosintéticos, podría tener un efecto beneficioso adicional sobre la tolerancia de las plantas. Sin embargo, si los aumentos de ascorbato en la fruta tendrían o no un efecto sobre la tolerancia al estrés, no está tan claro, aunque se propone que durante el desarrollo de la fruta y la maduración puede ocurrir estrés oxidativo (Brennan y Frenkel, 1977; Huan et al., 2016; Jimenez et al., 2002; Rogiers et al., 1998). La mayoría de los intentos utilizados para aumentar los niveles de ascorbato se basan en herramientas moleculares y consisten básicamente en la sobreexpresión de genes involucrados en diferentes aspectos del metabolismo del ascorbato (biosíntesis, reciclaje o regulación). Un segundo enfoque para aumentar el contenido de ascorbato sería a través de la selección de regiones genómicas específicas que determinan un alto ascorbato de un cultivador

donante (o especies relacionadas) y la introgresión en el cultivar de interés utilizando mejora genética asistida por marcadores (Singh y Singh, 2015). Mientras que en el primer enfoque es posible utilizar genes de diferentes especies y los promotores que impulsan la expresión alta o específica en los tejidos deseados (Amaya et al., 2015) en la medida en que la especie objetivo es susceptible de transformación, el segundo enfoque se basa en la identificación de variantes naturales que pueden usarse para entrecruzarse con estas líneas de interés. Aunque hasta la fecha existen informes limitados que utilizan este enfoque, la clara ventaja es que estas líneas se pueden poner directamente en producción porque no implica transgénesis y, por lo tanto, no están sujetas a la regulación de los organismos modificados genéticamente (Huang et al., 2016). La tecnología CRISPR/Cas9 ha mejorado enormemente nuestra capacidad para diseñar mutaciones específicas en genomas eucariotas (Doudna y Charpentier, 2014). En tomate, CRISPR/Cas9 se ha utilizado recientemente para generar un espectro de algunos rasgos agronómicos clave, como el tamaño del fruto, el número de inflorescencias y el tamaño de la planta en tomate (Rodríguez-Leal et al.2017). En un artículo reciente, la edición del elemento controlador de la expresión de VTC2 (uORF), una de las enzimas clave de la ruta de Smirnoff-Wheeler, aumentó el contenido de ascorbato en 1,5 veces, lo que condujo a una mejor tolerancia al estrés oxidativo (Zhang et al., 2018a). Una edición similar del VTC2 de tomate también condujo a un aumento de ascorbato de 1,5 veces en las hojas (Li et al., 2018). Por lo tanto, una práctica común en el futuro será utilizar la edición del genoma para modificar la expresión génica, la afinidad por un sustrato, la eficiencia catalítica o la generación de alelos específicos en las frutas. Todo esto se facilitará aún más mediante el reemplazo de secuencias mediante recombinación homóloga, como ya se ha conseguido en Arabidopsis haciendo uso de la tecnología CRISPR/Cas9 (Miki et al., 2018).

¿Qué encontramos en el Capítulo 1 de esta tesis doctoral?

Las concentraciones de ascorbato en plantas dependen del tejido en que se mida (Franceschi y Tarlyn, 2002; Lorence et al., 2004; Müller-Moulé, 2008; Zhang et al., 2011) y el contenido total se ajusta de acuerdo con las condiciones ambientales, especialmente a la luz (Bartoli et al., 2006; Page et al., 2012; Plumb et al., 2018). Sorprendentemente, a pesar de ser el antioxidante soluble más abundante, la comprensión de los mecanismos que regulan el contenido de ascorbato celular sigue siendo limitada. Si bien los pasos catalíticos están bien descritos, se ha reunido poca información sobre cómo se controla la ruta. Esto se complica aún más porque la concentración de ascorbato está determinada por un equilibrio entre la biosíntesis, su degradación, y su reciclaje. Parte del ascorbato que se oxida a monodehidroascorbato y deshidroascorbato como

resultado de sus funciones bioquímicas se puede reducir de nuevo a ascorbato a través del ciclo Halliwel-Foyer-Asada (Asada, 1999). Además, una proporción de ascorbato y deshidroascorbato puede degradarse a diversos productos como oxalato, treonato y tartrato si no se reduce rápidamente a ascorbato (Pallanca y Smirnoff, 2000; Green y Fry, 2005; deBolt et al., 2006, 2007; Truffault et al., 2017; Dewhirst et al., 2017; Terai et al., 2020). Estas reacciones de reciclaje y descomposición son importantes bajo estrés oxidativo severo, lo que resulta en una disminución del ascorbato celular (Terai et al., 2020; Waszczak et al., 2016).

Múltiples investigaciones apuntan a VTC2 como el paso catalítico crítico en la biosíntesis de ascorbato. La transcripción del gen *VTC2* (Urzica et al., 2012; Dowdle et al., 2007; Müller-Moulé, 2008) y la actividad de la enzima codificada (Dowdle et al., 2007) son altamente sensibles a los factores ambientales. Además, la traducción de *VTC2* está sujeta a una represión por retroalimentación a través de un marco de lectura abierto aguas arriba del gen principal (uORF) en el 5'-UTR (Laing et al., 2015). Como consecuencia, la eliminación del uORF aumenta la cantidad de ascorbato en Arabidopsis (Laing et al., 2015) además de los ya mencionados, tomate (Li et al., 2018) y lechuga (Zhang et al., 2018). Además, *VTC2* es el único gen de la vía cuya sobreexpresión aumenta consistentemente el contenido de ascorbato (Bulley et al., 2012; Yoshimura et al., 2014) y un análisis de QTL muestra que *VTC2* se encuentra dentro de las regiones del genoma asociadas a las frutas que contienen alto contenido. contenido de ascorbato (Mellidou, Chagne, et al., 2012). No obstante, ha habido artículos donde la sobreexpresión de otros genes de la ruta, como VTC1 o GME, también aumentan la concentración de ascorbato en Arabidopsis (Zhou et al., 2012 [1,3 veces]; Li et al., 2016 [1,5 veces]; Zhou et al., 2012 [1,4 veces]), arroz (Zhang et al., 2015 [1,4 veces]), tabaco (Wang et al., 2011 [2-4 veces]), tomate (Cronje et al. ., 2012 [1,7 veces]; Zhang et al., 2011 [1,4 veces]) y kiwi (Bulley et al., 2009 [1,2 veces]). Sin embargo, la sobreexpresión de estos genes no siempre tiene un efecto sobre la concentración de ascorbato (Yoshimura et al., 2014; Sawake et al., 2015).

En el capítulo 1 hemos estudiado el efecto de la sobreexpresión sistemática de todos los genes involucrados en la vía SW, de forma individual o en combinaciones, sobre el contenido de ascorbato endógeno usando hojas de *Nicotiana. benthamiana*. Hemos demostrado que las enzimas fusionadas a GFP son funcionales ya que sus inserciones en sus respectivos fondos mutantes aumentaron la concentración de ascorbato en Arabidopsis. En estas condiciones experimentales, solo la sobreexpresión de VTC2 aumentó la concentración de ascorbato, lo cual confirma estudios previos (Bulley et al., 2009; Bulley et al., 2012; Yoshimura et al., 2014; Laing et al., 2015; Li et al., 2018; Zhang et al., 2018; Ali et al., 2019). Curiosamente, el mutante *vtc2* transformado con una construcción *VTC2-GFP* cuya expresión estaba controlada por su propio promotor, también incluyendo la región 5'-UTR mostró una fluorescencia de GFP extremadamente baja en comparación con otras proteínas etiquetadas GFP. Esta diferencia en la cantidad de proteína es apreciable cuando se comparan

una misma inmunotransferencia. Probablemente, esta diferencia esté relacionada con la represión traduccional de *VTC2* a través del uORF conservado en el 5'-UTR (Laing et al., 2015). El bajo nivel esperado de proteína de VTC2 endógena en *N. benthamiana*, que también contiene el uORF (Laing et al., 2015), podría explicar el marcado aumento de ascorbato después de la sobreexpresión de *VTC2* sin el uORF.

Además, construimos un modelo cinético basado en las propiedades conocidas de las enzimas de la ruta que incluye la represión de GGP por ascorbato. Este modelo se usó para el análisis de control metabólico, un enfoque que determina la distribución del control del flujo y la concentración de intermedios de la ruta en respuesta a pequeños cambios en la actividad de cada enzima en la ruta calculando el control del flujo y los coeficientes de control de concentración para cada paso (Cayó, 1992). Este análisis mostró que el único paso en la ruta de biosíntesis que controla el flujo de la ruta y el tamaño del grupo de ascorbato es GGP (VTC2) siempre que se incluya la represión por retroalimentación. Las predicciones del modelo son consistentes con los resultados de la expresión transitoria que se muestran en esta tesis doctoral y con el efecto relativamente pequeño de sobre expresar enzimas distintas a VTC2.

Es importante destacar que el modelo muestra que la concentración de ascorbato responde a GGP (VTC2) en un amplio rango y, por lo tanto, explica cómo una combinación de transcripción y represión de retroalimentación controla la cantidad/actividad de GGP (VTC2) y proporciona un mecanismo para ajustar el nivel de ascorbato a las condiciones ambientales de crecimiento. La luz es el factor mejor estudiado y el ascorbato se ajusta a la intensidad de luz predominante durante varios días (Page et al., 2012; Capítulo 2).

Además de investigar el efecto de la sobreexpresión enzimática sobre la acumulación de ascorbato, utilizamos enzimas etiquetadas con GFP para investigar la localisación subcelular y la formación de complejos enzimáticos. Con la excepción de GLDH, la localisación citosólica de las enzimas de la ruta de Smirnoff-Wheeler es consistente con la predicción *in silico*. Curiosamente, además de VTC1 y VTC2 que previamente se encontraron en el núcleo (Wang et al., 2013; Müller-Moulé et al., 2008), VTC4 y L-GalDH también mostraron localisación nuclear a pesar de que carecen de señales de localisación nuclear. Aún no se ha determinado si esta localisación nuclear es funcionalmente importante o no, pero no es la primera vez que se detectan enzimas metabólicas en el núcleo (Boukouris et al., 2016).

Usando CoIP en *N. benthamiana*, hemos demostrado que, no solo las enzimas que catalizan pasos consecutivos en la ruta se asocian, sino que, además, dos proteínas que catalizan pasos enzimáticos distantes como son VTC1 y L-GalDH también se asocian. Sin embargo, no se encontraron interacciones directas utilizando el análisis de dos híbridos de levadura. La falta de interacción directa y las asociaciones positivas in vivo pueden indicar que las enzimas se unen a proteínas andamio que hacen que la interacción no se detecte

en levaduras, o bien, que la interacción por pares depende de la presencia de otras enzimas de la ruta. Aunque esto merece más investigación, es tentador especular que algunas de las enzimas de biosíntesis de ascorbato podrían formar un complejo enzimático funcional (metabolón) que, potencialmente, podría canalizar intermediarios de la ruta aumentando así el flujo y, quizás, ayudar a determinar si GDP-D-manosa y GDP-L- galactosa participan en la síntesis de ascorbato o en la de pared celular y glicoproteínas, como ocurre en otras rutas (Zhang et al., 2017; Sweetlove & Fernie, 2018; Smirnoff, 2019; Amorim-Silva et al., 2019).

En conclusión, los experimentos de ingeniería metabólica que usan las últimas seis enzimas de la ruta SW muestran que solo VTC2 (GGP) tiene un control significativo sobre la ruta. Está claro que el equilibrio de la cantidad de VTC2 está controlado por una combinación de transcripción y represión de la traducción en gran parte, pero no totalmente, mediada por el mecanismo uORF. Además, hemos producido un conjunto de mutantes complementados desde GME hasta L-GalDH etiquetados con GFP que proporcionan un recurso muy valioso para investigaciones posteriores sobre la ruta de Smirnoff-Wheeler.

¿Qué encontramos en el Capítulo 2 de esta tesis doctoral?

Entre las numerosas funciones que el ascorbato ejerce en las plantas, se propuso que el ascorbato participa en el crecimiento y la fotoprotección (Smirnoff et al., 2000), aunque experimentos recientes con el mutante deficiente en ascorbato *vtc2-1* sugieren que el ascorbato es esencial para el crecimiento, pero no es tan claro su papel fotoprotector (Plumb et al., 2018). Sin embargo, hay evidencias experimentales que respaldan lo contrario. Por ejemplo, el deshidroascorbato (DHA), la forma oxidada del ascorbato, es aceptor de electrones de la ferredoxina, el último componente de la cadena fotosintética de transporte de electrones en los cloroplastos (Asada, 1999), lo cual evita así la formación de $O_2^{\cdot-}$. Además, el ascorbato puede actuar como un donante de electrones del fotosistema II (Tóth et al., 2013) evitando que el grupo de manganeso resulte dañado en circunstancias tales como el estrés inducido por alta irradiancia (Tyystjärvi, 2008). Por lo tanto, estos datos si otorgan al ascorbato un papel esencial en la respuesta al estrés oxidativo debido a la intensidad lumínica. En el capítulo anterior hemos demostrado que solo la sobreexpresión de *VTC2* aumenta el flujo biosintético de la ruta y que su concentración de proteínas se regula en consecuencia. Más recientemente, se ha publicado que la acumulación de ascorbato bajo un alto estrés lumínico no solo requiere una mayor tasa de biosíntesis, sino también mecanismos para prevenir una degradación masiva del ascorbato, que se basa en reductasas de DHA y glutatión (Terai et al., 2020). Por lo tanto, el aumento de la reserva de ascorbato en condiciones ambientales adversas depende tanto de su biosíntesis como de

la reducción de deshidroascorbato a ascorbato. Asimismo, la tasa de biosíntesis dependerá tanto de la traducción de *VTC2* como de su degradación (VTC2). Está bien establecido que *VTC2* está regulado traduccionalmente (Laing et al., 2015), pero se sabe muy poco sobre su degradación. VTC1, la enzima que cataliza la conversión de D-manosa 1-fosfato en GDP-D-manosa actuando aguas arriba VTC2, a pesar de que un aumento en su contenido de proteína no conduce a la acumulación de ascorbato (Capítulo 1), está finamente regulada. Wang y sus colaboradores (2013) demostraron que el factor fotomorfogénico COP9 subunidad 5B (CSN5B), que forma parte del complejo CSN que regula la actividad de ubiquitina ligasa cullin-RING E3 (Schwechheimer e Isono, 2010), es requerido para la degradación de VTC1 a través de la ruta del proteasoma 26S en oscuridad. Así, la biosíntesis de ascorbato se reprime durante la noche, es decir, cuando no hay fotosíntesis. La alta intensidad de la luz conduce al estrés oxidativo causado por ROS producido como consecuencia de la reacción de Mehler durante la fotosíntesis. Este estrés oxidativo se reduce por el ascorbato en el ciclo Foyer-Asada (Asada, 1999).

En este capítulo hemos investigado la respuesta a la luz de todas las líneas transgénicas mutantes transformadas con su respectiva enzima fusionada a GFP utilizando diferentes enfoques. El tratamiento con luz alta de las líneas transgénicas, que causó un aumento en el contenido de ascorbato, condujo paradójicamente a una disminución del contenido de VTC2, VTC4 y L-GalDH, que son pasos enzimáticos de la vía SW dedicados a la biosíntesis de ascorbato. Por el contrario, GME, cuyo producto también participa en los polímeros de la pared celular y la biosíntesis de glicoproteínas, no cambió su concentración. La proporción de aumento de ascorbato debido a una mayor intensidad de luz fue similar (~2 veces) entre líneas, excepto en aquellas que contienen contenidos más bajos de ascorbato que WT (es decir, *gme/GME-GFP* y *vtc2*), que exhibieron un aumento más pronunciado de ascorbato en luz alta (~3,5 y 5 veces, respectivamente). Esto sugiere que otros mecanismos diferentes de la biosíntesis, como el reciclaje o la reducción de la degradación del ascorbato, están contribuyendo a compensar la deficiencia de ascorbato.

VTC2 mostró un patrón consistente de acumulación de proteínas durante el período de luz seguido de una fuerte disminución inmediatamente después de ingresar al período oscuro (dentro de 30 min), que no se correlacionan con el contenido de ascorbato. Sin embargo, el ascorbato total mostró una mejor correlación con la cantidad de proteína VTC2, lo que sugiere que el ascorbato biosintetizado se oxida rápidamente, manteniendo así un nivel estable de ascorbato, pero aumentando el de ascorbato total. Por tanto, la luz y los ciclos día/noche tienen un impacto en la concentración de las enzimas de biosíntesis de ascorbato, probablemente porque bajo una baja intensidad de luz la cantidad de ascorbato necesaria para eliminar las ROS es menor que bajo una alta irradiación. Así, es posible que la reducción de la biosíntesis de ascorbato en la oscuridad sea el resultado de la reducción de la actividad de VTC2. Aunque esto podría deberse a modificaciones postraduccionales de la proteína a través de la

fosforilación, nuestros datos respaldan que la regulación proteasomal de VTC2 es un importante punto de control. Además de la posibilidad de que la actividad del complejo CSN esté afectando a la estabilidad de VTC2, al igual que ocurre con VTC1, es posible que, de manera similar a la expresión de ARNm, la estabilidad de VTC2 podría estar también regulada por el reloj circadiano. Un cribado previo doble híbrido en levaduras identificó una proteína PAS/LOV como interactor tanto de VTC2 como de VTC5, cuya interacción disminuyó bajo la luz azul (Ogura et al., 2007). ZEITLUPE (ZTL), un regulador de proteínas del oscilador circadiano (Mas et al., 2003), también contiene un dominio LOV que contiene fotorreceptor de luz azul. Su interacción con TOC1, otro regulador circadiano, desencadena la degradación de TOC1 en la oscuridad, que puede ser estabilizada por un inhibidor de proteasoma (Mas et al., 2003). Por lo tanto, es posible que ZTL esté promoviendo la degradación de VTC2 en la oscuridad, aumentando así el control del reloj circadiano sobre la concentración de ascorbato.

Para concluir, en este capítulo hemos caracterizado la respuesta de la ruta de biosíntesis de ascorbato y el nivel de proteína y la evolución de VTC2, el regulador principal de la ruta en respuesta a condiciones de alta luz y durante el ciclo día / noche. Aquí, hemos demostrado que una alta irradiación conduce a una concentración reducida de enzimas de biosíntesis de ascorbato (Figura 20) y que la acumulación de VTC2 no se correlaciona necesariamente con un mayor contenido de ascorbato (Figura 19E). Además, hemos demostrado que el proteasoma es un determinante importante de la estabilidad de la proteína VTC2 cuya interacción potencialmente abre un nuevo enfoque en la ingeniería de la estabilidad de VTC2 para aumentar el ascorbato en las plantas de cultivo. Esto podría conducir a una mayor tolerancia a una serie de tensiones abióticas (Akram et al., 2017) como la salinidad (Huang et al., 2005; Zhang et al., 2012; Wang et al., 2013) y el estrés oxidativo en los cultivos de interés (Cai et al., 2016; Hu et al., 2016) (Fenech et al., 2019). Otro aspecto positivo en la identificación del mecanismo regulador de la acumulación de ascorbato es un mejor valor nutricional, una mayor conservación de las propiedades nutricionales después de la cosecha y una mayor vida útil de la fruta (Stevens et al., 2007; Antunes et al., 2013).

INTRODUCTION

This introduction has been published as a Review Article in the journal "Frontiers in Plant Science" in which this PhD candidate is the first author and it is attached at the end of this thesis in the section "Publication":

Fenech M, Amaya I, Valpuesta V and Botella MA (2019). **Vitamin C Content in Fruits: Biosynthesis and Regulation**. *Front. Plant Sci.* 9:2006. doi: 10.3389/fpls.2018.02006

The introduction presented here corresponds to the cited paper and it has been modified for coherence along the manuscript, but no essential information has been changed.

Multiple roles of vitamin C in humans

L-Ascorbic Acid (L-threo-hex-2-enono-1,4-lactone, ascorbate), also called vitamin C, is an essential antioxidant molecule in plant and animal metabolism and also functioning as a cofactor in many enzymes. While many animals are able to synthesize ascorbate in the liver or in the kidney, others, such as humans, non-human primates, guinea pigs, and certain groups of bats and birds have lost this ability due to the accumulation of mutations in the coding sequence of the last committed enzyme of the pathway (L-gulono-1,4-lactone oxidase, GULO; Chatterjee, 1973; Drouin et al., 2011; Nishikimi et al., 1994). Dietary changes with the inclusion of abundant fruits and vegetables in the diet resulted in the loss of selective pressure to keep the pathway functional (Macknight et al., 2017). Thus, this molecule must be incorporated in the diet (hence classified as a vitamin), with vegetables and fruits as the major sources of ascorbate.

The role of ascorbate in mammals has extensively been studied throughout time, particularly since the 18th century with the discovery of its role in preventing scurvy (Baron, 2009; Lind, 1753). However, this was not obvious at the time because the lack of ascorbate in the diet takes about a month before the symptoms to occur. Thus, this disease was typically manifested during long sea travels with a diet scarce in fresh vegetables and fruits. In the earlies 1930's, Albert Szent-Györgyi identified and isolated the molecule responsible for this anti-scurvy activity. Thus, that molecule, previously called hexuronic acid, was renamed as ascorbic acid. One of the main symptoms in scurvy is skin impairment and injuries due to the involvement of ascorbate in the biosynthesis and stability of collagen. Ascorbate functions as a cofactor in the enzymatic hydroxylation catalysed by Fe^{2+}/αKG-dependent dioxygenases prolyl 4-hydroxylase, prolyl 3-hydroxylase and lysyl hydroxylase (Myllylä et al., 1984; Padayatty and Levine, 2016; Pekkala et al., 2003; Peterkofsky, 1991) through the reduction of Fe^{3+} to the active Fe^{2+} (de Jong et al., 1982; Gorres and Raines, 2010). Prolyl hydroxylation is an essential post-translational modification that occurs in proline residues located at X and Y sites of procollagen Gly-X-Y tandem repeats during collagen biosynthesis. Whereas Prolyl 4-hydroxylases catalyse hydroxylation on Y locations, Prolyl 3-hydroxylases hydroxylate residues located at X sites, thus enabling the trimerization of collagen providing high thermal stability (Koide and Nagata, 2005). The hydroxylation catalysed by these

enzymes requires an Fe^{2+} ion located at the active centre, which is oxidized to Fe^{3+} in the catalytic cycle and ascorbate is responsible of keeping the iron active by reducing it back to Fe^{2+}.

In addition to preventing scurvy, ascorbate is involved in many other processes which also require the action of other members of this family of mono- and dioxygenases. For these enzymes, ascorbate functions as a cofactor, maintaining activity of the metal ions located in the active centres. For example, ascorbate is important for the synthesis of carnitine, the lack of which is related to the common fatigue found in scorbutic patients. Trimethyllysine hydroxylase and γ-butyrobetaine hydroxylase require ascorbate to enhance their activity in the biosynthesis of carnitine (Rebouche, 1991). In addition, ascorbate is also known to act as a cofactor of dopamine β-monooxygenase (Rush and Geffen, 1980), and in peptide hormone metabolism, by acting as a cofactor of peptidylglycine α-amidating monooxygenase, involved in the C-terminal amidation of these regulatory molecules (Prigge et al., 1999). More recently, the activity of other key Fe^{2+}/αKG-dependent dioxygenases have been showed to be enhanced by ascorbate, as is the case of Ten-Eleven Translocations (TETs) enzymes. TETs are involved in DNA demethylation through an oxidation cascade from 5-methylcytosine to 5-hydroxymethylcytosine, 5-formylcytosine, 5-carboxylcytosine and, then, to cytosine by the Base Excision Repair (BER) mechanism (Blaschke et al., 2013; Hu et al., 2015; Minor et al., 2013). Importantly, ascorbate functions as a cofactor of histone demethylases harbouring a Jumonji C (JmjC) domain (JHDMs), the same catalytic domain present in TETs (Young et al., 2015). Tri-, di- and monomethylated lysines in histones can be oxidized to hydroxymethyl lysines by JHDM and ascorbate in a similar way as occurring with DNA demethylation and TETs, with an spontaneous removal of this hydroxymethyl group (Young et al., 2015). All together, these findings show that ascorbate participates in the response to environmental stimuli, not only by buffering the cell redox state, but also by its involvement in the epigenetic control on gene expression. In addition, ascorbate enhances iron absorption (Hallberg et al., 1989, 1987), which is not only important to keep the Fe^{2+}/αKG-dependent dioxygenases active, but also for many other roles (Lieu et al., 2001; Muckenthaler et al., 2008).

Major fruit supplies of ascorbate in humans

Fresh fruits and vegetables are the major sources of this vitamin, therefore increasing its concentration will have an important impact in human nutrition. Ascorbate deficiency in developed countries has registered a decrease throughout time. At the end of last century, ascorbate deficiency in USA was around 13% of the population (Hampl et al., 2004), but it dropped to 7% in the last survey effectuated during 2003-2004 period (Schleicher et al., 2009). According to early experiments, a daily dose of less than 10 mg was found to

prevent scurvy (Baker et al., 1969, 1971, Hodges et al., 1969, 1971; Johnstone et al., 1946; Peters et al., 1953). However, an Average Requirement (AR) of 90 mg/day for men and 80 mg/day for women, and a Population Reference Intake (PRI) of 110 mg/day for men and 95 mg/day for women, has been established by the European Food Safety Authority (EFSA Panel on Dietetic Products and Nutrition Allergies, 2013). This is based on maintaining a plasma concentration around 50 µmol/L of ascorbate, indicative of an adequate status (Kallner et al., 1979). In USA and Canada, the Recommended Dietary Allowance (RDA) is 90 mg/day for men and 75 mg/day for women (Food and Nutrition Board, 2000).

It is accepted that a diet rich in ascorbate has various health advantages (Carr and Maggini, 2017; Reczek and Chandel, 2015; van Gorkom et al., 2018; Wintergerst et al., 2006). Furthermore, in the last few years, ascorbate has been proposed as a treatment against different types of cancer through various mechanisms, such as increasing TET's activity, inducing oxidative stress in cancer cells or enhancing the activity of various chemical treatments (Agathocleous et al., 2017; Cimmino et al., 2017; Ko et al., 2015; Lu et al., 2018; Miura et al., 2018; Shenoy et al., 2017; Yun et al., 2015). Daily intake of ascorbate provided by fruits is dependent on several factors, but clearly the content of ascorbate as well as the amount that is consumed are the most important factors. However, it is important to take into account the way it is consumed as this might have important consequences on ascorbate reduction and oxidation, and can also alter the bioavailability of ascorbate due to interactions with other phytochemicals such as Vitamin E or flavonoids (Carr and Vissers, 2013; Packer et al., 1979; Tanaka et al., 1997).

Ascorbate overall intake is dependent on the intrinsic amount of ascorbate of a specific fruit and its consumption (Figure 1B). According to FAOSTAT[1], tomato has been the most produced fruit in the world in the last twenty years, a trend that has increased during the last years (Figure 1A). The production has been 177 million tonnes in 2016, followed by banana (~113 million tonnes), apple (~89 million tons), cucumber (~80 million tons) and grape (~77 million tonnes). In the European Union in 2016, fruit production was dominated by grape (~24 million tonnes), followed by tomato (~18 million tonnes), apple (~12,5 million tonnes) and orange (~6,3 million tonnes) (Eurostat, 2017). However, a large proportion of tomato (61,5%), apple (26,8%) and grape (96.5%) is processed (Eurostat, 2017), leading both to a reduction of ascorbate content and a lower bioavailability of other nutrients that are ascorbate dependent (Hallberg et al., 1987, 1982). This is particularly evident in grape, with ~90 % of the harvest destined to wine production (Eurostat, 2017), leading to negligible amounts of ascorbate (USDA Food Composition Databases[2]). Therefore, considering production along with consumption data (Figure 1C), ascorbate intake through orange surpasses that of grape. Tomato and apple fruits, although important dietary sources of ascorbate. It is obvious that even a moderate increase in the content of ascorbate in these highly consumed fruits would rise their nutritional value. Therefore, the large consumption of tomato, its relatively low ascorbate and its high raw intake

makes it an excellent target for increasing its ascorbate content from a nutritional point of view (Figure 1).

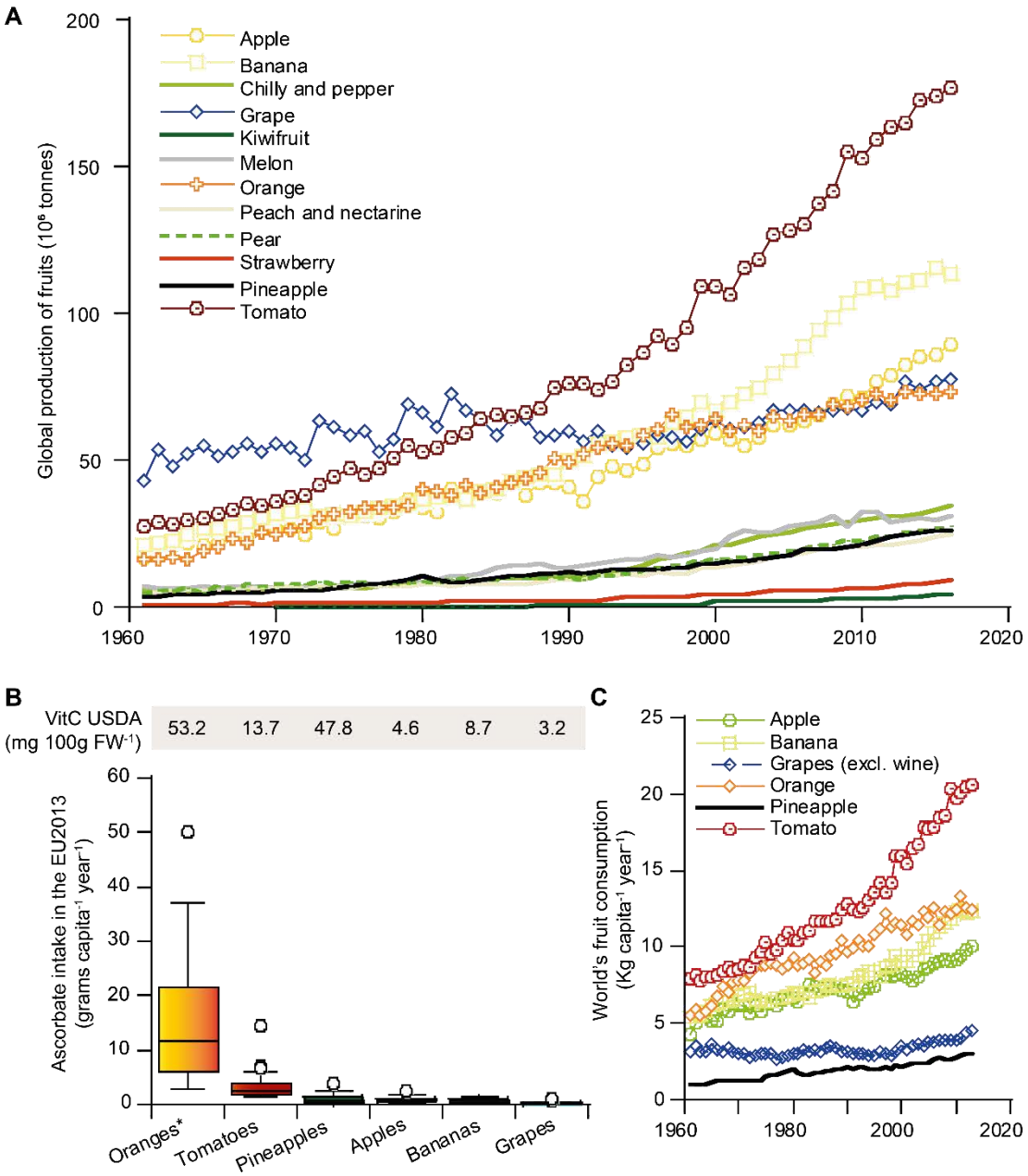

Figure 1. Main fruit crops yield and consumption according to FAO. (A) Global fruit production, in million tons, and its evolution from 1961 to 2016. (B) Fruit ascorbate intake, in grams of ascorbate capita^{-1} year^{-1}, in the countries from the European Union in 2013. Data were generated considering ascorbate (VitC) levels of raw fruit available in USDA database (https://ndb.nal.usda.gov/ndb/search/list) and consumption data of each fruit (Kg capita^{-1} year^{-1}) from FAOSTAT. USDA IDs consulted: 9200 (Oranges *includes mandarins, raw, all commercial varieties), 11529 (Tomatoes, red, ripe, raw, year average), 9003 (Apples, raw with skin), 9132 [Grapes, red or green (European type, such as Thompson seedless), raw], 9266 (Pineapple, raw, all varieties), 9040 (Bananas, raw). Consumption data was obtained from Eurostat (http://ec.europa.eu/eurostat). (C) Evolution in the global consumption of fruits, in Kg capita^{-1} year^{-1}, from 1961 to 2013.

The role of ascorbate in plants and fruits

Ascorbate plays a plethora of roles in plant cells. Important properties of ascorbate are its antioxidant capacity and the finalization of oxidative chain reactions resulting in non-oxidative products such as dehydroascorbate (DHA) and 2,3-diketogulonic acid (Davey et al., 2000). The importance of ascorbate in scavenging ROS became evident when several of the genes involved in the ascorbate biosynthetic pathway were identified in genetic screenings searching for mutants hypersensitive to ozone, a powerful oxidant (Conklin et al., 1996). This screening resulted in the identification of five vitamin C-deficient (*vtc*) mutants, with four of those mutations affecting genes encoding enzymes of the Smirnoff-Wheeler pathway: *VTC1* (Lukowitz et al., 2001), *VTC2* and *VTC5* (Dowdle et al., 2007; Linster et al., 2007) and *VTC4* (Conklin et al., 2006).

Hydrogen peroxide (H_2O_2) plays essential roles in plants development and defence (Exposito-Rodriguez et al., 2017; Mittler, 2017; Mullineaux et al., 2018; Waszczak et al., 2018) and it can be found in different organelles within the plant cells (Exposito-rodriguez et al., 2013). However, H_2O_2 is also partly responsible for light-induced oxidative damage. Ascorbate is involved in the scavenging of the excess of H_2O_2 produced during the photosynthesis in high-irradiance conditions by the function of ascorbate peroxidases (APX), enzymes not present in animals (Wheeler et al., 2015).

Together with APX, catalases also perform H_2O_2 scavenging (Mhamdi et al., 2012, 2010). However, plants lack catalases in chloroplasts, which experience a high production of H_2O_2 in thylakoids due to photosynthesis, as a consequence of the Mehler reaction. In these organelles, a thylakoidal APX (tAPX) catalyses the reduction of H_2O_2 (Asada, 1999). Surprisingly, single and double mutants in chloroplastic APX (tAPX and stromal APX) are viable, suggesting alternative mechanisms for H_2O_2 detoxification (Giacomelli et al., 2007). 2-Cys peroxiredoxins (2-Cys PRX), localised in the chloroplast, reduce H_2O_2 and prevent oxidation of the thylakoidal membrane by reducing lipid hydroperoxide from thylakoid phospholipids (Baier and Dietz, 1997). Therefore, 2-Cys PRXs have been proposed as alternative H_2O_2 scavengers to APX in an alternative water-water cycle (Awad et al., 2015; Pérez-Ruiz et al., 2017) using glutathione, thioredoxin, glutaredoxin, cyclophilin, and/or tryparedoxin instead of ascorbate as cofactors (Stork et al., 2005). Together with APX and 2-Cys PRX, vitamin E (α-tocopherol) is a major lipophilic antioxidant also involved in preventing photodamage in the membrane of thylakoid lipids (Semchuk et al., 2009). Ascorbate also has a role in vitamin E function by the non-enzymatical reduction of α-tocopheryl radicals, hydroxyl radicals (·OH) and superoxide ions (O_2^-) (Asada, 1999; Davey et al., 2000; Mittler, 2017).

The use of ascorbate as a cofactor by other enzymes, such as the Fe^{2+}/α-KG-dependent dioxygenases and Cu^+-monooxygenases, is conserved among plants and animals. However, one of these common enzymes, a Fe^{2+}-dependent

4-hydroxyphenylpyruvate dioxygenase, has different functions in plants. Whereas in animals this enzyme is involved in tyrosine metabolism (Lindblad et al., 1970), in plants it is required for plastoquinone and tocopherols synthesis (Norris et al., 1998). Other light-responsive pigments that are very abundant in fruits, like anthocyanins, fail to accumulate in *vtc1* and *vtc2* mutant plants when exposed to high light. This finding, combined with the UV-B absorption by anthocyanin, suggests that ascorbate-mediated redox reactions act upstream of anthocyanin synthesis (Page et al., 2012).

Ascorbate was proposed to directly participate in photosynthesis as an electron carrier, although later a role as a photoprotectant was revealed (Smirnoff, 2000). The electron transfer from ascorbate to the primary oxidising agent of photolysis was first coupled to the photophosphorylation reaction (Marrè et al., 1959). Then, the reduction of monodehydroascorbate (MDA) and DHA were suggested to rely on reductants formed in photosystem I (PSI). It is now established that inside the thylakoid, luminal ascorbate acts as an electron donor of photosystem II (PSII) (Tóth et al., 2013) where the Oxygen-Evolving Complex is impaired (Katoh and San Pietro, 1967; Mano et al., 1997; Tóth et al., 2009), thus allowing the reduction of $NADP^+$ to NADPH by the electron-transport chain (Tóth et al., 2013, 2009). This is particularly important during abiotic stresses such as heat and high light that alter this complex by damaging the manganese cluster (Tyystjärvi, 2008). In addition, ascorbate can also dissipate energy from an excess of light irradiance acting as a cofactor of violaxanthin de-epoxidase, an enzyme involved in preventing photodamage by non-photochemical quenching (NPQ) (Yamamoto et al., 1972). When the irradiance is too high, the excess of energy normally transferred to chlorophyll *a* is used to de-epoxidize the carotenoid violaxanthin into zeaxanthin using the thylakoid luminal ascorbate as a cofactor in the xanthophyll cycle (Hieber et al., 2000). This has been supported experimentally by mutations in the enzyme's residues that bind ascorbate (Saga et al., 2010) and by the analysis of Arabidopsis mutants with low ascorbate content (Müller-Moulé et al., 2002).

Biosynthesis and Metabolism of ascorbate in plants

The predominant pathway through which ascorbate is synthesized in plants is the Smirnoff-Wheeler (SW) pathway (Wheeler et al., 1998). Contrary to the animal pathway, in the plant pathway there is no carbon inversion, as the carbon 1 in the D-glucose molecule remains as carbon 1 in ascorbate after conversion. In this pathway, a molecule of D-glucose-6-phosphate is transformed into D-fructose-6-phosphate by the action of phosphoglucose isomerase (PGI; Figure 2). Then, it is transformed into D-mannose-6-phosphate and D-mannose-1-phosphate by the action of phosphomannose isomerase (PMI; Maruta et al., 2008) and phosphomannomutase (PMM; Qian et al., 2007). Then, GDP-D-

mannose pyrophosphorylase (GMP, encoded by *VTC1* in *Arabidopsis thaliana*) transfers guanosine monophosphate from GTP to form GDP-D-mannose (Conklin et al., 1999, 1997, 1996; Lukowitz et al., 2001). GDP-D-mannose is further transformed into GDP-L-galactose by the GDP-D-mannose-3',5'-epimerase (GME), an enzyme that belongs to the extended short chain dehydratase/reductase (SDR) protein family, harbouring a modified NAD^+ binding Rossman fold domain. Interestingly, GDP-L-galactose is not the only result of GME activity, since GDP-L-gulose can also be produced if GME catalyses a 5' epimerization instead of a 3',5' epimerization (Major et al., 2005; Wolucka et al., 2001; Wolucka and Van Montagu, 2003). Since GDP-L-gulose is a very rare sugar in plants with no structural function, it has been suggested that it is directly channelled to synthesize ascorbate. After GME releases GDP-L-galactose, this compound is then transformed into L-galactose-1-phosphate, L-galactose and L-galactono-1,4-lactone by GDP-L-galactose-phosphorylase (GGP, encoded by *VTC2* and *VTC5* in *A. thaliana*; Dowdle et al., 2007; Laing et al., 2007), L-galactose-1-phosphate phosphatase (GPP, encoded by *VTC4* in *A. thaliana*; Conklin et al., 2006; Laing et al., 2004; Nourbakhsh et al., 2015; Torabinejad et al., 2009) and L-galactose dehydrogenase (L-GalDH; Gatzek et al., 2002; Laing et al., 2004b), respectively. Interestingly, for the final production of L-ascorbic acid, L-galactono-1,4-lactone must move from the cytosol to the intermembrane space of the mitochondria, where the active site of L-galactono-1,4-lactone dehydrogenase (GLDH) is located (Imai et al., 1998; Mapson and Breslow, 1958; Pineau et al., 2008; Schertl et al., 2012; Schimmeyer et al., 2016). The fact that the oxidation of L-galactono-1,4-lactone is carried out in plants by a dehydrogenase instead of an oxidase (GULO) as occurs in animals, is not trivial. Contrary to paradoxical GULO activity, GLDH does not release H_2O_2 and therefore the production of ascorbate in plants does not have side effects over the redox state of the cell (Wheeler et al., 2015). Although some data support the existence of a side branch of the pathway that converges with that of animals (Jain and Nessler, 2000; Maruta et al., 2010; Radzio et al., 2003), there is strong evidence that most of the ascorbate in plants is produced through GLDH (Pineau et al., 2008). A recent phylogenetic study on the origin of GLDH identified an ancient paralog arisen from the original GULO, followed by a loss of paralogs (Wheeler et al., 2015). Thus, in species with the SW pathway, GULO has been functionally replaced by GLDH following chloroplast acquisition in photosynthetic organisms, since the presence of both proteins seems mutually exclusive (Wheeler et al., 2015). Interestingly, L-gulose, a previously mentioned rare sugar in plants and also a product of GME activity, is proposed to be transformed into L-gulono-1,4-lactone by as yet unidentified enzymes (Wolucka and Van Montagu, 2003). Supporting the presence of GULO activity in plants are (1) external supplementation of L-gulono-1,4-lactone in the growth media increased ascorbate levels in WT tobacco leaves (Jain and Nessler, 2000) and (2) the synthesis rate of ascorbate can increase up to 15% when L-gulono-1,4-lactone is externally supplied in Arabidopsis cell culture (Davey et al., 1999). One possibility

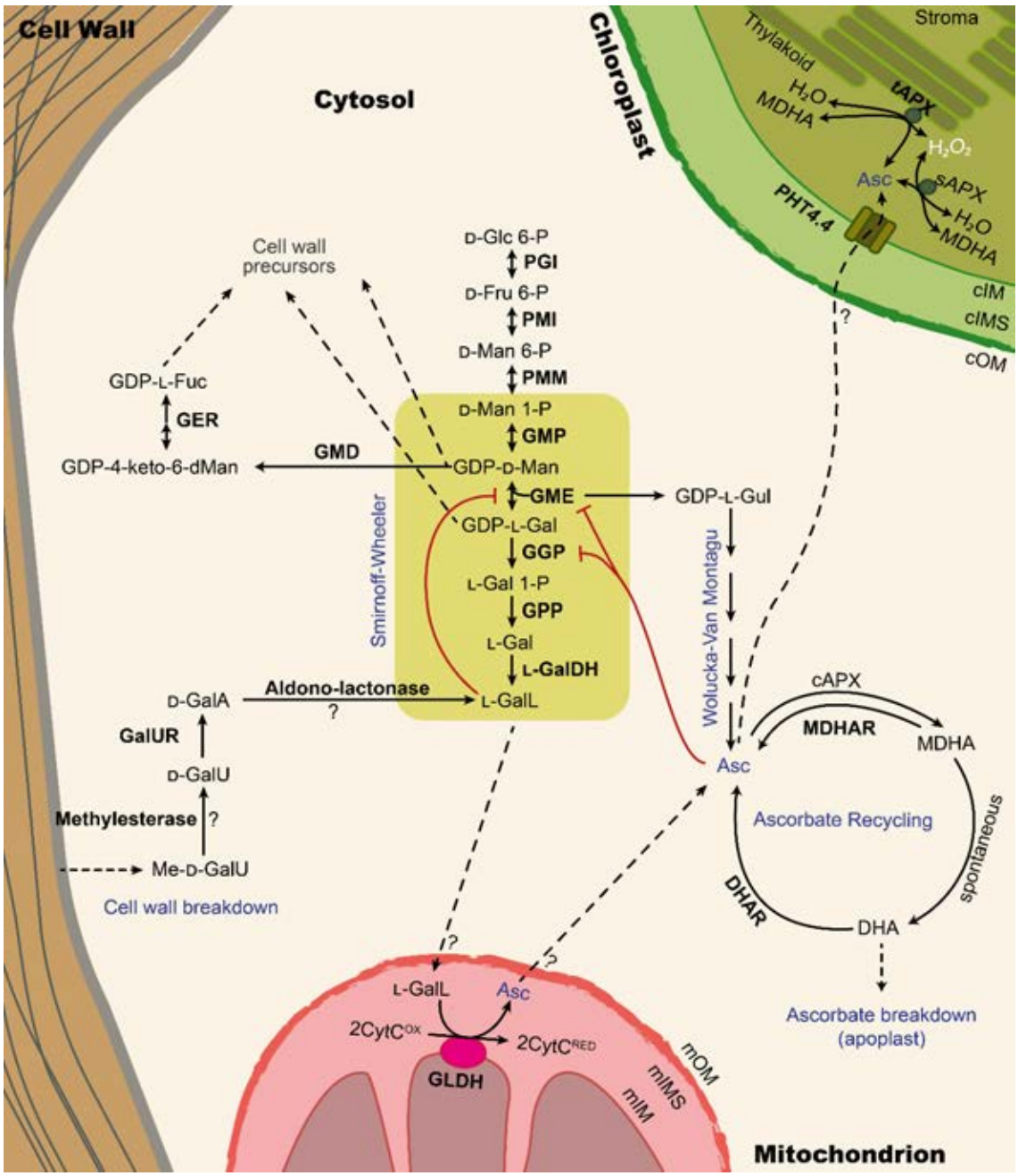

Figure 2. Biosynthesis pathways of ascorbate in the plant cell. Solid lines represent the committed reactions within a pathway. Dashed lines represent the translocation of a molecule from a cellular compartment to another. Enzymes are displayed in bold: PGI=phosphoglucose isomerase, PMI=phosphomannose isomerase, PMM=phosphomannomutase, GMP=GDP-D-mannose pyrophosphorylase (Arabidopsis VTC1), GME=GDP-D-mannose-3',5'-isomerase, GGP=GDP-L-galactose phosphorylase (Arabidopsis VTC2/VTC5), GPP=L-galactose-1-phosphate phosphatase (Arabidopsis VTC4), L-GalDH=L-galactose dehydrogenase, GLDH=L-galactono-1,4-lactone dehydrogenase, cAPX= cytosolic Ascorbate Peroxidase, MDHAR= monodehydroascorbate reductase, DHAR= dehydroascorbate reductase, PHT4.4=inorganic phosphate transporter, sAPX=stromal ascorbate peroxidase, tAPX=thylakoidal ascorbate peroxidase, GMD=GDP-D-mannose-4,6-dehydratase (Arabidopsis MUR1/GMD1), GER= GDP-4-keto-6-deoxymannose-3,5-epimerase-4-reductase (Arabidopsis GER1/GER2), GalUR=D-Galacturonate Reductase. Substrates and products are shown in regular shape: Glc=glucose, Fru=fructose, Man=mannose, Gal=galactose, Gul=gulose, GalU=Galacturonate, Me-D-GalU=methyl galacturonate, GalA=Galactonate, GalL=L-galactono-1,4-lactone, Asc=ascorbate, $CytC^{OX}$= oxidized cytochrome c, $CytC^{RED}$=reduced cytochrome c, MDHA=monodehydroascorbate, DHA=dehydroascorbate, GDP-α-keto-6-dMan=GDP-4-keto-6-deoxymannose, Fuc=fucose. Other abbreviations: mOM=mitochondrial outer membrane, mIMS=mitochondrial inter membrane space, mIM=mitochondrial inner membrane, cOM=chloroplastic outer membrane, cIMS=chloroplastic inter membrane space, cIM=chloroplastic inner membrane.

is that GLDH also uses L-gulono-1,4-lactone as substrate. However, this seems unlikely since GLDH is highly specific for L-galactono-1,4-lactone (Mapson and Breslow, 1958; Oba et al., 1995; Østergaard et al., 1997; Rodríguez-Ruiz et al., 2017). Transgenic tobacco BY2 cells overexpressing several Arabidopsis homologs of GULO from rat resulted in increased ascorbate content in lines overexpressing GULO2, GULO3 and GULO5 but only after external application of L-gulono-1,4-lactone (Maruta et al., 2010). However, GULO has lower substrate specificity than GLDH and can catalyse the oxidation of other aldono-lactones, including L-galactono-1,4-lactone (Davey et al., 2000). Interestingly, the overexpression of rat liver GULO increased ascorbate levels in tobacco leaves (Jain and Nessler, 2000) as well as in Arabidopsis leaves, and rescued the Arabidopsis *vtc1* mutant ascorbate levels to WT (Radzio et al., 2003).

Alternative ascorbate biosynthesis pathways have been proposed in plants. One is through myo-inositol, following a pathway similar to animals, since the oxidation of myo-inositol oxidation produces D-glucuronate by a *MYO-INOSITOL OXYGENASE* (*MIOX*). Arabidopsis plants overexpressing *MIOX4* showed a 2-3-fold ascorbate content (Lorence et al., 2004). However, based on early radiotracer experiments (Loewus, 1963) and more recent reports (Endres and Tenhaken, 2011, 2009; Ivanov Kavkova et al., 2018), its contribution to the ascorbate pool remains unclear. The second is through the D-galacturonate pathway. In this pathway, a D-galacturonate reductase (GalUR) uses D-galacturonate, to produce L-galactonic acid that is converted to L-galactono-1,4-lactone, the last intermediate within the SW pathway (Mapson and Isherwood, 1956; Shigeoka et al., 1979).

In addition to its biosynthesis, the ascorbate pool also depends on its recycling by the Foyer-Halliwell-Asada cycle (Asada, 1999; Foyer and Halliwell, 1976) and degradation (Green and Fry, 2005; Loewus, 1999). Although the biochemistry of biosynthesis and recycling of ascorbate is well established, its degradation is not clear and might not follow a single pathway. In the apoplast, it can be degraded through the conversion of ascorbate to 2-keto-L-gulonic acid that leads to L-tartaric acid formation in cytoplasm, a compound important for fruit quality particularly in the *Vitaceae* family (DeBolt et al., 2006). Ascorbate can also be degraded through the direct oxidation of DHA or through the oxidation of 4-O-oxalyl-L-threonic acid, leading to the production of both oxalic acid and L-threonic acid (Green and Fry, 2005). Additionally, it can also be degraded through the hydrolysis of DHA to 2,3-diketo-gulonic acid, and to oxalic acid and its esters, or to L-threonic acid under strong oxidative conditions (Parsons et al., 2011). In tomato, the main degradation products are oxalic acid, threonic acid and oxalyl threonic acid, but no tartaric acid has been detected (Truffault et al., 2017), suggesting that ascorbate degradation occurs mainly through DHA oxidation rather than DHA hydrolysis, a pathway previously proposed in *Rosa sp.* cell cultures (Green and Fry, 2005). A broad perspective of ascorbate breakdown pathways in different species is provided by DeBolt and collaborators (2007).

Biosynthesis and Metabolism of ascorbate in fruits

Mutant analyses indicate that the SW pathway is the predominant if not the only pathway involved in ascorbate biosynthesis in green tissues (Dowdle et al., 2007; B. Lim et al., 2016). In heterotrophic tissues like fruits, the SW pathway is functional, as showed in several species including acerola, kiwi, strawberry, peach, tomato and apple (Badejo et al., 2012, 2009; Bulley et al., 2009; Cruz-Rus et al., 2010; Imai et al., 2009; Ioannidi et al., 2009; Mellidou et al., 2012a, 2012b). However, depending on the fruit ripening stage, alternative pathways might become relevant, especially the D-galacturonate pathway (Mapson and Isherwood, 1956; Shigeoka et al., 1979), for which the degradation of cell wall pectin can provide abundant substrate (Agius et al., 2003; Badejo et al., 2012; Cruz-Rus et al., 2010; Di Matteo et al., 2010). Analyses of tomato introgression lines from a cross between *Solanum lycopersicum cv*. M82 and *S. pennellii* was used to find genetic elements associated with high ascorbate content in fruits. This was done through the identification of genes induced in the IL12-4 line, which contains 19.9 mg ascorbate/g FW, relative to *S. lycopersicum cv.* M82, which contains 12.2 mg ascorbate/g FW (Di Matteo et al., 2010). Interestingly, while genes of the SW pathway were not differentially expressed, a pectinesterase gene (TC177576) involved in breakdown of pectins was 4.4-fold more expressed in the IL12-4 line than in the parental M82. This result suggests that an additional supply of D-galacturonate due to cell wall degradation might be the cause of the ascorbate increase in this line. In addition, an ascorbate peroxidase (TC172881) was down-regulated in fruits of IL12-4 compared to M82 parental line, which may cause a higher ascorbate accumulation due to a lower degradation (Di Matteo et al., 2010). While the D-galacturonate pathway is more active as the fruit ripens, the SW pathway and ascorbate translocation from the leaves provide the bulk of ascorbate in fruits at immature green stage. The fact that the photosynthesis inhibitor DCMU diminished the pool of ascorbate only at green stage (Badejo et al., 2012) not only supports this, but also reinforces the tight relationship between the SW pathway and photosynthesis.

Considering the variety of functions that ascorbate exerts in plant cells and its tight regulation in green tissues, it is remarkable how variable the content of ascorbate can be among the fruits of different species (Davey et al., 2000) or even between varieties or cultivars from the same species (Cruz-Rus et al., 2011; Mellidou et al., 2012b). An obvious question is: what is the functional significance of this high variability in fruit ascorbate content? Fruit crops have different environmental requirements to optimize yield and, in addition, the pool of ascorbate is affected by abiotic factors such as light or temperature (Gautier et al., 2008; Suzuki et al., 2014; Zechmann et al., 2011), due to its role in the antioxidant cellular system (Jimenez et al., 2002; Massot et al., 2013). Therefore, small differences within species can depend on their cultivation requirements,

harvest time or post-harvest conditions (Akhatou and Fernández-Recamales, 2014; Davey et al., 2007; Kevers et al., 2011; Oms-Oliu et al., 2011). However, the observed large differences in ascorbate content in closely related species likely have other causes. For example, several fold differences in ascorbate can be found between wild and cultivated tomato. Whereas domesticated tomato cultivars contain roughly 15 mg/100g FW, wild varieties *Solanum pimpinelifollium* and *Solanum pennellii* contain around 40 mg/100g FW (Lima-Silva et al., 2012) and up to 70 mg/100g FW (Stevens et al., 2007), respectively. In fact, back-crosses with *Solanum peruvianum*, another wild species (Atherton and Rudich, 1986), have been shown to contain the highest amount of ascorbate in *Solanum* species, around 50 mg/100g FW (Top et al., 2014). These wild tomato species grow naturally in Peru and Mexico, in coastal areas and river valleys less than 1000 m above sea level with abundant rainfalls. These two countries lie within the tropics of Capricorn and Cancer, respectively, with high irradiance and warm temperatures that may have favoured the selection of individuals with high ascorbate content over time. Current evidence suggests that domestication of wild tomatoes by cross-breeding different species of *Solanum* started in these two countries (Esquinas-Alcazar, 1981) likely driven by the selection of higher fruit size and resistance to diseases like *Fusarium* wilt (Atherton and Rudich, 1986). However, the most important advances in tomato breeding have taken place during the last 200 years in Europe, mainly in France, Italy and England, with a strong participation of the United States since the early 1920s (Atherton and Rudich, 1986). It is likely that growing under more controlled and less harsh conditions has decreased the selective pressure to keep alleles conferring high ascorbate content, particularly because an apparent association between high ascorbate levels and low productivity has been reported in this species (Atherton and Rudich, 1986). However, in addition to the metabolic regulatory mechanisms that might explain these differences in ascorbate content, other factors such as water content must be considered. A known example is that of two tomato cultivars, Matador and Elin, subjected to salinity treatment. This increased their ascorbate content on fresh weight basis, but it was decreased on dry weight basis. In both cultivars, water and ascorbate content were reduced, but the loss of water was higher than that of ascorbate (Dumas et al., 2003). Fruit size and weight were directly related with water content, and they have been key traits selected during breeding programs, while this is not the case for ascorbate.

In most fruits, such as tomato, acidity decreases while sugar content increases during ripening (Gautier et al., 2008; Mellidou et al., 2012b). Major organic acids in tomato, contributing to fruit acidity, are malic and citric acids (Davies and Hobson, 1981). However, the change in ascorbate levels during fruit ripening is a trait dependent on the species. In tomato (Badejo et al., 2012; Dumas et al., 2003; Gautier et al., 2008; Ioannidi et al., 2009), grape (Cruz-Rus et al., 2010) and strawberry (Cruz-Rus et al., 2011), ascorbate content increases as the fruit ripens. This correlated with changes in the activity of enzymes affecting the redox state of the fruit during the breaker stage (Gautier et al., 2008;

Jimenez et al., 2002). Unlike tomato, grape and strawberry, kiwifruit showed a maximal ascorbate level at the immature green stage due to its high biosynthesis rate, it decreased as it ripened and then remained fairly stable until complete ripening (Li et al., 2010; J. Y. Zhang et al., 2018). In peach fruits, ascorbate content gradually decreased during ripening (Imai et al., 2009). In different studies, the pattern of ascorbate accumulation does not match the expression of a specific gene involved in ascorbate biosynthesis or recycling, and therefore there is no clear connection between the expression of biosynthetic genes and ascorbate content (Imai et al., 2009; Li et al., 2010; Lima-Silva et al., 2012). However, evidences gathered in these studies show that the overall size of the ascorbate pool correlated well with the oxidative status (i.e. activity of enzymes involved in redox state, H_2O_2 content) of the fruit, which is usually triggered at breaker stage (Gautier et al., 2008; Imai et al., 2009; Jimenez et al., 2002; Li et al., 2010).

Relationship between ascorbate and cell wall biosynthesis

A significant aspect of the ascorbate biosynthetic pathway is the intimate relationship shared with cell wall biosynthesis. Some of the early precursors of the SW pathway such GDP-D-mannose and GDP-L-galactose are among the non-cellulosic cell wall glycosyl residues forming pectins and hemicelluloses (Figure 3). For this reason, mutations or knock-downs in genes related to the early steps of the SW pathway lead to growth reduction or even arrest, due to impairment of cell wall formation during plant growth, including different stages of fruit development (Hoeberichts et al., 2008; Lukowitz et al., 2001; Mounet-Gilbert et al., 2016). Thus, knock-down mutants of the Arabidopsis *PMM* gene show between 20 and 50% of ascorbate levels relative to WT, altered protein N-glycosylation (specially a protein-disulphide isomerase post-translational modification, an abundant protein in the ER) and glycosylphosphatidylinositol (GPI) anchoring of proteins, leading to cell death after heat stress (Hoeberichts et al., 2008). Supplementation with L-galactono-1,4-lactone (Hoeberichts et al., 2008) or ascorbate (Cho et al., 2016) in the media recovered ascorbate levels but the mutants remained hypersensitive to heat. A null mutation in the Arabidopsis *GMP* gene (*cyt1* mutant) results in embryo arrest due to defects in *N*-glycosylation of proteins and altered composition of the cell wall (Figure 3; Lukowitz et al., 2001). The product of GMP activity, GDP-D-mannose, is used in the glycosylation of proteins, ascorbate biosynthesis and as a precursor of cell wall carbohydrates (Conklin et al., 1999). GDP-D-mannose is converted to GDP-L-galactose by the action of GME, but can also be converted to GDP-L-fucose by the sequential function of GDP-D-mannose-4,6-dehydratase (MUR1/GMD1; Bonin et al., 1997, 2003) and GDP-4-keto-6-deoxy-mannose-3,5-epimerase/4-reductase (GER1/GER2; Bonin and Reiter, 2000; Nakayama et al., 2003; Figure

3). All these three compounds, GDP-D-mannose, GDP-L-galactose and GDP-L-fucose are precursors of hemicelluloses and pectins (RG-II) when converted to D-mannosyl, L-galactosyl and L-fucosyl residues (Conklin et al., 1999; Reiter and Vanzin, 2001).

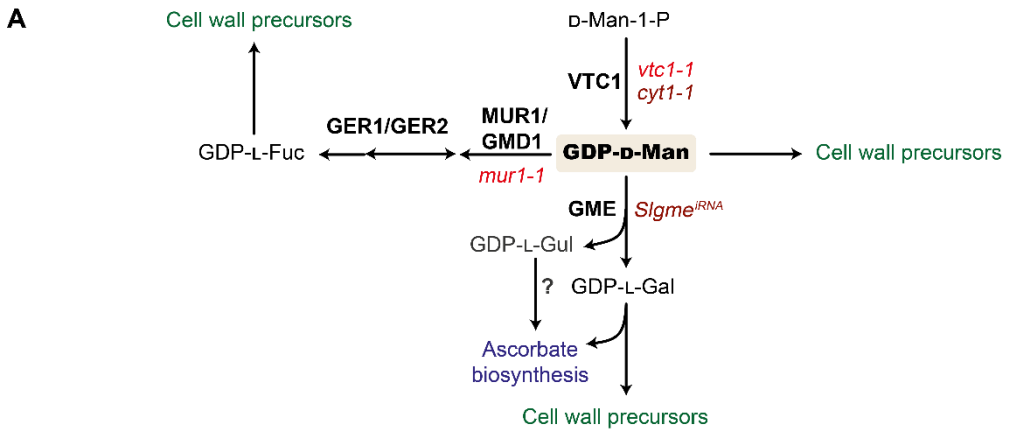

B

	Cell Wall impairment	RG-II impairment (Boron rescue)	Asc (Asc rescue)
vtc1-1/cyt1-1	Defect in cellulose biosynthesis; reduced CW D-Man content/ desorganized CW	? (?)	25-30% (No) / ? (No)
mur1-1	Virtual lack of L-Fuc in non-cellulosic CW polymers	Impaired dimerization (Yes)	? (?)
Slgme^iRNA	Increase in mannan content	Impaired dimerization in gme2^iRNA and gme^iRNA lines, but not in gme1^iRNA lines (Yes)	Leaves: 40-60%, Fruits: 60-80%. gme1^iRNA and gme2^iRNA equal to WT (No)

Figure 3. GDP-D-mannose and its biological relevance for ascorbate and cell wall biosynthesis in plants. A) Reaction scheme for the novo synthesis of GDP-D-mannose in *Arabidopsis thaliana*. Mutants described for each step are indicated in lower case italic red letters. B) Biological impairment over cell wall (RG-II=rhamnogalacturonate II) and ascorbate content in mutants of genes controlling the GDP-D-mannose pool. MUR1 and GMD1 encode two GDP-D-mannose-4,6-dehydratases. GER1 and GER2 encode two GDP-4-keto-6-deoxymannose-3,5-epimerase-4-reductases. The epimerase reaction is reversible whereas the reduction is not (Bonin et al., 1997). VTC1 encodes GMP, a GDP-D-mannose pyrophosphorylase, GME encodes a GDP-D-mannose-3',5'-isomerase. D-Man-1-P= D-mannose-1-phosphate, GDP-D-Man= GDP-D-mannose, GDP-L-Gul= GDP-D-gulose, GDP-D-Gal= GDP-D-galactose, GDP-D-Fuc= GDP-D-fucose, Asc= Ascorbate.

All the above evidences support the conclusion that a reduction in the production of GDP-D-mannose in the *cyt1* mutant is expected to have a significant impact on the structure of the cell wall. The importance of GDP-D-mannose in cell wall structure was further supported by the identification of the *mur1* mutant (Bonin et al., 1997). Mutations in *MUR1* produce a dwarf phenotype, mainly caused by a reduced content in fucose, since the supply of exogenous L-fucose reverted the dwarf phenotype (O'Neill et al., 2001). Interestingly, L-fucosyl residues in *mur1* cell wall xyloglucans are replaced by L-galactosyl residues (Bonin et al., 1997; Reiter et al., 1993; Zablackis et al., 1996). One possibility is that this substitution is the direct cause the dwarf phenotype of *mur1*. However, this does not seem to be the case since the Arabidopsis *mur2* mutant, affected in a xyloglucan-specific fucosyltransferase (*AtFUT1*), grows indistinguishably from

WT despite having around 1% of the L-fucose content of the WT (Perrin et al., 1999; Vanzin et al., 2002). Moreover, the xyloglucans of jojoba seeds naturally contain L-galactosyl residues, and not fucosyl residues (Hantus et al., 1997; Pauly and Keegstra, 2016), suggesting that xyloglucan substitution of L-fucose by L-galactose residues is not the cause of growth impairment in *mur1*. In addition to this replacement of fucosyl by L-galactosyl residues in xyloglucan, the *mur1* mutant also has the same substitution in their RG-II fraction of pectins. In the RG-II structure, cross-linking mediated by boron is essential for a proper dimerization (O'Neill et al., 2001). Therefore, an alternative possibility was that changes in monosaccharide composition in the pectic RG-II *mur1* can impair this dimerization, which in turn would lead to dwarfism. In fact, the impaired dimerization in RG-II seems to be the cause of this dwarf phenotype because exogenous application of boron restored the wild type phenotype (O'Neill et al., 2001). This is consistent with the finding that mur2 mutants are neither affected in RG-II cross-linking nor L-fucose content (O'Neill et al., 2001). Furthermore, Arabidopsis *cgl* mutants, lacking the N-acetyl glucosaminyl transferase I in their Golgi apparatus (and hence, L-fucosylation), do not present altered growth (von Schaewen et al., 1993). Altogether, growth defects in *mur1* point to a structural defect which is due to impairment in RG-II dimerization, and not due to defects in protein fucosylation. However defective interactions with different cell wall polymers cannot be completely ruled out, since the α-1,3-xylosyltransferase activity carried out by RGXT enzyme family, involved in RG-II synthesis, transfers D-xylose residues from UDP-xylose onto fucose (Egelund et al., 2006).

An additional link between ascorbate and cell wall biosynthesis comes from studies of tomato lines silencing *GME* (Gilbert et al., 2009; Mounet-Gilbert et al., 2016). Those lines with both copies of *GME* silenced showed reduced growth, higher fragility, lower fruit firmness and a 35-55% reduced ascorbate content in leaves and 20-40% of WT ascorbate levels in fruits (Gilbert et al., 2009). Consistent with the expected accumulation of GDP-D-mannose, the silenced lines showed an increase in mannose-linked cell wall and defects in dimerization of RG-II by boron-mediated cross-linking, since phenotypic defects could be rescued by the application of external boron, but not with ascorbate (Gilbert et al., 2009; Mounet-Gilbert et al., 2016; Qi et al., 2017; Voxeur et al., 2011). All these results strongly suggest that this impairment has a cell wall structural basis rather than reduced ascorbate levels, similar to what was previously found in an Arabidopsis *mur1-1* mutant (O'Neill et al., 2001). Supporting this connection between ascorbate and cell wall biosynthesis at the GDP-D-mannose level, inactivation of GMP activity by knocking down Arabidopsis *KONJAC* genes involved in the activation of GMP resulted in reduced glucomannan content of cell walls and severe dwarfism (Sawake et al., 2015). The overexpression of *KONJAC1* caused a slight increase in ascorbate, whereas it resulted in a significant increase in the glucomannan content of plant cell walls, suggesting the presence of a mechanism that limits ascorbate accumulation.

This interaction between cell wall and ascorbate biosynthesis does not rely only on sharing common intermediates. As an enzyme cofactor, ascorbate is required for the activities of proline and lysine hydroxylases that, as previously mentioned, are involved in collagen biosynthesis in animals. In plants, proline hydroxylation is required for the production of hydroxyproline-rich glycoproteins (HRGP) such as arabinogalactans (AGPs) and extensins (EXTs). These proteins are part of cell wall structural glycoproteome acting as scaffolding components (Kishor et al., 2015; Marzol et al., 2018). AGPs are highly glycosylated HRGP proposed to function as cross-linkers of different cell wall polymers, thus conferring plasticity to the cell wall (Lamport et al., 2006). Recently, AGPs have been shown to be structural components of the cell wall by covalent attachment to pectins (rhamnogalacturonan I/homogalacturonate) and hemicelluloses (arabinoxylan), giving rise to the Arabinoxylan Pectin Arabinogalactan Protein complex APAP1 (Tan et al., 2013). In plants, EXTs have a role similar to that played by collagen in animals but contrary to collagen, EXTs can undergo *O*-glycosylation. This post-translational modification leads to oligo-arabinosylation of hydroxyproline residues that allow the formation of a three-dimensional network *in muro*, attaching to other cell wall components such as pectins (Hijazi et al., 2014; Kishor et al., 2015). Indeed, proline hydroxylation is the preceding step to *O*-glycosylation of extensins and arabinogalactans (Showalter and Basu, 2016). Overall, proline hydroxylase activity, promoted by ascorbate, is essential for cell wall assembly and stiffening. Conversely, ascorbate has been implicated in fruit softening through non-enzymatic mechanisms, mainly by solubilizing pectins due to •OH radicals arising as a result of the Fenton reaction in the apoplast (Dumville and Fry, 2003). Because the architecture of pectins in the seed coat is important in interactions with other cell wall polymers (Turbant et al., 2016), this ascorbate-driven decrease in pectins might lead to seed abortion. These seemingly opposite effects of ascorbate in the cell wall can be explained by a fine-tuned regulation of the ascorbate content and its compartmentalization, aspects that are still poorly understood.

Regulation of ascorbate content

As an essential antioxidant, regulation of the ascorbate content is closely related with abiotic stresses that normally cause oxidative stress. High light in particular is translated into a ROS burst caused by an increased photoreduction and photorespiration. This, in turn, leads to increased ascorbate biosynthesis in order to detoxify these ROS (Asada, 1999). Low light, in contrast, causes a reduction of ascorbate. For example, *Arabidopsis* plants grown in continuous dark for two days only contained 20% of ascorbate relative to plants grown in light (Conklin et al., 2013).

Regulatory mechanisms that control ascorbate biosynthesis have been found at the level of transcription, translation, protein stability and activity for

different components of the SW pathway. Light modulation of ascorbate content involves GMP stability (Wang et al., 2013), since GMP protein is degraded in the dark by the CONSTITUTIVE PHOTOMORPHOGENIC9-Signalosome subunit 5B (CSN5B; Wang et al., 2013). At the transcriptional level, low light decreases the expression of *GGP*, whereas high light causes its induction (Dowdle et al., 2007). Similarly, high light also induces the expression of *GLDH* in melon (Pateraki et al., 2004). NO treatment, which induces oxidative stress, causes an increase of *GLDH* mRNA levels in pepper (Rodríguez-Ruiz et al., 2017). At the activity level, *Arabidopsis* and barley plants exposed to high light showed an increment of GGP and GLDH activity (Dowdle et al., 2007; Smirnoff, 2000). A redox regulation has also been reported for the activities of L-GalDH in kiwifruit (William A Laing et al., 2004), GME (Wolucka and Van Montagu, 2003) and GLDH (Leferink et al., 2009) in Arabidopsis. For GLDH in particular, Cys-340 has been identified as a redox-sensitive thiol residue required for an optimal conversion of L-galactono-1,4-lactone into ascorbate. This residue can be irreversibly oxidized by H_2O_2 unless it is previously S-glutathionylated (Leferink et al., 2009). This oxidation might be involved in the programmed cell death induced by some stresses like heat, since GLDH activity decreases during early stages of programmed cell death resulting in the inhibition of ascorbate biosynthesis (de Pinto et al., 2015). Therefore, the increased conversion of L-galactono-1,4-lactone to ascorbate under oxidative stress or high light might be an important control point of ascorbate biosynthesis (Smirnoff, 2000).

Probably, the best described regulatory control point of ascorbate biosynthesis is exerted by GGP (Laing et al., 2015). This study reports that the amount of GPP protein in Arabidopsis is controlled by a cis-acting upstream Open Reading Frame (uORF). Thus, at high ascorbate concentration there is a decrease of the translation of *GGP* mRNA, functioning as a negative feedback loop (Laing et al., 2015). More importantly, since this uORF has been identified in *GGP* genes from mosses to angiosperms, this ascorbate posttranslational regulation is likely conserved throughout many plant species. Another possible control point exerted by ascorbate is L-GalDH, since the activity of this enzyme purified from spinach leaves is inhibited by ascorbate (Mieda et al., 2004). However, this is now under debate based on activity studies of the purified L-GalDH from kiwifruit (William A Laing et al., 2004). The role of GLDH in ascorbate biosynthesis has also been studied during fruit development of tomato and pea. GLDH activity is inhibited by high ascorbate levels (Mellidou et al., 2012b; Pallanca and Smirnoff, 2000), a feedback control also found to affect GME activity in Arabidopsis (Wolucka and Van Montagu, 2003). Another link related with stress came with the finding that the activity of PMM is enhanced by a Ca^{2+}-dependent interaction with Calmodulin-Like 10 (CML10; Cho et al., 2016), of which the expression is boosted by H_2O_2 and biotic stress (Zimmermann et al., 2004). Accordingly, *Arabidopsis* transgenic lines expressing an artificial microRNA against CML10 fail to increase ascorbate levels under heat stress (Cho et al., 2016).

Other genes involved in the regulation of ascorbate levels are *AMR1* (Zhang et al., 2009) and *ERF98* (Zhang et al., 2012). AMR1 encodes an F-Box protein that represses the expression of virtually all the SW genes, particularly the expression of *GME* and *GGP*. Interestingly, this negative regulator of the pathway is barely expressed under high light conditions, pointing out the importance of the *de novo* biosynthesis of ascorbate in the response to light (Zhang et al. 2009). In contrast, *ERF98* is a positive regulator of the pathway since overexpression of this gene increase the content of ascorbate by enhancing the expression of genes of the SW pathway, in particular *GMP*, *GGP* and *L-GalDH*. Further analysis indicated that ERF98 can directly bind the promoter of the *GMP* gene (Zhang et al., 2012), supporting its regulatory role of the SW pathway.

An important aspect concerning ascorbate regulation is how it is distributed at the subcellular level. Cytohistochemical analysis, based on immunogold labelling and high-resolution immuno electron microscopy in tobacco and Arabidopsis leaves have shown that ascorbate is unevenly distributed at the subcellular levels (Zechmann et al., 2011). The estimated concentrations of ascorbate in Arabidopsis are: mitochondria (10.4 mM), chloroplasts (10.8 mM), peroxisomes (22.8 mM), nuclei (16.3 mM), vacuole (2.3 mM) and cytosol (21.7 mM) (Zechmann et al., 2011). In addition, low concentrations of ascorbate (0.002 mM) and DHA (0.36 mM) have been reported in the apoplast (Booker et al., 2012). These concentrations vary when plants are exposed to high light, which translates into an increase of ascorbate content in most cell compartments (Zechmann, 2011; Zechmann et al., 2011) with the exception of peroxisomes, whose content diminishes under high light. Interestingly, vacuolar ascorbate increases 4-fold when plants are exposed high light. This might be necessary to reduce the phenoxyl radicals that are oxidized by the high light associated-increase of H_2O_2 (Takahama, 2004). However, it is unknown whether the increase in ascorbate content in vacuole is due to the reduction of vacuolar MDHA through trans-membrane ascorbate-mediated electron transporters like cytochrome b561 (Asard et al., 2013; Griesen et al., 2004) or by direct transport of cytosolic ascorbate into the vacuole under high light using a transporter not identified yet.

Interestingly, despite the low concentration of ascorbate, the apoplast ratio of ascorbate/DHA ascorbate is important to determine the redox state of this compartment, which in turn controls redox-dependent signalling processes (Waszczak et al., 2018), such as stomata closure (Chen and Gallie, 2004) and chloroplast reprogramming leading to light acclimation (Karpinska et al., 2018). All these processes would be compromised if DHA and MDHA were not reduced back into ascorbate. Considering the little amount in the apoplast of glutathione and the enzymes in the Halliwell-Asada cycle other mechanisms must keep the redox homeostasis or the apoplast. First, apoplastic DHA produced by the spontaneous oxidation of MDHA enters the cytosol in exchange with ascorbate through facilitated diffusion using a yet-unknown protein (Horemans et al., 1998,

1997, 1996). Once in the cytosol, DHA is reduced to ascorbate by DHAR through the glutathione cycle. Second, MDHA is reduced to ascorbate in the apoplast by a cytochrome b-mediated trans-plasma membrane electron transport that uses cytosolic ascorbate as an electron donor (Horemans et al., 2000, 1994), which resembles the ascorbate restoration by electron transport across the tonoplast membrane (Asard et al., 2013), thus suggesting the involvement of cytochrome b561 in the reduction of apoplastic MDHA.

A similar question remains concerning MDHA and DHA reduction back to ascorbate in the thylakoid lumen. Taking into account the importance of luminal ascorbate in the maintenance of the functionality of the photosynthetic apparatus and energy dissipation (NPQ) commented above, MDHA and DHA must be reduced back to ascorbate. Since, to the best of our knowledge, there are no DHA reductases (DHAR) nor MDHA reductases (MDHAR) in the thylakoid lumen, other mechanisms should be involved. It has been shown that luminal DHA, produced by MDHA disproportionation in the lumen, crosses the thylakoidal membrane to the stroma (Mano et al., 1997), where it is reduced by the Halliwel-Asada cycle (Asada, 1999). The mechanism by which DHA crosses the thylakoidal membrane is not clear. Since no DHA transporter has been yet described in thylakoids (Foyer and Lelandais, 1996; Foyer and Noctor, 2011), the difference in DHA concentration between stroma and thylakoid lumen, and the lack of charge, would favour a high diffusion rate towards the stroma. On the other hand, ascorbate (newly synthetized and recycled from DHA) has to enter the lumen of the thylakoid. The diffusion hypothesis might also apply if the concentration of ascorbate in the stroma is much higher than that in the lumen, consistent with a non-active transport of ascorbate into the lumen previously reported (Foyer and Lelandais, 1996). However, unlike DHA, ascorbate has a negative charge making it a less suitable molecule to diffuse across the thylakoid membrane (Horemans et al., 2000). It has been recently reported that AtPHT4;4 transports ascorbate from the chloroplastic intermembrane space into the stroma (Miyaji et al., 2015). Interestingly, the homologous AtPHT4;1 is localised in the thylakoid membrane (Pavón et al., 2008) and its expression is modulated by light (Guo et al., 2008; Miyaji et al., 2015). Therefore, AtPHT4;1 is a good candidate to transport ascorbate across the thylakoid membrane.

Approaches to increase ascorbate in fruits

Increasing ascorbate content in highly consumed fruits would clearly have an impact on human nutrition. A concomitant increase of ascorbate in tissues or organs that are submitted to oxidative stress, i.e. photosynthetic tissues, might have an additional beneficial effect on plant tolerance. However, whether or not ascorbate increases in fruit would have an effect on stress tolerance is not so clear, although is proposed that during fruit development and ripening oxidative stress might occur (Brennan and Frenkel, 1977; Huan et al., 2016; Jimenez et

al., 2002; Rogiers et al., 1998). Most of the attempts used to increase ascorbate levels are based on biotechnology and basically consist in the overexpression of genes involved in different aspects of ascorbate metabolism (biosynthesis, recycling or regulation). A second approach to increase the content of ascorbate would be through the selection of specific genomic regions that determine high ascorbate from a donor cultivar (or related species) and introgression into the cultivar of interest using molecular-assisted breeding (Singh and Singh, 2015). While in the first approach it is possible to use genes from different species and promoters that drive high or specific expression is desired tissues (Amaya et al., 2015), as far as the target species is amenable of transformation, the second approach relies in the identification of natural variants that can be used to inter-cross with these lines of interest. Although to date there are limited reports using this approach, the clear advantage is that these lines can be directly put into production because it does not involve transgenesis and therefore are not subjected to GMO regulation (Huang et al., 2016).

Biotechnological Approaches

There are abundant reports in the literature showing an increase of ascorbate in plants using biotechnological approaches (Macknight et al., 2017; Mellidou and Kanellis, 2017; Valpuesta and Botella, 2004). However, most of the studies have been performed in plants that do not produce edible fruits such as Arabidopsis, tobacco or rice and thus, most of the analyses were focused on vegetative tissues. Within fruits, tomato has been the preferred model due to its adoption as a model of fleshy fruits, its commercial value and the availability of efficient transformation protocols. The highest increase of ascorbate in tomato fruits reported so far has been about 6-fold and was achieved by ectopically expressing *GGP* from kiwi (Bulley et al., 2012). Interestingly, the transgenic tomato lines with the highest increase of ascorbate showed fruits with developmental defects and did not produce seeds (Bulley et al., 2012). A possible explanation is that an increase of metabolic flux to the synthesis of ascorbate had the effect of draining metabolites that are required for cell wall biosynthesis, particularly during seed development. Alternatively, this sharp increase of ascorbate might cause an increase in pectin solubilization (Dumville and Fry, 2003), which might provoke defects in seed development. Interestingly, in the same study, overexpression of *GGP* also caused an increase in ascorbate content of approximately two-fold in strawberry without obvious defects during seed formation. There can be several explanations for these differences in fruit development, first the ascorbate increase in strawberry fruit is smaller, thus not being enough to solubilize pectins, second strawberry is a false fruit with the real fruits (the achenes) located outside the fleshy part, and third the composition of the cell wall surrounding the fruits might be different in terms of pectin composition.

Genes involved in ascorbate biosynthesis from alternative pathways have also been used to increase ascorbate content in tomato fruit. Three different studies in tomato have been published expressing the *D-Galaturonate Reductase* (*GalUR*) gene from strawberry (Agius et al., 2003). In two reports, overexpression of *GalUR* caused an increase between 2 and 2.5-fold, which resulted in enhanced tolerance to various abiotic stresses (Cai et al., 2015; M. Y. Lim et al., 2016). In the third study, *GalUR* is driven by the constitutive 35S promoter or the tomato fruit-specific *polygalacturonase* (*PG*) promoters (Amaya et al., 2015). In both cases, transgenic lines showed a modest (1.3-fold) increase of ascorbate content. However, a comprehensive metabolomic analysis indicated complex changes in metabolites as well as concomitant increase of total antioxidant capacity in transgenic tomato fruits, suggesting that the increase of ascorbate is associated with a tight regulation of the cellular redox state of fruits.

Other approaches have employed genes involved in ascorbate recycling or transcription factors involved in the regulation of genes of the SW pathway. Overexpression of the cytosolic *DHAR1* gene from potato increased the ascorbate content by 1.9-fold in transgenic tomato fruits (Li et al., 2012). Two additional reports using regulatory factors also show a modest increase of ascorbate in fruits. Identification and overexpression of SlHZ24, a transcription factor that binds the promoter of the tomato *SlGMP3* gene (Hu et al., 2016), caused a 1.6-fold increase of total ascorbate in tomato fruits at the breaker stage. Further analysis indicated that SlHZ24 also can bind *in vitro* *SlGME2* and *SlGGP* promoters, suggesting that this transcription factor can target multiple genes involved in ascorbate biosynthesis. The tomato *SlDof22* negatively regulates ascorbate accumulation in tomato, and reduction of the endogenous expression of this gene by RNAi increased the levels of ascorbate 1.3-1.6-fold in mature fruits. Transcriptomic analysis indicated that the *SlDof22* silenced lines had increased expression of several genes involved in the SW pathway and recycling of ascorbate (Cai et al., 2016). Further, the authors showed that *SlDof22* can bind the promoter of the tomato *SOS1*, a Na^+/H^+ antiporter involved in Na^+ homeostasis and essential for salt tolerance (Zhu, 2002). However, how the *SOS* pathway and the ascorbate biosynthetic pathway are connected remains elusive.

From a breeding perspective, the increases of ascorbate between 1,5 and 2-fold using biotechnological approaches in tomato here reported might not seem outstanding (Amaya et al., 2015; Cai et al., 2015; M. Y. Lim et al., 2016). However, considering the large consumption of tomato, its relatively low ascorbate and its high raw intake, we believe that the reported increments would have a positive impact from a nutritional point of view, more so considering the recent reports on the health beneficial effects of a rich ascorbate diet. The 6-fold ascorbate increase reported by Bulley and co-workers (Bulley et al., 2012) would have a tremendous impact on ascorbate intake. Although the reported developmental defects make it unviable for agricultural use, from a scientific perspective it might be a useful model to investigate the role that high ascorbate has in tomato physiology.

Molecular Breeding and Genome Selection for ascorbate improvement

Improving fruit ascorbate content using marker-assisted selection requires prior identification of the genetic basis for natural variation of ascorbate. This can be achieved by genetic mapping and quantitative trait loci (QTL) analysis or genome-wide association studies (GWAS) in a developed mapping population, or alternatively in a diverse set of genotypes within the species, that are genotyped and phenotyped to determine molecular markers associated to specific traits (Mackay et al., 2009; Singh and Singh, 2015). Next, identified markers need to be validated for their application to select new cultivars with increased ascorbate content.

Several studies have shown that ascorbate content in fruits exhibit a quantitative inheritance, with several loci involved in ascorbate variation (Stevens et al., 2007; Zorrilla-Fontanesi et al., 2011). These studies have rarely identified the genes controlling the variation in ascorbate content, but they mark the genomic regions, and associated markers, and provide relevant information about the genetic architecture of the trait (how many loci and their quantitative contribution), as well as environmental effects. In some studies, candidate genes in those regions have been identified, with examples described below in apple, strawberry and tomato.

Apple

In this species (*Malus domestica*), a population derived from the cultivars 'Telamon' and 'Braeburn' was used to identify several QTLs for ascorbate content in fruit skin and flesh on linkage groups (LG) 6, 10, and 11 in the apple genome (Davey et al., 2006). The QTL identified on LG10 collocates with a major QTL controlling flesh browning (Sun et al., 2014). Four regions on LG 10, 11, 16 and 17 controlling ascorbate were detected over different years in another study using the same population (Mellidou et al., 2012a). Collocations between *GGP*, *DHAR* and a nucleobase-ascorbate transporter and some of the QTL were identified. In the case of *GGP,* allelic variations in two different *GGP* genes (*MdGGP1* and *MdGGP3*) were associated with ascorbate content (QTL on LG 11 and LG 10) both in the population and across commercial apple cultivars (Mellidou et al., 2012a). In particular, differences in the expression of *MdGGP1* between fruits from high- and low-ascorbate cultivars indicate a key role for *MdGGP1* in the regulation of fruit ascorbate content (Mellidou et al., 2012a). An allele-specific SNP in this gene represents a promising tool for molecular breeding for enhanced fruit ascorbate content in apple. In the same study, the gene *MdDHAR3-3* was associated with a stable QTL for flesh browning on LG 17, suggesting that regulation of redox status of the ascorbate pool via DHAR is important for postharvest fruit quality traits in apple. In agreement with this, transcriptomic studies revealed that prolonged postharvest storage downregulated *DHAR* expression, resulting in the oxidation of ascorbate and thus enabling browning to occur (Mellidou et al., 2014). Therefore, besides the nutritional relevance of

increasing ascorbate content in fruits, it has been shown that increased ascorbate is associated with improved post-harvest quality in fruits such as pear and apple (Davey et al., 2006; Mellidou et al., 2012a). For example, increased flesh browning in apple fruits is associated with the presence of a less reduced ascorbic acid pool (Davey et al., 2006).

Strawberry

Strawberry (*Fragaria* × *ananassa*) is the fruit with the highest global production among berries, reaching a value of over nine million tonnes (FAOSTAT[1]) and it typically contains high ascorbate. However, ascorbate content varies widely between strawberry cultivars and *Fragaria* species, ranging from 10 to 80 mg/100 g FW (Cruz-Rus et al., 2011; Mezzetti et al., 2016). Using a biparental population of 95 F1 progenies derived from two strawberry breeding lines, three QTL explaining a total of 45% variation were identified on LG IV-2, LG V-1 y LG VII-1 (Zorrilla-Fontanesi et al., 2011). Two of the detected QTLs were stable in different years and candidate genes were identified based in orthologous positions in the diploid *F. vesca* reference genome. The gene *FaGalUR* collocated with the position of the stable QTL on LG IV-2 and a gene encoding a myoinositol oxygenase (*FaMIOX*) was located within the stable QTL on LG V-1 (Zorrilla-Fontanesi et al., 2011), although the role of this pathway remains controversial.

FaDHAR and *FaGMP* collocated with the QTL detected only one year on LG VII-1. Recently, a transcriptomic analysis by RNA-seq in pools of progeny lines contrasting in ascorbate content derived from the same population identified differential expression of gene *MANNOSE-6-PHOSPHATE ISOMERASE 1* (*FaM6PI1*) while *FaMIOX* was not differentially expressed (Vallarino et al., 2019). The *FaM6PI1* gene was also located within the confidence interval of the major QTL detected on LG V-I, and it is highly similar to the Arabidopsis *PMI* gene that encodes the first enzyme in the SW pathway (Maruta et al., 2008). Therefore, gene *FaM6PI1* was proposed as a candidate gene contributing to the natural variation in ascorbate content in strawberry.

Tomato

Several loci controlling ascorbate content have been detected using different populations derived from crosses between cultivated varieties (*Solanum lycopersicum*) and related wild *Solanum* species. Common genomic regions controlling ascorbate content have been identified on chromosomes 2, 8, 9, 10, and 12 (Stevens et al., 2007). In general, wild alleles increased ascorbate content and QTL were relatively stable across years or environments. The tomato gene *GME2* lies within the QTL interval on chromosome 9 (bin 9-J) and other candidate genes localised within QTL intervals were *MDHAR3* in bin 9-D, *GMP2* in bin 9-E, and *GLDH* in bin 10-E (Stevens et al., 2007). Further studies confirmed that this MDHAR activity was linked to ascorbate content in tomato fruits, which was found beneficial for an extended shelf life after chilling (Stevens et al., 2007). The role

of MDHAR in governing ascorbate pool size was demonstrated through assessing expression and activity profiles throughout fruit ripening (Mellidou et al., 2012b). In an independent report, 163 tomato accessions were analysed for several traits including ascorbate content by a GWAS approach and, again, significant SNPs associated to *MDHAR* were identified (Sauvage et al., 2014). All together, these reports indicate a relevant role of MDHAR in governing natural variation in ascorbate content in tomato.

Using transcriptomic analysis, a QTL detected in three trials on introgression line IL12-4 (*S. pennellii* in a *S. lycopersicum* background) was associated with up-regulation of genes involved in pectin degradation (Di Matteo et al., 2010). Further analyses of mutant variants and expression studies in introgression sublines from IL12-4 supported that pectinesterases might have a crucial role in determining ascorbate content in fruits of IL12-4 (Ruggieri et al., 2015). These studies suggested that ascorbate accumulation in IL12-4 fruits was achieved by increasing flux through the D-galacturonate pathway, as indicated above.

Recombinant Inbred Lines (RIL) have also been used to identify QTL/candidate genes linked to ascorbate content in tomato fruits. Thus, transcriptomic analyses in fruits of two groups of contrasting RILs suggested that ascorbate content co-regulates with genes involved in hormone signalling, and that they are dependent on the oxidative status of the fruit (Lima-Silva et al., 2012). Another study in tomato using the same RIL population, derived from the wild-relative *Solanum pimpinellifolium* TO-937, detected four QTL with a joint contribution of 42.1% to the variation of ascorbate content (Capel et al., 2015).

Melon

A limited number of genetic studies on ascorbate have been conducted in melon, although this fruit serves a significant source of this vitamin. There is considerable variation within the species. Ascorbate content in different varieties of the most widely consumed Cantaloupe and Honeydew melons range from about 10 to 29 mg/100 g FW, with the former types having higher content than the latter (Laur and Tian, 2011). This crop has a high global production (~31 million tonnes; FAOSTAT) and it is also amongst the highest productions in the European Union (~3 million tonnes; Eurostat, 2017). A single QTL for ascorbate has been mapped on LG 5 using different populations (Park et al., 2009; Sinclair et al., 2006). However, low reproducible RAPD markers were used in these studies, hampering their application in breeding programs.

Overall, the number of studies identifying QTLs affecting fruit ascorbate content is still rather limited to draw conclusions on common loci across different species. In order to effectively introduce QTLs using marker-assisted selection in order to develop new fruit varieties with increased ascorbate content, loci must be validated in independent studies. Also, it is important to use additional populations and to perform the QTL analysis in different locations in order to determine QTL stability. To date, only natural variation in *GGP* and *MDHAR* alleles have been shown in independent studies to be useful in increasing ascorbate in apple and tomato, respectively (Mellidou et al., 2012a; Stevens et al., 2008). Pyramiding QTLs has the potential to increase ascorbate content, particularly in those cases when an individual QTL has a limited effect. There are already reports in which *Solanum lycopersicum* lines containing two chromosomal fragments from *Solanum pennellii* double the ascorbate content in ripe tomato fruit (Rigano et al., 2014; Sacco et al., 2013). Furthermore, with the recent establishment of high-throughput genotyping platforms, the selection of lines that include only specific genomic regions of interest will now be performed in a very efficient manner (Crossa et al., 2017).

Conclusions and future perspectives

The importance of ascorbate for humans has been recently highlighted through the characterization of its role in the activity of TETs and histone demethylases. Therefore, it is important to understand the mechanisms that determine the levels of ascorbate in fruits, a major source for ascorbate in human diet. An essential role for ascorbate in plants and animals is to maintain the oxidative status in the active centre of several enzymes. It is also essential for scavenging ROS produced during photosynthesis. The identification of *vtc* mutants clearly highlighted an essential role of ascorbate in oxidative stress tolerance (Conklin et al., 1996). Ascorbate has additional roles during plant growth since early reports indicated that external application of ascorbate caused a significant increase in seedling growth and effects on cell division (Hausen, 1935; Havas, 1935), although the molecular mechanisms are not completely understood.

Most of the molecular studies have been performed in the model plant *Arabidopsis thaliana*, allowing the identification of all the catalytic steps of the SW pathway. However, with the exception of the established role of GGP as a key biosynthetic control step, very little is known about the factors that determine the final content of ascorbate in different tissues.

In fruits from different species or even within the same species large differences can be observed, with fruits that show extremely high content of ascorbate such as camu (Castro et al., 2015) and acerola (Badejo et al., 2009). How these fruits can accumulate such large amounts, or what is the advantage of having such a high content of ascorbate in these fruits is not known. As

previously indicated, an important aspect of ascorbate is the close interconnection between its biosynthesis and that of the non-cellulosic cell wall components, which might hamper a proper understanding of the regulation of ascorbate biosynthesis. Since degradation of the cell wall is a common process during fruit ripening, alternative pathways such as that using D-galacturonate may have an important role in the final accumulation of ascorbate in this organ. Considering all this, it is important to extend the research to ascorbate-rich fruits to identifying regulators that determine high-ascorbate accumulation. An advantage is that the high conservation of proteins of the SW pathway among plant species makes it relatively easy to identify the orthologous genes. With the current genomic tools and high throughput sequencing technology, GWAS could be a good approach to identify these components. The use of segregating populations using contrasting parental lines can also be a good choice, considering the expedition of gene identification through combination of bulk segregant analysis (BSA), high-throughput next-generation sequencing, efficient SNP arrays, mapping by sequencing approaches (Takagi et al., 2013), or global gene expression studies (Amaya et al., 2016).

The CRISPR/Cas9 technology has greatly improved our capacity to engineer targeted mutations in eukaryotic genomes (Doudna and Charpentier, 2014). In tomato, CRISPR/Cas9 has been recently used to modify quantitative trait variation in some key agronomical traits such as fruit size, inflorescence number and plant size in tomato (Rodríguez-Leal et al. 2017). In a recent report, genome editing of the uORF of *GGP* in lettuce increased the ascorbate content by 1.5-fold, leading to oxidative stress tolerance (H. Zhang et al., 2018). A similar edition of tomato *GGP1* also led to an ascorbate increase of ~1.5-fold in leaves (Li et al., 2018). Thus, a future trend will be to use genome editing to target gene determinants in either the cis-regulatory elements to modify their gene expression, substrate affinity, catalytic efficiency, generation of specific alleles or targeting interacting partners to modulate the ascorbate content in fruits. All this will be further facilitated by increasing sequence replacements via homologous recombination as has been already reported in Arabidopsis through CRISPR/Cas9 (Miki et al., 2018).

HYPOTHESIS & OBJECTIVES

Hypothesis

Most of the enzymes that catalyse the biosynthesis of ascorbate through the Smirnoff-Wheeler pathway are predicted to be localized in the cytosol. It is becoming clear that enzymes in different metabolic pathway tend to form metabolons in order to improve the efficiency. In this thesis we investigated whether enzymes that catalyse ascorbate biosynthesis through the Smirnoff-Wheeler pathway associate forming an enzymatic complex, hence facilitating its biosynthesis. Ascorbate content is also regulated by environmental conditions. Furthermore, several metabolic pathways are regulated by a limiting catalytic step. Thus, ascorbate biosynthesis might also be controlled by a limiting catalytic step whose activity is an integrated response to endogenous (inner ascorbate level) and exogenous (light intensity, time of the day) cues. Our working hypothesis is that the regulation of its stability must be finely tuned to balance the biosynthesis rate to meet the cell requirements. Moreover, the identification of regulators of this limiting step and those controlling the formation of this functional unity of enzymes could lead to a marker-assisted breeding programme or biotechnological strategy to engineering ascorbate biosynthesis in crop plants of interest without compromising fruit development or fertility. Therefore, in order to answer the previous questions, we defined the following objectives.

Objectives

1. To investigate whether the ascorbate biosynthesis enzymes associate *in vivo*.
2. Identifying the ascorbate biosynthesis limiting activities.
3. To study the protein dynamics of ascorbate biosynthesis enzymes with a special focus on VTC2, the enzyme proposed to catalyse the limiting step of the ascorbate biosynthesis pathway.

CHAPTER 1

A brief introduction

L-Ascorbate (ascorbate, vitamin C) is the most abundant soluble antioxidant in plants and functions as a cofactor in many enzymatic reactions (Fenech et al., 2019; Smirnoff, 2018). Some groups of animals, among which humans are included, lost the ability to biosynthesize ascorbate (Smirnoff, 2018).

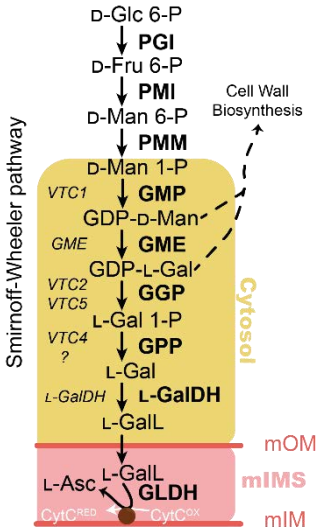

Figure 4. The ascorbate biosynthesis via GDP-mannose and L-galactose (the Smirnoff-Wheeler [SW] pathway) in Arabidopsis thaliana. Yellow area refers to the cytosolic enzymes used in this work. mOM: mitochondrion outer membrane, mIMS: mitochondrion intermembrane space, mIM: mitochondrion inner membrane. In the left-hand side of the arrows, the genes encoding each enzyme are displayed while in the right-hand side the encoded proteins/enzymatic activities are shown. Glc: glucose, Fru: fructose, Man: mannose, Gal: galactose, GalL: galactono-1,4-lactone, Asc: ascorbic acid. PGI: phosphoglucose isomerase, PMI: phosphomannose isomerase, PMM: phosphomannomutase, GMP: GDP-mannose pyrophosphorylase, GME. GDP-mannose 3',5' epimerase, GGP: GDP-L-galactose phosphorylase, GPP: L-galactose 1-phosphate phosphatase, L-GalDH: L-galactose dehydrogenase, GLDH: L-galactono-1,4-lactone dehydrogenase. $CytC^{RED}$: cytochrome c reduced, $CytC^{OX}$: cytochrome c oxidized.

Therefore, we need to incorporate this essential nutrient through the diet, with fruits and vegetables being the major source. In plants, ascorbate is synthesized from the hexose phosphate pool *via* D-mannose/L-galactose through the Smirnoff-Wheeler (SW) pathway (Wheeler et al., 1998; Figure 4). The pathway is supported by abundant biochemical and genetic studies (Bulley and Laing, 2016; Wheeler et al., 2015). D-Glucose 6-P is sequentially transformed into D-fructose 6-P, D-mannose 6-P and D-mannose 1-P by phosphoglucose isomerase (PGI), phosphomannose isomerase (PMI) and phosphomannomutase (PMM). GDP-D-mannose pyrophosphorylase (VTC1; GMP) then converts D-mannose 1-P into GDP-D-mannose, which is subsequentially epimerized by GDP-D-mannose epimerase (GME) into GDP-L-galactose. GDP-D-mannose and GDP-L-galactose are additionally used in synthesis of cell wall polysaccharides and protein glycosylation thereby interconnecting the SW pathway with cell wall biosynthesis (Conklin et al., 1999; Fenech et al., 2019; Reiter and Vanzin, 2001). The next step is catalysed by GDP-L-galactose phosphorylase (GGP), producing L-galactose 1-P. This step is proposed to be the main control point of the pathway (Dowdle et al., 2007; Laing et al., 2015, 2007; Linster et al., 2007; Yoshimura et al., 2014). In *Arabidopsis thaliana* (Arabidopsis), GGP activity is encoded by two paralogues, *VTC2* and *VTC5*. Next, L-galactose 1-phosphate phosphatase (VTC4, GPP) and other unidentified phosphatases (Conklin et al., 2006; Torabinejad et al., 2009), transform L-galactose 1-phosphate into L-galactose. L-Galactose is then oxidized to L-galactono-1,4-lactone by a L-galactose dehydrogenase (L-GalDH). All these steps are believed to occur in the cytosol while L-galactono-1,4-lactone crosses the outer membrane of the mitochondria

to be oxidized by L-galactono-1,4-lactone dehydrogenase (GLDH) which is an integral component of mitochondrial electron transport Complex 1 on the inner membrane (Pineau et al., 2008; Schimmeyer et al., 2016).

Ascorbate concentration is dependent on the tissue (Franceschi and Tarlyn, 2002; Lorence et al., 2004; Müller-Moulé, 2008; Zhang et al., 2011) and the ascorbate pool adjusts to changes in environmental conditions, particularly light (Bartoli, 2006; Page et al., 2012; Plumb et al., 2018). Surprisingly, despite being the most abundant soluble antioxidant, a good understanding of the mechanisms that control ascorbate concentration remains limited. While mutant analyses of genes involved in biosynthetic pathway have corroborated the involvement of the various enzymes (Table 1), they provide little information on how the pathway is controlled. This is further complicated because the ascorbate pool is determined by the balance between synthesis, oxidation, recycling and breakdown. The oxidation product of ascorbate is the monodehydroascorbate radical. This is either directly reduced back to ascorbate or can give rise to dehydroascorbate (DHA) in its hydrated bicyclic hemiketal form, which is reduced back to ascorbate through the Halliwell-Foyer-Asada cycle (Asada, 1999). In addition, a proportion of ascorbate and DHA can be degraded to various products such as oxalate, threonate, and tartrate (Debolt et al., 2007; DeBolt et al., 2006; Dewhirst et al., 2017; Green and Fry, 2005; Pallanca and Smirnoff, 2000; Terai et al., 2020; Truffault et al., 2017). These recycling and breakdown reactions are evident under severe oxidative stress, which results in decreased cellular ascorbate (Terai et al., 2020; Waszczak et al., 2018).

Table 1. Phenotypes associated to Arabidopsis mutants affected in the genes involved in ascorbate biosynthesis available in the literature. Phenotype analyses show that VTC2 is the first enzyme fully dedicated to ascorbate synthesis since growth arrest occurring in the vtc2/vtc5 double mutant and downstream mutants is rescued by ascorbate supplementation. Although a reduced function (knock-down mutation) of genes upstream of GGP (*VTC2, VTC5*) also results in lower ascorbate concentration, the lethality occurring in knock-out mutants cannot be prevented by exogenous ascorbate supplementation.

Enzyme	Mutant	Allele	Phenotype	Reference
GMP	*cyt1-1*	Knock-out	Embryo lethal	Lukowitz et al., 2001
	vtc1-1	Knock-down	30% of WT ascorbate	Conklin et al., 1996, 2000.
GME	*gme-1*	Knock-out	Male gametophyte lethal. Growth defect, rescued by boron but not by ascorbate supplementation.	Qi et al., 2017
	gme-2	Knock-down	30% of WT ascorbate	
GGP	*vtc2-4*	Single knock-out	20% of WT ascorbate	Lim et al., 2016
	vtc5-2	Single knock-out	80% of WT ascorbate	Dowdle et al., 2007
	vtc2/vtc5	Double knock-out	Growth arrest, rescued by ascorbate supplementation	Dowdle et al., 2007; Lim et al., 2016
GPP	*vtc4-4*	Knock-out	65% of WT ascorbate	Torabinejad et al., 2009
L-GalDH	*lgaldh*	Not reported	30% of WT ascorbate in antisense suppression lines	Gatzek et al., 2002
L-GalLDH	*gldh*	Knock-out	Growth arrest, rescued by ascorbate supplementation	Pineau et al., 2008

Multiple lines of evidence point to VTC2 as the critical controlling step of ascorbate biosynthesis. The transcription of *VTC2* gene (Dowdle et al., 2007; Müller-Moulé, 2008; Urzica et al., 2012) and the activity of the encoded enzyme (Dowdle et al., 2007) are highly responsive to environmental factors. Furthermore, *VTC2* translation is subject to feedback repression *via* a conserved upstream open reading frame (uORF) in the 5'-UTR (Laing et al., 2015). As a consequence, removing the uORF results in increased ascorbate in Arabidopsis (Laing et al., 2015), tomato (Li et al., 2018) and lettuce (H. Zhang et al., 2018). In addition, *VTC2* is the only gene of the pathway whose overexpression consistently increases the ascorbate content (Bulley et al., 2012; Yoshimura et al., 2014) and QTL analysis shows that *GGP* paralogs located within regions of the genome associated to fruits containing high ascorbate content (Mellidou et al., 2012a). There have been reports where overexpression of other genes of the pathway such as *VTC1* or *GME* also increase ascorbate concentration in Arabidopsis (Zhou et al., 2012 [1.3-fold]; Li et al., 2016 [1.5-fold]), rice (Zhang et al., 2015 [1.4-fold]), tobacco (Wang et al., 2011 [2-4-fold]), tomato (Cronje et al., 2012 [1.7-fold]; Zhang et al., 2011 [1.4-fold]) and kiwifruit (Bulley et al., 2009 [1.2-fold]). However, overexpression of these genes does not always have an effect on ascorbate concentration (Sawake et al., 2015; Yoshimura et al., 2014). In addition, various studies have reported ascorbate feedback inhibition of the biosynthetic enzymes PMI (Maruta et al., 2008), GME (Wolucka and Van Montagu, 2003) and L-GalDH (Mieda et al., 2004). This feedback control is further supported by the decreased incorporation of labelled sugars into ascorbate *in vivo* after feeding ascorbate (Pallanca and Smirnoff, 2000; Wolucka and Van Montagu, 2003).

In order to increase our understanding of the organization of the ascorbate biosynthesis pathway, we have performed a systematic over-expression of single and multiple combinations of all the enzymes of the pathway from VTC1 downstream in *Nicotiana benthamiana.* This allowed the systematic investigation of their effects on the ascorbate pool and supported the formation of a multiprotein complex. In addition, complementation of the Arabidopsis mutants with the respective GFP-tagged enzymes confirmed the functionality of the constructs and provided information on their subcellular localisations. Finally, we constructed a kinetic model based on the known properties of the pathway whose predictions support that activity of VTC2 is the only significant controlling step and which also explains other observed features of the pathway. In addition to this information, this work provides a set of tools that will allow a better understanding of ascorbate biosynthesis at the molecular and cellular level.

Results

Generation and analyses of GFP-tagged ascorbate biosynthesis enzymes in Arabidopsis complementation lines reveal major differences in protein expression along the pathway

In order to study the function of SW proteins we aimed to generate Arabidopsis lines transformed with genomic regions (including their promoters) of ascorbate biosynthesis genes that resulted in proteins fused to GFP at their C-terminus. To investigate the functionality of these constructs, they were introduced into Arabidopsis mutants and the complementation of their phenotypes was analysed. Arabidopsis mutants in SW genes typically show lower ascorbate concentration and/or lethality in early stages of development (Table 1). Selfing of Arabidopsis heterozygous mutants for *GME* (SALK_150208, *gme-3*, hereafter *gme*; Figure 5A) and *L-GalDH* (SALK_056664, Figure 5B) did not produce homozygous mutants (Figure 6). Since exogenous supplementation of ascorbate prevented growth arrest of several SW mutants (Dowdle et al., 2007; Pineau et al., 2008) we germinated seeds from heterozygous *gme* and *lgaldh* plants on solid media without and supplemented with 0.5 mM ascorbate (Figure 7A). As a control we included seeds from a heterozygous *gldh* mutant plant, whose growth arrest is prevented by exogenous ascorbate (Pineau et al., 2008). The analysis of heterozygous *gme* progeny identified 40 wild-type (WT) seedlings, 46 heterozygous seedlings and no homozygous for the T-DNA, confirming the lethality of a loss-of-function allele of *GME* (Qi et al., 2017; Voxeur et al., 2011) (Figure 6A; Figure 7A). Similarly, no homozygous *gme* seedlings were identified when the growth medium was supplemented with 0.5 mM ascorbate in contrast to *gldh* (Pineau et al., 2008; Figure 6B), confirming that GME, similarly to VTC1 (Lukowitz et al., 2001), has additional roles to that of ascorbate biosynthesis (Figure 6A; Gilbert et al., 2009; Qi et al., 2017; Voxeur et al., 2011). On the other hand, diagnostic PCR of heterozygous *lgaldh* progeny identified 23 WT seedlings and 69 heterozygous T-DNA seedlings while no homozygous mutants were found in the medium not supplemented with ascorbate. Remarkably, a number of seedlings showed growth arrest and yellowing similarly to *gldh* progeny (Figure 7A, magnified square). In contrast, we identified 25 WT, 41 heterozygous T-DNA and 25 homozygous T-DNA seedlings by diagnostic PCR in ascorbate containing medium (Figure 6C, Figure 7A). Therefore, and in contrast to *gme* mutants, *lgaldh* mutants could be rescued by supplementation with exogenous ascorbate. This supports that the expression product of *L-GalDH* is responsible for the L-galactose dehydrogenase activity present in Arabidopsis. Additionally, the finding that, like *gldh*, *lgaldh* is an ascorbate auxotroph also indicates that the activity of this enzyme is essential for ascorbate biosynthesis.

In order to investigate the functionality of a GME protein fused with a GFP at the C-terminus, we transformed WT plants with a *GMEp:GME-GFP* construct. Of the several transformants that showed high expression of GME-GFP and a single insertion (Figure 8A), line 6 (L6) was selected to introduce the transgene

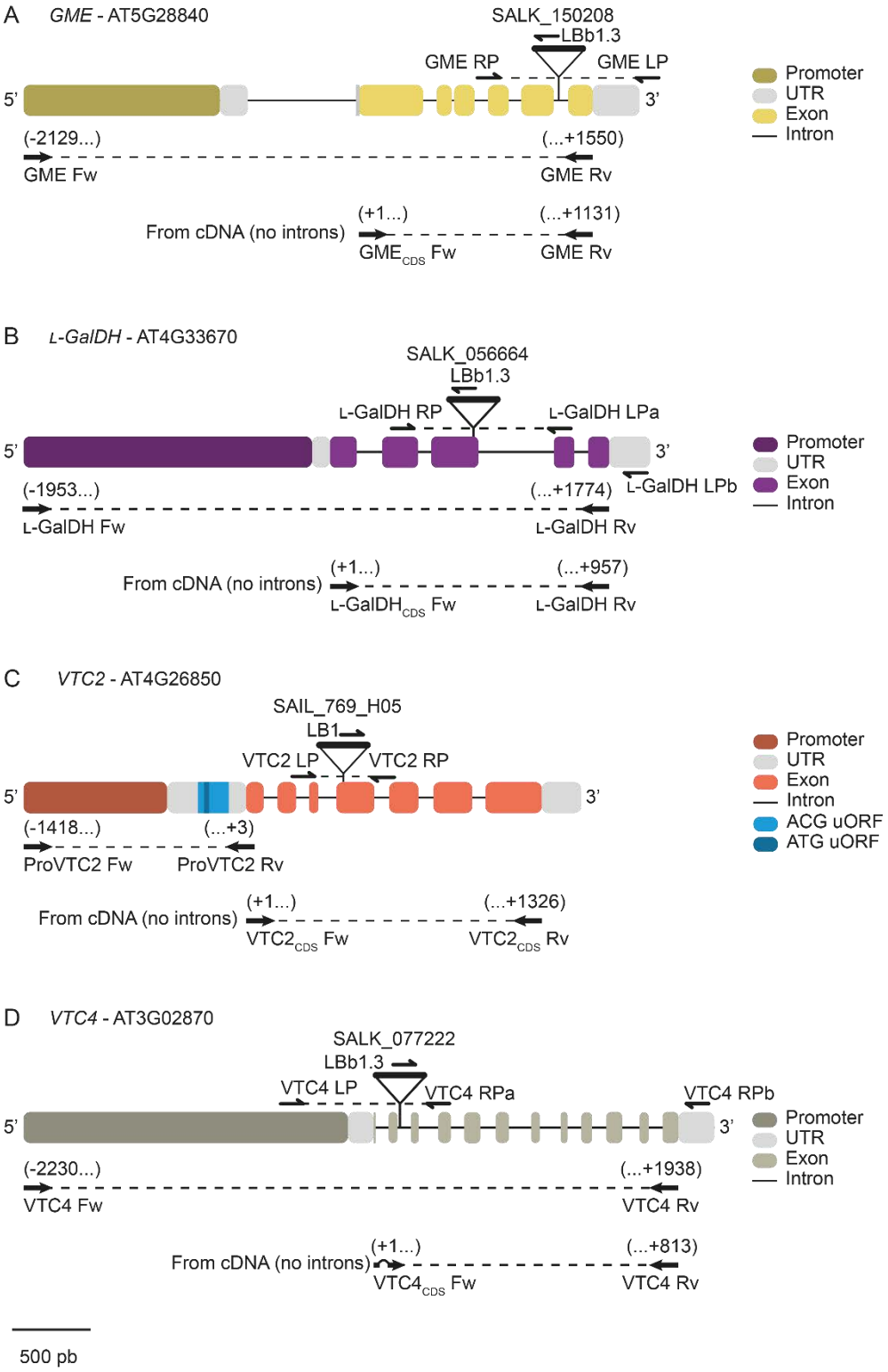

Figure 5. Gene structure, primers disposition and mutants' T-DNA location. Primers' sequences are available in Material and Methods section.

into the *gme* mutant background using reciprocal crosses. Using heterozygous *gme* plants as male parent, we did not obtain F1 *gme/GMEp:GME-GFP* (hereafter named *gme*/*GME-GFP* L6) descendants, supporting the role of *GME* in pollen development and pollen tube elongation (Qi et al., 2017). However,

when L6 was used as a male parent we obtained viable *gme/GME-GFP* F1 seedlings that allowed the identification in the F2 of homozygous *gme/GME-GFP* L6 seedlings (Figure 8B). Surprisingly, while the GME-GFP fusion protein complement the sterility defects, it contained ~55% of the ascorbate content of WT plants (Figure 7B) which, considering the lower ascorbate content of knock-down *gme* Arabidopsis mutants (Qi et al., 2017), indicates that it complements only partially the ascorbate content. Similarly, a *L-GalDHp:L-GalDH-GFP* construct was transformed into WT plants and selected line 1 (L1) that showed high expression and a single insertion (Figure 8C). Then, reciprocal crosses between heterozygous *lgaldh* plants and *L-GalDHp:L-GalDH-GFP* L1 were performed. In this occasion, we did obtain F1 plants when *lgaldh* plants were used as male or female parent. Homozygous *lgaldh/GalDH-GFP* L1 seedlings were identified in F2 progeny using diagnostic PCR in medium lacking ascorbate (Figure 8D), indicating that the L-GalDH-GFP protein driven by the *L-GalDH* promoter restores the enzyme activity lost in *lgaldh* mutant. In addition, ascorbate content of *lgaldh/L-GalDH-GFP* L1 plants contained WT levels of ascorbate (Figure 7B).

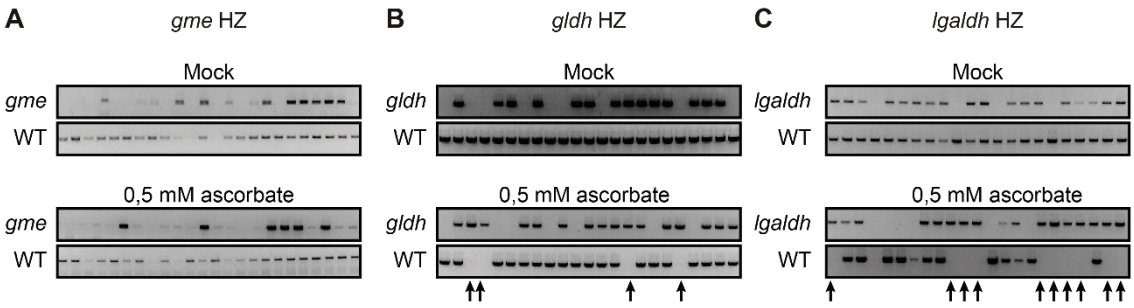

Figure 6. Diagnostic PCR of the *gme*, *gldh* and *lgaldh* seedlings analysed in the complementation assay. Whereas ascorbate does not recover the lethality of *gme* mutation (A), it does recover *lgaldh* (C). As a control, we used *gldh* (B), previously published to be recovered by ascorbate (Pineau et al., 2008). Arrows at the bottom indicate homozygous mutants.

In contrast to *gme* and *lgaldh*, loss of function *vtc2* and *vtc4* homozygous mutants are viable and show WT growth at standard conditions despite presenting a 20% and 55% of WT ascorbate content, respectively (Figure 7B; Conklin et al., 2000; Dowdle et al., 2007; Torabinejad et al., 2009). In the case of *vtc2* mutant, GDP-L-galactose phosphorylase activity is also provided by the paralogous *VTC5* gene. Consistently, *vtc2/vtc5* double mutants, like *lgaldh* and *gldh* mutants show growth arrest (Figure 7A) that can be complemented with exogenous ascorbate (Figure 6B, C; Dowdle et al., 2007; Lim et al., 2016). However, considering the phenotypes described (Table 1) the viability of *vtc4* must rely on other enzymes with L-galactose 1-phosphate phosphatase activity (Nourbakhsh et al., 2015; Torabinejad et al., 2009). In order to test the functionality of GFP-tagged VTC2 and VTC4, we relied on restoring WT ascorbate content by introducing *VTC2p:VTC2-GFP* and *VTC4p:VTC4-GFP* constructs into their respective mutants. T-DNA knock-out mutant *vtc2-4* (SAIL_769_H05; hereafter named *vtc2*; Figure 5C; Lim et al., 2016) was directly transformed and lines with single

insertion were selected (Figure 8E). Among these lines, line 13 (L13) was selected because it showed the highest accumulation of VTC2-GFP (Figure 8F). Also, *VTC4p:VTC4-GFP* was introduced into *vtc4-4* mutant (Figure 5D) following the same strategy described for *GME* and *L-GalDH* (Figure 8G). A single insertion *VTC4p: VTC4-GFP* line 5 was selected to cross with *vtc4* homozygous mutant and the homozygous *vtc4/VTC4-GFP* line was isolated by diagnostic PCR (Figure 8H). Ascorbate concentration of *vtc2/VTC2-GFP* and vtc4/VTC4-GFP lines was restored to WT levels validating the functionally of the GFP-tagged enzyme (Figure 7B).

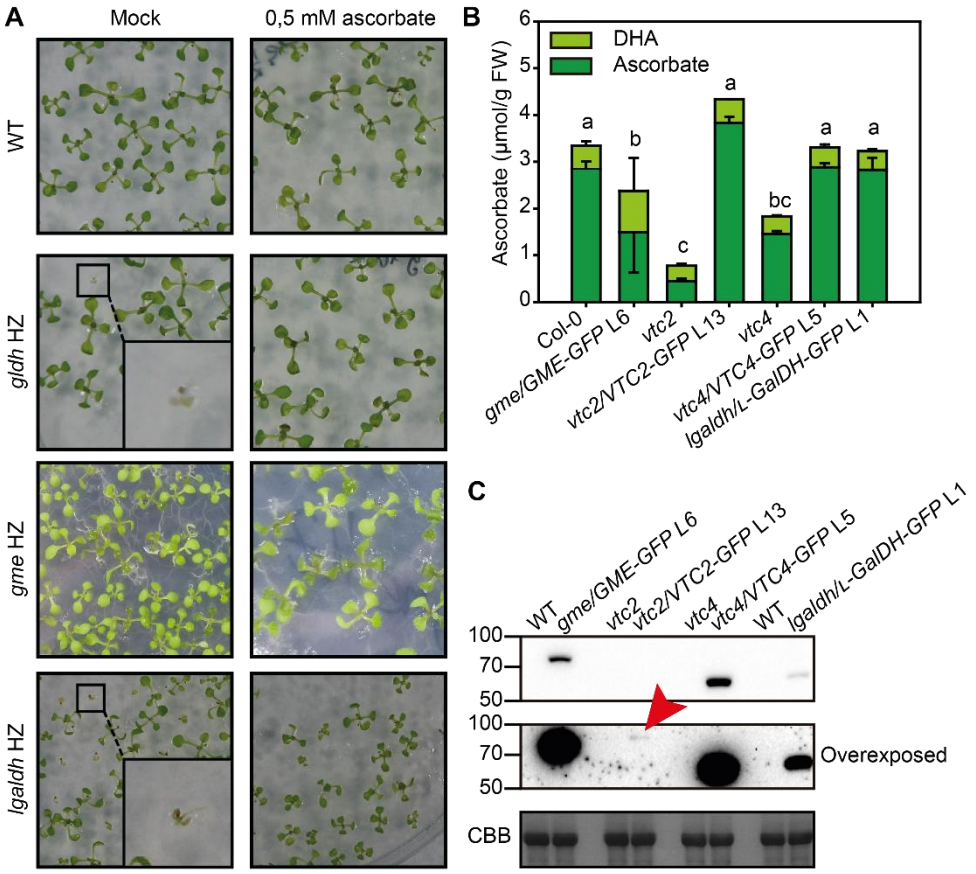

Figure 7. Characterization of C-terminal GFP fusions of ascorbate biosynthesis enzymes. A) Ascorbate complementation assay rescues growth arrest from *gldh* and *lgaldh* mutants but not *gme* lethality. In *gldh* and *lgaldh* mutants, small squares show that homozygous mutants undergo growth arrest in media lacking ascorbate, but not in media supplemented with ascorbate. B) Complementation of ascorbate concentration by expression of GFP fusion proteins in ascorbate deficient Arabidopsis mutants. Different letters denote statistically significant differences for ascorbate concentration (One-Way ANOVA, α=0,05, post-hoc Tukey test). Ascorbate was extracted from three independent samples composed of three 6-weeks old fully expanded rosettes grown in short day regime at 150 µmol photons m^{-2} s^{-1}, one and a half hours after lights turned on. C) Immunoblot (α-GFP) of complemented lines show that little amount of protein VTC2 compared other components restores ascorbate content. Red arrowhead indicates VTC2-GFP. A representative sample for each genotype is shown out of the three tested by immunoblot (not shown).

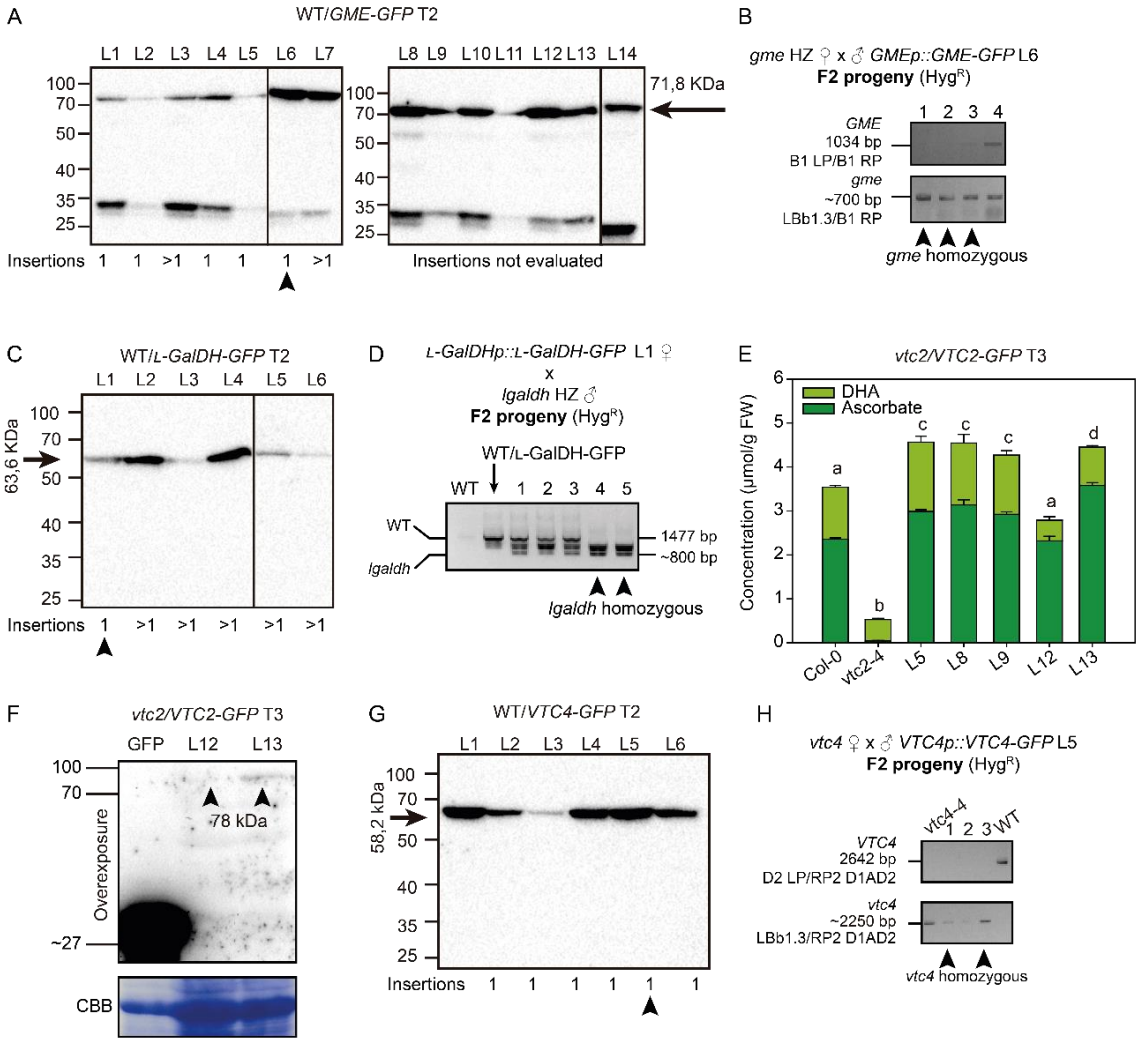

Figure 8. Generation of Arabidopsis transgenic lines containing ascorbate biosynthesis enzymes fused to GFP. A) Immunoblot (α-GFP) analysis of fourteen GME-GFP T2 lines identifies several lines expressing different amounts of GME-GFP protein (background WT). After the identification of lines harbouring single insertions (T2 Hyg^R:Hyg^S=3, χ^2 (α=0.05)), we selected line L6 (arrowhead) to introduce the *GMEp:GME-GFP* construct into the *gme* mutant (SALK_150208) background using reciprocal crosses. B) Diagnostic PCR of F2 generation from the cross indicated identified plants harbouring *GME-GFP* in homozygous mutant background (arrowheads). Ascorbate content of this line is shown in Figure 7B). C) Immunoblot (α-GFP) analysis of L-GalDH-GFP T2 generation showing the six lines expressing L-GalDH-GFP protein (background WT). After the identification of lines harbouring single insertions (T2 Hyg^R:Hyg^S=3, χ^2 (α=0.05)), we selected line L1 to introduce the *L-GalDHp:L-GalDH-GFP* construct into the *lgaldh* mutant (SALK_056664) background using reciprocal crosses. D) Diagnostic PCR of F2 generation from the cross indicated identified plants harbouring *L-GalDH-GFP* in homozygous mutant background (arrowheads). Ascorbate content of this line is showed in Figure 7B. E) Ascorbate content of the T3 generation of lines generated consisting of *vtc2* mutants harbouring *VTC2p:VTC2-GFP*. Three fully expanded leaves were collected on five-week-old T3 plants grown on soil in a growth chamber under short-day conditions (10 h light at 22°C/14 h dark at 19°C), at 60% humidity and 200 µmol m^{-2} s^{-1} light intensity. Different letters denote statistically significant differences for ascorbate content (One-Way ANOVA, α=0,05, post-hoc Tukey test). F) Immunoblot (α-GFP) analysis of VTC2-GFP of two lines containing ascorbate maximum and minimum values. Four days old seedlings were grown under long day conditions in solid half-strength MS agar plates. G) Immunoblot (α-GFP) analysis of VTC4-GFP T2 generation showing the six lines expressing VTC4-GFP protein (background WT). After the identification of lines harbouring single insertions (T2 Hyg^R:Hyg^S=3, χ^2 (α=0.05)), we selected line L5 to introduce the *VTC4p:VTC4-GFP* construct into the *vtc4* mutant (SALK_077222) background using reciprocal crosses. H) Diagnostic PCR of F2 generation from the cross indicated identified plants harbouring *VTC4-GFP* in homozygous mutant background (arrowheads). Ascorbate content of this line is showed in Figure 7B.

We analysed the protein levels of the different lines generated in a single blot in order to compare the amount of proteins accumulated in each line. Immunoblot analysis indicated that GME-GFP and VTC4-GFP were easily detectable while L-GalDH-GFP showed reduced levels of proteins (Figure 7C). Interestingly, despite the complementation of ascorbate levels in L13, VTC2-GFP protein was not detected (Figure 7C, upper panel) and was detected only after overexposure of the blot using a high sensitivity ECL substrate for the detection of femtogram amounts of protein. This low amount of VTC2 protein cannot be explained by a low expression of *VTC2* at the transcriptomic level because, based on public available transcriptomic databases, *VTC2* and *GME* show the highest expression of all SW genes in vegetative tissue (Figure 9).

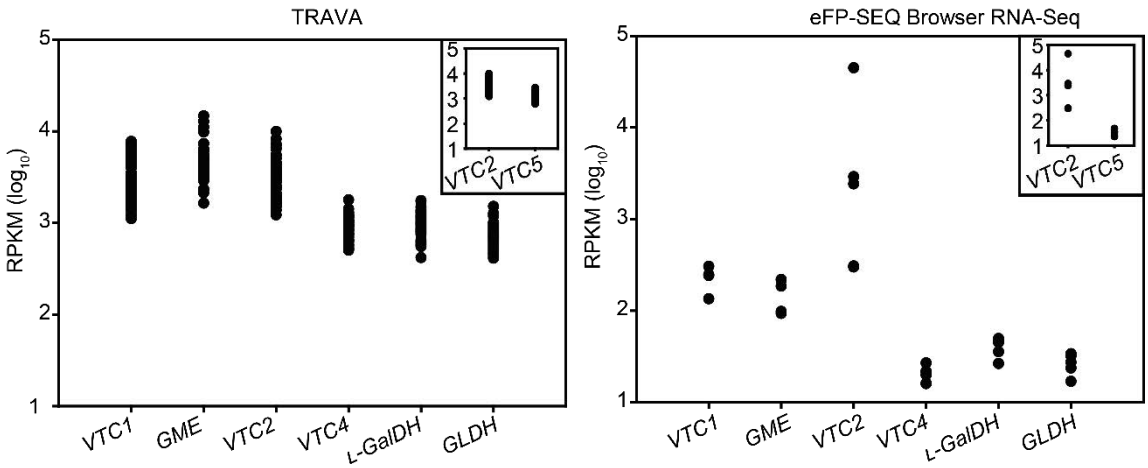

Figure 9. VTC2 mRNA levels are similar to those of VTC1 and GME, although VTC2 protein is hardly detectable. Data were taken from two different public RNA sequencing (RNA-seq) data sets: Transcriptome Variation Analysis (TRAVA, travadb.org; Klepikova et al., 2016) and the eFP-Seq Browser (https://bar.utoronto.ca/eFP-Seq_Browser/; Sullivan et al., 2019) corresponding to different adult plants' vegetative and green tissues, respectively.

Combinatorial expression of ascorbate biosynthesis genes in *N. benthamiana* leaves identifies VTC2 as the main control point of ascorbate biosynthesis

We have shown that that SW proteins are functional when a tag is added to their C-terminus and that a small amount of VTC2-GFP protein is required to increase the content of *vtc2* ascorbate to WT levels. In order to investigate the effect of the activity of ascorbate biosynthesis genes on ascorbate concentration we cloned the coding sequences (CDS) of Arabidopsis *VTC1*, *GME*, *VTC2*, *VTC4*, *L-GalDH* and GLDH with C-terminal GFP and HA, driven by the CaMV35S promoter (Figure 10A) and transiently expressed them in *N. benthamiana* leaves. Immunoblot analysis of the SW GFP tagged proteins showed that the molecular masses of the different fusion proteins were consistent with their predicted sizes (Figure 10B). Moreover, based on the low concentration of low molecular weight

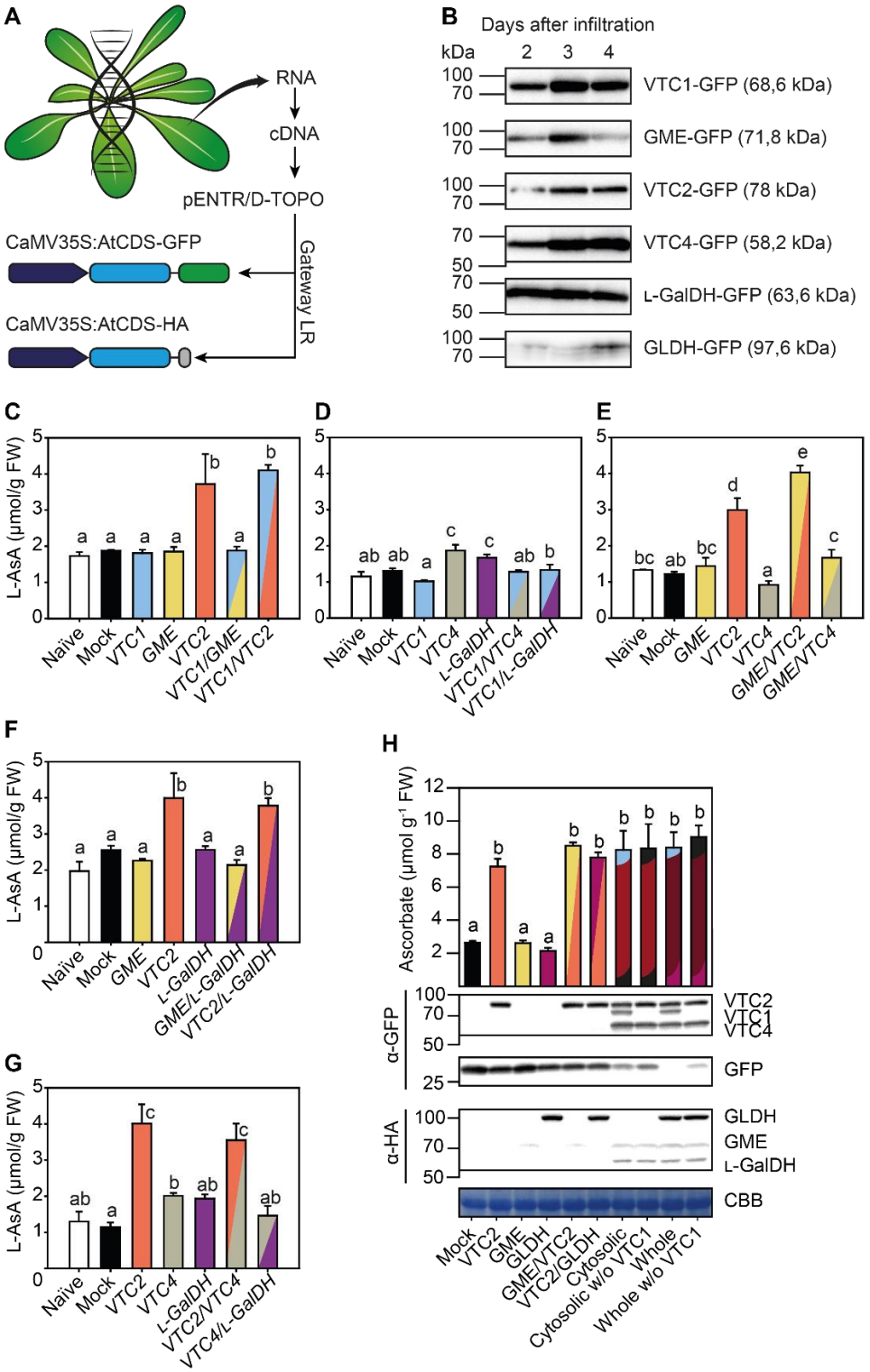

Figure 10. The effect of transient expression of C-terminal GFP and HA fusions of ascorbate biosynthesis enzymes on ascorbate concentration in *Nicotiana benthamiana* leaves. A) Strategy followed to clone and to overexpress in *N. benthamiana* leaves ascorbate biosynthesis genes from Arabidopsis translationally fused to GFP and HA at the protein C-terminus. B) Immunoblots (α-GFP) of fusion protein accumulation 2, 3 and 4 days after agroinfiltration. Expression was driven by the 35S promoter. Protein amount was measured and loaded to obtain similar intensities in the blot at 2 days after infiltration. C-H) Leaf ascorbate concentration 3 days after agroinfiltration with different combinations of C-terminal GFP ad HA fusions of ascorbate biosynthesis enzymes. Constructs used in each infiltration are shown in Supplementary Table 1. Two leaves of at least three *N. benthamiana* plants were infiltrated and samples were collected at 3 days after infiltration. Different letters denote statistically significant differences (One-Way ANOVA, α=0,05, post-hoc Tukey test)

fragments of the protein, all the fusion proteins showed little degradation of the proteins at all time points tested (Figure 11). Three days after agroinfiltration, VTC1-GFP, GME-GFP, VTC2-GFP and VTC4-GFP proteins showed the highest expression while L-GalDH-GFP and GLDH-GFP were also well expressed (Figure 10B).

Then, we performed a systematic analysis of the effect of transient overexpression of individual or multiple combinations of these *SW* Arabidopsis genes on the ascorbate concentration in *N. benthamiana* leaves. Based on the expression data showed in Figure 10B, we analysed the ascorbate content 3 days after agroinfiltration. All genes were expressed either individually or in pairs (Figure 10C-G; Appendix 1), and due to the large number of possible combinations, three genes were expressed individually and two genes out of the three were co-expressed in order to analyse the ascorbate content in the same experiment (Figure 10C-G). This experimental design validated the reproducibility of our experimental system since individual genes have been analysed three times with their proper controls (except for *VTC1,* with only two). As shown in Figure 10C, the transient expression of individual *VTC1-GFP* and *GME-GFP* genes did not increase ascorbate content relative to the naïve (not agroinfiltrated) or control (infiltrated with GFP) in *N. benthamiana* leaves. However, expression of *VTC2-GFP* increased ascorbate concentration between 2 and 3-fold. The expression of individual *VTC1, GME* and *L-GalDH* genes or any combination of these three genes without *VTC2-GFP* did not significantly increase ascorbate concentration in any of the multiple assays (Figure 10D-G). It also demonstrates that higher levels of VTC1 (Figure 10C), VTC4 (Figure 10G) and L-GalDH (Figure 10F) do not contribute to increase the ascorbate content, either individually or combined. The combination of *VTC2* with *GME* caused a significant increase in ascorbate relative to *VTC2* (Figure 10E), although the effect was not consistent in all experiments (Figure 10E, H). An increased ascorbate content by combining *GME* and *VTC2* has been previously reported using transient overexpression of kiwifruit *GME* and *VTC2* homologs in tobacco leaves (Bulley et al., 2009).

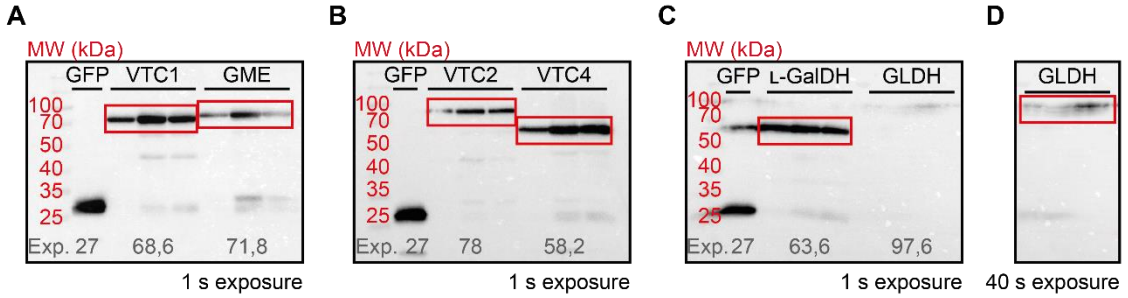

Figure 11. Complete blots corresponding to Figure 10B (red rectangle) show little degradation of the proteins transiently expressed in *N. benthamiana* leaves. Blots A, B and C have the same time of exposure using an ultra-sensitive enhanced chemiluminescent substrate for low femtogram protein level detection. Blot C and D are the same membrane with different exposure times. Protein loads were calculated using FIJI so the amount of protein at the first timepoint were similar among constructs. In red letters, protein mass weigh (in kDa); In grey letters, the expected size of the GFP-tagged protein calculated *in silico*.

Finally, we tested the effect of the simultaneous transient overexpression of all SW cytosolic Arabidopsis genes on the ascorbate concentration in *N. benthamiana* leaves. The expression of all cytosolic components was confirmed by immunoblot analysis (Figure 10H) and increased the ascorbate content to similar levels as produced by expressing *VTC2* alone (Figure 10H). Expressing all the cytosolic enzymes together with the final mitochondrial enzyme *GLDH* also did not increase ascorbate concentration (Figure10H). Overall, these results point to *VTC2* as the main control point in the biosynthesis of ascorbate.

Subcellular localisation of ascorbate biosynthesis enzymes using GFP-tagged proteins

The biosynthesis of ascorbate up to the L-galactose dehydrogenase step is proposed to take place in the cytosol with the exception of the last step that occurs at the intermembrane space of the mitochondria (Dunkley et al., 2006; Heazlewood et al., 2004; Østergaard et al., 1997; Pineau et al., 2008; Schimmeyer et al., 2016). *In silico* analysis using the software *Compartments* (https://compartments.jensenlab.org/Search) predicted a cytosolic subcellular localisation for GME, VTC4 and L-GalDH, an annotated dual cytosolic-nuclear localisation of VTC1 and VTC2 and a mitochondrial localisation of GLDH (Figure 12). Confocal microscopy imaging of C-terminal GFP-tagged proteins transiently

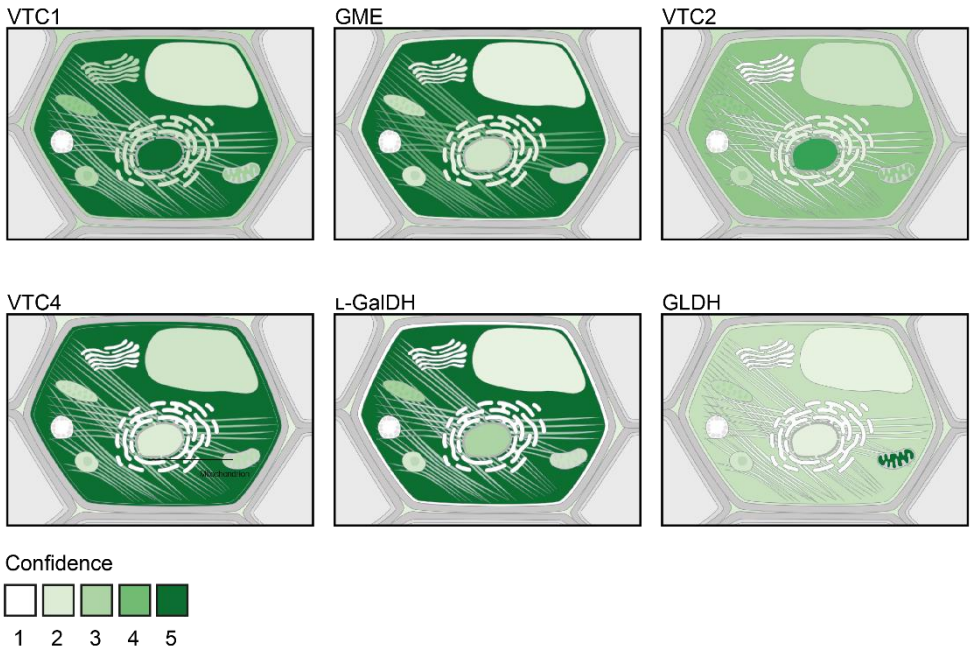

Figure 12. Predicted and/or annotated subcellular localisation of the SW proteins in the plant cell according to Compartments (https://compartments.jensenlab.org/Search).

expressed in *N. benthamiana* revealed a cytosolic subcellular localisation for VTC1, GME, VTC2, VTC4 and L-GalDH while GLDH-GFP appeared in structures that resembled mitochondria (Figure 13). Interestingly, VTC1-GFP, VTC2-GFP,

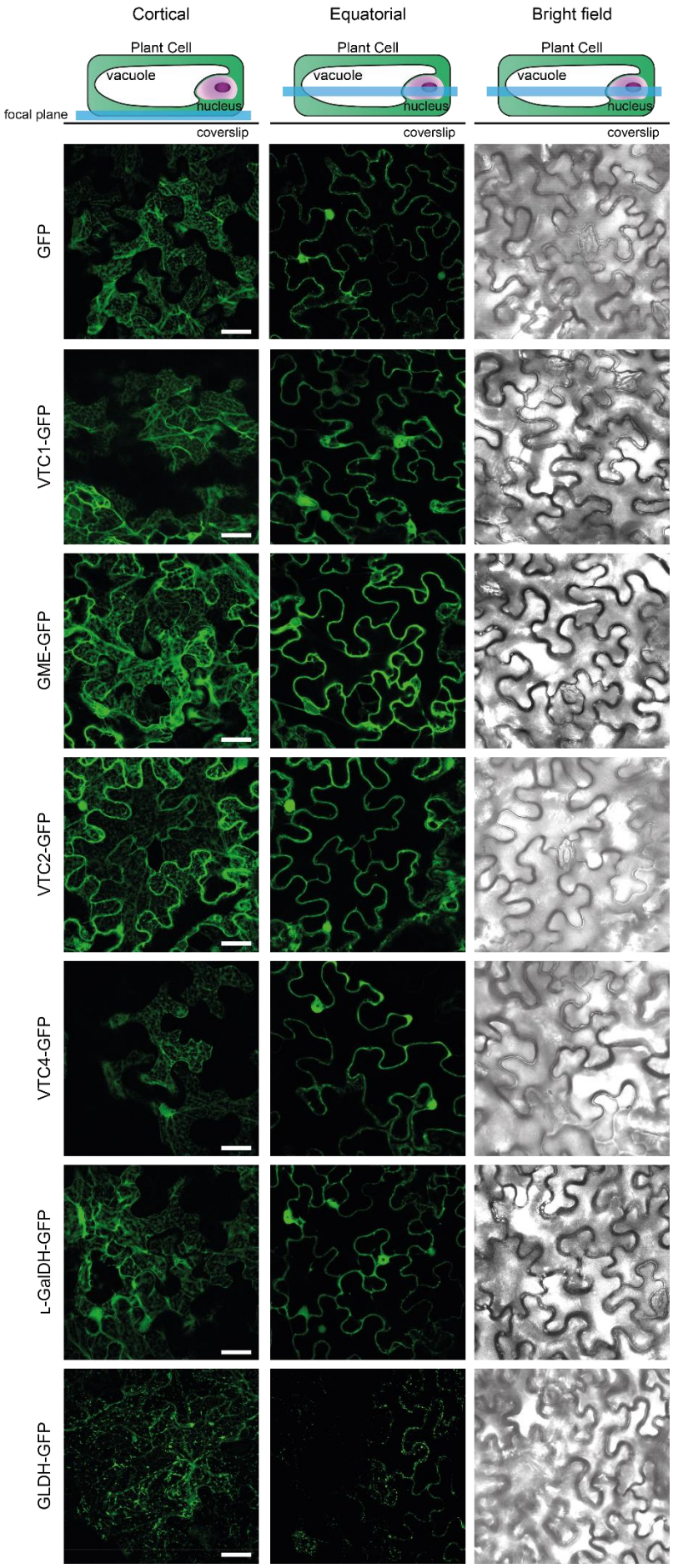

Figure 13. Subcellular localisation of free GFP and C-terminal GFP fusions of ascorbate biosynthesis enzymes transiently expressed in *N. benthamiana* leaves under the control of the 35S promoter 3 days after agroinfiltration. GFP was visualized by laser scanning confocal microscopy. Scale bar = 30 µm.

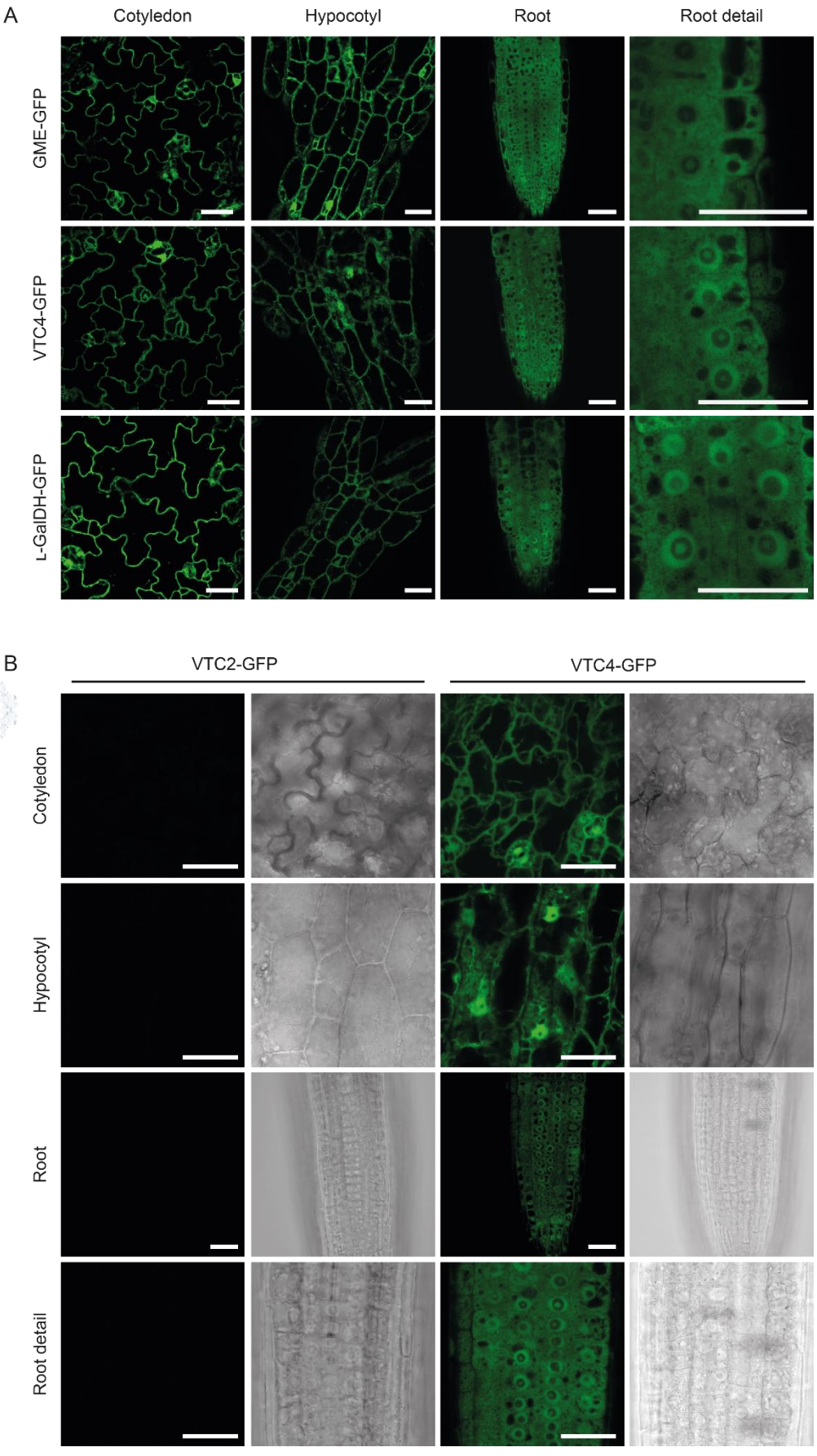

Figure 14. Subcellular localisation of transgenic Arabidopsis lines expressing ascorbate biosynthesis enzymes fused to GFP at the C-terminus under the control of their native promoters. A) The expression of GFP-tagged enzymes is ubiquitous in four days-old seedlings and their subcellular localisation is compatible with cytosol and nucleus except for GME, which only locates in cytosol. B) GFP signal of a functional VTC2-GFP (line 13) protein was not detectable. GFP was visualized by laser scanning confocal microscopy. Scale bar = 30 μm

VTC4-GFP and L-GalDH-GFP also showed a nuclear localisation in addition to their cytoplasmic localisation, whereas we observed a GME-GFP signal surrounding the nuclei (Figure 13). Evidence for a dual cytosolic-nuclear localisation has been provided for VTC1 and VTC2 using stable transgenic Arabidopsis lines (Müller-Moulé, 2008; Wang et al., 2013), suggesting a potential nuclear function of these proteins. Remarkably, similarly to VTC1, nuclear localisation signals are not predicted for VTC4 or L-GalDH and, therefore, the localisation reported here was unexpected (Appendix 2).

Because overexpression can result in ectopic localisation of proteins, we used the Arabidopsis transgenic lines that carry functional biosynthetic ascorbate proteins C-terminally fused to GFP and driven by their own promoters to analyse their *in vivo* subcellular localisation as well as their tissue distribution. Cotyledons, cotyledon-hypocotyl junction, hypocotyl and root tip of four-day-old Arabidopsis seedlings were analysed. GME-GFP, VTC4-GFP and L-GalDH-GFP lines showed a strong fluorescence signal in the cytoplasm (Figure 14A). In addition, VTC4-GFP and L-GalDH-GFP were present within nuclei-like structures. In roots, these two proteins were present within nucleus as a dot that resembles nucleolus, but they also displayed a ring-like pattern in nucleus whereas GME-GFP showed an even distribution across cytosol (Figure 14A). We did not detect fluorescence signal for VTC2-GFP above the background level (Figure 14B) consistent with the weak signal previously observed in immunoblot analysis (Figure 7C; Figure 8F). Except for VTC2, these data are consistent with the over-expression data of *SW-GFP* constructs in *N. benthamiana*.

Protein-protein interaction assays support a physical association of proteins involved in ascorbate biosynthesis

Enzymes involved in metabolic pathways can associate in order to increase the efficiency of consecutive enzymatic transformations (Smirnoff, 2019; Sweetlove and Fernie, 2018). Since VTC1, GME, VTC2, VTC4 and L-GalDH proteins showed cytoplasmic localisation (Figure 13, Figure 14) we investigated their interaction *in viv*o using yeast two-hybrid (Y2H) (Figure 15; Figure 16A). For this, all ascorbate biosynthesis CDSs (including the mitochondria-localised GLDH as a negative control) were cloned into both binding domain (BD, pGBKT7) and activation domain (AD, pGADT7) yeast vector and tested all 36 possible interactions resulting from the combination of all the enzymes of the pathway in both directions (fused to AD or to BD; Figure 15). As positive controls, we included SNF1/SNF2 (Fields and Song, 1989) and p53/SV40-Large AgT (Iwabuchi et al., 1993; Li and Fields, 1993) interactions, whereas Laminin C/SV40-Large AgT was used as a negative control (Bartel et al., 1993; Ye and Worman, 1995). This analysis did not provide evidence of direct interactions between the enzymes of the pathway, although VTC1, GME and VTC4 showed self-interaction, showing that these proteins were expressed in yeast (Figure 16A). A dimerization interface is predicted for GME and VTC4, while a trimerization domain is predicted for VTC1 (Figure 16B), consistent with our yeast two-hybrid interaction results.

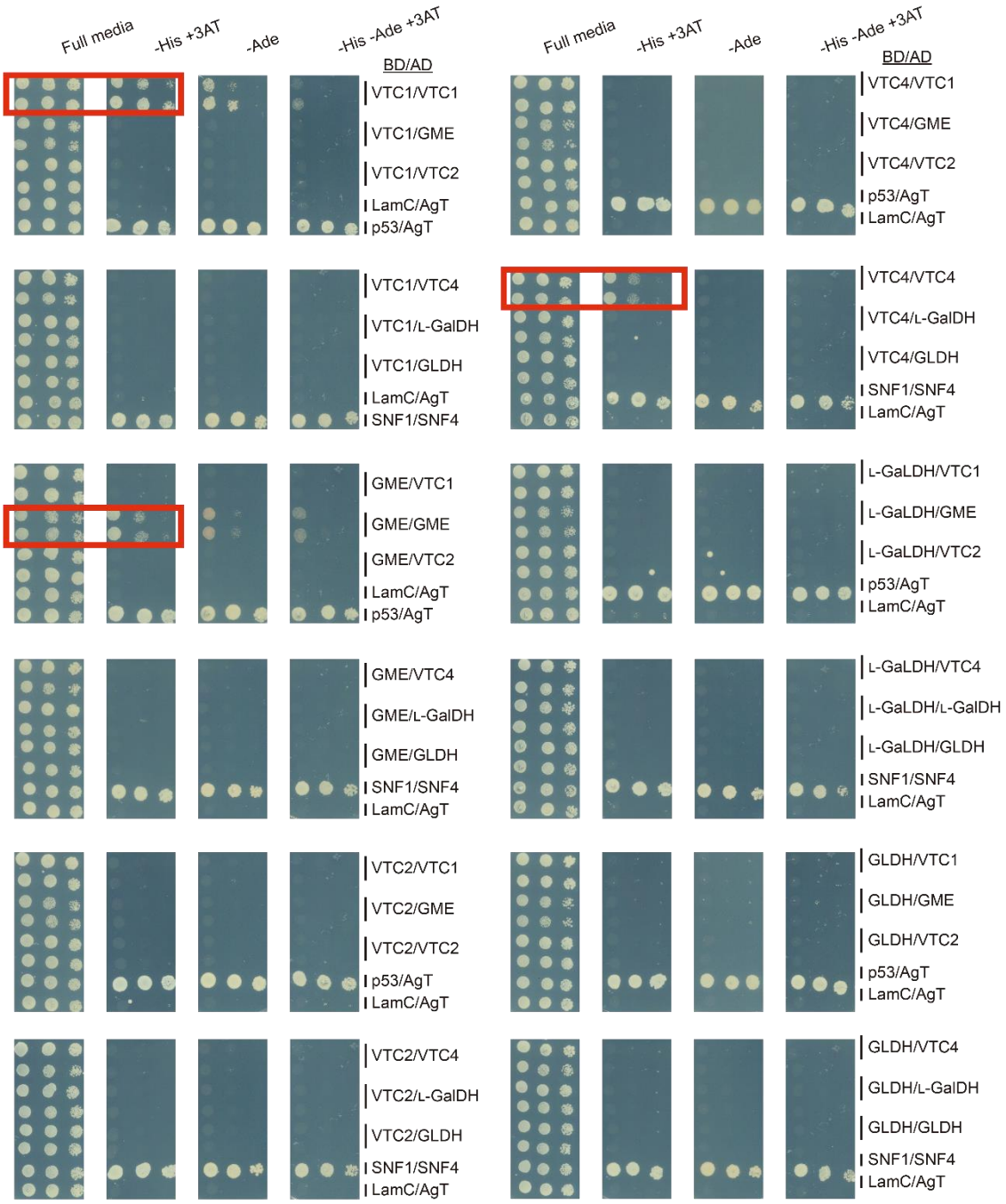

Figure 15. Yeast two-hybrid whole screening. Red rectangles correspond to the spotting presented in Figure 16A. As positive interaction controls, we used SNF1/SNF4 (Fields and Song, 1989) and p53/SV40-Large AgT (AgT; Li and Fields, 1993; Iwabuchi et al., 1993). As a negative control, we included LamC/AgT cotransformation (Bartel et al., 1993; Ye & Worman, 1995). His: histidine, 3-AT: 3-amino-1,2,4-triazole, Ade: adenine.

Despite the apparent lack of direct interactions of ascorbate biosynthesis enzymes in yeast, we investigated whether these proteins could indirectly associate in a model plant. For this, we co-expressed biosynthesis enzymes of the pathway tagged with C-terminal GFP and HA in *N. benthamiana* and performed coimmunoprecipitation (CoIP) assays. We used GFP-Trap beads to inmunoprecipitate GFP tagged proteins and α-HA antibodies to detect coimmu-

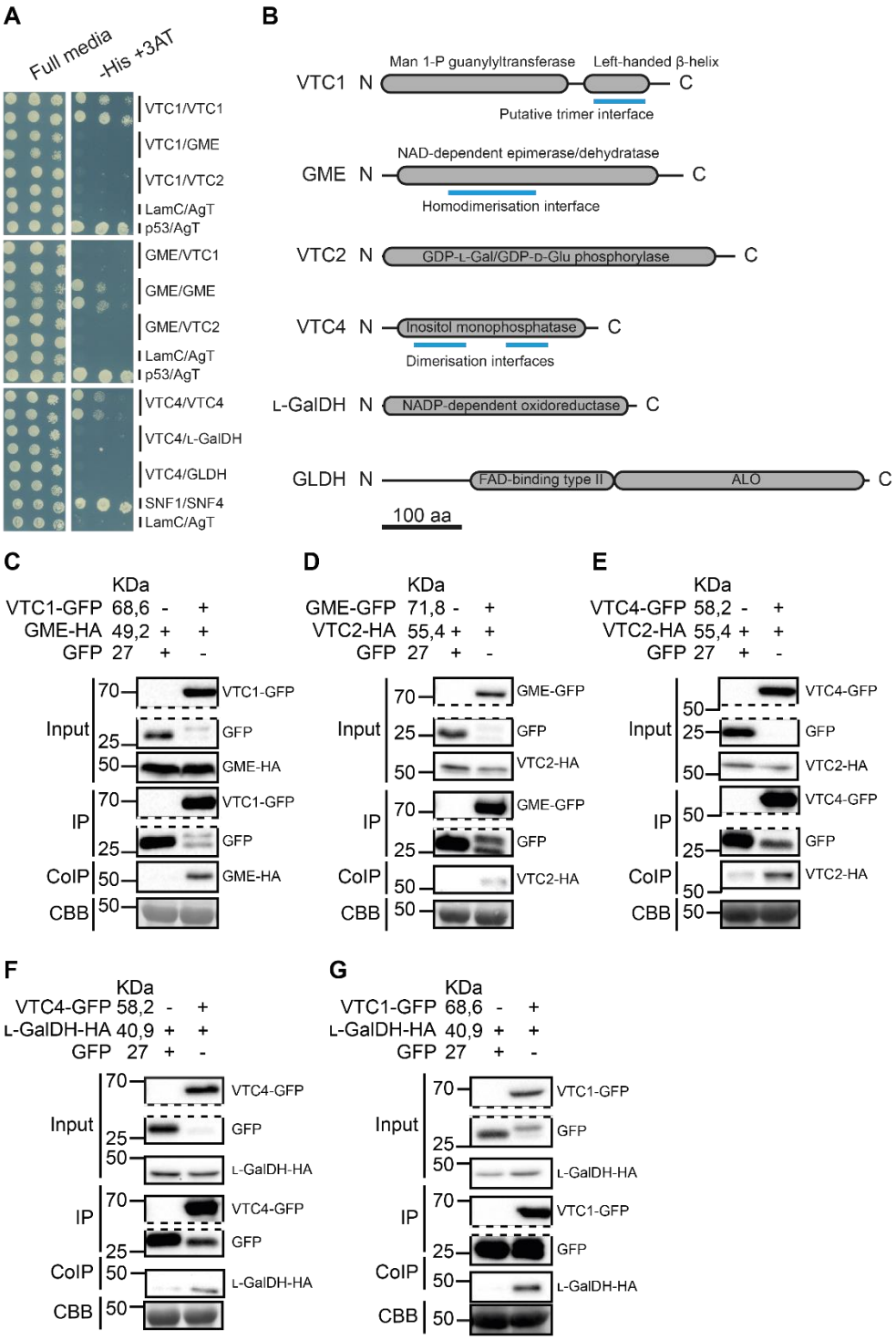

Figure 16. Interaction of ascorbate biosynthesis enzymes assessed by yeast two-hybrid analysis and coimmunoprecipitation (CoIP). (A) Yeast two-hybrid assay (also Figure 15) detected no direct interaction between the enzymes, but VTC1, GME and VTC4, which contain predicted dimerization/trimerization domains (B), form dimers/trimers. B) Protein scheme for each of the enzymes assayed in yeast two-hybrid showing length (in amino acids), annotated domains and dimer/trimerization interfaces. (C-G) CoIP assay reported association in vivo in Nicotiana between consecutive steps as well as between the first (VTC1) and the last (L-GalDH) steps occurring in cytosol. GFP-tagged enzyme from Nicotiana crude protein extracts containing two overexpressed consecutive enzymes, GFP and HA-tagged, was pulled-down using α-GFP agarose beads and coimmunoprecipitated protein was detected using α-HA antibody.

noprecipitated HA-fused proteins using immunoblot. We first tested biosynthesis proteins that are consecutive in the pathway (Figure 16C-F), i.e., VTC1/GME, GME/VTC2, VTC2/VTC4, VTC4/L-GalDH. We co-expressed VTC1-GFP and GME-HA to test the interaction, and GFP together with GME-HA as a negative control (Figure 16C) and checked by immunoblot if protein expression was suitable for immunoprecipitation prior to the assay (Figure 17). After immunoprecipitation of VTC1-GFP and free GFP, we detected a specific association between GME-HA with VTC1-GFP but not with free GFP (Figure 16C). Following the same strategy, we found associations between all consecutive enzymes of the pathway (Figure 16D-F). In addition, we also performed CoIP between the first and last cytosolic enzymes of the pathway, i.e., VTC1 and L-GalDH and found a specific association between VTC1-GFP and L-GalDH-HA (Figure 16G).

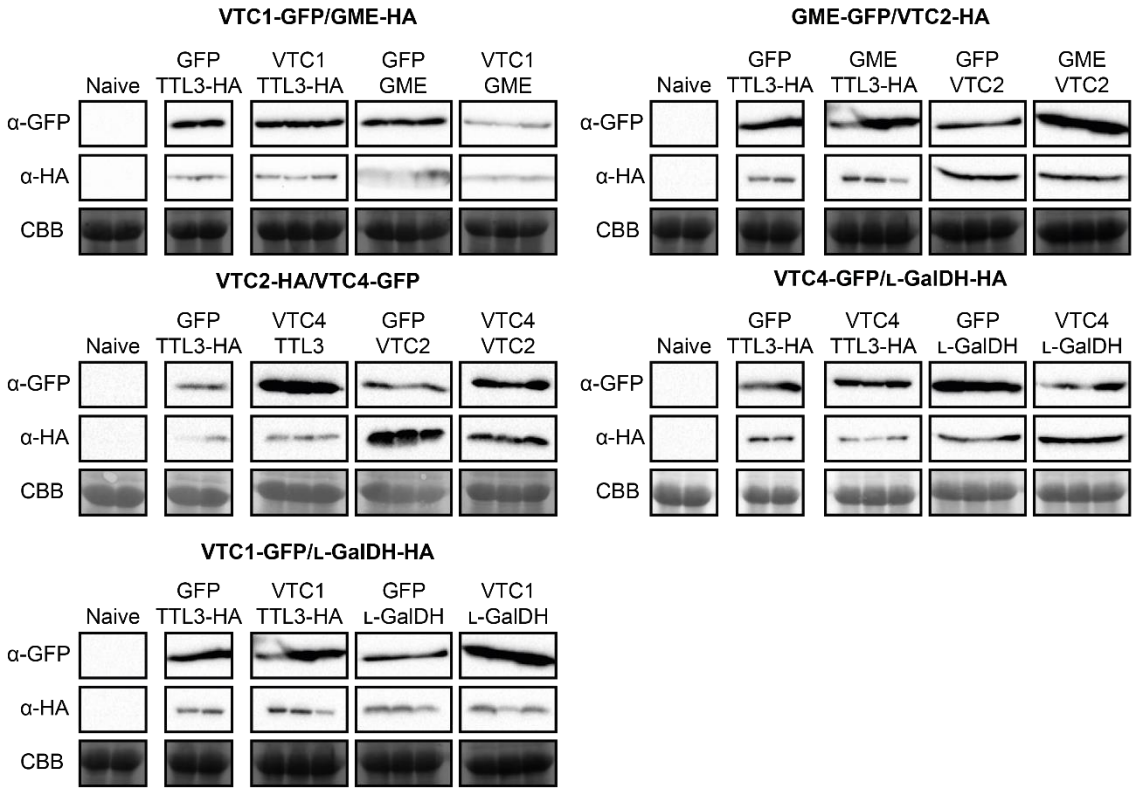

Figure 17. Immunoblot (α-GFP) of *N. benthamiana* leaves crude extracts following agroinfiltration of above-indicated combinations of proteins (also see Appendix 1). Two leaves of 2 or 3 independent plants were infiltrated, using GFP or TTL3-HA (an HA-tagged protein non-related to ascorbate synthesis; Amorim-Silva et al., 2019) to set optical density up to 1.

A kinetic model of ascorbate biosynthesis indicates GDP-L-galactose phosphorylase as the main control point

To further understand the results of over-expression, a kinetic model of ascorbate biosynthesis was constructed using Complex Pathway Simulator (COPASI; Hoops et al., 2006). Reactions were described by reversible Michaelis-Menten kinetics, except for L-Gal 1-P phosphatase/VTC4 and GLDH which were described by irreversible Michaelis-Menten kinetics (Figure 18A). Published Km values were used except for GGP, which was set to 0.1 mM in the absence of published data (Gatzek et al., 2002; Hoeberichts et al., 2008; Laing et al., 2004; Linster et al., 2007; Maruta et al., 2008; Østergaard et al., 1997; Wolucka and Van Montagu, 2003). The relative activity of enzymes has been reported in only one case (Dowdle et al., 2007) but these are not guaranteed to reflect the maximum rate of each enzyme. Low expression of GGP compared to other pathway enzymes is suggested from very low expression of the GFP fusion which nevertheless rescues ascorbate concentration in the mutant background (Figure 7B, C; Figure 8E, F). However, conservatively, the relative activity of each enzyme (V) was set to the same value (10 mM s^{-1}) but was varied during simulations. Evidence from radiolabelling suggests that ascorbate synthesis is subject to feedback inhibition by ascorbate (Conklin et al., 1997; Laing et al., 2015; Pallanca and Smirnoff, 2000; Wolucka and Van Montagu, 2003). The proposed uORF-mediated feedback repression of GGP translation (Laing et al., 2015) was modelled by including non-competitive inhibition by ascorbate. Competitive inhibition of PMI and L-GalDH by ascorbate (Maruta et al., 2008; Mieda et al., 2004) were included, although in the case of L-GalDH, the inhibition could be an assay artefact (Laing et al., 2004). Once synthesised, ascorbate and its oxidation product dehydroascorbate (DHA) can be broken down to a wide range of products (Dewhirst et al., 2020; Dewhirst and Fry, 2018; Green and Fry, 2005). The oxidation of ascorbate to monodehydroascorbate (MDHA) and DHA was included in simplified form including only ascorbate and DHA. The breakdown rate of DHA was described by irreversible 1st order kinetics (Conklin et al., 1997; Pallanca and Smirnoff, 2000). It is assumed in the model that all breakdown products are recycled to D-Glc 6-P. This is unlikely to be correct but did not affect model predictions.

The starting parameters used in the model are shown in Appendix 3. The model carried out metabolic control analysis (MCA) at steady state. The effect of changing the strength of feedback repression of GGP by ascorbate on the flux control coefficients for each step are shown in Figure 18B (and data in Appendix 4). At the highest Ki value (relatively weak feedback), all steps up to GGP contributed equally to flux, indicated by similar flux control coefficients. However, biosynthesis steps beyond GGP had very low flux control coefficients and changes in activity of these enzymes would be predicted to have a very small effect on pathway flux. The turnover step also had a significant effect on flux. Decreasing Ki by ten-fold or more resulted in all flux control being shared between GGP and turnover, the pre-GGP steps having very low flux control coefficients. Therefore, for the biosynthesis steps, the model predicts that only GGP controls the flux through the pathway if feedback repression is sufficiently strong.

Correspondingly, concentration control coefficients (i.e. the change in the concentration of each pathway intermediate caused by a change in enzyme activity) for each step were calculated. The results for ascorbate are shown in Figure 18C and for all intermediates in Appendix 5. At the highest Ki value, all steps up to GGP had similar concentration control coefficients indicating change in activity at each step would exert a similar effect on ascorbate concentration.

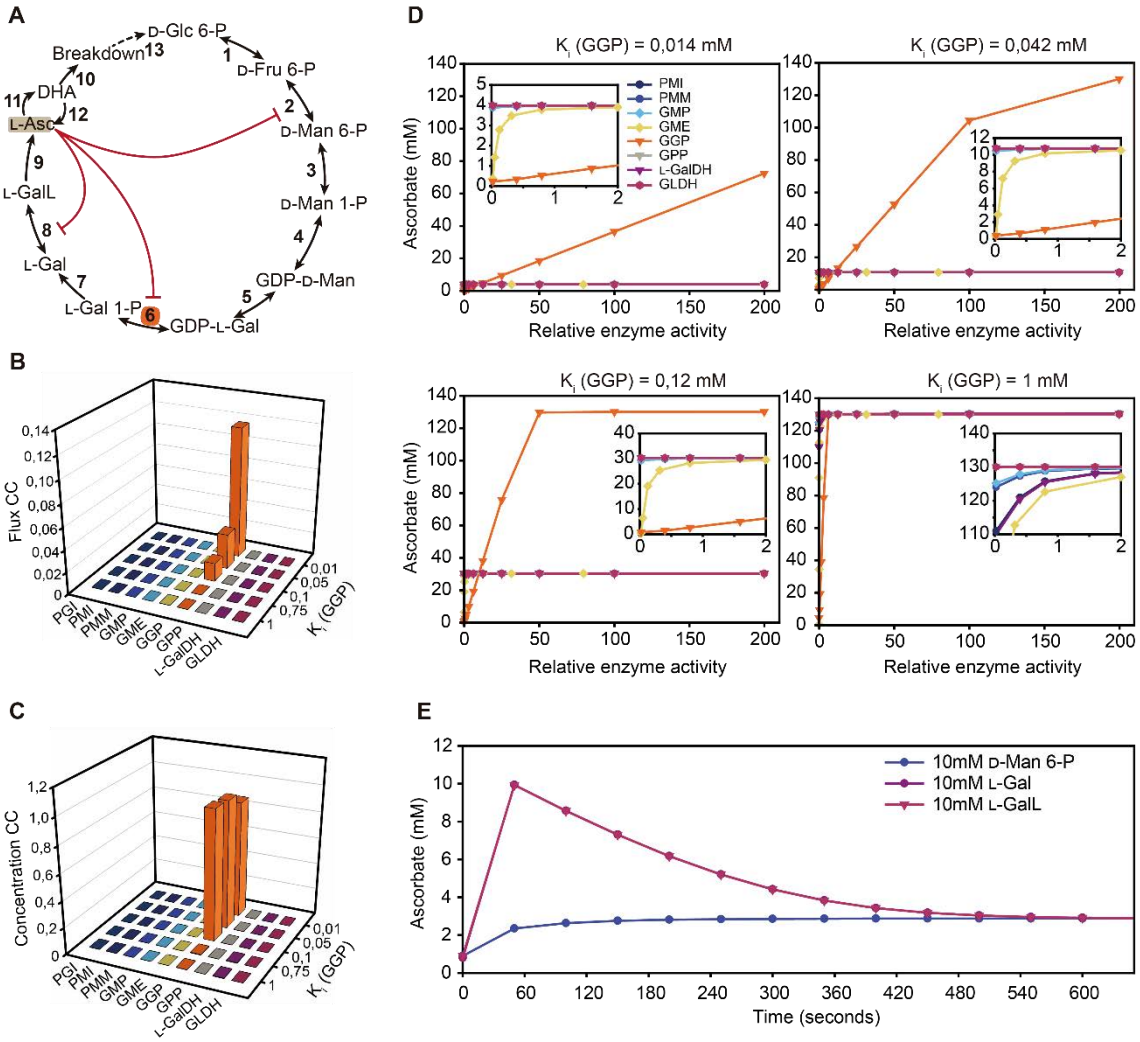

Figure 18. A kinetic model of ascorbate biosynthesis, recycling and turnover. A) Scheme of the pathway modelled in COPASI showing intermediates catalytic steps (arrows) and feedback (red lines). The initial model parameters are shown in Supplementary Table 3. B) Metabolic control analysis at steady state was used to calculate flux control coefficients (CC) for each enzyme with various strengths of non-competitive inhibition exerted by ascorbate (indicated by Ki values) on GGP (step 6). C) Metabolic control analysis at steady state was used to calculate concentration control coefficients (CC) for ascorbate with various strengths of non-competitive inhibition exerted by ascorbate (indicated by Ki values) on GGP (step 6). D) The effect of varying enzyme activity on ascorbate concentration with various strengths of non-competitive inhibition exerted by ascorbate (indicated by Ki values) on GGP (step 6). E) Time course of the change in ascorbate concentration in response to the addition of D-mannose 6-phosphate (D-Man 6-P), L-galactose (L-Gal) and L-galactono-1,4-lactone (L-GalL). 1: PGI, 2: PMI, 3: PMM, 4: GMP, 5: GME, 6: GGP, 7: GPP, 8: L-GalDH, 9: GLDH, 10: Turnover, 11: Oxidation, 12: Reduction).

Increasing feedback strength decreased the concentration control coefficients of all steps except GGP predicting that only this step controls ascorbate concentration. The outcome could be affected by the starting conditions (relative enzyme activities and kinetic constants) but testing the model with varying Km values or with and without competitive feedback inhibition of PMI and L-GalDH had little effect on ascorbate concentration (Appendix 6). To simulate metabolic engineering experiments, the enzyme activity of each step was increased over a large range and the predicted change in ascorbate concentration at various feedback repression strengths was determined (Figure 18D and Appendix 7). As expected from the MCA, only varying GGP activity had a significant effect on ascorbate over a very wide range of activities and this effect was strongly dependent on the extent of feedback repression. In comparison, it was necessary to decrease the activity of the other enzymes to very low values before ascorbate concentration was affected and this behaviour was particularly marked for the post-GGP steps. The kinetic model therefore reflects the effect of transient expression of the pathway enzymes in *N. benthamiana*: only increasing GGP activity increases ascorbate concentration. Simulation of mannose 6-P addition caused a small transient increase in ascorbate accumulation, while L-galactose and L-galactono-1,4-lactone addition had a large effect (Figure 18E). This differential response reflects the operation of feedback repression at the GGP step.

Discussion

Here, we report the effect of systematic overexpression, individually and in combination, of all genes involved in the SW pathway have on the endogenous ascorbate content using *N. benthamiana* leaves. The GFP-tagged enzymes were functional since translational fusion of GFP at the C-termini of all enzymes increased ascorbate concentration in their respective Arabidopsis mutants. Further, immunoblots of the expressed enzymes showed that they were all well expressed in *N. benthamiana* (Figure 17). Under these experimental conditions, only VTC2/GGP over-expression was able to increase ascorbate concentration, which confirms previous studies (Ali et al., 2019; Bulley et al., 2012, 2009; Laing et al., 2015; Li et al., 2018; Yoshimura et al., 2014; H. Zhang et al., 2018). Interestingly, a *vtc2* mutant containing a VTC2-GFP construct driven by its own promoter and including the 5'-UTR showed an extremely low GFP fluorescence compared to other SW GFP-tagged proteins. This low expression of VTC2-GFP was also reflected in the immunoblot comparing the expression of all the components of the pathway at the protein level (Figure 7C), likely reflecting the translational repression of VTC2 via the conserved uORF in the 5'-UTR (Laing et al., 2015). This is further confirmed by the finding that the overexpression in *N. benthamiana* of VTC2 without the uORF showed a similar amount of VTC2 proteins to other proteins of the pathway (Figure 17). The expected low level of endogenous VTC2 protein in *N. benthamiana*, which also contains the uORF

(Laing et al., 2015), may explain the marked increase of ascorbate after the overexpression of Arabidopsis VTC2 lacking the uORF.

Based on the data presented here and other reports, we constructed a kinetic model based on the known properties of the pathway enzymes that includes the repression of GGP by ascorbate. However, it does not explicitly distinguish between transcriptional, translational, post-translational and metabolite feedback on enzyme activity as the mechanism of repression. This model was used for metabolic control analysis, an approach which determines the distribution of the control of flux and concentration of pathway intermediates in response to small changes in activity of each enzyme in the pathway by calculating flux control and concentration control coefficients for each step (Fell, 1992). This analysis showed that the only step in the biosynthesis pathway that controls pathway flux and ascorbate pool size is GGP as long as feedback repression is included. The other critical step is ascorbate breakdown while the flux control coefficients of all the other steps were negligible. Decreasing the strength of feedback repression by ascorbate on GGP eventually decreased its flux and concentration control coefficients, resulting in control being more evenly distributed across the steps up to GGP. The model predicts that the steps post GGP exert little control and that in the presence of feedback repression, GGP is the only critical step. Consequently, in virtual metabolic engineering experiments, in which each enzyme was changed over a large range, only GGP affected ascorbate concentration.

The model prediction is consistent with the transient expression results shown in this report and with the relatively small effect of over-expressing enzymes other than GGP. In a previous study of transient expression in *Nicotiana tabacum*, GME alone did not affect ascorbate, in accordance with the model, but enhanced the effect of expressing GGP (Bulley et al., 2009). However, in our hands this increase in ascorbate was not always reproducible suggesting that other factors need to be considered such as different carbohydrate status caused by growth conditions. Stable over-expression of GMP and GME has been reported to increase ascorbate in tomato and *N. tabacum* (Badejo et al., 2008, 2007; Li et al., 2019) and the model predicts that these enzymes could be effective if endogenous activity is low. Similarly, increasing the expression of L-GalDH in *N. tabacum* had no effect on ascorbate while antisense suppression in Arabidopsis only had a small effect in high light (Gatzek et al., 2002).

The model outcomes are robust over a range of starting conditions and are minimally affected by the Km values tested nor by the presence/absence of competitive inhibition of PMI and L-GalDH. The model also explains another feature of the pathway, which is that VTC2 and VTC5, the paralogues of GGP in Arabidopsis, do not compensate for each other when knocked out (Dowdle et al., 2007). The control features of the pathway appear to emerge from its architecture in which a strongly repressible GGP step is followed by the irreversible L-Gal 1-P phosphatase and L-galactonolactone dehydrogenase steps. In a previous study comparing the activity of SW enzymes where ascorbate pool size differs under low and high light intensity, only GGP showed increased activity in high light in Arabidopsis (Dowdle et al., 2007). Transcript levels suggest that only VTC2 and VTC5 (and sometimes GME) are responsive to environmental conditions (Li et

al., 2013), and that there is not a coordinated induction of SW genes under high light and low temperature, conditions that increase ascorbate concentration (Laing et al., 2017). The control of ascorbate biosynthesis therefore differs from pathways in which there is coordinated induction of multiple pathway enzymes by transcription factors, for example anthocyanin synthesis (Zhang et al., 2014).

Importantly, the model shows that ascorbate pool size responds to GGP over a wide range and thereby explains how a combination of transcription and feedback repression controls the amount/activity of GGP and provide a mechanism to adjust ascorbate pool size to prevailing conditions. Light is the best studied factor and ascorbate adjusts to the prevailing light intensity over several days (Page et al., 2012). The mechanism likely involves a changed balance between increased transcription of GGP via a possible photosynthesis-derived signal and light response promoter elements (Gao et al., 2011; Yabuta et al., 2007) and ascorbate repression of translation via the uORF. In addition to the transient expression assays showing the role of the uORF in translational repression of GGP (Laing et al., 2015), CRISPR-Cas9 editing of the uORF in Arabidopsis, lettuce and tomato increases ascorbate, confirming its role in repression of ascorbate synthesis in diverse species (Li et al., 2018; H. Zhang et al., 2018). Faster control could also occur if ascorbate status more directly affects GGP activity via direct inhibition or post-translational modification. These latter possibilities have not been investigated but could operate since ascorbate addition relatively rapidly decreases incorporation of ^{14}C-glucose or mannose into ascorbate (Pallanca and Smirnoff, 2000; Wolucka and Van Montagu, 2003). It is not known if ascorbate or a proxy of ascorbate concentration exerts repression and, also, the mechanism by which the uORF controls GGP translation is not known.

In addition to investigating the effect of enzyme overexpression on ascorbate accumulation, we used tagged enzymes to investigate subcellular localisation and the formation of enzymatic complexes. With the exception of GLDH, the cytosolic localisation of the SW enzymes is consistent with the in-silico prediction (Figure 12). In this study, we have shown that all SW proteins are present in the cytosol (Figure 13; Figure 14). Interestingly, in addition to VTC1 and VTC2 that were previously reported to localise in the nucleus (Müller-Moulé, 2008; Wang et al., 2013) VTC4 and L-GalDH also showed nuclear localisation (Figure 13; Figure 14) despite the lack of nuclear localisation signals (Appendix 2). Whether or not this nuclear localisation is functionally important remains to be determined but several metabolic enzymes moonlighting in the nucleus have been previously reported (Boukouris et al., 2016).

Using CoIP in *N. benthamiana* we have shown that enzymes catalysing consecutive steps in the pathway associate (Figure 16C-F) as well as proteins catalysing distant enzymatic steps such as VTC1 and L-GalDH (Figure 16G). However, no direct interactions were found using yeast two-hybrid analysis (Figure 15). It could be possible that the N-terminal position of both AD and BD could be impairing the interactions involving VTC2 or L-GalDH but not the other enzymes, since self-interactions of VTC1, GME and VTC4 proved otherwise. Furthermore, previous studies reported ascorbate-producing yeasts by heterologous expression of the plant pathway in *Saccharomyces cerevisiae*, thus

lightening that these proteins can be stabilised in yeast (Branduardi et al., 2007; Fossati et al., 2011). The lack of direct interaction in yeast but the positive associations in *N. benthamiana* may indicate that the enzymes might require the presence of each other so that the interaction would not be detectable in the yeast two-hybrid assay. Although this deserves further investigation it is tempting to speculate that some of the ascorbate biosynthesis enzymes might form a functional enzymatic complex (metabolon) that could potentially channel pathway intermediates to increase flux and perhaps aid partitioning of GDP-D-mannose and GDP-L-galactose between ascorbate and polysaccharide synthesis. Such channeling has been shown for a number of pathways (Amorim-Silva et al., 2019; Smirnoff, 2019; Sweetlove and Fernie, 2018; Zhang et al., 2017).

In conclusion, metabolic engineering experiments using the last six enzymes of the SW pathway show that only GGP has significant control over the pathway, and we have developed a kinetic model that provides a rationale for this result. It is clear that the balance of VTC2/VTC5 amount is controlled by a combination of transcription and translation repression, largely, but not entirely mediated by the uORF mechanism. In addition, we have produced a set of complemented mutants from GME to L-GalDH tagged with GFP that provides a resource for further investigation of the SW pathway.

CHAPTER 2

A brief introduction

Ascorbate is known to exert a plethora of roles in plants, some of which are extensively described in the introduction of this thesis. Among them, ascorbate was proposed to have a role in growth and photoprotection (Smirnoff et al., 2000), although recent experiments using the ascorbate deficient mutant *vtc2-1* suggest that ascorbate is essential for growth but it is not so clear its photoprotective role (Plumb et al., 2018). However, there are experimental evidences supporting otherwise. For example, dehydroascorbate (DHA), the oxidised form of ascorbate, is an electron acceptor from ferredoxin, the last component of the photosynthetic electron transport chain in chloroplasts (Asada, 1999), hence preventing the formation of O_2^-. Also, ascorbate can act as an electron donor of photosystem II (Tóth et al., 2013) preventing the manganese cluster from photodamaging under circumstances such as high light-induced stress (Tyystjärvi, 2008). Therefore, this data support that ascorbate is essential for the response to the oxidative stress caused by high irradiance. In the previous chapter we have shown that only the overexpression of *VTC2* increases the biosynthetic flux of the pathway and, therefore, its protein concentration is regulated accordingly. More recently, it has been reported that ascorbate accumulation under high light stress not only requires a higher rate of biosynthesis but also mechanisms to prevent a massive degradation of ascorbate, which rely on DHA reductases and glutathione (Terai et al., 2020). Therefore, increase of the ascorbate pool under adverse environmental conditions depends on both ascorbate biosynthesis and turnover. Likewise, the stationary ascorbate content will depend on the translation of *VTC2* as well as on its degradation. It has been well stablished that *VTC2* is translationally regulated (Laing et al., 2015), but very little is known about its degradation. VTC1, the enzyme catalysing the conversion of D-mannose 1-phosphate into GDP-D-mannose acting upstream VTC2, is finely regulated even though an increase in its protein content does not lead to ascorbate accumulation (Figure 10C, D). Wang and collaborators (2013) have shown that the photomorphogenic factor CONSTITUTIVE PHOTOMORPHOGENESIS9 (COP9) signalosome subunit 5B (CSN5B), which is part of the CSN complex that regulates the cullin-RING E3 ubiquitin ligase activity (Schwechheimer and Isono, 2010), is required for VTC1 degradation through the 26S proteasome pathway in the dark, hence repressing ascorbate biosynthesis during the night, i.e., in conditions with no photosynthesis. We have reported that VTC2, the main regulator of the pathway is also subjected to proteasome regulation, although the exact molecular mechanism remains elusive.

In this chapter, we investigated the effect that high irradiance, which leads to increase ascorbate, has on ascorbate biosynthesis enzymes concentration. We used transgenic Arabidopsis plants containing functional GFP-tagged proteins of the SW pathway under the control of their own promoter in their respective mutant backgrounds previously generated (Chapter 1). In addition, we

have generated *vtc2/VTC2-GFP* transgenic lines expressing *VTC2-GFP* under the 35S promoter due to the low amount of VTC2 protein produced in those lines when driven by the *VTC2* promoter. Taking advantage of this biological tools, we studied the evolution in the content of SW proteins along a day/night cycle.

Results

Higher ascorbate content as a response to high light correlates with lower amounts of enzymes involved in ascorbate biosynthesis.

Light intensity is considered one of the main factors determining the amount of ascorbate in green tissues in such a way that the greater the irradiance the higher the content (Laing et al., 2017). However, how the ascorbate content correlates to the concentration of biosynthetic enzymes remains elusive. Therefore, we investigated if the increase in the content of ascorbate during high light acclimation was caused by a rise in the SW protein concentration.

To perform this study, we generated Col-0 Arabidopsis transgenic lines harbouring the genomic regions (including promoter region) of Arabidopsis genes involved in the cytosolic steps of the pathway. The resulting proteins (from GME to L-GalDH) contained a GFP fused to C-terminus (Figure 5; Figure 7, Figure 8; Figure 19A). Transgenic T2 lines carrying single insertion also showing high expression based on immunoblot analysis were selected. These lines were then crossed with their respective mutants in order to generate complementing lines with C-terminal GFP-tagged proteins (Figure 19B). As showed in Chapter 1, all enzymes tagged with GFP where functional and rescued ascorbate levels. The only exception was GME-GFP, which prevented the lethality of the mutation although contained ~50% of WT ascorbate content (Figure 7B).

Due to the impossibility to amplifying the complete genomic region of *VTC2* despite several attempts, we generated a construct that contained the promotor region including 5' UTR/uORF and the CDS of *VTC2* (*VTC2p:VTC2-GFP*) (Figure 19C). Remarkably, VTC2-GFP protein was either not detected or weakly detected in all the T2 transformants analysed by immunoblot despite using an ultra-sensitive enhanced chemiluminescent substrate for low femtogram protein level detection. Therefore, based on the WT growth of *vtc2* mutants and the easily scored phenotype (20% of ascorbate), we transformed *vtc2-4* plants and selected transformants based on increased ascorbate content and the presence of a single insertion (Figure 19D, F). This allowed the selection of two independent lines, C12 and C13, with significantly higher ascorbate than *vtc2-4* (Figure 19F). However, while line C12 showed an amount of ascorbate similar to WT plants, line C13 showed a greater content than the WT. This content correlated with the higher amount of protein in C13 than C12, however, both lines presented hardly detectable amounts of VTC2-GFP protein, further supporting that the amount of endogenous VTC2 protein is very little compared with the other cytosolic proteins of the SW pathway.

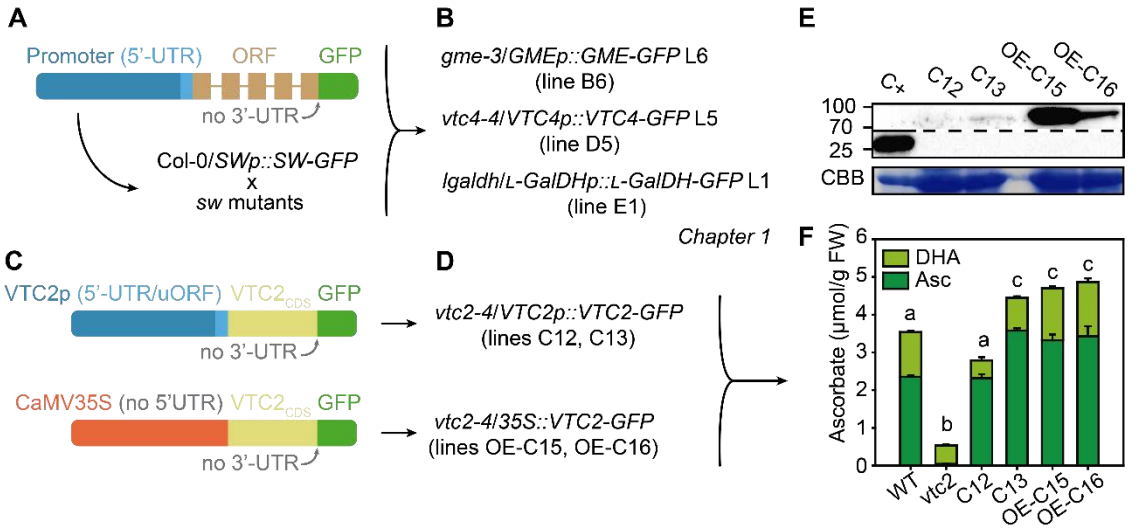

Figure 19. Genomic constructs used to generate Arabidopsis transgenic lines. A, B) Genomic constructs used to generate Arabidopsis transgenic lines in Chapter 1 (Line B6: GMEp::GME-GFP line 6; Line D5: VTC4p::VTC4-GFP line 5; line E1: L-GalDH::L-GalDH-GFP line 1). C, D) Transgenic lines generated for this chapter (lines C12, C13: VTC2p::VTC2-GFP; lines OE-C15, OE-C16: 35S::VTC2-GFP). E) T3 generation of homozygous vtc2/VTC2-GFP lines showed a broad range of VTC2-GFP concentration that, however, rescued ascorbate content (F). Ascorbate was extracted from three fully expanded leaves from five-week-old T3 plants grown on soil in a growth chamber under short-day conditions (10 h light at 22°C/14 h dark at 19°C), at 60% humidity and 200 µmol m^{-2} s^{-1} light intensity. Means±SD are shown, and different letters denote statistically significant differences for ascorbate content (One-Way ANOVA, α=0,05, post-hoc Tukey test).

In addition, we generated transgenic lines in *vtc2-4* background with the *VTC2* CDS driven by *CaMV35S* promoter. This construct lacks the 5' UTR/uORF and therefore is not subjected to translational control (Figure 19C, D, E). Two homozygous lines with single insertions, *OE-C15* and *OE-C16* were selected that showed an increased amount of ascorbate content relative to WT plants (Figure 19F). Consistent with the regulatory role of *VTC2* uORF, these lines presented high amounts of VTC2-GFP protein that could be readily monitored by immunoblot (Figure 19E). Notably, total ascorbate level in line C13 was similar to that in VTC2-overexpressing lines and greater than WT under the same growth conditions (Figure 19F), meaning that despite the large difference in the concentration of VTC2-GFP, the increase in ascorbate level is limited.

Overall, we described above the generation of homozygous lines carrying loss-of-function mutations in their endogenous SW genes of the cytosolic steps harbouring their respective GFP-tagged enzymes driven by their endogenous promoters that resulted in functional translational fusions. In addition, we have generated *vtc2* plants complemented with a VTC2-GFP but using two different approaches. In the first approach, the transcription and the translation of VTC2 is controlled by the *VTC2* promoter and its 5'-UTR/uORF, respectively. In the second approach, the VTC2-GFP is driven by the constitutive *CaMV35S* promoter (Figure 19D, E) not including the 5' UTR, thus lacking both transcriptional and translational control.

In order to investigate how differences in light intensity that translated into differences in ascorbate affect the content of SW proteins plants were grown for 7 weeks at 100 µmol m^{-2} s^{-1} (standard irradiance). Then, plants were transferred to low light intensity (57.5±2 µmol m^{-2} s^{-1}) and high light intensity (770±10 µmol m^{-2} s^{-1}) for 4 days and collected the samples half-way through the light period. As expected, high light caused an increase in ascorbate content in WT plants, from 1,25 µmol/g FW in low light to 2,4 µmol/g FW in high light. This 90% difference in ascorbate levels between high and low light indicated that these conditions were suitable for further analysis. We then analysed the ascorbate content and the protein levels of transgenic lines expressing GME-GFP, VTC4-GFP and L-GalDH-GFP. In addition to the GFP-tagged lines in mutant background, we analysed the content of the transgenic lines in WT background in order to discard differences at protein levels that might be caused for differences in gene copy number.

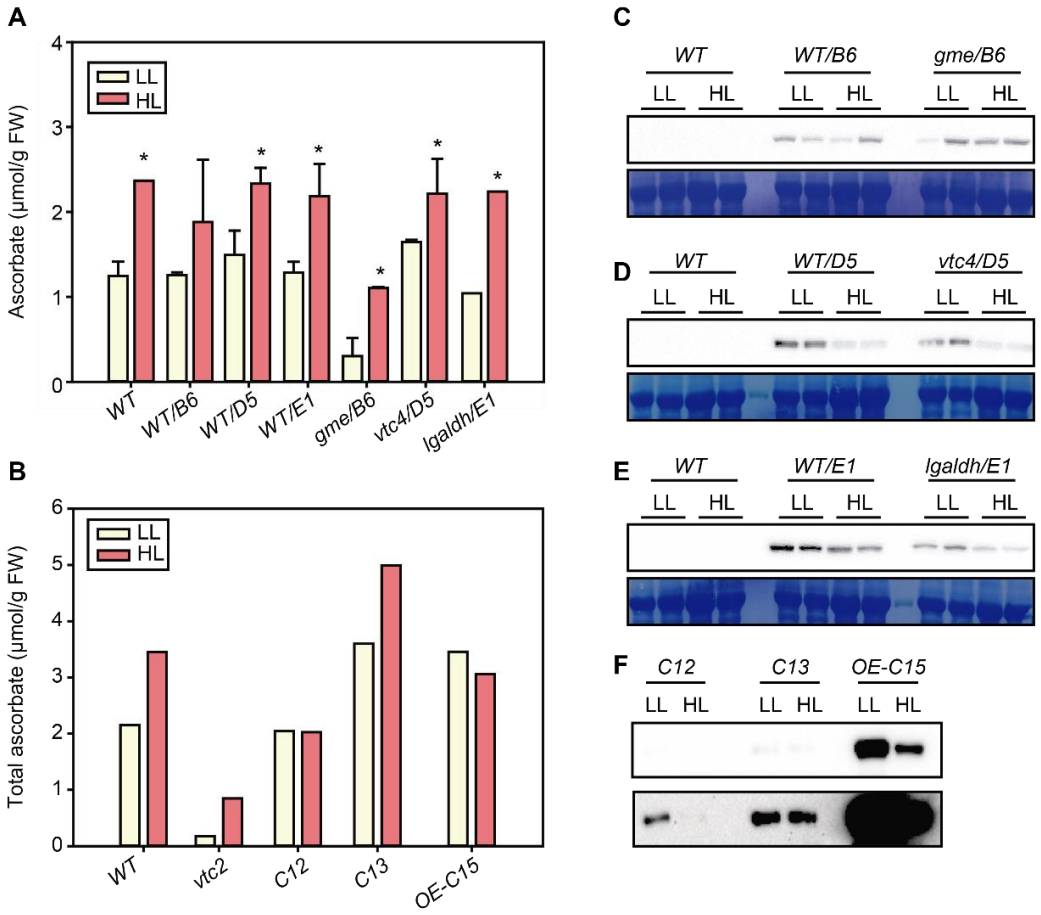

Figure 20. Effect of light intensity on the Arabidopsis transgenic lines generated in this work. Ascorbate levels increased up to 2-fold in response to high light (A, B). Mean and standard deviation are displayed (n=2) in A. Asterisks denote significant differences between low (LL) and high light (HL) based on confidence intervals (α=0.05). Values displayed in B represent ascorbate levels for 12-plants pools. C) α-GFP immunoblot shows that GME-GFP protein level did not change when grown under different light intensities. Two independent biological replicates are shown for each light treatment and genotype. D) α-GFP immunoblot shows that VTC4-GFP and L-GalDH-GFP (E) did respond to light intensity accumulating enzyme under high light. F, α-GFP immunoblot following VTC2-GFP concentration using GFP-Trap columns, above – 11s exposure, below – 1000s exposure. LL, low light. HL, high light. Asc, ascorbate. DHA, dehydroascorbate.

As shown in Figure 20A, most of the transgenic lines showed an ascorbate content between 1.3 to 2-fold higher in high light than in low light, similar to the increase shown by WT plants. The only exception was *gme/GME-GFP*, that showed 3,6-fold increase in ascorbate content under high light conditions.

For *VTC2*, we analysed five-week old plants of C12, C13 and OE-C15 at the same light conditions previously described. In addition to WT plants we also included *vtc2-4* (*vtc2*) in the analysis. At high light, WT and *vtc2* plants showed higher ascorbate content than plants grown at low light intensity (Figure 20B). Interestingly, ascorbate content of *vtc2* was 5-fold greater in high irradiance than in low irradiance, while WT plants showed a 1.6-fold difference. Therefore, ascorbate content in vtc2 mutants was 8% of WT under low irradiance but 25% under high irradiance. Surprisingly, C12 and OE-C15 lines did not increase the ascorbate content in high light conditions, suggesting that the activation of VTC2 in these lines was not happening properly. This is not the case for line C13, in which the ascorbate content was ~40% higher in high light thus behaving as WT plants.

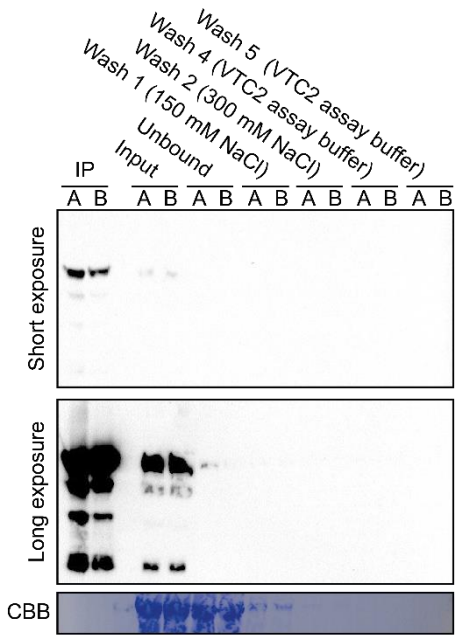

A - ~350 mg fresh tissue. Resuspended in 70,4 µL
B - ~260 mg fresh tissue. Resuspended in 52 µL

Figure 21. GFP-Trap column-mediated VTC2-GFP concentration from Arabidopsis OE-C15 line quality control. Two independent extracts from different amounts of tissue belonging to plants grown under high light intensity were performed from a single 12-plants pool.

To determine whether there is a correlation between the light-dependent ascorbate content and the amount of SW enzymes, we performed immunoblot analyses using GFP antibodies of protein extracts from the different lines previously analysed. When we analysed the expression of GME-GFP we did not find differences in the protein amount. This is somewhat expected because, in addition to ascorbate biosynthesis, GME has an essential role in the biosynthesis of cell wall polysaccharides. Surprisingly, VTC4-GFP and L-GalDH-GFP, two enzymes entirely dedicated to ascorbate biosynthesis, showed higher protein concentration when plants were grown under low light intensity (Figure 20D, E).

Our previous data, together with published data covered in the introduction, indicate that VTC2 is the main regulatory step on ascorbate biosynthesis (Chapter 1). Although VTC2-GFP is detected using a highly sensitive immunoblot detection system in crude extracts of the overexpressing lines (Figure 19E, Figure 20F), it did not provide enough sensitivity in lines in which *VTC2-GFP* is driven by its own promoter. Therefore, we first concentrated the VTC2-GFP protein of C12 and C13 lines using GFP-

Trap columns which allowed the detection of VTC2-GFP (Figure 20F; Figure 21). In addition to C12 and C13 lines we used the OE-C15 line as a control (Figure 20F, bottom panel). In order to further validate the functionality of VTC2-GFP fusion protein, we used extract A from immunoprecipitation showed in Figure 21 to measure the conversion of GDP-D-glucose into D-glucose 1-P by GC/MS (Figure 22). VTC2 catalyses the conversion of GDP-D-glucose into D-Glucose 1-P in a phosphate-dependent manner (Linster et al., 2007). The incubation of VTC2-GFP attached to α-GFP agarose beads used to concentrate this protein with GDP-D-glucose led to an increase of D-glucose 1-P concentration only in the presence of phosphate after 1 hour. Therefore, VTC2-GFP exerts its enzymatic activity not only *in vivo* but also *in vitro*.

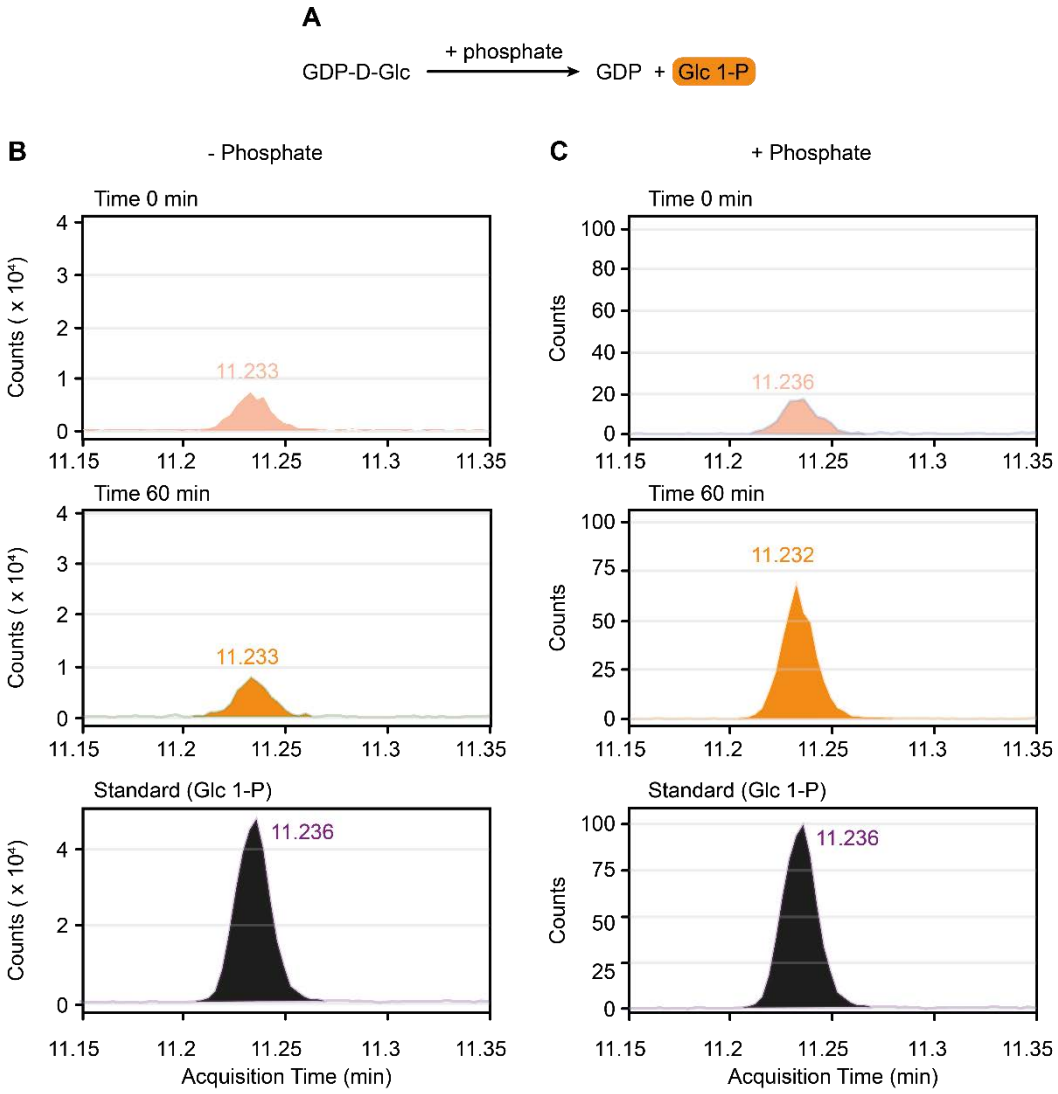

Figure 22. Immunoprecipitated VTC2-GFP shows enzymatic activity. A) VTC2 catalyses the conversion of GDP-D-glucose into D-glucose 1-P (Linster et al., 2007) in a phosphate-dependent manner. VTC2 enzymatic activity was measured as the increase in D-glucose 1-P eluted at the same retention time than the standard (bottom panel) by GC/MS. Reaction was measured at time 0 (prior to mock/phosphate addition) and after 60 minutes of mock (B) or phosphate (C) addition.

The concentration of VTC2-GFP was lower in plants exposed to high irradiance compared with those grown under low light intensity. This reduction of VTC2-GFP protein occurred regardless of the promoter driving VTC2-GFP expression and the response of ascorbate. The finding that C13 and OE-C15 presented similar amounts of ascorbate despite the significantly higher amount of VTC2-GFP in OE-C15 (Fig. 19E, F; 20F) suggests that the rise of ascorbate is dependent on an increased activity rather than on the content of VTC2. Since the reduction in the amount of VTC2 protein in response to light also occurs in the OE-C15, it is tempting to speculate that factors other than mRNA amount and translation are involved. Post-translational modifications such as phosphorylation could trigger an enhanced VTC2 activity given that the phosphorylated state of both, VTC2 and VTC5, was detected in all thirty tissues studied in the recently released Arabidopsis' phosphoproteome (Mergner et al., 2020). The phosphorylation occurs in a highly conserved N-terminal threonine among photosynthetic organisms' VTC2-like proteins (Figure 23). Its substitution by a serine residue, which is also a substrate for Ser/Thr kinases-mediated phosphorylation, occurs in some species of higher plants that also contain a Thr-containing copy, with the only exception of *Setaria italica*.

In summary, our results show that those enzymes exclusively dedicated to ascorbate biosynthesis such as VTC2, VTC4 and L-GalDH, decrease their protein content when growing at high light intensity. These results are rather unexpected but are compatible with a high irradiance-induced VTC2 increased activity reported in previous studies (Dowdle et al., 2007), which adds a new layer of regulation of VTC2. Further studies of the enzymatic activities are needed in order to shed light on the regulation of this pathway in response to different light conditions.

VTC2-GFP accumulates during the day and falls after entering the dark period

Previously, we analysed the responses of ascorbate and protein amount of VTC2 to different light intensities. Considering that previous studies showed that VTC2 maximum enzymatic activity takes place a few hours after the transcript curve peaks during the light period (Dowdle et al., 2007), we aimed to investigate the responses of ascorbate and VTC2 protein amount of during a day/night cycle. During the light period, the transcript levels of *VTC2* and enzyme activity vary despite growing under constant light intensity. Using available expression data (http://bar.utoronto.ca/; Michael et al., 2008), *VTC2* shows dramatic changes in expression during short days (8 hours light, 16 hours dark) (Figure 24). The maximum of *VTC2* expression occurs around 4 hours into the light period and then decreases ~4-fold at the end of the light-beginning of the night period. Therefore, we hypothesized that the high expression of *VTC2* in light could result in higher protein content.

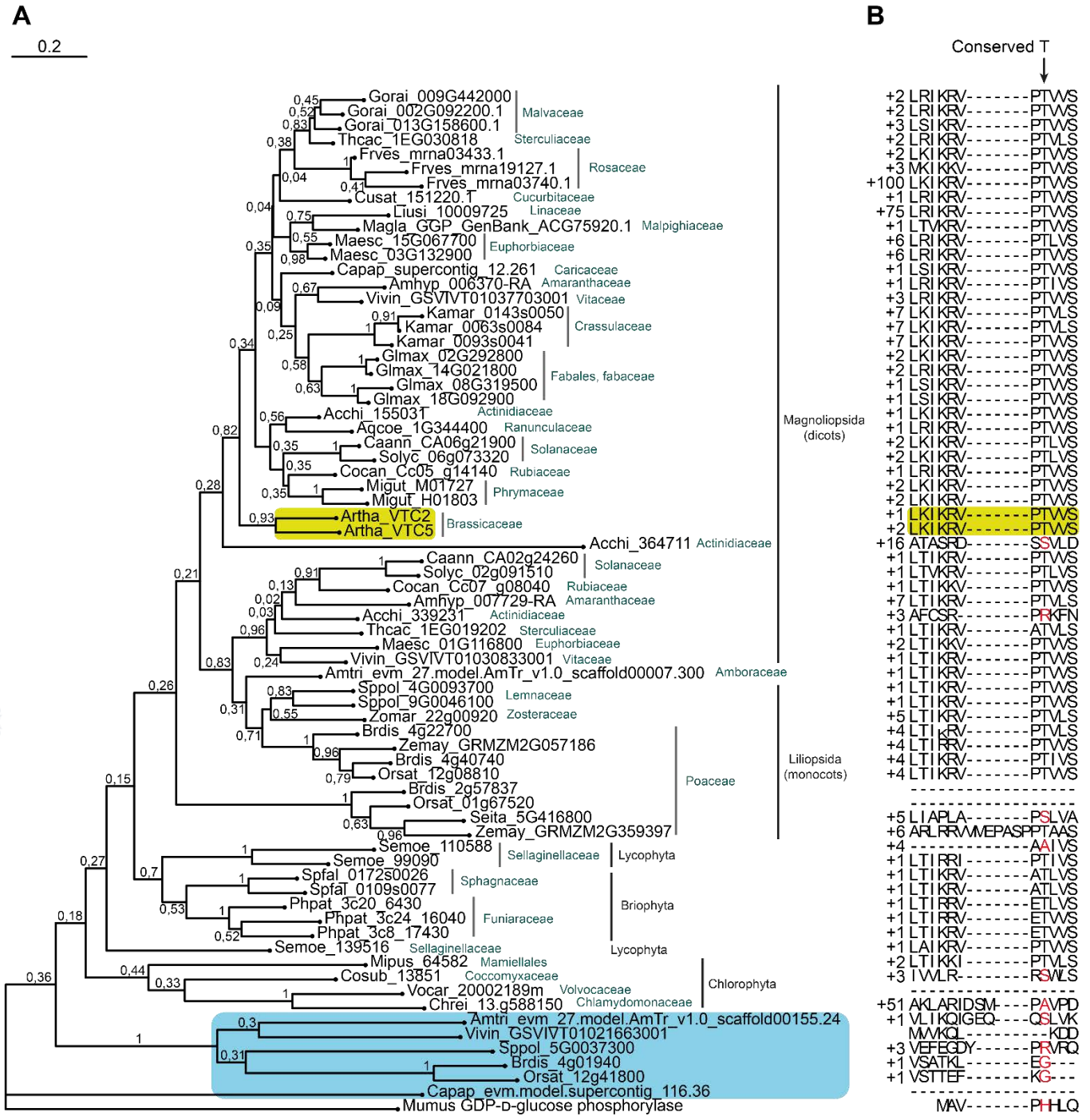

Figure 23. Arabidopsis VTC2 N-terminal threonine is highly conserved among photosynthetic organisms. The evolutionary history was inferred by using the Maximum Likelihood method and JTT matrix-based model (Jones et al., 1992). The tree with the highest log likelihood (-35643.28) is shown. A) Evolutionary analysis by Maximum Likelihood method. The percentage of trees in which the associated taxa clustered together is shown next to the branches. Initial tree(s) for the heuristic search were obtained automatically by applying Neighbor-Join and BioNJ algorithms to a matrix of pairwise distances estimated using the JTT model, and then selecting the topology with superior log likelihood value. This analysis involved 71 amino acid sequences. There was a total of 985 positions in the final dataset. Numbers at the nodes are bootstrap values (0-1). B) Multiple alignment of the various species' N-terminus of all proteins used in this study (see Appendix 8) show that threonine (arrow at the top), its position and its aminoacidic context are highly conserved. Substitutions of threonine by serine (S), which is also a substrate for Ser/Thr Kinases. Only *Setaria italica* (Seita) presents one Ser-containing sequence but not Thr. Blue-shaded sequences refer to outgroups with large dissimilarities to VTC2. All species containing these sequences also had a copy highly similar to VTC2. The number of N-terminal aminoacids preceding the sequence displayed are indicated at the beginning of the alignment. Evolutionary analyses were conducted in MEGA X (Kumar et al., 2018).

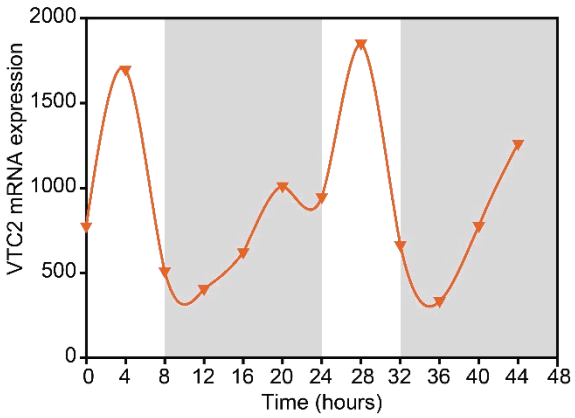

Figure 24. VTC2 expression during two light/dark cycles in short day conditions. Data extracted from Michael et al., 2008.

First, we measured ascorbate (Figure 25) and total ascorbate levels (Figure 26) at different time points along the day focussing on the light/dark transition period. We used 5-week-old WT, *vtc2*, C12, C13, OE-C15 and OE-C16 plants growing at short days (8h light/16h dark). Ascorbate contents of WT and *vtc2* plants were barely altered during the entire light/dark cycle (Figure 25A) even though there was a large difference in the amount of ascorbate between these two lines. Line C12 showed a similar pattern and ascorbate remained constant. The level of ascorbate of line OE-C16 was similar to that of WT plants (Figure 25C) while lines C13 and OE-C15 contained higher content of ascorbate during the light period (Figure 25A, C), despite substantial differences in the content of VTC2-GFP (Figure 19E). Immediately after entering the dark period, the high VTC2 expressing lines C13, OE-C15 and OE-C16, underwent a decrease in ascorbate level (Figure 25A, C) and it remained steady until the end of the night with similar values to WT. We then measured total ascorbate, which included ascorbate and its oxidised forms (monodehydroascorbate and dehydroascorbate) and normalised the values to that measured at time 0.5 hours. Total ascorbate increased during the day and accumulated by the end of the light period in WT and *vtc2* (Figure 26A, B) as previously described (Dowdle et al., 2007). During the dark period, total ascorbate decreased within the first 30 minutes and increased until the middle of the night (Figure 26A, B). Similarly, line C12 followed this pattern with an early drop of total ascorbate content during the light period, and a more acute increase at the beginning of the night (Figure 26C). However, in those lines with high expression of VTC2-GFP, total ascorbate did not change during the day (Figure 26D, E, F), while the evolution of total ascorbate during the dark period was similar to WT. Noticeably, the evolution pattern of total ascorbate of the lines with high expression of VTC2-GFP mirrored that of ascorbate, meaning that these variations solely depended on ascorbate and not on its oxidised forms.

We then determined the content of VTC2-GFP protein in the transgenic lines using immunoblot analysis. As shown in Figure 25, VTC2-GFP accumulated towards the end of the light period in all lines, including those driven by their own promoter (Figure 25B) and driven by the 35S (Figure 25D). Additionally, VTC2-GFP protein amount decreased shortly after the light/dark transition, independently of the promoter driving the expression of *VTC2*. These results suggest that the amount of VTC2 is dependent on its stability (i.e., on its

degradation) rather than translational regulation. Despite ascorbate levels and the amount of VTC2-GFP did not perfectly correlate during the light period (Figure 25), lines with high expression of VTC2-GFP showed that ascorbate and total ascorbate changed according to protein amount, in the night period (Figure 26).

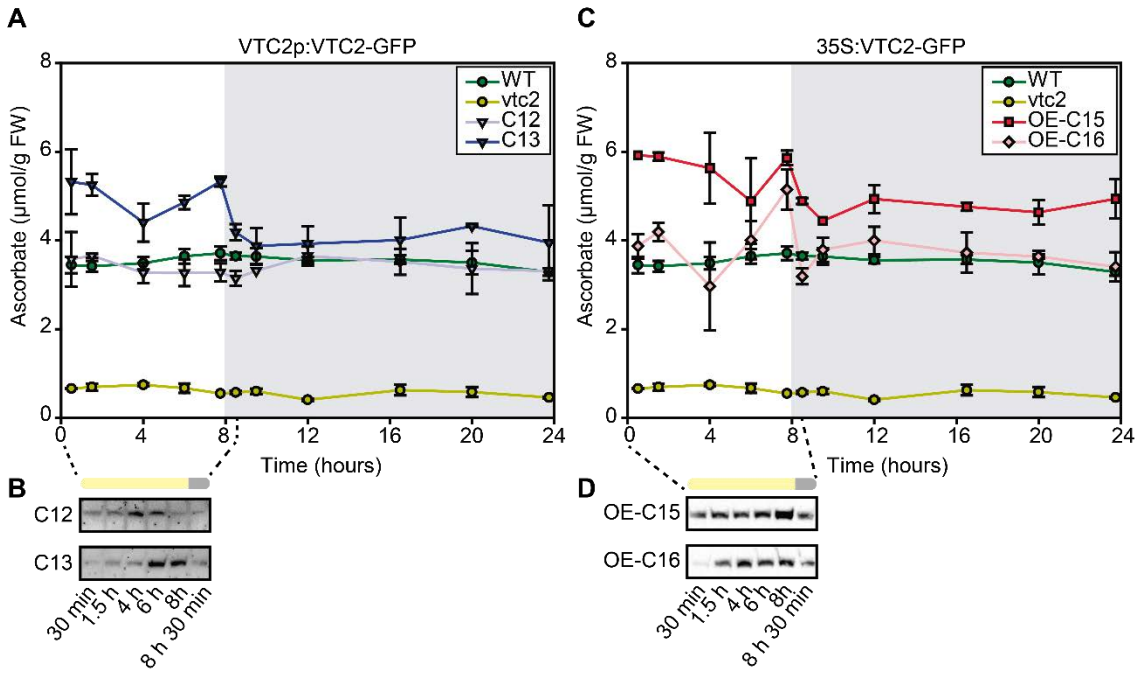

Figure 25. Evolution of ascorbate (A, C) and protein (B, D) concentration along a short day in Arabidopsis transgenic lines expressing VTC2-GFP under the control of VTC2 promoter (A, B) or 35S promoter (C, D). Wild type and *vtc2* plants were also included as controls. The shaded area represents the night period. Ascorbate data showed represent mean±SD (n=2).

Interestingly, VTC2-GFP in line C12, which virtually behaves like WT plants, only correlated to the concentration of total ascorbate. The fact that during the dark period the transgenic lines presented roughly WT levels of ascorbate supports that the activity and not the amount of VTC2-GFP determines the production of ascorbate.

Proteasomal regulation of proteins involved in ascorbate biosynthesis

Using available expression data, we analysed the expression at the transcriptional level of the last five genes of the pathway, i.e., *GME*, *VTC2*, *VTC4*, *L-GalDH* and *GLDH* genes in plants grown under long day conditions (16h light/8h dark). Interestingly, all genes encoding cytoplasmic proteins showed differential expression throughout the day except for *GLDH* (Figure 27A). Genes that encode cytosolic proteins showed one peak in their expression except *VTC2,* with two peaks of expression, at 4 and 16 hours in the day period. Remarkably, at 4 hours of into the light period, the expression of all genes showed a change in their tendency. Although there are differences in the amplitude of the changes, *VTC4* and *GME* showed opposed expression patterns with peaks at 4 and 24 hours. *L-GalDH* expression increased during the light period peaking at 8 hours in the

daytime. These genes showed day/night rhythmicity and it is known that *VTC2* is controlled by the circadian oscillator. Using available data (Covington and Harmer, 2007) we found that in addition to *VTC2*, the expression of *VTC5* and *L-GalDH* also showed a circadian regulation (Figure 27B, C).

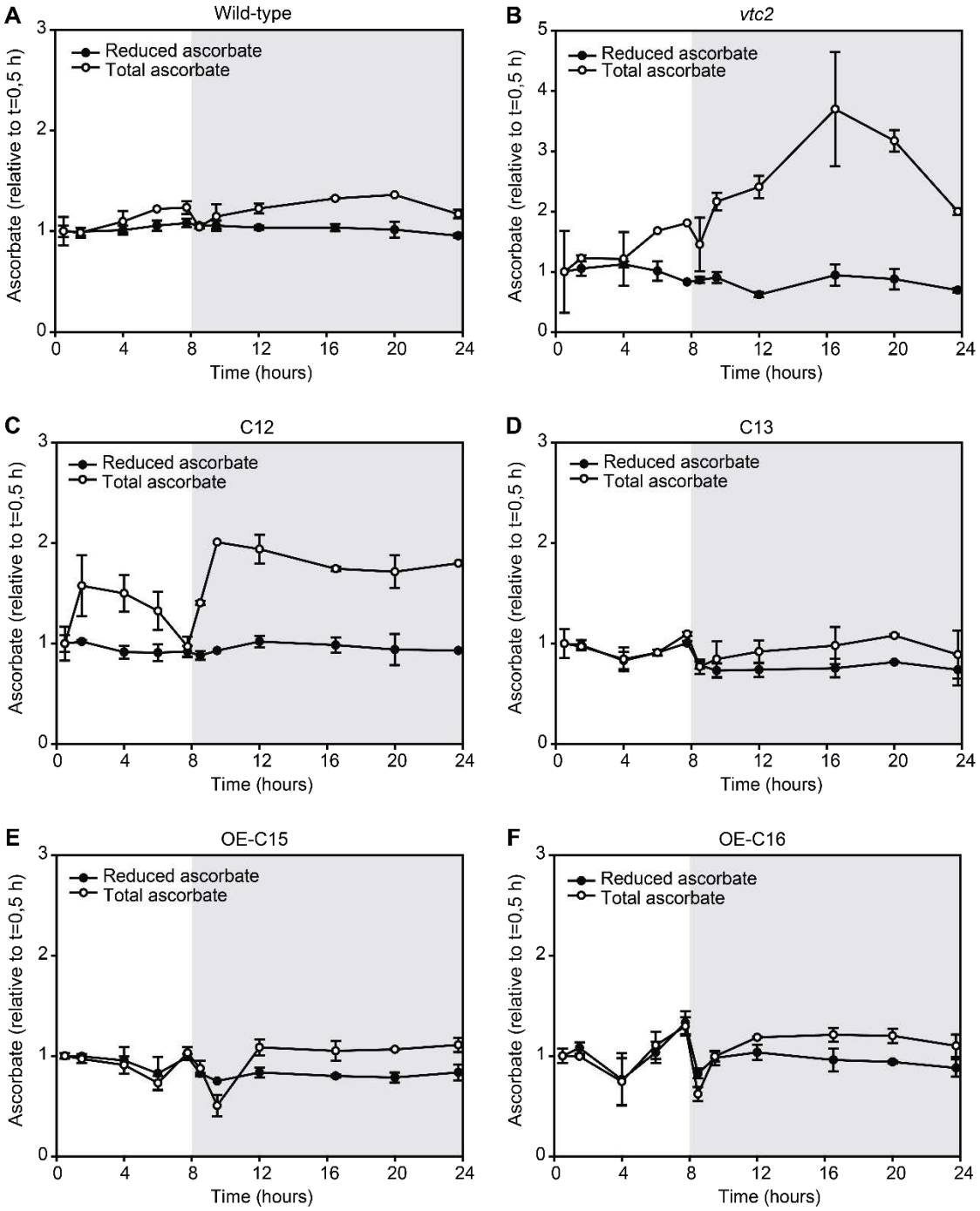

Figure 26. Evolution of ascorbate and total ascorbate (i.e., ascorbate + MDHA + DHA) in a normalised scale along a short day in Arabidopsis transgenic lines expressing VTC2-GFP under the control of VTC2 promoter (C, D) or 35S promoter (E, F). Wild type (A) and *vtc2* (B) plants were also included as controls. The shaded area represents the night period. Ascorbate data showed represent mean and SD (n=2). Values are normalised to that measured at time 0.5 hours.

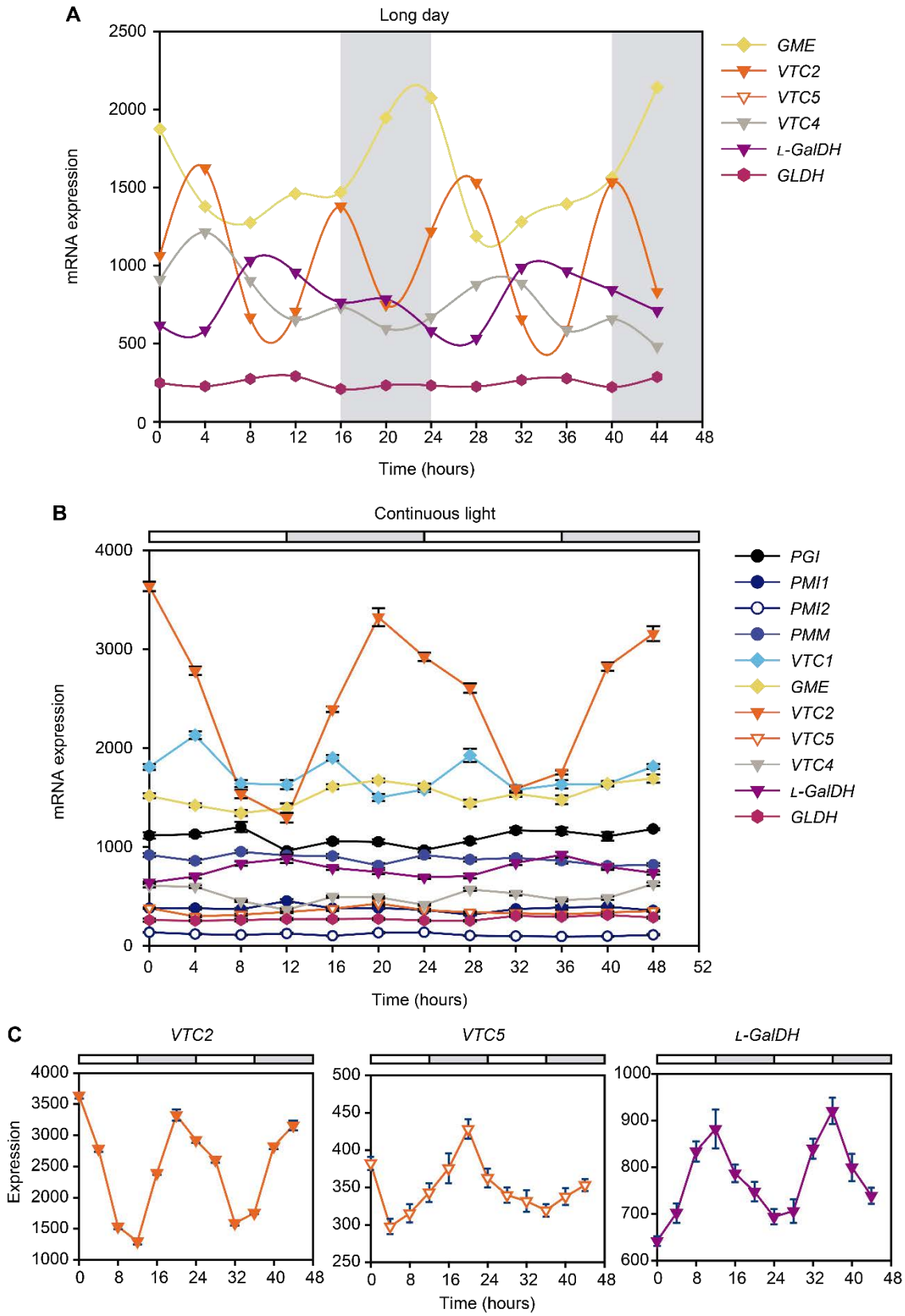

Figure 27. The expression of the Smirnoff-Wheeler genes shows day/night rhythmicity. A) Ascorbate biosynthesis genes expression for two light/dark cycles under long day conditions (extracted from Michael et al., 2008). B) Gene expression of the SW genes in seedlings entrained in 12-h white light (light source was cool white fluorescence tubes; fluence rate ~120 µmol m^{-2} sec^{-1})/12-h dark cycles for 7 d before being released into free-running conditions of continuous white light at 22 °C. Starting at subjective dawn of day 9, tissue was harvested every 4 h over the course of the next 44 h. C) *VTC2*, *VTC5* and *L-GalDH* are considered circadian regulated according to Covington and Harmer (2007) (pMMC-β < 0.05 and 19 ≤ period ≤ 29 h). Data extracted from (Covington and Harmer, 2007).

Protein stability has previously been shown to affect ascorbate biosynthesis. More specifically, VTC1 degradation requires the photomorphogenic factor CSN5B for protein degradation through the 26S proteasome pathway in the dark (Wang et al., 2013). VTC2-GFP accumulates at the end of the day and that its content is reduced after entering the dark period. The finding that this reduction also occurs in lines lacking the translational regulator 5'-UTR/uORF suggests that protein stability is important for the regulation of VTC2. Therefore, we investigated whether a similar mechanism could be also playing a role in the regulation of the stability of other ascorbate biosynthesis proteins such as GME, VTC2, VTC4 and L-GalDH using the transgenic lines previously developed (Figure 19C, D).

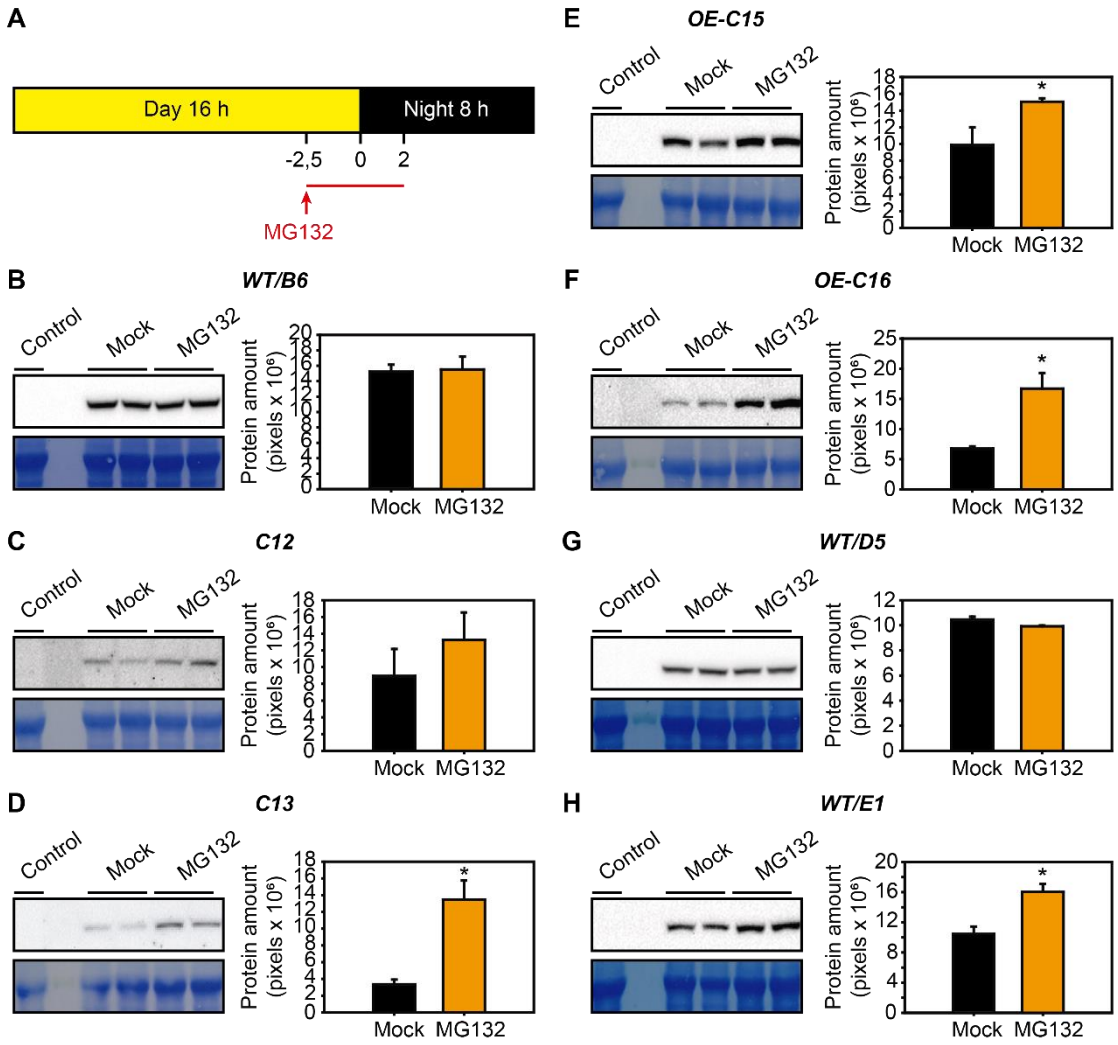

Figure 28. Proteasome inhibitor MG132 leads to the accumulation of VTC2 and L-GalDH in Arabidopsis transgenic lines during the dark period. A) 12 days-old seedlings were submitted to 4,5 hours of 10 µM MG132 treatment in liquid half-strength MS after three days of acclimation or the equivalent volume of DMSO (Mock), starting 2,5 hours prior to the beginning of the dark period. B-H) Immunoblot (α-GFP) and its quantification using Fiji (Schindelin et al., 2012; Schneider et al., 2012) of two independent replicates consisting of at least 30 seedlings under mock and MG132 treatment at the end of the 4,5 hours of treatment of the various transgenic lines generated in this thesis. Arabidopsis transgenic lines used in this assay are described in Figure 19. Bar charts display mean+SD. Statistical significance (*) was inferred from confidence intervals (α=0.05) due to the difference between standard deviations.

Ten-days old seedlings were grown in solid media and transferred to liquid media for three days for acclimation in long day conditions to maximise biomass yield in a shorter time on plates. Two and a half hours prior to the beginning of the dark period, seedlings were treated either with DMSO (mock) or with 26S proteasome inhibitor MG132 and collected duplicated samples after two hours into the dark period (Figure 28A). Immunoblot analysis showed that proteasome inhibition did not affect the amount of GME or VTC4 protein (Figure 28B, G). However, VTC2-GFP and L-GalDH-GFP showed protein accumulation in the presence of MG132, supporting that these proteins are regulated by the proteasome (Figure 28C, D, E, F, H). Particularly striking was the 4-fold increase after MG132 treatment compared to mock in seedlings of L16 line in which *VTC2* expression is driven by its own promoter (Figure 28F). The finding that *VTC2* lines driven by the constitutive 35S promoter also increase the amount of protein in the presence of MG132 further supports that VTC2 is regulated by the proteasome. Taken together, our results indicate that GME and VTC4 are not regulated by the 26S proteasome while L-GalDH showed a 1,5-fold increase after proteasome inhibition by MG132. Interestingly, inhibition of the proteasome caused a significant increase in the content of VTC2 (between 3-4-fold) regardless the promoter driving *VTC2* expression or the presence of the 5'-UTR/uORF.

Discussion

High light intensity leads to oxidative stress caused by ROS produced as a consequence of the Mehler reaction during photosynthesis. This oxidative stress is reduced by ascorbate in the Foyer-Asada cycle (Asada, 1999). In this study we have investigated the response to light of all *sw-mutant*/*SW-GFP* transgenic lines generated in this work using different approaches. High light treatment of the transgenic lines, which caused an increase in ascorbate content, paradoxically led to a decrease of VTC2, VTC4 and L-GalDH content, which are enzymatic steps of the SW pathway committed to ascorbate biosynthesis. In contrast, GME, whose product is also involved in non-cellulosic cell wall polymers and glycoprotein biosynthesis, did not change its concentration. Interestingly, the proportion of ascorbate increase due to higher light intensity was similar (~2-fold) among lines except in those containing lower contents of ascorbate than WT (i.e., *gme/GME-GFP* and *vtc2*), which exhibited a more pronounced increase of ascorbate in high light (~3.5 and 5-fold, respectively). This suggests that other mechanisms different from biosynthesis, such as recycling or reduced degradation of ascorbate, are contributing to compensate ascorbate deficiency.

VTC2 is translationally regulated by an upstream open reading frame located within its 5'UTR (Laing et al., 2015). VTC2 showed a consistent pattern of protein accumulation during the light period followed by a sharp decrease immediately after entering the dark period (within 30 min), that do not correlate with the ascorbate content. However, total ascorbate showed a better correlation

with the amount of VTC2 protein, suggesting that the biosynthesised ascorbate is rapidly oxidised thus keeping a stable level of ascorbate but increasing that of total ascorbate. Considering these results, light and the day/night cycles have an impact in the concentration of ascorbate biosynthesis enzymes, likely because under low light intensity the requirement of ascorbate supply to scavenge ROS is lower than under high irradiance. Therefore, it is possible that the decrease of ascorbate biosynthesis in the dark is the result of the reduction of VTC2 activity. caused by post-translational modifications of the protein through phosphorylation. However, our data support that proteasomal regulation of VTC2 concentration is an important regulatory control point. It has been previously described that VTC1 degradation is promoted by COP9-signalosome subunit 5B. As a consequence, *csn5b* mutant has 30% more ascorbate content than WT plants due to a higher concentration of VTC1 (Wang et al., 2013). However, under the growing conditions set in our laboratory and according to a simulation analysis of metabolic control of ascorbate biosynthesis (Figure 10; Figure 18), the increase of VTC1 protein amount and enzymatic activity do not lead to an increase in the content of ascorbate. The fact that the CSN complex also regulates VTC2 protein amount becomes a plausible possibility since an additional biochemical evidence brings to the table a putative coordinated regulation of VTC1 and VTC2 in the cell wall biosynthesis of non-cellulosic compounds. The convergence of ascorbate and cell wall precursors biosynthetic pathways has been extensively covered in the introduction of this thesis. However, the fact that VTC1 catalyses the conversion of D-glucose 1-phosphate into GDP-D-glucose in the presence of Mn^{2+} (Jamil, 2018) was not discussed. GDP-D-glucose is involved in the biosynthesis of cell wall glucomannans (Liepman et al., 2005). The reverse reaction to that described by Jamil (2018) for VTC1, i.e., the conversion of GPD-D-glucose into D-glucose 1-P, is known to be catalysed by VTC2 (Linster et al., 2007). The opposition between these two enzymatic activities would need a coordinated regulation of these two proteins leading to the activation/deactivation of cell wall biosynthesis regulated by VTC1 and VTC2, respectively. Therefore, we proposed the alternative hypothesis by which the increased ascorbate content in *csn5b* mutant could be due to an accumulation of VTC2. Furthermore, the CSN complex also regulates the circadian function in *Neurospora* (Z. Zhou et al., 2012) so VTC2 protein stability, similarly to mRNA expression, might be regulated by the circadian clock. Alternatively, but also suggesting the importance of the circadian clock in VTC2 stability, previous yeast two-hybrid screening identified a PAS/LOV (Light-Oxygen-Voltage) protein as an interactor of both VTC2 and VTC5 whose interaction was diminished under blue light (Ogura et al., 2008). A LOV domain containing blue-light photoreceptor is also found in ZEITLUPE (ZTL), a protein regulator of the circadian oscillator (Más et al., 2003). Its interaction with TOC1, another circadian regulator, triggers TOC1 degradation in the dark, which can be stabilised by a proteasome inhibitor (Más et al., 2003). Therefore, it is possible that ZTL could be promoting VTC2 degradation in the dark hence increasing the control of the circadian clock over ascorbate concentration. Supporting this

hypothesis, L-GalDH, whose gene expression also displays circadian rhythm (Figure 27C; Covington and Harmer, 2007), also accumulated upon proteasome inhibition. Moreover, GME and VTC4, whose gene expression did not display circadian rhythm, were not affected by proteasome inhibitor treatment (Figure 28).

To conclude, in this chapter we have characterised the response of the ascorbate biosynthesis pathway and the protein level and the dynamic of VTC2, the main regulator of the pathway in response to high light conditions and during the day/night cycle. Here, we have shown that high irradiance leads to a reduced concentration of ascorbate biosynthesis enzymes (Figure 20) and that the accumulation of VTC2 does not necessarily correlates with higher ascorbate content (Figure 19E). Furthermore, we have shown that the proteasome is an important determinant of VTC2 protein stability whose interaction potentially opens a new approach on engineering VTC2 stability to increase ascorbate in crop plants. This could lead to increased tolerance to a number of abiotic stresses (Akram et al., 2017) such as salinity (Wang et al., 2013; Zhang et al., 2012) and oxidative stress in crops of interest (Cai et al., 2016; Fenech et al., 2019; Hu et al., 2016). Other positive aspects on identifying regulatory mechanism of ascorbate accumulation are improving nutritional value, enhancing post-harvesting preservation of nutritional properties and extending fruit shelf life (Antunes et al., 2013; Stevens et al., 2007).

CONCLUSIONS

1. In this thesis we have developed a set of tools consisting of *Arabidopsis thaliana* mutants in the SW genes complemented with their respective enzyme fused to GFP whose expression is driven by its own promoter.

2. Molecular analysis of the transgenic lines generated in this work have provided information on the expression of SW enzymes downstream of VTC1. While GME and VTC4 show detectable expression, the levels of VTC2 proteins are hardly detectable supporting a regulatory role.

3. Metabolic engineering studies reveal that only the overexpression of *VTC2* leads to a biologically significant increase of ascorbate concentration, which is further enhanced by the coexpression with *GME*.

4. Overexpression of the whole SW pathway in *Nicotiana benthamiana* supports the lack of substrate limitation during the biosynthesis of ascorbate, at least, downstream from VTC1.

5. Metabolic Control Analysis performed using the available kinetics data on SW proteins supports that VTC2 provides the most relevant activity controlling ascorbate concentration and ascorbate feedback inhibition.

6. All ascorbate biosynthesis enzymes localise in cytosol and nucleus, except GME, which only locates in cytosol after transient overexpression in *N. benthamiana*. This is further supported by the confocal analysis of the *A. thaliana* complemented transgenic lines.

7. The protein-protein interaction studies performed in *N. benthamiana* suggest that the cytosolic enzymes associate in an indirect manner pointing to the formation of an enzymatic complex assembly.

8. Ascorbate concentration does not correlate with the protein concentration under high and low light intensities in *A. thaliana* since, with the exception of GME, the amount of cytosolic enzymes were lower in high light than in low light.

9. VTC2 accumulates during the day and decrease after 30 minutes after entering the dark period. This regulation of VTC2 stability after entering the dark period is determined by the proteasome.

10. The dynamics of ascorbate concentration during a day/night cycle does not correlate well to VTC2-GFP amount, although dehydroascorbate does.

MATERIAL & METHODS

Plant material

Arabidopsis thaliana (L.) Heynh wild-type (WT) and transgenic lines generated were in Col-0 ecotype. Arabidopsis mutants *vtc2-4* (SAIL_769_H05; Lim et al., 2016), *vtc4-4* (SALK_077222; Torabinejad et al., 2008) and *gldh* (SALK_060087; Pineau et al., 2008) used in this study have been previously described. However, to the best of our knowledge, this is the first time that SALK_150208 (here named *gme-3*) and SALK_056664 (here named *lgaldh-1*), obtained from the European Arabidopsis Stock Centre (NASC: http://arabidopsis.info/), were described (M&M Table 1). Diagnostic PCR was performed to identify the presence of T-DNA insertion in individuals plants using the allele-specific primers listed in M&M Table 2A. The generation of transgenic lines either in WT or in the respective mutant backgrounds is described in the "Generation of transgenic lines" section and lines are listed in (M&M Table 1).

M&M Table 1. Arabidopsis mutants and lines used in this work.

Line	Background	T-DNA	Reference
WT	Col-0		-
gme-3	Col-0	SALK_150208	-
vtc2-4	Col-0	SAIL_769_H05	Lim et al., 2016.
vtc4-4	Col-0	SALK_077222	Torabinejad et al., 2009.
lgaldh-1	Col-0	SALK_056664	-
gldh	Col-0	SALK_060087	Pineau et al., 2008.
Transgenic lines			
GME-GFP L6	Col-0	GMEp:GME-GFP line 6	This work
VTC4-GFP L5	Col-0	VTC4p:VTC4-GFP line 5	This work
L-GalDH-GFP L1	Col-0	L-GalDHp:L-GalDH-GFP line 1	This work
Complemented mutants			
gme/GME-GFP L6	*gme-3*	GMEp:GME-GFP line 6	This work
vtc2/VTC2-GFP L12	*vtc2-4*	VTC2p:$_{CDS}$VTC2-GFP line 12	This work
vtc2/VTC2-GFP L13	*vtc2-4*	VTC2p:$_{CDS}$VTC2-GFP line 13	This work
vtc2/VTC2-GFP OE-L15	*vtc2-4*	35Sp:$_{CDS}$VTC2-GFP line 15	This work
vtc2/VTC2-GFP OE-L16	*vtc2-4*	35Sp:$_{CDS}$VTC2-GFP line 16	This work
vtc4/VTC4-GFP L5	*vtc4-4*	VTC4p:VTC4-GFP line 5	This work
lgaldh/L-GalDH-GFP L1	*lgaldh-1*	L-GalDHp:L-GalDH-GFP line 1	This work

Standard growth conditions

Arabidopsis seeds were surface sterilized using chlorine gas by pouring 3 mL of 37% HCl into 100 mL of commercial bleach and airtight sealed for 4 hours. Then, seeds were air-cleared for at least 4 hours in a laminar flow cabinet and stored at 4ºC for 3-days stratification. Seeds were sowed on half-strength Murashige-Skoog (MS) agar-solidified (0.6% [w/v] agar) medium supplemented with 1,5% [w/v] sucrose under sterile conditions and grown with a long-day photoperiod (16-h light/8-h darkness cycle, 22±1 ^{o}C, 150±50 µmol photons m^{-2} s^{-1}) for 7-10 days. Seedlings were then collected for analysis, transferred to liquid media or to soil (4:1 (v/v) soil:vermiculite).

M&M Table 2. Oligonucleotides used in this work.

A. Oligonucleotides used as primers in diagnostic PCR. LB: Left Border primer; LPa/b: Left Primer; RPa/b: Right Primer

Gene	Mutant line	LB	LPa	RPa	Tm
GME	SALK_150208	LBb1.3	TCACCGTGAGTGATCCCTAAC	TGCTTGGATCAACTTAGGTGG	60
VTC2	SAIL_769_H05	LB1	CTTCCGATCTCCTCTTTCTCG	GAGGCAAGCAGTCAAGAACAC	55
VTC4	SALK_077222	LBb1.3	GGCAGAAGCAGTAGACGATTG	TCACACCAAATGCAGCTGTAG	60
L-GalDH	SALK_056664	LBb1.3	CTGTGAGACAGAGCTCATCCC	AAAGGCTTTGCAAGTCCCTAG	60
L-GalLDH	SALK_060087	LBb1.3	GAAGCTTGTTTTGTGGCTCTG	CTAGCAAGACAGCCACAAACC	60

LBb1.3: ATTTTGCCGATTTCGGAAC
LB1: GCCTTTTCAGAAATGGATAAATAGCCTTGCTTCC
VTC4 RPb: TGAGTTTGTTTTCTTTCTACCGAA
L-GalDH LPb: CACAATGACACAACAACGAATGC

Primers VTC4 RPb and L-GalDH LPb were used to genotyping the mutant background when it was complemented with the GFP-tagged sequence to avoid crossed-amplification with the GFP-tagged cassette

Gene	Forward primer	Reverse primer	Tm
B. Oligonucleotides used as primers to amplify **genomic fragments** from Arabidopsis thaliana's genomic DNA			
GME	**CACC**TGCTTCCATCACGTTCTGTTT	CTCTTTTCCATCAGCCGCG	
ProVTC2	AAGCTTACCGAACGAACGATGGTAGTCA	AAGCTTCATTCTCAAAAAAGACAAATTTCG	57 °C
VTC4	**CACC**GAGAAGGAGTTGGATCACCGA	TGCCCCTGTAAGCCGCAA	
L-GalDH	**CACC**CAAGGTGCAAAGGTCAGTGC	GTTCTGATGGATTCCACTTGGC	
C. Oligonucleotides used to amplify the gene of interest's **CDS** from Arabidopsis cDNA			
VTC1	**CACC**ATGAAGGCACTCATTCTTGTTGG	CATCACTATCTCTGGCTTCAAGATG	
GME	**CACC**ATGGGAACTACCAATGGAACAGA	CTCTTTTCCATCAGCCGCG	
VTC2	**CACC**ATGTTGAAAATCAAAAGAGTTCCGACC	CTGAAGGACAAGGCACTCGG	59 °C
VTC4	**CACC**ATGGCGGACAATGATTCTCTAGA	TGCCCCTGTAAGCCGCAA	
L-GalDH	**CACC**ATGACGAAAATAGAGCTTCGAGC	GTTCTGATGGATTCCACTTGGC	
L-GalLDH	**CACC**ATGCTCCGGTCACTTCTTCTC	AGCAGTGGTGGAGACTGGG	

CACC was added to the 5' end of forward primers as a requirement to clone in pENTR/D-TOPO vector (except VTC2)

CACC was added to the 5' end of forward primers as a requirement to clone in pENTR/D-TOPO vector

Gene	Forward primer	Reverse primer	Tm
D. Oligonucleotides used to perform **colony PCR**			
	See M&M Table 2B	**See** M&M Table 2B). Also: GFP Rv: GAACAGCTCCTCGCCCTTG GFP Rv2: TGCTCAGGTAGTGGTTGTCG	59 ºC

E. Oligonucleotides used for DNA sequencing in addition to B and D	
VTC1	ATGAAGGCACTCATTCTTGTTGG
	CTTGATGGATCTGGAGAGC
	GGGTTTGAGACTCTACTTAGACTC
GME	GTTTGGTGCACCAATAAAGAAAAT
	GGTTTTAAAATCCCAGATTCCTG
	AACAGATTTGTTTTGCAATTTTG
	GAGTTCCATCTTGTTGATCTTAG
	CTCAAGATGCTTATGGTTTGG
	GGAAGCGATGAGATGGTGA
VTC4	CGGCCCATATTCAGAATAAGG
	CGACATTGATTTGACGCAG
	TCCTCGCGTTGATCATTAGAG
	GGTGTCCAAGGGAAAGG
	AGGTCAGGTCCCTTAGGAT
L-GalDH	GAGTTAAAATAATGTCGTTTCCATTG
	GCTTTCCGTCTCGGTATCAA
	TGTCTCAAACCTTTACTAAGTGTTC
	GGCAGGTTAAATTCTATAGATGCT
	GGTTTGTTCTCTGTTTGATATTTTG
L-GalLDH	CTCAGAAGCTCAATTCCGTAAA
	CATTAGAGAGCAGCAGATTGG
	TTTCTGCGTATGAACATTGGG

Plasmid Constructs

Two different types of DNA fragments were used as templates (genomic and coding DNA sequence) to generate the constructs used in this work. First, genomic fragments were amplified starting from at least 2 kb upstream the +1 ATG unless otherwise specified (Figure 5) until the stop codon (not included) using genomic Col-0 DNA as template. Second, coding DNA sequences (CDS) were amplified, starting at +1 ATG until the stop codon (not included), using as template Col-0 Arabidopsis cDNA that was generated using total RNA. In the case of VTC2, due to a failure in amplifying the entire VTC2p:VTC2 product, about 1.4 kb (according to Gao et al., 2011) of the VTC2 promoter including the 5'UTR was amplified (Figure 5; M&M Table 3). The primers used to generate these above-mentioned DNA fragments are detailed in M&M Table 2B and 2C. A proofreading DNA polymerase was used for all these PCR amplifications (TAKARA PrimeSTAR Max DNA Polymerase, CAT. #R045A).

M&M Table 3. Summary of the constructs used in this work.

A. Sizes of constructs generated in this work using the vectors listed in B)

Construct	Size	VTC1	GME	VTC2	VTC4	L-GalDH	GLDH
Genomic	bp	-	3680	ProVTC2: 1421	4172	3727	-
CDS		1083	1131	1326	813	957	1830
C'-GFP	kDa	68,6	71,8	78	58,2	63,6	97,6
C'-HA		46	49,2	55,4	35,5	40,9	75

B. Vectors used in this work and the resulting construct

Name	Vector type	Final construct (selective marker)
pENTR/D-TOPO	Entry	attL1::GeneX::attL2 (Kan^R)
pGWB4	Expression	PromoterX::GeneX-GFP (Kan^R/Hyg^R)
pGWB5	Expression	CaMV35S::GeneX-GFP (Kan^R/Hyg^R)
pGWB504	Expression	VTC2p:$VTC2_{CDS}$-GFP (Kan^R/Hyg^R)
pGWB14	Expression	CaMV35S::GeneX-HA (Kan^R/Hyg^R)
pGADT7	Y2H prey	ADH1::AD-GeneX (Kan^R/Leu^+)
pGBKT7	Y2H bait	ADH1::BD-GeneX (Kan^R/Trp^+)

VTC2 promoter was digested with HindIII and directly cloned into the pGWB504 vector. All other DNA fragments (excluding VTC2 promoter) were cloned into pENTR/D-TOPO using the pENTR Directional TOPO cloning kit (Invitrogen). Next, on the one hand, DNA genomic fragments (which includes promoter and lacks the stop codon) were recombined from pENTR/D-TOPO into pGWB4 by LR reaction (Invitrogen) to generate SWp:SW-GFP constructs for GME, VTC4 and L-GalDH. On the other hand, all CDS fragments (without promoter, 5'-UTR and stop codon) were sub-cloned into pGWB5 and pGWB14 to generate CaMV35S:SW_{CDS}-GFP and CaMV35S:SWCDS-HA, respectively. In

the case of VTC2, the CDS was also recombined to VTC2p-pGWB504 by LR reaction (Invitrogen) thus obtaining the VTC2p:VTC2CDS-GFP construct Likewise, CDS (pENTR/D-TOPO) were recombined into both pGADT7-GW (activation domain, AD) and pGBKT7-GW (binding domain, BD) to generate SWCDS-AD and SWCDS-BD, respectively, for yeast two-hybrid assay (see Yeast two-hybrid assay section). The expression vectors generated using the destination vectors pGWB5 and pGWB14 contain a kanamycin and a hygromycin resistance gene for bacteria and plant selection, respectively. The yeast two-hybrid vectors pGADT7 and pGBKT7 contain an ampicillin and kanamycin resistance gene, respectively for selection in bacteria. A summary of generated constructs is showed in M&M Table 3. All constructs were analysed by colony PCR (using the primers indicated in M&M Table 2D), enzymatic DNA restriction and sequencing (using the primers indicated in M&M Table 2E).

The plasmids used from the pGWB vector series were provided by Tsuyoshi Nakagawa (Department of Molecular and Functional Genomics, Shimane University; Nakagawa et al., 2007). The pGADT7(GW) and pGBKT7(GW) destination vectors were provided by Salomé Prat (Nacional de Biotecnología-Consejo Superior de Investigaciones Científicas).

Generation of Arabidopsis transgenic lines

The constructs generated using pGWB4 plasmid for native expression of the SW genes (pGWB504 for VTC2) were transformed into *Agrobacterium tumefaciens* GV3101::pMP90 by electroporation and confirmed by colony PCR using the primers indicated in M&M Table 2D. Arabidopsis WT (Col-0) plants were then transformed using these *A. tumefaciens* strains by floral dipping (Clough and Bent, 1998). T2 plants were analysed for hygromycin resistance ratio resistant:sensitive (R:S) and lines with single insertion (T2 Hyg^R:Hyg^S=3, χ^2 (α=0.05), n>300) were selected. Selected T2 plants were grown in long day photoperiod and a sample of rosette leaf was taken to perform immunoblot analysis (Figure 8). Seeds from different T2 lines with a high expression were selected and homozygous T3 and T4 plants were used in this work.

For generation of the complementation lines, selected T2 plants (with single insertion) were crossed with their respective mutants in both directions as male and female. In order to obtain homozygous plants for both the T-DNA insertion and the SWp:SW-GFP construct (Hyg^R), we selected hygromycin resistant plants and performed diagnostic PCR to identify T-DNA insertion using the primers in M&M Table 2A. Homozygous F3 plants for T-DNA and SWp:SW-GFP insertion were used in this work.

Ascorbate complementation assay

WT, *gme* (SALK_150208), *lgaldh* (SALK_056664) and *gldh* (SALK_060087) seeds were surface sterilized and stratified for 3 days at 4 ºC. Seeds were then sowed in agar-solidified (0.5% [w/v] agar) modified Scholl medium with or without 0,5 mM ascorbate as described elsewhere (B. Lim et al., 2016) and grown with a long-day photoperiod. After 10 days, plants were individually collected and PCR-diagnosed to identify homozygous mutants.

Ascorbate measurements

High Performance Liquid Chromatography (HPLC) for combinatorial expression in Nicotiana benthamiana

Ascorbate was extracted from approximately 250 mg fresh tissue using 2 mL of a 2% (w/v) metaphosphoric acid, 2 mM EDTA ice-cold buffer (modified from Davey et al., 2006). Samples were centrifuged at 18000 g for 20 min at 4^{o}C, and supernatants were filtered (0.45 µm) before injection into a HPLC (Agilent Technologies 1200 series; Rx-C18, 4.6x100 mm 3.5 µm column (Agilent Technologies 861967-902), diode array detector (Agilent Technologies G1315D). Samples were measured at 254 nm using filtered (0.45 µm) 0.1 M NaH_2PO_4, 0.2 mM EDTA, pH 3.1 (orthophosphoric acid) as mobile phase (Harapanhalli et al., 1993) at 4 ^{o}C (column at 20 ^{o}C; 5 µL sample injection, 0.7 mL/min flow, 200 bar). Standards were prepared using ascorbic acid dissolved in extraction buffer, with concentrations ranging from 0 mM to 2.5 mM.

Ascorbate oxidase (AO) activity for Arabidopsis transgenic lines

Ascorbate and dehydroascorbate were extracted from approximately 80 mg fresh tissue using 1 mL of a 3% (w/v) ice cold metaphosphoric acid plus 1 mM EDTA. Samples were centrifuged at 16000 g for 10 min at 4^{o}C. Absorbance measurements were carried out at 265 nm using 20 µL sample/standard aliquots in a 96 well UV-transparent plate (Greiner UV-Star® 96-Well Microplate) mixed with 100 µL of either phosphate buffer (0.2 M KH_2PO_4, pH 7 to measure ascorbate) or Tris(2-carboxyethyl)phosphine (TCEP)-phosphate buffer (0.2 M KH_2PO_4, pH7, 2 mM TCEP, to measure ascorbate and dehydroascorbate). Then, 5 µL 40 U/mL AO was added to each well, mixed and incubated at room temperature for 20 minutes, when the absorbance was again measured. The difference in the absorbance was interpolated in the standard curve, using standards ranging from 0 mM to 1 mM in extraction buffer. TCEP and AO stocks were prepared in phosphate buffer.

Immunoblot

Proteins were separated by size through a sodium dodecyl sulphate-polyacrylamide gel electrophoresis (SDS-PAGE) and transferred onto a polyvinylidene difluoride (PVDF) membrane (Immobilon-P, Millipore, 0.45 µm pore size; CAT. #IPVH00010) previously methanol-equilibrated. Next, the PVDF membrane was blocked with 5% (w/v) skimmed milk followed by an incubation with a primary antibody synthesised in mouse against GFP (Santa Cruz Biotechnology, CAT. #sc-9996; 1:600) or HA (Sigma-Aldrich, CAT. #H3663; 1:3000) epitopes. Then, the membrane was subsequentially incubated with a horseradish peroxidase (HRP)-conjugated α-mouse whole IgG antibody produced in rabbit (Sigma-Aldrich, CAT. #A9044; 1:80000). Protein-HRP chemiluminescence was detected using Chemidoc XRS1 System (Bio-Rad) after incubation with Clarity ECL Western Blotting Substrate or SuperSignal West Femto Maximum Sensitivity Substrate according to the manufacturer's instructions.

Transient expression in *Nicotiana benthamiana* leaves

Agrobacterium tumefaciens GV3101::pMP90 was transformed by electroporation with the constructs generated using pGWB5 and pGWB14 positive colonies were confirmed by colony PCR. Two leaves per plant (leaves 3 and 4 from apex) 4-week-old *N. benthamiana* were infiltrated in the abaxial side of using 1 mL syringe (without needle). Agrobacterium cultures were grown overnight in liquid Luria-Bertani medium containing rifampicin (50 µg/mL), gentamycin (25 µg/mL), and the construct-specific antibiotic kanamycin (50 µg/mL). Cells were then harvested by centrifugation (for 15 min at 3000 g in 50-mL falcon tubes) at room temperature, pellets were resuspended in agroinfiltration solution (10 mM MES, pH 5.6, 10 mM $MgCl_2$, and 1 mM acetosyringone), and kept for 2-3 h in dark conditions at room temperature. In order to avoid overexpression-associated gene silencing, an *Agrobaterium* strain containing a p19 expression vector was coinfiltrated. For single gene expression, the gene of interest and p19 were mixed in such a way that the optical densities (600 nm, OD_{600}) were 0.8 and 0.2, respectively. For multiple co-infiltration experiments, the genes of interest were diluted in the same proportion so the final OD_{600} was 1 (0,8 for the combination of genes of interest and 0,2 for p19). Agrobacterium strains expressing either free GFP or TTL3-HA (an ascorbate biosynthesis non-related protein (Amorim-Silva et al., 2019) were used to compensate OD_{600} in co-infiltration experiments.

To achieve optimal protein expression, immunoblot time course analysis was addressed 2, 3 and 4 days after infiltration (Figure 9B). Protein loads were adjusted so comparable amounts of GFP-tagged protein were detected two days after infiltration for each construct using the Java-based image-processing program FIJI (Schindelin et al., 2012; Schneider et al., 2012).

Confocal laser scanning microscopy

All confocal images of *N. benthamiana* (Figure 13) were obtained using a Leica TCS SP5 II confocal microscope equipped with a 488-nm argon laser for GFP excitation and a PMT for its detection. The HCX PL APO CS 40x1,25 OIL objective was used with additional 2x digital zoom for images acquisition. Arabidopsis imaging was carried out using a Leica TCS SP8 equipped with a solid state 488-nm laser used to excite GFP and a high-sensitivity SP hybrid detector (objective HC PL APO CS2 40x/1,30 OIL, Figure 14A) and a Zeiss LSM 880 (objective C-Apochromat 40x/1.2 W Korr M27, Figure 14B) with a 488-nm argon laser and PMT detectors for GFP and transmitted light (bright field). All image processing was performed using FIJI (Schindelin et al., 2012; Schneider et al., 2012).

Yeast two-hybrid assay

The Gal4-based yeast two-hybrid system (Clontech Laboratories) was used for testing the interaction. *Saccharomyces cerevisiae* Meyen ex E. C. Hansen strain PJ69-4A was transformed with the constructs described in the plasmid constructs section (SW genes clones into pGADT7 and pGBKT7) as described elsewhere (Gietz and Schiestl, 1995). Constructs transformed are explained in the plasmid constructs section (pGADT7 and pGBKT7). Transformants were grown on plasmid-selective medium (synthetic defined (SD)/ -Trp -Leu) and grown at 28 ^{o}C for 4 days. Two independent colonies were taken per transformation event and resuspended in 200 µL of sterile water. Ten-fold serial dilutions were made and 5 µL of each dilution were spotted onto three different interaction-selective medium: SD -Trp (minus tryptophan) -Leu (minus leucin) -His (minus histidine) +2 mM 3-AT (3-amino-1,2,4-triazole); SD -Trp -Leu -Ade; SD -Trp -Leu -Ade +3-AT. Full SD medium was also used to check strain survival. Plates were grown at 28 ^{o}C and pictures were taken after 3, 5 and 9 days (only 5 days is shown). Concentrations are available in Rodríguez-Negrete et al. (2014).

Bioinformatic analyses

Protein domains predictions were performed using Protein Basic Local Alignment Search from the National Center for Biotechnology Information (Altschul et al., 1997), BLASTp; https://blast.ncbi.nlm.nih.gov/Blast.cgi?PAGE=Proteins) followed by functional annotation of protein domain using the Conserved Domain Database (Marchler-Bauer et al., 2017, 2015, 2011; Marchler-Bauer and Bryant, 2004; https://www.ncbi.nlm.nih.gov/Structure/cdd/cdd.shtml). Protein subcellular localisation was predicted using COMPARTMENTS (Binder et al., 2014; https://compartments.jensenlab.org/Search). Predicted subcellular localisation

signals were performed using LOCALISER (Sperschneider et al., 2017; http://localiser.csiro.au/). Metabolic control Analysis was carried out using Complex Pathway Simulator (COPASI, Hoops et al., 2006; http://copasi.org/). All the details needed for the simulations are collected in Appendices 3-7). VTC2 mRNA expression datasets were extracted from Transcriptome Variation Analysis database (Klepikova et al., 2016, TRAVA; http://travadb.org/) and eFP-seq Browser (Sullivan et al., 2019; https://bar.utoronto.ca/eFP-Seq_Browser/). Evolutionary analyses were conducted in MEGA X (Kumar et al., 2018) using the species' genomes listed in Appendix 8, downloaded from Phytozome database (https://phytozome.jgi.doe.gov/pz/portal.html). BLAST against these genomes was performed using Arabidopsis *VTC2* protein sequence (TAIR: AT4G26850; UniProt: Q8RWE8) as a query. Results were filtered (E-value ≤ 10^{-10}, percentage of identical matches ≥ 50%, High Score Pairing query coverage ≥ 70%,) using Linux (bash) scripts available in Fenech (2015, MsD thesis, University of Málaga).

Coimmunoprecipitation assay

Four-week-old *N. benthamiana* plants were used for transient expression assays as described above. Leaves were ground to fine powder in liquid nitrogen. ~0.5 g of ground leaves per sample was used, and total proteins were extracted with 1 mL of non-denaturing extraction buffer (50 mM Tris-HCl pH7.5, 150 mM NaCl, 1% (v/v) Nonidet P-40, 10 mM EDTA, 1mM Na_2MoO_4, 1 mM NaF, 10 mM DTT, 0.5 mM PMSF, 1% (v/v) protease inhibitor (Sigma P9599)) and incubated for 30 min at 4 ºC using an end-over-end rocker. Protein extracts were centrifuged at 20000 g for 20 min at 4 ºC and then filtered by gravity using Poly-Prep chromatography columns (731-1550, Bio-Rad). Supernatants were filtered by gravity through Poly-Prep chromatography columns (731-1550, Bio-Rad), and 100 mL was reserved for immunoblot analysis as input. The remaining supernatants were used for immunoprecipitation of GFP-fused proteins agarose using GFP-Trap coupled to agarose beads (Chromotek) and following the manufacturer's instructions. Total (input), immunoprecipitated (IP), and CoIP samples were resuspended with 2x concentrated Laemmli sample buffer and heated at 95°C for 5 min protein denaturation. Finally, samples were separated in a 10% SDS-PAGE gel and analysed as described above.

GFP-Trap column-mediated VTC2-GFP concentration from Arabidopsis plants grown under high and low light intensities

Arabidopsis plants from WT, *vtc2*, *C12*, *C13* and *OE-C15* lines were grown for five weeks, when plants were transferred to low light intensity (57.5±2 µmol m^{-2} s^{-1}) and high light intensity (770±10 µmol m^{-2} s^{-1}) for 4 days and collected the samples half-way through the light period. Samples were collected and ground in liquid nitrogen and non-denaturing protein extraction was performed as described in "Coimmunoprecipitation assay" section. Following the incubation of the beads

with the protein extracts as described in the section above, an aliquot of the unbound fraction was taken. Beads were then washed once with 150 mM NaCl wash buffer (50 mM Tris-HCl pH7.5, 0,1% (v/v) Nonidet P-40, 150 mM NaCl, 10 mM EDTA, 1mM Na_2MoO_4, 1 mM NaF, 10 mM DTT, 0.5 mM PMSF, 1% (v/v) protease inhibitor (Sigma P9599)) and two more times with 300 mM wash buffer. Beads were further washed twice with a buffer compatible with VTC2 enzymatic assay (50 mM HEPES, 3mM $MgCl_2$, pH 7,5 KOH), described below. Then, samples were resuspended in one fifth of the extraction volume using VTC2 assay buffer.

VTC2 enzymatic assay

Sample preparation

Following VTC2-GFP concentration explained above, the experiment was set up as shown in M&M Table 4. Samples were collected at time 0 and after 1 hour of incubation at room temperature with soft agitation to prevent the beads to settle. The reaction was stopped by heating the samples at 95 °C for 1 minute and then centrifuged at maximum speed for 30 minutes at 4 °C. Supernatant was transferred to a fresh tube avoiding carrying over the pellet. GDP-D-Glucose and D-glucose 1-P 2 mM were prepared in assay buffer as standards (5 µL sugar + 5µL phosphate buffer + 90µL assay buffer). Prior to the injection into the GC/MS analyser, 300 µL acetonitrile were added to all samples and standards, centrifuged under the same conditions previously mentioned and supernatant was transferred to a fresh tube.

M&M Table 4. Design of VTC2-GFP enzymatic assay. Phosphate buffer (KH_2PO_4 100mM in Assay Buffer) was used to trigger the reaction.

Volumes to add (µL)	Assay	Blank
Assay Buffer	70	75
Protein Extract	20	20
2 mM GDP-Glc	5	5
Phosphate Buffer	5	0
Total Volume (µL)	100	100

From this supernatant, 50 µl were transferred to glass vials and completely dried down using an evaporator (GeneVac EZ-2). 20 µl of methoxyamine hydrochloride (20 mg/ml dissolved in pyridine) was added to each sample and they were incubated at 37 °C for 2 hours. Then, 30 µl of MSTFA (N-Methyl-N-(trimethylsilyl)trifluoroacetamide) was added and the samples were heated again at 37 °C for 30 minutes before analysis on the GC-MS. Derivatising agents were all from Sigma-Aldrich. GDP-glucose and glucose 1-phosphate standards were prepared at 1 µM, 10 µM and 100 µM.

Gas chromatography-Mass spectrometry analysis

Derivatised samples were analysed using an Agilent 7200 series accurate mass Q-TOF GC-MS together with a 7890A GC system (Agilent Technologies,

Santa Clara, USA), equipped with an EI (electron ionisation) ion source. 0.6 µl of each sample was injected into a non-deactivated, baffled glass liner with a 10:1 split ratio (12.04 mL/min split flow) and the inlet temperature was maintained at 250 °C. A 3mL/minute septum purge flow was applied. A Zebron semi-volatiles (Phenomenex, Torrance, USA) column (30 m x 250 µm x 0.25 µm) coupled with a 10m guard column, was maintained at a constant helium flow of 1.2ml/min. The temperature gradient of the GC was ramped up at a rate of 15 °C/min, from 70 °C to 310 °C, over 16 min, and then held at 310 °C for a further 6 minutes. The total run time of 22 min, was followed by a 7 min backflush at 310 °C to clean the column at the end of every run. The MS emission current and emission voltage were held at 35 µA and 70 eV respectively, and the MS was automatically calibrated after every run. The mass range was set from 50 to 600 amu, with an acquisition rate of 5 spectra/s, and a solvent delay of 3,5 min. DCM and extraction solvent blanks were run at the beginning and end of the run.

Data were analysed using Agilent technologies MassHunter qualitative (v B.07.00) and quantitative (v B.08.00) software.

Proteasome inhibitor MG132 assay

Arabidopsis seeds were germinated and grown for 10 days in half-strength MS with 1.5% sucrose under long day conditions and then transferred to liquid half-strength MS with 1.5% sucrose (7.5 mL/well) for 2 days under same grow conditions in transparent 6-well plates. Liquid medium in the wells was exchanged with 5 mL fresh medium containing 0.241% (v/v) dimethyl sulfoxide (DMSO, mock) or proteasome inhibitor (10 µM MG132 in DMSO), 2.5 hours prior to the dark period. Samples were collected and weighed 2 hours after the beginning of the dark period and frozen in liquid nitrogen.

Statistical analysis

All analyses were performed using SigmaPlot v11 for Windows considering $n>3$ and $\alpha=0.05$.

Accession Numbers

Sequence data were sourced from the The Arabidopsis Information Resource (TAIR) (https://www.arabidopsis.org/) under the following accession numbers: AT2G39770 for VTC1, AT5G28840 for GME, AT4G26850 for VTC2, AT3G02870 for VTC4, AT4G33670 for L-GalDH, and AT3G47930 for GLDH.

APPENDICES

Appendix 1. Infiltration in *N. benthamiana* corresponding to Figure 10C-H. * Data transformed with log_{10} to accomplish normality and homoscedasticity required for ANOVA. Free GFP and TTL3-HA were used to rise the OD_{600} up to 1 when necessary. p19 OD_{600} was always 0,2.

0Panel	Description			Label	ANOVA-1 (α=0,05)
C	Not infiltrated			Naïve	a
	GFP	TTL3-HA	p19	Mock	a
	VTC1-GFP	TTL3-HA	p19	VTC1	a
	GME-HA	GFP	p19	GME	a
	VTC2-HA	GFP	p19	VTC2	b
	VTC1-GFP	GME-HA	p19	VTC1/GME	a
	VTC1-GFP	VTC2-HA	p19	VTC1/VTC2	b
D	Not infiltrated			Naïve	ab
	GFP	TTL3-HA	p19	Mock	ab
	VTC1-GFP	TTL3-HA	p19	VTC1	a
	VTC4-HA	GFP	p19	VTC4	c
	L-GalDH-HA	GFP	p19	L-GalDH	c
	VTC1-GFP	VTC4-HA	p19	VTC1/VTC4	ab
	VTC1-GFP	L-GalDH-HA	p19	VTC1/L-GalDH	b
E*	Not infiltrated			Naïve	bc
	GFP	TTL3-HA	p19	Mock	ab
	GME-GFP	TTL3-HA	p19	GME	bc
	VTC2-HA	GFP	p19	VTC2	d
	VTC4-HA	GFP	p19	VTC4	a
	GME-GFP	VTC2-HA	p19	VTC2/GME	e
	GME-GFP	VTC4-HA	p19	GME/VTC4	c
F	Not infiltrated			Naïve	a
	GFP	TTL3-HA	p19	Mock	a
	L-GalDH-GFP	TTL3-HA	p19	L-GalDH	a
	GME-HA	GFP	p19	GME	a
	VTC2-HA	GFP	p19	VTC2	b
	L-GalDH-GFP	GME-HA	p19	GME/L-GalDH	a
	L-GalDH-GFP	VTC2-HA	p19	VTC2/L-GalDH	b
G	Not infiltrated			Naïve	ab
	GFP	TTL3-HA	p19	Mock	a
	VTC4-GFP	TTL3-HA	p19	VTC4	b
	VTC2-HA	GFP	p19	VTC2	c
	L-GalDH-HA	GFP	p19	L-GalDH	ab
	VTC4-GFP	VTC2-HA	p19	VTC2/VTC4	c
	VTC4-GFP	L-GalDH-HA	p19	VTC4/L-GalDH	ab
H	GFP		p19	Mock	a
	GFP, VTC2-GFP		p19	VTC2	b
	GFP, GME-HA		p19	GME	a
	GFP, GLDH-HA		p19	GLDH	a
	GFP, GME-HA, VTC2-GFP		p19	VTC2/GME	b
	GFP, VTC2-GFP, GLDH-HA		p19	VTC2/GLDH	b
	GFP, VTC1-GFP, GME-HA, VTC2-GFP, VTC4-GFP, L-GalDH-HA		p19	Cytosol	b
	GFP, VTC1-GFP, GME-HA, VTC2-GFP, VTC4-GFP, L-GalDH-HA		p19	Cytosol w/o VTC1	b
	VTC1-GFP, GME-HA, VTC2-GFP, VTC4-GFP, L-GalDH-HA, GLDH-HA		p19	Whole	b
	GFP, GME-HA, VTC2-GFP, VTC4-GFP, L-GalDH-HA, GLDH-HA		p19	Whole w/o VTC1	b

Appendix 2. Prediction of transit peptides and nuclear localisation signals within ascorbate biosynthesis proteins genes. Values in the brackets are (probability | residues involved). Results obtained from LOCALISER (http://localiser.csiro.au/).

Identifier	Chloroplast	Mitochondria	Nucleus
VTC1	-	Y (0,992 | 1-22)	-
GME	-	-	-
VTC2	-	-	Y (KKRP, LGEV)
VTC4	-	-	-
L-GalDH	-	-	-
GLDH	-	Y (0,999 | 1-27)	Y (RKRFPVDAYNKARRE)

Appendix 3. Initial conditions for the COPASI kinetic model of ascorbate biosynthesis and turnover.

Initial conditions (time = 0 sec)
Compartment size = 1 mL

Substrate	Initial concentration (mM)
D-Glc 6-P	5
D-Fru 6-P	0,410388
D-Man 6-P	0
D-Man 1-P	0,100795
GDP-D-Man	0,0978087
GDP-L-Gal	0,0954264
L-Gal 1-P	0,00030303
L-Gal	0
L-GalL	0
L-Asc	0,895145
DHA	1
Breakdown	124,057

#	Enzyme	K_{ms} (mM)	K_{mp} (mM)	V_f (mM/s)	V_r (mM/s)	K_i (mM)
1	PGI	5,9	0,5	10	10	
2	PMI	0,04	0,04	10	10	1
3	PMM	0,387	0,1	10	10	
4	GMP	0,1	0,1	10	10	
5	GME	0,045	0,045	10	10	
6	GGP	0,01	20	10	2,2	0,01
7	GPP	0,03		10		
8	L-GalDH	0,1	0,133	10	1	0,1
9	GLDH	0,12		10		
11	Oxidation	0,1		1		
12	Reduction	0,1		1,2		

10	Turnover	$k = 0,1\ s^{-1}$
13	Recycle	$k = 0,1\ s^{-1}$

Appendix 4. Flux control coefficients for ascorbate biosynthesis and turnover with various strengths of non-competitive feedback inhibition at the GDP-L-Gal phosphorylase step (Ki GGP). Values were calculated in COPASI using conditions indicated in Supplementary Table 3.

Ki (GGP) 1 mM	PGI	PMI	PMM	GMP	GME	GGP	GPP	L-GalDH	GLDH	Turnover	Oxidation	Reduction	Recycle
PGI	6,67337E-07	6,88165E-06	5,66712E-07	5,7709E-07	3,27957E-08	3,8955E-06	3,06121E-09	9,93702E-06	1,34534E-08	0,828315	4,30223	-4,13058	1,00709E-05
PMI	6,67337E-07	6,88165E-06	5,66712E-07	5,7709E-07	3,27957E-08	3,8955E-06	3,06121E-09	9,93702E-06	1,34534E-08	0,828315	4,30223	-4,13058	1,00709E-05
PMM	6,67337E-07	6,88165E-06	5,66712E-07	5,7709E-07	3,27957E-08	3,8955E-06	3,06121E-09	9,93702E-06	1,34534E-08	0,828315	4,30223	-4,13058	1,00709E-05
GMP	6,67337E-07	6,88165E-06	5,66712E-07	5,7709E-07	3,27958E-08	3,8955E-06	3,0612E-09	9,93702E-06	1,34535E-08	0,828315	4,30223	-4,13058	1,00709E-05
GME	6,67337E-07	6,88165E-06	5,66712E-07	5,7709E-07	3,27958E-08	3,8955E-06	3,0612E-09	9,93702E-06	1,34535E-08	0,828315	4,30223	-4,13058	1,00709E-05
GGP	6,67337E-07	6,88165E-06	5,66712E-07	5,7709E-07	3,27957E-08	3,8955E-06	3,06121E-09	9,93702E-06	1,34535E-08	0,828315	4,30223	-4,13058	1,00709E-05
GPP	6,67337E-07	6,88165E-06	5,66712E-07	5,7709E-07	3,27957E-08	3,8955E-06	3,06121E-09	9,93702E-06	1,34535E-08	0,828315	4,30223	-4,13058	1,00709E-05
L-GalDH	6,67337E-07	6,88165E-06	5,66712E-07	5,7709E-07	3,27957E-08	3,8955E-06	3,06121E-09	9,93702E-06	1,34535E-08	0,828315	4,30223	-4,13058	1,00709E-05
GLDH	6,67337E-07	6,88165E-06	5,66712E-07	5,7709E-07	3,27957E-08	3,8955E-06	3,06121E-09	9,93702E-06	1,34535E-08	0,828315	4,30223	-4,13058	1,00709E-05
Turnover	6,67337E-07	6,88165E-06	5,66712E-07	5,7709E-07	3,27957E-08	3,8955E-06	3,06121E-09	9,93702E-06	1,34534E-08	0,828315	4,30223	-4,13058	1,00709E-05
Oxidation	1,55108E-07	1,59949E-06	1,31719E-07	1,34132E-07	7,62264E-09	9,05422E-07	7,11511E-10	2,30964E-06	3,12695E-09	-5,8834E-06	0,999957	4,10121E-05	2,34075E-06
Reduction	1,33821E-07	1,37998E-06	1,13643E-07	1,15724E-07	6,57653E-09	7,81165E-07	6,13865E-10	1,99267E-06	2,69782E-09	-0,034428	0,862726	0,171695	2,01951E-06
Recycle	6,67337E-07	6,88165E-06	5,66712E-07	5,7709E-07	3,27957E-08	3,8955E-06	3,06121E-09	9,93702E-06	1,34534E-08	0,828315	4,30223	-4,13058	1,00709E-05

Ki (GGP) 0,75 mM	PGI	PMI	PMM	GMP	GME	GGP	GPP	L-GalDH	GLDH	Turnover	Oxidation	Reduction	Recycle
PGI	6,77549E-07	6,87913E-06	5,78996E-07	5,89599E-07	4,02187E-08	1,26711E-05	3,07081E-09	9,91568E-06	1,34328E-08	0,828308	4,30219	-4,13054	1,00554E-05
PMI	6,77549E-07	6,87913E-06	5,78996E-07	5,89599E-07	4,02187E-08	1,26711E-05	3,07081E-09	9,91568E-06	1,34328E-08	0,828308	4,30219	-4,13054	1,00554E-05
PMM	6,77549E-07	6,87913E-06	5,78996E-07	5,89599E-07	4,02187E-08	1,26711E-05	3,07081E-09	9,91568E-06	1,34328E-08	0,828308	4,30219	-4,13054	1,00554E-05
GMP	6,77549E-07	6,87913E-06	5,78996E-07	5,89599E-07	4,02186E-08	1,26711E-05	3,07081E-09	9,91568E-06	1,34328E-08	0,828308	4,30219	-4,13054	1,00554E-05
GME	6,77549E-07	6,87913E-06	5,78996E-07	5,89599E-07	4,02186E-08	1,26711E-05	3,07081E-09	9,91568E-06	1,34328E-08	0,828308	4,30219	-4,13054	1,00554E-05
GGP	6,77549E-07	6,87913E-06	5,78996E-07	5,89599E-07	4,02187E-08	1,26711E-05	3,07081E-09	9,91568E-06	1,34329E-08	0,828308	4,30219	-4,13054	1,00554E-05
GPP	6,77549E-07	6,87913E-06	5,78996E-07	5,89599E-07	4,02187E-08	1,26711E-05	3,07081E-09	9,91568E-06	1,34329E-08	0,828308	4,30219	-4,13054	1,00554E-05
L-GalDH	6,77549E-07	6,87913E-06	5,78996E-07	5,89599E-07	4,02187E-08	1,26711E-05	3,07081E-09	9,91568E-06	1,34329E-08	0,828308	4,30219	-4,13054	1,00554E-05
GLDH	6,77549E-07	6,87913E-06	5,78996E-07	5,89599E-07	4,02187E-08	1,26711E-05	3,07081E-09	9,91568E-06	1,34329E-08	0,828308	4,30219	-4,13054	1,00554E-05
Turnover	6,77549E-07	6,87913E-06	5,78996E-07	5,89599E-07	4,02187E-08	1,26711E-05	3,07081E-09	9,91568E-06	1,34328E-08	0,828308	4,30219	-4,13054	1,00554E-05
Oxidation	1,57481E-07	1,5989E-06	1,34575E-07	1,37039E-07	9,34795E-09	2,94512E-06	7,13743E-10	2,30468E-06	3,12217E-09	-7,57419E-06	0,999949	4,94256E-05	2,33715E-06
Reduction	1,35869E-07	1,37948E-06	1,16106E-07	1,18233E-07	8,06507E-09	2,54095E-06	6,15792E-10	1,9884E-06	2,69369E-09	-0,0344294	0,862719	0,171702	2,01641E-06
Recycle	6,77549E-07	6,87913E-06	5,78996E-07	5,89599E-07	4,02187E-08	1,26711E-05	3,07081E-09	9,91568E-06	1,34328E-08	0,828308	4,30219	-4,13054	1,00554E-05

Ki (GGP) 0,1 mM	PGI	PMI	PMM	GMP	GME	GGP	GPP	L-GalDH	GLDH	Turnover	Oxidation	Reduction	Recycle
PGI	6,09882E-08	6,893E-08	7,05553E-08	7,18478E-08	3,89454E-08	0,0165875	1,19463E-11	7,6177E-09	5,27689E-11	0,817616	4,19902	-4,03322	3,95064E-08
PMI	6,09882E-08	6,893E-08	7,05553E-08	7,18478E-08	3,89454E-08	0,0165875	1,19414E-11	7,6177E-09	5,27778E-11	0,817616	4,19902	-4,03322	3,95064E-08
PMM	6,09881E-08	6,893E-08	7,05553E-08	7,18478E-08	3,89454E-08	0,0165875	1,19398E-11	7,6177E-09	5,27776E-11	0,817616	4,19902	-4,03322	3,95064E-08
GMP	6,09882E-08	6,893E-08	7,05553E-08	7,18478E-08	3,89455E-08	0,0165875	1,19591E-11	7,6177E-09	5,27561E-11	0,817616	4,19902	-4,03322	3,95065E-08
GME	6,09882E-08	6,893E-08	7,05553E-08	7,18478E-08	3,89455E-08	0,0165875	1,19553E-11	7,61771E-09	5,27526E-11	0,817616	4,19902	-4,03322	3,95065E-08
GGP	6,09882E-08	6,893E-08	7,05553E-08	7,18478E-08	3,89454E-08	0,0165875	1,19457E-11	7,6177E-09	5,27689E-11	0,817616	4,19902	-4,03322	3,95064E-08
GPP	6,09882E-08	6,893E-08	7,05553E-08	7,18478E-08	3,89454E-08	0,0165875	1,19457E-11	7,6177E-09	5,27688E-11	0,817616	4,19902	-4,03322	3,95064E-08
L-GalDH	6,09882E-08	6,893E-08	7,05553E-08	7,18478E-08	3,89454E-08	0,0165875	1,19456E-11	7,6177E-09	5,27687E-11	0,817616	4,19902	-4,03322	3,95064E-08
GLDH	6,09882E-08	6,893E-08	7,05553E-08	7,18477E-08	3,89454E-08	0,0165875	1,1933E-11	7,61771E-09	5,27713E-11	0,817616	4,19902	-4,03322	3,95064E-08
Turnover	6,09882E-08	6,893E-08	7,05553E-08	7,18478E-08	3,89454E-08	0,0165875	1,19468E-11	7,6177E-09	5,27685E-11	0,817616	4,19902	-4,03322	3,95064E-08
Oxidation	1,42835E-08	1,61434E-08	1,65241E-08	1,68268E-08	9,12104E-09	0,0038848	2,79769E-12	1,78407E-09	1,23585E-11	-0,00322992	0,983412	0,0159329	9,25243E-09
Reduction	1,23635E-08	1,39735E-08	1,4303E-08	1,4565E-08	7,89503E-09	0,00336262	2,42186E-12	1,54426E-09	1,06973E-11	-0,0369729	0,851226	0,182384	8,00876E-09

Recycle	6,09882E-08	6,893E-08	7,05553E-08	7,18478E-08	3,89454E-08	0,0165875	1,19457E-11	7,6177E-09	5,27689E-11	0,817616	4,19902	-4,03322	3,95064E-08

Ki (GGP) 0,05 mM	PGI	PMI	PMM	GMP	GME	GGP	GPP	L-GalDH	GLDH	Turnover	Oxidation	Reduction	Recycle
PGI	1,0211E-07	1,11114E-07	1,18275E-07	1,20442E-07	6,54876E-08	0,0317267	1,79562E-11	5,84883E-09	7,93134E-11	0,80849	4,09703	-3,93724	5,93911E-08
PMI	1,0211E-07	1,11114E-07	1,18275E-07	1,20442E-07	6,54876E-08	0,0317267	1,79584E-11	5,84883E-09	7,93057E-11	0,80849	4,09703	-3,93724	5,93911E-08
PMM	1,0211E-07	1,11114E-07	1,18275E-07	1,20442E-07	6,54876E-08	0,0317267	1,79578E-11	5,84883E-09	7,93065E-11	0,80849	4,09703	-3,93724	5,93911E-08
GMP	1,0211E-07	1,11114E-07	1,18275E-07	1,20442E-07	6,54876E-08	0,0317267	1,79515E-11	5,84883E-09	7,93234E-11	0,80849	4,09703	-3,93724	5,93911E-08
GME	1,0211E-07	1,11114E-07	1,18275E-07	1,20442E-07	6,54876E-08	0,0317267	1,7951E-11	5,84883E-09	7,93249E-11	0,80849	4,09703	-3,93724	5,93911E-08
GGP	1,0211E-07	1,11114E-07	1,18275E-07	1,20442E-07	6,54876E-08	0,0317267	1,7956E-11	5,84883E-09	7,93134E-11	0,80849	4,09703	-3,93724	5,93911E-08
GPP	1,0211E-07	1,11114E-07	1,18275E-07	1,20442E-07	6,54876E-08	0,0317267	1,7956E-11	5,84883E-09	7,93134E-11	0,80849	4,09703	-3,93724	5,93911E-08
L-GalDH	1,0211E-07	1,11114E-07	1,18275E-07	1,20442E-07	6,54876E-08	0,0317267	1,79561E-11	5,84883E-09	7,93134E-11	0,80849	4,09703	-3,93724	5,93911E-08
GLDH	1,0211E-07	1,11114E-07	1,18275E-07	1,20442E-07	6,54876E-08	0,0317267	1,79523E-11	5,84883E-09	7,93196E-11	0,80849	4,09703	-3,93724	5,93911E-08
Turnover	1,0211E-07	1,11114E-07	1,18275E-07	1,20442E-07	6,54876E-08	0,0317267	1,79564E-11	5,84883E-09	7,93123E-11	0,80849	4,09703	-3,93724	5,93911E-08
Oxidation	2,41323E-08	2,62603E-08	2,79526E-08	2,84648E-08	1,5477E-08	0,00749814	4,24365E-12	1,38229E-09	1,87445E-11	-0,00626093	0,968273	0,03049	1,40362E-08
Reduction	2,09678E-08	2,28167E-08	2,42871E-08	2,47322E-08	1,34475E-08	0,00651489	3,68724E-12	1,20102E-09	1,62863E-11	-0,0393254	0,841301	0,19151	1,21956E-08
Recycle	1,0211E-07	1,11114E-07	1,18275E-07	1,20442E-07	6,54876E-08	0,0317267	1,7956E-11	5,84883E-09	7,93132E-11	0,80849	4,09703	-3,93724	5,93911E-08

Ki (GGP) 0,01 mM	PGI	PMI	PMM	GMP	GME	GGP	GPP	L-GalDH	GLDH	Turnover	Oxidation	Reduction	Recycle
PGI	3,1267E-07	3,31508E-07	3,62518E-07	3,69176E-07	2,01227E-07	0,118434	5,07844E-11	3,8222E-09	2,2423E-10	0,755675	3,50461	-3,37872	1,68108E-07
PMI	3,1267E-07	3,31508E-07	3,62518E-07	3,69176E-07	2,01227E-07	0,118434	5,07844E-11	3,8222E-09	2,2423E-10	0,755675	3,50461	-3,37872	1,68108E-07
PMM	3,1267E-07	3,31508E-07	3,62518E-07	3,69176E-07	2,01227E-07	0,118434	5,07844E-11	3,8222E-09	2,2423E-10	0,755675	3,50461	-3,37872	1,68108E-07
GMP	3,1267E-07	3,31508E-07	3,62518E-07	3,69176E-07	2,01227E-07	0,118434	5,07845E-11	3,8222E-09	2,2423E-10	0,755675	3,50461	-3,37872	1,68108E-07
GME	3,1267E-07	3,31508E-07	3,62518E-07	3,69176E-07	2,01227E-07	0,118434	5,07844E-11	3,8222E-09	2,2423E-10	0,755675	3,50461	-3,37872	1,68108E-07
GGP	3,1267E-07	3,31508E-07	3,62518E-07	3,69176E-07	2,01227E-07	0,118434	5,07844E-11	3,8222E-09	2,2423E-10	0,755675	3,50461	-3,37872	1,68108E-07
GPP	3,1267E-07	3,31508E-07	3,62518E-07	3,69176E-07	2,01227E-07	0,118434	5,07844E-11	3,8222E-09	2,2423E-10	0,755675	3,50461	-3,37872	1,68108E-07
L-GalDH	3,1267E-07	3,31508E-07	3,62518E-07	3,69176E-07	2,01227E-07	0,118434	5,07853E-11	3,8222E-09	2,2423E-10	0,755675	3,50461	-3,37872	1,68108E-07
GLDH	3,1267E-07	3,31508E-07	3,62518E-07	3,69176E-07	2,01227E-07	0,118434	5,0783E-11	3,8222E-09	2,24231E-10	0,755675	3,50461	-3,37872	1,68108E-07
Turnover	3,1267E-07	3,31508E-07	3,62518E-07	3,69176E-07	2,01227E-07	0,118434	5,07844E-11	3,8222E-09	2,2423E-10	0,755675	3,50461	-3,37872	1,68108E-07
Oxidation	7,86502E-08	8,33887E-08	9,11892E-08	9,28639E-08	5,06175E-08	0,0297914	1,27745E-11	9,61451E-10	5,64036E-11	-0,0255375	0,881564	0,114182	4,22866E-08
Reduction	6,99307E-08	7,41439E-08	8,10796E-08	8,25687E-08	4,50059E-08	0,0264886	1,13583E-11	8,54861E-10	5,01505E-11	-0,0546451	0,78383	0,244326	3,75985E-08
Recycle	3,1267E-07	3,31508E-07	3,62518E-07	3,69176E-07	2,01227E-07	0,118434	5,07843E-11	3,8222E-09	2,2423E-10	0,755675	3,50461	-3,37872	1,68108E-07

Appendix 5. Concentration control coefficients at each step for pathway intermediates with various strengths of non-competitive feedback inhibition at the GDP-L-Gal phosphorylase step (Ki GGP). Values were calculated in COPASI using conditions indicated in Appendix 3.

Ki (GGP) 1 mM	PGI	PMI	PMM	GMP	GME	GGP	GPP	L-GalDH	GLDH	Turnover	Oxidation	Reduction	Recycle
D-Glc 6-P	-7,25E-02	-6,90E-01	-5,27E-02	-5,27E-02	-2,94E-03	-0,297629	-2,96E-07	2,95E-03	4,00E-06	0,963552	4,98916	-4,7901	2,99E-03
D-Fru 6-P	0,00021205	-0,737938	-0,0564157	-0,0564124	-0,00314951	-0,31833	-3,16E-07	0,00315754	4,27E-06	0,966123	5,00144	-4,80189	0,00320008
D-Man 6-P	2,43E-04	2,50E-03	-2,13E-01	-2,13E-01	-1,19E-02	-1,20482	-3,75E-06	3,61E-03	4,89E-06	1,35376	7,01243	-6,73264	3,66E-03
D-Man 1-P	3,06E-04	3,15E-03	2,60E-04	-2,69E-01	-1,50E-02	-1,51831	-4,73E-06	4,55E-03	6,16E-06	1,48301	7,67882	-7,37245	4,61E-03
GDP-D-Man	4,14E-04	4,27E-03	3,52E-04	3,58E-04	-2,04E-02	-2,0581	-6,41E-06	6,17E-03	8,35E-06	1,70799	8,83885	-8,48619	6,25E-03
GDP-L-Gal	0,000420902	0,00434039	0,000357436	0,000363982	2,07E-05	-2,09171	-6,52E-06	0,00626747	8,49E-06	1,71873	8,89411	-8,53925	0,00635189
L-Gal 1-P	6,70E-07	6,91E-06	5,69E-07	5,79E-07	3,29E-08	3,91E-06	-1,00E+00	9,98E-06	1,35E-08	0,83163	4,31945	-4,14711	1,01E-05
L-Gal	0,000202299	0,00208612	0,000171795	0,000174941	9,94E-06	0,00118089	9,28E-07	-1,00087	-0,00012437	0,823987	4,26395	-4,09382	0,00305291
L-GalL	6,70E-07	6,91E-06	5,69E-07	5,79E-07	3,29E-08	3,91E-06	3,07E-09	9,98E-06	-1,00E+00	0,83163	4,31945	-4,14711	1,01E-05
L-Asc	2,02E-04	2,08E-03	1,71E-04	1,75E-04	9,92E-06	0,00117834	9,26E-07	3,01E-03	4,07E-06	-0,00765678	-0,055592	0,053374	3,05E-03
DHA	6,67E-07	6,88E-06	5,67E-07	5,77E-07	3,28E-08	3,90E-06	3,06E-09	9,94E-06	1,35E-08	-0,171685	4,30223	-4,13058	1,01E-05
Breakdown	6,67E-07	6,88E-06	5,67E-07	5,77E-07	3,28E-08	3,90E-06	3,06E-09	9,94E-06	1,35E-08	0,828315	4,30223	-4,13058	-1,00E+00

Ki (GGP) 0,75 mM	PGI	PMI	PMM	GMP	GME	GGP	GPP	L-GalDH	GLDH	Turnover	Oxidation	Reduction	Recycle
D-Glc 6-P	-6,38E-02	-5,97E-01	-4,67E-02	-4,67E-02	-3,13E-03	-0,838064	-6,65E-07	4,30E-03	5,83E-06	1,31541	6,8096	-6,53791	4,36E-03
D-Fru 6-P	0,000311405	-0,633106	-0,0494608	-0,0494559	-0,00331411	-0,888117	-7,05E-07	0,0045573	6,17E-06	1,3377	6,92402	-6,64777	0,00462151
D-Man 6-P	4,95E-04	5,03E-03	-1,34E-01	-1,34E-01	-9,00E-03	-2,41203	-3,49E-06	7,24E-03	9,81E-06	2,21246	11,4534	-10,9964	7,35E-03
D-Man 1-P	5,67E-04	5,76E-03	4,85E-04	-1,54E-01	-1,03E-02	-2,76361	-4,00E-06	8,30E-03	1,12E-05	2,40713	12,4589	-11,9618	8,41E-03
GDP-D-Man	6,65E-04	6,75E-03	5,68E-04	5,78E-04	-1,21E-02	-3,23961	-4,69E-06	9,73E-03	1,32E-05	2,67188	13,8266	-13,2749	9,86E-03
GDP-L-Gal	0,000669761	0,00680006	0,000572341	0,000582822	3,98E-05	-3,26503	-4,73E-06	0,00980171	1,33E-05	2,68273	13,8825	-13,3286	0,00993979
L-Gal 1-P	6,80E-07	6,91E-06	5,81E-07	5,92E-07	4,04E-08	1,27E-05	-1,00E+00	9,96E-06	1,35E-08	0,831624	4,31941	-4,14707	1,01E-05
L-Gal	0,00020529	0,0020843	0,00017543	0,000178642	1,22E-05	0,00383922	9,30E-07	-1,00088	-0,000124467	0,821787	4,25254	-4,08287	0,00304667
L-GalL	6,80E-07	6,91E-06	5,81E-07	5,92E-07	4,04E-08	1,27E-05	3,08E-09	9,96E-06	-1,00E+00	0,831624	4,31941	-4,14707	1,01E-05
L-Asc	2,05E-04	2,08E-03	1,75E-04	1,78E-04	1,22E-05	0,0038309	9,28E-07	3,00E-03	4,06E-06	-0,0098522	-0,0669626	0,0642909	3,04E-03
DHA	6,78E-07	6,88E-06	5,79E-07	5,90E-07	4,02E-08	1,27E-05	3,07E-09	9,92E-06	1,34E-08	-0,171692	4,30219	-4,13054	1,01E-05
Breakdown	6,78E-07	6,88E-06	5,79E-07	5,90E-07	4,02E-08	1,27E-05	3,07E-09	9,92E-06	1,34E-08	0,828308	4,30219	-4,13054	-1,00E+00

Ki (GGP) 0,1 mM	PGI	PMI	PMM	GMP	GME	GGP	GPP	L-GalDH	GLDH	Turnover	Oxidation	Reduction	Recycle
D-Glc 6-P	-2,43E-03	-2,02E-03	-1,45E-03	-1,33E-03	-6,42E-04	-0,237338	1,13E-06	7,19E-04	4,98E-06	0,200793	1,01207	-0,972111	3,73E-03
D-Fru 6-P	0,00575478	-0,00202508	-0,00144901	-0,00132705	-0,00064228	-0,237549	1,13E-06	0,000718799	4,98E-06	0,194167	0,978037	-0,93942	0,00372779
D-Man 6-P	5,76E-03	6,51E-03	-1,45E-03	-1,33E-03	-6,43E-04	-0,238481	1,13E-06	7,19E-04	4,98E-06	0,187845	0,945553	-0,908218	3,73E-03
D-Man 1-P	5,76E-03	6,51E-03	6,66E-03	-1,33E-03	-6,43E-04	-0,238675	1,13E-06	7,19E-04	4,98E-06	0,181257	0,911716	-0,875717	3,73E-03
GDP-D-Man	5,76E-03	6,51E-03	6,67E-03	6,79E-03	-6,43E-04	-0,238869	1,13E-06	7,20E-04	4,99E-06	0,174666	0,877864	-0,843202	3,73E-03
GDP-L-Gal	0,00576154	0,0065118	0,00666534	0,00678744	3,68E-03	-0,238943	1,13E-06	0,000719643	4,99E-06	0,171134	0,859725	-0,825779	0,00373216
L-Gal 1-P	6,12E-08	6,92E-08	7,08E-08	7,21E-08	3,91E-08	1,67E-02	-1,00E+00	7,65E-09	5,30E-11	0,820845	4,2156	-4,04915	3,97E-08
L-Gal	3,66939E-06	4,14721E-06	0,000004245	4,32276E-06	2,34E-06	0,997996	7,19E-10	-1,00332	-0,000656703	0,00495423	0,0254311	-0,024427	2,37693E-06
L-GalL	6,12E-08	6,92E-08	7,08E-08	7,21E-08	3,91E-08	1,67E-02	1,20E-11	7,65E-09	-1,00E+00	0,820845	4,2156	-4,04915	3,97E-08
L-Asc	3,63E-06	4,10E-06	4,20E-06	4,28E-06	2,32E-06	0,987145	7,11E-10	4,53E-07	3,14E-09	-0,820737	-4,21506	4,04863	2,35E-06
DHA	6,10E-08	6,89E-08	7,06E-08	7,18E-08	3,89E-08	1,66E-02	1,19E-11	7,62E-09	5,28E-11	-0,182384	4,19902	-4,03322	3,95E-08
Breakdown	6,10E-08	6,89E-08	7,06E-08	7,18E-08	3,89E-08	1,66E-02	1,19E-11	7,62E-09	5,28E-11	0,817616	4,19902	-4,03322	-1,00E+00

Ki (GGP) 0,05 mM	PGI	PMI	PMM	GMP	GME	GGP	GPP	L-GalDH	GLDH	Turnover	Oxidation	Reduction	Recycle
D-Glc 6-P	-2,38E-03	-1,91E-03	-1,42E-03	-1,30E-03	-6,32E-04	-0,106165	9,91E-07	3,23E-04	4,38E-06	0,092556	0,452411	-0,434767	3,28E-03
D-Fru 6-P	0,00563929	-0,00191079	-0,00142172	-0,00130201	-0,000632068	-0,106449	9,92E-07	0,000323016	4,38E-06	0,0860998	0,41969	-0,403322	0,00328002
D-Man 6-P	5,64E-03	6,14E-03	-1,42E-03	-1,30E-03	-6,32E-04	-0,107015	9,92E-07	3,23E-04	4,38E-06	0,0798507	0,388017	-0,372884	3,28E-03
D-Man 1-P	5,64E-03	6,14E-03	6,54E-03	-1,30E-03	-6,32E-04	-0,107291	9,92E-07	3,23E-04	4,38E-06	0,0734342	0,355498	-0,341633	3,28E-03
GDP-D-Man	5,64E-03	6,14E-03	6,54E-03	6,66E-03	-6,33E-04	-0,107567	9,92E-07	3,23E-04	4,38E-06	0,0670149	0,322964	-0,310369	3,28E-03
GDP-L-Gal	0,00564355	0,0061412	0,00653695	0,00665674	3,62E-03	-0,107703	9,92E-07	0,000323259	4,38E-06	0,0635779	0,305547	-0,293631	0,00328249
L-Gal 1-P	1,03E-07	1,12E-07	1,19E-07	1,21E-07	6,57E-08	3,19E-02	-1,00E+00	5,87E-09	7,96E-11	0,811631	4,11294	-3,95254	5,96E-08
L-Gal	3,19478E-06	3,47649E-06	3,70053E-06	3,76834E-06	2,05E-06	0,992649	5,62E-10	-1,00265	-0,00128383	0,00941023	0,047677	-0,0458176	1,8582E-06
L-GalL	1,03E-07	1,12E-07	1,19E-07	1,21E-07	6,57E-08	3,19E-02	1,80E-11	5,87E-09	-1,00E+00	0,811631	4,11294	-3,95254	5,96E-08
L-Asc	3,13E-06	3,40E-06	3,62E-06	3,69E-06	2,01E-06	0,971975	5,50E-10	1,79E-07	2,43E-09	-0,811597	-4,11278	3,95238	1,82E-06
DHA	1,02E-07	1,11E-07	1,18E-07	1,20E-07	6,55E-08	3,17E-02	1,80E-11	5,85E-09	7,93E-11	-0,19151	4,09703	-3,93724	5,94E-08
Breakdown	1,02E-07	1,11E-07	1,18E-07	1,20E-07	6,55E-08	3,17E-02	1,80E-11	5,85E-09	7,93E-11	0,80849	4,09703	-3,93724	-1,00E+00

Ki (GGP) 0,01 mM	PGI	PMI	PMM	GMP	GME	GGP	GPP	L-GalDH	GLDH	Turnover	Oxidation	Reduction	Recycle
D-Glc 6-P	-2,13E-03	-1,67E-03	-1,28E-03	-1,17E-03	-5,69E-04	-0,0196985	8,19E-07	6,16E-05	3,61E-06	0,0207316	0,083581	-0,0805787	2,71E-03
D-Fru 6-P	0,00504082	-0,00166874	-0,00127593	-0,00116859	-0,000568679	-0,0205524	8,19E-07	0,000061621	3,62E-06	0,015317	0,058467	-0,0563668	0,00271022
D-Man 6-P	5,04E-03	5,34E-03	-1,28E-03	-1,17E-03	-5,69E-04	-0,0214312	8,19E-07	6,16E-05	3,62E-06	0,010058	0,0340762	-0,0328522	2,71E-03
D-Man 1-P	5,04E-03	5,35E-03	5,85E-03	-1,17E-03	-5,69E-04	-0,0222785	8,19E-07	6,16E-05	3,62E-06	0,00467777	0,00912184	-0,00879417	2,71E-03
GDP-D-Man	5,04E-03	5,35E-03	5,85E-03	5,95E-03	-5,69E-04	-0,0231262	8,19E-07	6,16E-05	3,62E-06	-0,000704408	-0,0158415	0,0152725	2,71E-03
GDP-L-Gal	0,00504303	0,00534686	0,00584702	0,00595441	3,25E-03	-0,0235782	8,19E-07	0,000061648	3,62E-06	-0,00358695	-0,02921	0,0281608	0,0027114
L-Gal 1-P	3,14E-07	3,33E-07	3,64E-07	3,70E-07	2,02E-07	1,19E-01	-1,00E+00	3,84E-09	2,25E-10	0,758307	3,51682	-3,39049	1,69E-07
L-Gal	2,53355E-06	2,68619E-06	2,93747E-06	2,99142E-06	1,63E-06	0,959669	4,12E-10	-0,998178	-0,00550829	0,0377199	0,174928	-0,168645	1,36217E-06
L-GalL	3,14E-07	3,33E-07	3,64E-07	3,70E-07	2,02E-07	1,19E-01	5,10E-11	3,84E-09	-1,00E+00	0,758307	3,51682	-3,39049	1,69E-07
L-Asc	2,34E-06	2,48E-06	2,71E-06	2,76E-06	1,50E-06	0,884626	3,79E-10	2,85E-08	1,67E-09	-0,75831	-3,51684	3,39051	1,26E-06
DHA	3,13E-07	3,32E-07	3,63E-07	3,69E-07	2,01E-07	1,18E-01	5,08E-11	3,82E-09	2,24E-10	-0,244325	3,50461	-3,37872	1,68E-07
Breakdown	3,13E-07	3,32E-07	3,63E-07	3,69E-07	2,01E-07	1,18E-01	5,08E-11	3,82E-09	2,24E-10	0,755675	3,50461	-3,37872	-1,00E+00

Appendix 6. Flux (A) and concentration (B) control coefficients at each step with competitive feedback inhibition of PMI and L-GalDH relaxed to 100 mM (compare Supplementary Tables 4 and 5 for published Ki values). Values were calculated in COPASI using conditions indicated in Appendix 3.

A. Flux control coefficients. Ki (GGP) = 0,01 mM

Ki (PMI) 100 mM	PGI	PMI	PMM	GMP	GME	GGP	GPP	L-GalDH	GLDH	Turnover	Oxidation	Reduction	Recycle
PGI	3,12654E-07	3,2903E-07	3,62518E-07	3,69176E-07	2,01228E-07	0,118434	5,07823E-11	3,82205E-09	2,24221E-10	0,755675	3,50461	-3,37872	1,68101E-07
PMI	3,12654E-07	3,2903E-07	3,62518E-07	3,69176E-07	2,01228E-07	0,118434	5,07825E-11	3,82205E-09	2,24221E-10	0,755675	3,50461	-3,37872	1,68101E-07
PMM	3,12654E-07	3,2903E-07	3,62518E-07	3,69176E-07	2,01228E-07	0,118434	5,07825E-11	3,82205E-09	2,24221E-10	0,755675	3,50461	-3,37872	1,68101E-07
GMP	3,12654E-07	3,2903E-07	3,62518E-07	3,69176E-07	2,01228E-07	0,118434	5,07823E-11	3,82205E-09	2,24221E-10	0,755675	3,50461	-3,37872	1,68101E-07
GME	3,12654E-07	3,2903E-07	3,62518E-07	3,69176E-07	2,01228E-07	0,118434	5,07823E-11	3,82205E-09	2,24221E-10	0,755675	3,50461	-3,37872	1,68101E-07
GGP	3,12654E-07	3,2903E-07	3,62518E-07	3,69176E-07	2,01228E-07	0,118434	5,07823E-11	3,82205E-09	2,24221E-10	0,755675	3,50461	-3,37872	1,68101E-07
GPP	3,12654E-07	3,2903E-07	3,62518E-07	3,69176E-07	2,01228E-07	0,118434	5,07823E-11	3,82205E-09	2,24221E-10	0,755675	3,50461	-3,37872	1,68101E-07
L-GalDH	3,12654E-07	3,2903E-07	3,62518E-07	3,69176E-07	2,01228E-07	0,118434	5,0781E-11	3,82205E-09	2,24221E-10	0,755675	3,50461	-3,37872	1,68101E-07
GLDH	3,12654E-07	3,2903E-07	3,62518E-07	3,69176E-07	2,01228E-07	0,118434	5,07829E-11	3,82205E-09	2,24222E-10	0,755675	3,50461	-3,37872	1,68101E-07
Turnover	3,12654E-07	3,2903E-07	3,62518E-07	3,69176E-07	2,01228E-07	0,118434	5,07824E-11	3,82205E-09	2,24221E-10	0,755675	3,50461	-3,37872	1,68101E-07
Oxidation	7,86461E-08	8,27654E-08	9,11891E-08	9,28638E-08	5,06175E-08	0,0297914	1,2774E-11	9,61413E-10	5,64014E-11	-0,0255375	0,881564	0,114182	4,22849E-08
Reduction	6,99271E-08	7,35897E-08	8,10795E-08	8,25686E-08	4,50059E-08	0,0264886	1,13578E-11	8,54827E-10	5,01485E-11	-0,0546451	0,78383	0,244326	3,7597E-08
Recycle	3,12654E-07	3,2903E-07	3,62518E-07	3,69176E-07	2,01228E-07	0,118434	5,07823E-11	3,82205E-09	2,24221E-10	0,755675	3,50461	-3,37872	1,68101E-07

Ki (L-GalDH) 100 mM	PGI	PMI	PMM	GMP	GME	GGP	GPP	L-GalDH	GLDH	Turnover	Oxidation	Reduction	Recycle
PGI	3,1261E-07	3,31444E-07	3,62448E-07	3,69105E-07	2,01189E-07	0,118434	5,07718E-11	1,74873E-10	2,24174E-10	0,755675	3,50461	-3,37872	1,68066E-07
PMI	3,1261E-07	3,31444E-07	3,62448E-07	3,69105E-07	2,01189E-07	0,118434	5,07717E-11	1,74873E-10	2,24174E-10	0,755675	3,50461	-3,37872	1,68066E-07
PMM	3,1261E-07	3,31444E-07	3,62448E-07	3,69105E-07	2,01189E-07	0,118434	5,07718E-11	1,74873E-10	2,24174E-10	0,755675	3,50461	-3,37872	1,68066E-07
GMP	3,1261E-07	3,31444E-07	3,62448E-07	3,69105E-07	2,01189E-07	0,118434	5,07719E-11	1,74873E-10	2,24174E-10	0,755675	3,50461	-3,37872	1,68066E-07
GME	3,1261E-07	3,31444E-07	3,62448E-07	3,69105E-07	2,01189E-07	0,118434	5,07721E-11	1,74873E-10	2,24174E-10	0,755675	3,50461	-3,37872	1,68066E-07
GGP	3,1261E-07	3,31444E-07	3,62448E-07	3,69105E-07	2,01189E-07	0,118434	5,07717E-11	1,74873E-10	2,24174E-10	0,755675	3,50461	-3,37872	1,68066E-07
GPP	3,1261E-07	3,31444E-07	3,62448E-07	3,69105E-07	2,01189E-07	0,118434	5,07719E-11	1,74873E-10	2,24174E-10	0,755675	3,50461	-3,37872	1,68066E-07
L-GalDH	3,1261E-07	3,31444E-07	3,62448E-07	3,69105E-07	2,01189E-07	0,118434	5,07714E-11	1,74873E-10	2,24174E-10	0,755675	3,50461	-3,37872	1,68066E-07
GLDH	3,1261E-07	3,31444E-07	3,62448E-07	3,69105E-07	2,01189E-07	0,118434	5,07715E-11	1,74873E-10	2,24174E-10	0,755675	3,50461	-3,37872	1,68066E-07
Turnover	3,1261E-07	3,31444E-07	3,62448E-07	3,69105E-07	2,01189E-07	0,118434	5,07718E-11	1,74873E-10	2,24174E-10	0,755675	3,50461	-3,37872	1,68066E-07
Oxidation	7,86351E-08	8,33728E-08	9,11717E-08	9,28461E-08	5,06079E-08	0,0297915	1,27713E-11	4,39884E-11	5,63896E-11	-0,0255376	0,881564	0,114182	4,22761E-08
Reduction	6,99173E-08	7,41298E-08	8,10641E-08	8,25529E-08	4,49973E-08	0,0264887	1,13555E-11	3,91116E-11	5,01381E-11	-0,0546451	0,78383	0,244326	3,75892E-08
Recycle	3,1261E-07	3,31444E-07	3,62448E-07	3,69105E-07	2,01189E-07	0,118434	5,07717E-11	1,74873E-10	2,24174E-10	0,755675	3,50461	-3,37872	1,68066E-07

B. Concentration control coefficients. Ki (GGP) = 0,01 mM

Ki (PMI) 100 mM	PGI	PMI	PMM	GMP	GME	GGP	GPP	L-GalDH	GLDH	Turnover	Oxidation	Reduction	Recycle
D-Glc 6-P	-0,00213012	-0,00165597	-0,0012757	-0,00116838	-0,000568578	-0,0197112	8,18563E-07	6,16078E-05	3,61423E-06	0,0207319	0,0835826	-0,0805802	0,00270963
D-Fru 6-P	0,00504082	-0,00165635	-0,001276	-0,00116865	-0,000568709	-0,0205651	8,1875E-07	6,16218E-05	3,61505E-06	0,0153174	0,0584686	-0,0563683	0,00271025
D-Man 6-P	0,00504092	0,00530495	-0,00127603	-0,00116868	-0,000568721	-0,0213904	8,18765E-07	0,000061623	3,61512E-06	0,0100576	0,0340748	-0,0328508	0,0027103
D-Man 1-P	0,00504182	0,0053059	0,00584592	-0,00116889	-0,000568824	-0,0222377	8,18911E-07	0,000061634	3,61576E-06	0,00467735	0,0091204	-0,00879279	0,00271079
GDP-D-Man	0,00504273	0,00530685	0,00584697	0,00595436	-0,000568928	-0,0230854	8,19059E-07	6,16451E-05	3,61641E-06	-0,00070482	-0,0158429	0,0152738	0,00271127
GDP-L-Gal	0,00504277	0,00530689	0,00584702	0,0059544	0,00324558	-0,0235374	8,19065E-07	6,16456E-05	3,61644E-06	-0,00358736	-0,0292114	0,0281621	0,0027113
L-Gal 1-P	3,13743E-07	3,30176E-07	3,6378E-07	3,70461E-07	2,01928E-07	0,118847	-1,00348	3,83536E-09	2,25002E-10	0,758307	3,51682	-3,39049	1,68687E-07
L-Gal	2,53342E-06	2,66611E-06	2,93747E-06	2,99142E-06	1,63054E-06	0,959669	4,11486E-10	-0,998178	-0,00550829	0,03772	0,174929	-0,168645	1,36212E-06

L-GalL	3,13743E-07	3,30176E-07	3,6378E-07	3,70461E-07	2,01928E-07	0,118847	5,09598E-11	3,83536E-09	-1,00348	0,758307	3,51682	-3,39049	1,68687E-07
L-Asc	2,33531E-06	2,45763E-06	2,70776E-06	2,7575E-06	1,50304E-06	0,884626	3,79311E-10	2,85482E-08	1,67478E-09	-0,75831	-3,51684	3,39051	1,25561E-06
DHA	3,12654E-07	3,2903E-07	3,62518E-07	3,69176E-07	2,01228E-07	0,118434	5,07824E-11	3,82205E-09	2,24221E-10	-0,244325	3,50461	-3,37872	1,68101E-07
Breakdown	3,12654E-07	3,2903E-07	3,62517E-07	3,69176E-07	2,01228E-07	0,118434	5,07823E-11	3,82205E-09	2,24221E-10	0,755674	3,50461	-3,37872	-1

Ki (L-GalDH) 100 mM	PGI	PMI	PMM	GMP	GME	GGP	GPP	L-GalDH	GLDH	Turnover	Oxidation	Reduction	Recycle
D-Glc 6-P	-0,00213012	-0,00166836	-0,00127564	-0,00116832	-0,000568548	-0,0196386	8,18505E-07	2,81918E-06	3,61397E-06	0,0207307	0,0835774	-0,0805752	0,00270944
D-Fru 6-P	0,00504081	-0,00166874	-0,00127593	-0,00116859	-0,000568679	-0,0204924	8,18692E-07	2,81982E-06	3,61479E-06	0,0153161	0,0584635	-0,0563634	0,00271006
D-Man 6-P	0,00504117	0,0053449	-0,00127602	-0,00116868	-0,000568721	-0,0213712	8,18749E-07	2,82002E-06	3,61505E-06	0,0100571	0,0340727	-0,0328488	0,00271025
D-Man 1-P	0,00504207	0,00534585	0,00584592	-0,00116889	-0,000568824	-0,0222185	8,18896E-07	2,82053E-06	3,61569E-06	0,00467687	0,0091184	-0,00879085	0,00271074
GDP-D-Man	0,00504298	0,00534682	0,00584697	0,00595435	-0,000568928	-0,0230662	8,19043E-07	2,82104E-06	3,61634E-06	-0,0007053	-0,0158449	0,0152757	0,00271122
GDP-L-Gal	0,00504302	0,00534686	0,00584701	0,0059544	0,00324558	-0,0235182	8,1905E-07	2,82106E-06	3,61637E-06	-0,00358784	-0,0292134	0,028164	0,00271124
L-Gal 1-P	3,13698E-07	3,32599E-07	3,63711E-07	3,70391E-07	2,0189E-07	0,118847	-1,00348	1,75483E-10	2,24955E-10	0,758307	3,51682	-3,39049	1,68652E-07
L-Gal	3,73044E-07	3,95519E-07	4,32517E-07	4,40461E-07	2,40083E-07	0,14133	6,05867E-11	-0,899071	-0,108413	0,742463	3,44334	-3,31965	2,00557E-07
L-GalL	3,13698E-07	3,32599E-07	3,63711E-07	3,70391E-07	2,0189E-07	0,118847	5,09483E-11	1,75482E-10	-1,00348	0,758307	3,51682	-3,39049	1,68652E-07
L-Asc	2,33498E-06	2,47566E-06	2,70724E-06	2,75697E-06	1,50275E-06	0,884626	3,79231E-10	1,30619E-09	1,67443E-09	-0,75831	-3,51684	3,39051	1,25534E-06
DHA	3,1261E-07	3,31444E-07	3,62448E-07	3,69105E-07	2,01189E-07	0,118434	5,07718E-11	1,74873E-10	2,24174E-10	-0,244325	3,50461	-3,37872	1,68066E-07
Breakdown	3,1261E-07	3,31444E-07	3,62448E-07	3,69105E-07	2,01189E-07	0,118434	5,07717E-11	1,74873E-10	2,24174E-10	0,755675	3,50461	-3,37872	-1

Appendix 7. The effect of varying relative enzyme activity (V or Vf) on the concentration of pathway intermediates with various strengths of non-competitive feedback inhibition at the GDP-L-Gal phosphorylase step (Ki GGP). Values were calculated in COPASI using conditions indicated in Appendix 3.

Phosphomannose isomerase

K_i (GGP)	Relative activity	D-Glc 6-P	D-Fru 6-P	D-Man 6-P	D-Man 1-P	GDP-D-Man	GDP-L-Gal	L-Gal 1-P	L-Gal	L-GalL	L-Asc	DHA	Breakdown
	0,2	116,5840	9,8073	0,1596	0,0406	0,0399	0,3976	0,0001	0,0110	0,0004	3,8972	0,3598	0,3598
	0,399052	115,8200	9,7430	0,3517	0,0899	0,0889	0,8850	0,0001	0,0111	0,0004	3,9458	0,3602	0,3602
	0,796214	114,3950	9,6231	0,7282	0,1864	0,1848	1,8401	0,0001	0,0112	0,0004	3,9668	0,3604	0,3604
	1,58866	111,6810	9,3947	1,4527	0,3723	0,3693	3,6780	0,0001	0,0112	0,0004	3,9766	0,3605	0,3605
	3,16979	106,6440	8,9709	2,8004	0,7181	0,7125	7,0971	0,0001	0,0112	0,0004	3,9813	0,3606	0,3606
0,014427	6,32456	97,8441	8,2305	5,1564	1,3225	1,3126	13,0741	0,0001	0,0112	0,0004	3,9837	0,3606	0,3606
	12,6191	84,0149	7,0670	8,8597	2,2725	2,2558	22,4691	0,0001	0,0112	0,0004	3,9848	0,3606	0,3606
	25,1785	65,5359	5,5122	13,8085	3,5421	3,5163	35,0236	0,0001	0,0113	0,0004	3,9854	0,3606	0,3606
	50,2377	45,5503	3,8307	19,1607	4,9152	4,8795	48,6018	0,0001	0,0113	0,0004	3,9857	0,3606	0,3606
	100,237	28,3237	2,3813	23,7742	6,0987	6,0545	60,3057	0,0001	0,0113	0,0004	3,9858	0,3606	0,3606
	200	16,1486	1,3569	27,0348	6,9352	6,8850	68,5775	0,0001	0,0113	0,0004	3,9859	0,3606	0,3606
	0,2	110,4730	9,2886	0,1478	0,0375	0,0368	0,3666	0,0001	0,0309	0,0005	10,5063	0,3842	0,3842
	0,399052	109,6540	9,2197	0,3294	0,0841	0,0831	0,8269	0,0001	0,0314	0,0005	10,6585	0,3844	0,3844
	0,796214	108,2670	9,1029	0,6854	0,1754	0,1736	1,7288	0,0001	0,0316	0,0005	10,7231	0,3845	0,3845
	1,58866	105,6830	8,8857	1,3704	0,3510	0,3479	3,4645	0,0001	0,0316	0,0005	10,7530	0,3845	0,3845
	3,16979	100,9150	8,4847	2,6449	0,6778	0,6722	6,6938	0,0001	0,0317	0,0005	10,7675	0,3845	0,3845
0,0416277	6,32456	92,5945	7,7850	4,8732	1,2492	1,2392	12,3399	0,0001	0,0317	0,0005	10,7746	0,3846	0,3846
	12,6191	79,5198	6,6854	8,3767	2,1476	2,1307	21,2172	0,0001	0,0317	0,0005	10,7781	0,3846	0,3846
	25,1785	62,0437	5,2157	13,0604	3,3485	3,3225	33,0847	0,0001	0,0317	0,0005	10,7798	0,3846	0,3846
	50,2377	43,1344	3,6255	18,1284	4,6481	4,6121	45,9262	0,0001	0,0317	0,0005	10,7807	0,3846	0,3846
	100,237	26,8281	2,2542	22,4989	5,7687	5,7242	57,0001	0,0001	0,0317	0,0005	10,7812	0,3846	0,3846
	200	15,2993	1,2847	25,5889	6,5611	6,5104	64,8296	0,0001	0,0317	0,0005	10,7814	0,3846	0,3846
	0,2	93,1177	7,8274	0,1204	0,0305	0,0298	0,2970	0,0001	0,0878	0,0005	29,3572	0,3942	0,3942
	0,399052	92,0478	7,7374	0,2723	0,0694	0,0685	0,6817	0,0001	0,0894	0,0005	29,9011	0,3943	0,3943
	0,796214	90,7279	7,6264	0,5700	0,1457	0,1442	1,4356	0,0001	0,0901	0,0005	30,1276	0,3944	0,3944
	1,58866	88,4946	7,4387	1,1430	0,2926	0,2899	2,8867	0,0001	0,0904	0,0005	30,2316	0,3944	0,3944
	3,16979	84,4722	7,1005	2,2090	0,5659	0,5611	5,5865	0,0001	0,0906	0,0005	30,2816	0,3944	0,3944
0,120112	6,32456	77,4971	6,5140	4,0731	1,0438	1,0352	10,3074	0,0001	0,0907	0,0005	30,3062	0,3944	0,3944
	12,6191	66,5534	5,5938	7,0043	1,7953	1,7808	17,7308	0,0001	0,0907	0,0005	30,3184	0,3944	0,3944
	25,1785	51,9304	4,3643	10,9235	2,8001	2,7777	27,6563	0,0001	0,0907	0,0005	30,3244	0,3944	0,3944
	50,2377	36,1075	3,0340	15,1652	3,8875	3,8565	38,3985	0,0001	0,0907	0,0005	30,3275	0,3944	0,3944
	100,237	22,4610	1,8866	18,8237	4,8254	4,7871	47,6639	0,0001	0,0907	0,0005	30,3290	0,3944	0,3944
	200	12,8114	1,0752	21,4108	5,4886	5,4451	54,2158	0,0001	0,0907	0,0005	30,3298	0,3944	0,3944
	0,2	18,0209	1,5131	0,0064	0,0012	0,0008	0,0081	0,0001	0,3342	0,0005	110,9750	0,3985	0,3985
	0,399052	8,7631	0,7348	0,0069	0,0014	0,0010	0,0095	0,0001	0,3645	0,0005	120,9780	0,3986	0,3986
	0,796214	4,3412	0,3630	0,0072	0,0015	0,0010	0,0102	0,0001	0,3789	0,0005	125,7560	0,3986	0,3986
	1,58866	2,1728	0,1807	0,0074	0,0015	0,0011	0,0106	0,0001	0,3860	0,0005	128,0990	0,3987	0,3987
1	3,16979	1,0972	0,0903	0,0074	0,0015	0,0011	0,0108	0,0001	0,3895	0,0005	129,2610	0,3987	0,3987
	6,32456	0,5608	0,0452	0,0075	0,0015	0,0011	0,0109	0,0001	0,3912	0,0005	129,8410	0,3987	0,3987
	12,6191	0,2926	0,0226	0,0075	0,0015	0,0011	0,0110	0,0001	0,3921	0,0005	130,1300	0,3987	0,3987
	25,1785	0,1584	0,0113	0,0075	0,0015	0,0011	0,0110	0,0001	0,3925	0,0005	130,2750	0,3987	0,3987
	50,2377	0,0911	0,0057	0,0075	0,0015	0,0011	0,0110	0,0001	0,3927	0,0005	130,3480	0,3987	0,3987

	100,237	0,0575	0,0028	0,0075	0,0015	0,0011	0,0110	0,0001	0,3929	0,0005	130,3850	0,3987	0,3987

Phosphomannomutase

K_i (GGP)	Relative activity	D-Glc 6-P	D-Fru 6-P	D-Man 6-P	D-Man 1-P	GDP-D-Man	GDP-L-Gal	L-Gal 1-P	L-Gal	L-GalL	L-Asc	DHA	Breakdown
	0,2	108,415	9,12005	9,05398	0,0378789	0,0372489	0,370859	0,000108305	0,0109676	0,000433221	3,8909	0,359719	0,359719
	0,399052	107,902	9,07679	9,01092	0,0838663	0,0829053	0,825619	0,000108451	0,0111237	0,000433805	3,94289	0,360202	0,360202
	0,796214	106,96	8,99753	8,9322	0,174464	0,172851	1,72152	0,000108513	0,0111913	0,000434054	3,96542	0,360408	0,360408
	1,58866	105,158	8,84587	8,78161	0,350685	0,347806	3,46416	0,000108542	0,011223	0,000434169	3,97596	0,360503	0,360503
	3,16979	101,75	8,5591	8,49688	0,685204	0,679921	6,77218	0,000108556	0,0112383	0,000434225	3,98107	0,360549	0,360549
0,014427	6,32456	95,5744	8,03953	7,98105	1,29185	1,28221	12,7712	0,000108563	0,0112459	0,000434252	3,98358	0,360572	0,360572
	12,6191	85,2537	7,17118	7,11893	2,30601	2,28908	22,8001	0,000108566	0,0112496	0,000434266	3,98483	0,360583	0,360583
	25,1785	70,1432	5,89982	5,85671	3,79093	3,76333	37,4844	0,000108568	0,0112515	0,000434273	3,98546	0,360589	0,360589
	50,2377	51,8213	4,35828	4,32624	5,59148	5,55094	55,2899	0,000108569	0,0112525	0,000434276	3,98577	0,360592	0,360592
	100,237	34,0719	2,8649	2,8436	7,33578	7,28271	72,5391	0,000108569	0,0112529	0,000434278	3,98593	0,360593	0,360593
	200	20,2473	1,70175	1,6888	8,69437	8,63154	85,9741	0,00010857	0,0112532	0,000434279	3,98601	0,360594	0,360594
	0,2	102,744	8,63859	8,57072	0,035266	0,0346134	0,344505	0,000115689	0,0308466	0,000462754	10,4891	0,384147	0,384147
	0,399052	102,164	8,58973	8,52216	0,0787243	0,0777385	0,773939	0,000115759	0,0313323	0,000463034	10,6501	0,384379	0,384379
	0,796214	101,234	8,5115	8,44451	0,164332	0,16269	1,61987	0,000115788	0,0315405	0,000463151	10,7191	0,384476	0,384476
	1,58866	99,5127	8,36675	8,30086	0,33085	0,327933	3,26534	0,000115801	0,0316374	0,000463206	10,7512	0,38452	0,38452
	3,16979	96,2843	8,09526	8,03144	0,646975	0,641635	6,38914	0,000115808	0,0316842	0,000463232	10,7667	0,384542	0,384542
0,0416277	6,32456	90,4466	7,60432	7,54426	1,22035	1,21061	12,055	0,000115811	0,0317073	0,000463244	10,7744	0,384552	0,384552
	12,6191	80,6926	6,78405	6,73026	2,17913	2,16205	21,5292	0,000115813	0,0317187	0,000463251	10,7782	0,384558	0,384558
	25,1785	66,4083	5,58278	5,53821	3,58353	3,55569	35,4069	0,000115813	0,0317245	0,000463254	10,7801	0,38456	0,38456
	50,2377	49,0799	4,12553	4,09212	5,28733	5,24643	52,2431	0,000115814	0,0317273	0,000463256	10,781	0,384562	0,384562
	100,237	32,2838	2,71304	2,69045	6,93883	6,88528	68,5625	0,000115814	0,0317288	0,000463256	10,7815	0,384562	0,384562
	200	19,1954	1,61235	1,59819	8,22578	8,16237	81,2796	0,000115814	0,0317295	0,000463257	10,7817	0,384563	0,384563
	0,2	86,6128	7,28047	7,21853	0,029442	0,0288182	0,28676	0,000118727	0,0877002	0,000474908	29,3233	0,394197	0,394197
	0,399052	85,7675	7,20938	7,1479	0,0657686	0,0648593	0,645614	0,000118759	0,0893726	0,000475037	29,8772	0,394303	0,394303
	0,796214	84,8358	7,13103	7,07012	0,137321	0,135849	1,35244	0,000118773	0,0900901	0,00047509	30,1149	0,394347	0,394347
	1,58866	83,3256	7,00405	6,94411	0,276499	0,273934	2,72732	0,000118779	0,0904244	0,000475115	30,2256	0,394368	0,394368
	3,16979	80,593	6,77429	6,71615	0,540726	0,536085	5,33751	0,000118782	0,0905861	0,000475127	30,2791	0,394378	0,394378
0,120112	6,32456	75,6973	6,36266	6,30775	1,02	1,01159	10,072	0,000118783	0,0906657	0,000475133	30,3055	0,394382	0,394382
	12,6191	67,5365	5,6765	5,62698	1,82151	1,80681	17,9898	0,000118784	0,0907053	0,000475136	30,3186	0,394385	0,394385
	25,1785	55,5917	4,67218	4,63055	2,99575	2,97182	29,5896	0,000118784	0,090725	0,000475137	30,3252	0,394386	0,394386
	50,2377	41,1014	3,45384	3,42178	4,42061	4,38549	43,6652	0,000118784	0,0907349	0,000475138	30,3284	0,394387	0,394387
	100,237	27,0539	2,27273	2,24995	5,80206	5,75608	57,3119	0,000118785	0,0907398	0,000475138	30,3301	0,394387	0,394387
	200	16,1055	1,35218	1,33663	6,87879	6,82435	67,9484	0,000118785	0,0907423	0,000475138	30,3309	0,394387	0,394387
	0,2	5,55867	0,465348	0,4418	0,00142386	0,00101552	0,00993217	0,000120063	0,373599	0,000480251	124,007	0,398614	0,398614
	0,399052	2,701	0,225095	0,202925	0,00147887	0,00107006	0,0104751	0,000120074	0,383643	0,000480295	127,333	0,39865	0,39865
	0,796214	1,44176	0,119227	0,0976639	0,00150407	0,00109504	0,0107239	0,000120078	0,388068	0,000480313	128,799	0,398665	0,398665
1	1,58866	0,847599	0,0692745	0,0479978	0,00151617	0,00110704	0,0108434	0,00012008	0,390156	0,000480322	129,49	0,398672	0,398672
	3,16979	0,558415	0,044962	0,0238247	0,00152212	0,00111293	0,010902	0,000120082	0,391173	0,000480326	129,827	0,398676	0,398676
	6,32456	0,415561	0,0329519	0,0118835	0,00152506	0,00111586	0,0109311	0,000120082	0,391675	0,000480328	129,993	0,398678	0,398678
	12,6191	0,344478	0,0269757	0,00594161	0,00152653	0,00111731	0,0109456	0,000120082	0,391925	0,000480329	130,076	0,398678	0,398678

	25,1785	0,30898	0,0239913	0,0029743	0,00152727	0,00111804	0,0109529	0,000120082	0,392049	0,00048033	130,117	0,398679	0,398679
	50,2377	0,29122	0,0224982	0,00148979	0,00152764	0,00111841	0,0109565	0,000120082	0,392112	0,00048033	130,138	0,398679	0,398679
	100,237	0,282328	0,0217506	0,000746438	0,00152782	0,00111859	0,0109583	0,000120082	0,392143	0,00048033	130,148	0,398679	0,398679

GDP-D-Mannose pyrophosphorylase

K_i (GGP)	Relative activity	D-Glc 6-P	D-Fru 6-P	D-Man 6-P	D-Man 1-P	GDP-D-Man	GDP-L-Gal	L-Gal 1-P	L-Gal	L-GalL	L-Asc	DHA	Breakdown
	0,2	106,497	8,95872	8,8938	2,28131	0,0369275	0,367657	0,000108303	0,0109652	0,000433212	3,89009	0,359712	0,359712
	0,399052	106,039	8,92007	8,85533	2,27142	0,081805	0,814659	0,00010845	0,011122	0,000433799	3,94231	0,360197	0,360197
	0,796214	105,204	8,84974	8,78547	2,25348	0,17033	1,69641	0,000108513	0,0111904	0,00043405	3,96511	0,360405	0,360405
	1,58866	103,603	8,71508	8,65176	2,21918	0,342954	3,41583	0,000108542	0,0112225	0,000434168	3,97581	0,360502	0,360502
	3,16979	100,564	8,45934	8,39784	2,15403	0,672232	6,69559	0,000108556	0,0112381	0,000434224	3,981	0,360549	0,360549
0,014427	6,32456	95,0082	7,99189	7,93375	2,03497	1,27474	12,6968	0,000108563	0,0112458	0,000434252	3,98357	0,360572	0,360572
	12,6191	85,578	7,19846	7,14602	1,83289	2,29769	22,886	0,000108567	0,0112497	0,000434266	3,98484	0,360583	0,360583
	25,1785	71,4342	6,00844	5,96455	1,52979	3,8321	38,1694	0,000108568	0,0112516	0,000434273	3,98548	0,360589	0,360589
	50,2377	53,7239	4,51836	4,48517	1,15027	5,75345	57,3069	0,000108569	0,0112525	0,000434276	3,98579	0,360592	0,360592
	100,237	35,9513	3,02303	3,00059	0,769414	7,68158	76,512	0,00010857	0,011253	0,000434278	3,98595	0,360593	0,360593
	200	21,6677	1,82125	1,80745	0,463326	9,23119	91,9469	0,00010857	0,0112532	0,000434279	3,98603	0,360594	0,360594
	0,2	100,93	8,48601	8,4193	2,1585	0,0343621	0,342002	0,000115688	0,0308403	0,000462751	10,487	0,384144	0,384144
	0,399052	100,403	8,44164	8,37521	2,14718	0,0767512	0,764107	0,000115758	0,0313272	0,000463031	10,6484	0,384376	0,384376
	0,796214	99,5734	8,37187	8,30594	2,12942	0,160359	1,59666	0,000115787	0,0315377	0,00046315	10,7181	0,384474	0,384474
	1,58866	98,0432	8,24318	8,17823	2,09666	0,323398	3,22018	0,000115801	0,031636	0,000463205	10,7507	0,38452	0,38452
	3,16979	95,1634	8,00099	7,93789	2,03504	0,634414	6,31723	0,000115808	0,0316837	0,000463231	10,7665	0,384542	0,384542
0,0416277	6,32456	89,9111	7,55929	7,49957	1,92264	1,20358	11,9849	0,000115811	0,0317071	0,000463244	10,7743	0,384552	0,384552
	12,6191	80,9993	6,80984	6,75586	1,73194	2,17017	21,6101	0,000115813	0,0317188	0,000463251	10,7782	0,384558	0,384558
	25,1785	67,63	5,68553	5,64017	1,44586	3,62059	36,0531	0,000115814	0,0317246	0,000463254	10,7801	0,38456	0,38456
	50,2377	50,8818	4,27706	4,24249	1,08747	5,43771	54,1478	0,000115814	0,0317275	0,000463256	10,7811	0,384562	0,384562
	100,237	34,0651	2,86284	2,8391	0,727614	7,26231	72,3169	0,000115814	0,031729	0,000463256	10,7816	0,384562	0,384562
	200	20,5429	1,72567	1,71064	0,438256	8,72947	86,9267	0,000115814	0,0317297	0,000463257	10,7818	0,384563	0,384563
	0,2	85,0866	7,15214	7,09121	1,81757	0,0286794	0,285379	0,000118727	0,0876859	0,000474907	29,3186	0,394196	0,394196
	0,399052	84,2932	7,08542	7,02491	1,80057	0,0641055	0,638109	0,000118759	0,0893566	0,000475035	29,8719	0,394302	0,394302
	0,796214	83,447	7,01426	6,95427	1,78246	0,13397	1,33374	0,000118772	0,0900808	0,00047509	30,1118	0,394347	0,394347
	1,58866	82,0967	6,90072	6,8416	1,75357	0,270207	2,69022	0,000118779	0,0904198	0,000475115	30,2241	0,394367	0,394367
	3,16979	79,6556	6,69547	6,63795	1,70136	0,530102	5,27793	0,000118782	0,0905842	0,000475127	30,2785	0,394377	0,394377
0,120112	6,32456	75,2494	6,325	6,27039	1,60713	1,00574	10,0138	0,000118783	0,0906652	0,000475133	30,3053	0,394382	0,394382
	12,6191	67,7931	5,69808	5,64839	1,44767	1,81358	18,0573	0,000118784	0,0907055	0,000475136	30,3187	0,394385	0,394385
	25,1785	56,6141	4,75814	4,71584	1,2086	3,02597	30,1288	0,000118784	0,0907256	0,000475137	30,3253	0,394386	0,394386
	50,2377	42,6099	3,58067	3,54762	0,909102	4,54522	45,2556	0,000118784	0,0907356	0,000475138	30,3287	0,394387	0,394387
	100,237	28,5462	2,3982	2,37444	0,608336	6,07107	60,4481	0,000118785	0,0907406	0,000475138	30,3303	0,394387	0,394387
	200	17,2355	1,4472	1,4309	0,366445	7,29828	72,6672	0,000118785	0,0907432	0,000475138	30,3312	0,394387	0,394387
	0,2	4,47974	0,374639	0,351625	0,0897407	0,00103433	0,0101195	0,000120067	0,377126	0,000480267	125,175	0,398627	0,398627
	0,399052	2,21718	0,184419	0,162488	0,0412562	0,00107891	0,0105633	0,000120075	0,385223	0,000480301	127,857	0,398656	0,398656
1	0,796214	1,21881	0,100483	0,0790305	0,0198621	0,00109921	0,0107654	0,000120079	0,388797	0,000480316	129,04	0,398668	0,398668
	1,58866	0,747514	0,0608601	0,039633	0,00976265	0,00110893	0,0108622	0,000120081	0,390483	0,000480323	129,599	0,398674	0,398674
	3,16979	0,518083	0,0415712	0,0204539	0,00484619	0,0011137	0,0109097	0,000120082	0,391304	0,000480327	129,871	0,398676	0,398676

	6,32456	0,404737	0,0320419	0,0109789	0,00241729	0,00111606	0,0109332	0,000120082	0,39171	0,000480328	130,005	0,398678	0,398678
	12,6191	0,348334	0,0272999	0,00626392	0,00120863	0,00111724	0,0109449	0,000120082	0,391912	0,000480329	130,072	0,398678	0,398678
	25,1785	0,320167	0,0249318	0,00390928	0,000605031	0,00111783	0,0109508	0,000120082	0,392013	0,000480329	130,105	0,398679	0,398679
	50,2377	0,306075	0,023747	0,00273127	0,000303053	0,00111812	0,0109537	0,000120082	0,392063	0,00048033	130,122	0,398679	0,398679
	100,237	0,299018	0,0231538	0,00214139	0,000151841	0,00111827	0,0109552	0,000120082	0,392088	0,00048033	130,13	0,398679	0,398679

GDP-D-Mannose 3',5'-epimerase

K_i (GGP)	Relative activity	D-Glc 6-P	D-Fru 6-P	D-Man 6-P	D-Man 1-P	GDP-D-Man	GDP-L-Gal	L-Gal 1-P	L-Gal	L-GalL	L-Asc	DHA	Breakdown
	0,02	108,054	9,12403	9,09187	2,34089	2,33249	0,000479364	0,000052898	0,000675835	0,000211592	0,3605	0,176016	0,176016
	0,0502377	107,053	9,01558	8,96044	2,30097	2,28667	0,00436079	9,18062E-05	0,00361475	0,000367225	1,42151	0,305087	0,305087
	0,126191	105,871	8,90857	8,84666	2,26986	2,25388	0,0204232	0,000104082	0,00765965	0,000416328	2,78677	0,345741	0,345741
	0,316979	105,249	8,85441	8,79104	2,25514	2,23881	0,0626237	0,000107032	0,00974966	0,000428126	3,48496	0,355504	0,355504
	0,796214	104,911	8,82542	8,76165	2,24745	2,23103	0,168868	0,000107991	0,0106436	0,000431963	3,78297	0,358678	0,358678
0,014427	2	104,589	8,79812	8,73433	2,24039	2,22396	0,435062	0,000108344	0,011009	0,000433377	3,90468	0,359848	0,359848
	5,02377	104	8,74845	8,68493	2,22769	2,21134	1,09884	0,000108481	0,0111559	0,000433924	3,95362	0,3603	0,3603
	12,6191	102,631	8,63325	8,57052	2,19834	2,18218	2,73584	0,000108535	0,0112146	0,000434139	3,97318	0,360478	0,360478
	31,6979	99,3774	8,35951	8,29873	2,12861	2,11295	6,6658	0,000108556	0,0112381	0,000434224	3,98098	0,360549	0,360549
	79,6214	92,059	7,74375	7,68739	1,97177	1,95725	15,5207	0,000108564	0,0112474	0,000434258	3,98409	0,360577	0,360577
	200	77,6932	6,53506	6,48739	1,66392	1,65161	32,9073	0,000108568	0,0112511	0,000434271	3,98532	0,360588	0,360588
	0,02	108,008	9,11797	9,08372	2,33824	2,3293	0,00020477	5,63764E-05	0,000781329	0,000225506	0,403691	0,187569	0,187569
	0,0502377	105,765	8,8992	8,83692	2,26725	2,25118	0,00330559	0,000104786	0,0080864	0,000419143	2,92954	0,34807	0,34807
	0,126191	102,2	8,59408	8,52825	2,18674	2,16993	0,0189559	0,000113596	0,0208748	0,000454384	7,18255	0,377225	0,377225
	0,316979	100,43	8,44434	8,37849	2,14812	2,13138	0,0590176	0,000115085	0,0271782	0,000460342	9,27303	0,382152	0,382152
	0,796214	99,6045	8,37463	8,30891	2,13021	2,11354	0,15939	0,000115543	0,0298774	0,000462171	10,1678	0,383665	0,383665
0,0416277	2	99,0919	8,33142	8,26588	2,11915	2,10255	0,410681	0,000115709	0,0309861	0,000462836	10,5353	0,384214	0,384214
	5,02377	98,4511	8,2775	8,21231	2,10541	2,0889	1,03723	0,000115773	0,0314331	0,000463091	10,6835	0,384426	0,384426
	12,6191	97,1251	8,16597	8,10161	2,07702	2,06072	2,58243	0,000115798	0,0316121	0,000463191	10,7428	0,384509	0,384509
	31,6979	94,0399	7,90651	7,84413	2,01099	1,9952	6,29233	0,000115808	0,0316835	0,000463231	10,7665	0,384542	0,384542
	79,6214	87,1234	7,32485	7,26693	1,86299	1,84833	14,6531	0,000115812	0,0317119	0,000463247	10,7759	0,384555	0,384555
	200	73,5495	6,18333	6,13415	1,57253	1,56009	31,0762	0,000115813	0,0317232	0,000463253	10,7796	0,38456	0,38456
	0,02	107,987	9,11529	9,08015	2,33708	2,32791	8,78975E-05	5,78601E-05	0,000830669	0,000231441	0,423526	0,192496	0,192496
	0,0502377	102,785	8,64366	8,57796	2,19959	2,18279	0,0026029	0,000112909	0,0188055	0,000451638	6,49586	0,374953	0,374953
	0,126191	92,291	7,75838	7,69478	1,97243	1,95667	0,016796	0,00011781	0,0569166	0,00047124	19,1269	0,391164	0,391164
	0,316979	87,0624	7,3184	7,25692	1,86009	1,84512	0,0508523	0,00011846	0,0758549	0,00047384	25,4	0,393314	0,393314
	0,796214	84,6188	7,11284	7,05242	1,80764	1,79306	0,134992	0,000118662	0,0845019	0,000474649	28,264	0,393982	0,393982
0,120112	2	83,4295	7,01281	6,95294	1,78212	1,76773	0,34504	0,000118737	0,0882017	0,000474947	29,4894	0,394229	0,394229
	5,02377	82,5792	6,9413	6,8819	1,76391	1,74966	0,868487	0,000118766	0,0897235	0,000475063	29,9934	0,394325	0,394325
	12,6191	81,3438	6,83742	6,77881	1,73748	1,72343	2,15934	0,000118777	0,0903377	0,000475109	30,1969	0,394362	0,394362
	31,6979	78,7152	6,6164	6,55951	1,68125	1,66765	5,25861	0,000118782	0,0905835	0,000475127	30,2783	0,394377	0,394377
	79,6214	72,9159	6,1288	6,07573	1,55723	1,5446	12,2438	0,000118783	0,0906816	0,000475134	30,3108	0,394383	0,394383
	200	61,5645	5,17437	5,1288	1,31447	1,30374	25,9672	0,000118784	0,0907207	0,000475137	30,3237	0,394386	0,394386
	0,02	107,976	9,11389	9,0783	2,33649	2,3272	0,000028052	5,86207E-05	0,000857057	0,000234483	0,43405	0,195021	0,195021
1	0,0502377	79,6347	6,69362	6,63537	1,70068	1,6869	0,00162639	0,000118984	0,103059	0,000475934	34,4102	0,395045	0,395045
	0,126191	32,8224	2,75752	2,72107	0,697147	0,691222	0,00576868	0,000119911	0,273604	0,000479643	90,8913	0,398111	0,398111

	0,316979	14,7344	1,23678	1,20891	0,309503	0,306649	0,00828588	0,000120021	0,339503	0,000480084	112,715	0,398476	0,398476
	0,796214	6,49133	0,54376	0,519804	0,132853	0,131401	0,00972044	0,000120058	0,369533	0,000480233	122,661	0,398599	0,398599
	2	2,86539	0,238916	0,216683	0,0551488	0,0543138	0,0104253	0,000120073	0,382743	0,000480291	127,035	0,398647	0,398647
	5,02377	1,34484	0,111079	0,0895693	0,0225636	0,0219874	0,0107361	0,000120079	0,388283	0,000480314	128,87	0,398666	0,398666
	12,6191	0,725232	0,0589868	0,0377715	0,00928549	0,00881465	0,0108655	0,000120081	0,39054	0,000480323	129,617	0,398674	0,398674
	31,6979	0,476145	0,0380453	0,0169485	0,00394758	0,00351913	0,0109179	0,000120082	0,391447	0,000480327	129,918	0,398677	0,398677
	79,6214	0,376588	0,0296753	0,00862579	0,00181409	0,00140259	0,010939	0,000120082	0,39181	0,000480329	130,038	0,398678	0,398678

GDP-L-Galactose phosphorylase

K_i (GGP)	Relative activity	D-Glc 6-P	D-Fru 6-P	D-Man 6-P	D-Man 1-P	GDP-D-Man	GDP-L-Gal	L-Gal 1-P	L-Gal	L-GalL	L-Asc	DHA	Breakdown
	0,2	91,8261	7,76164	7,74204	1,99536	1,99021	19,8745	3,78734E-05	0,000345022	0,000151493	0,214303	0,126085	0,126085
	0,399052	91,7621	7,74967	7,72373	1,98897	1,98217	19,7852	5,02102E-05	0,000603039	0,000200841	0,329956	0,167088	0,167088
	0,796214	91,6464	7,73241	7,69925	1,98076	1,97209	19,6744	6,43397E-05	0,00108264	0,000257359	0,522058	0,214007	0,214007
	1,58866	91,4303	7,7064	7,66581	1,97018	1,95959	19,5393	7,90511E-05	0,00199439	0,000316205	0,857218	0,262811	0,262811
	3,16979	91,0155	7,66434	7,61702	1,95584	1,94354	19,3697	9,25684E-05	0,00376059	0,000370274	1,47143	0,307612	0,307612
0,014427	6,32456	90,2036	7,59037	7,53796	1,93413	1,92056	19,1332	0,000103307	0,0072304	0,000413228	2,64302	0,343175	0,343175
	12,6191	88,5966	7,45136	7,3959	1,89672	1,88246	18,7486	0,000110691	0,0141067	0,000442766	4,9353	0,367615	0,367615
	25,1785	85,3996	7,18019	7,12388	1,82638	1,81208	18,0447	0,000115197	0,0277921	0,000460787	9,47655	0,38252	0,38252
	50,2377	79,0269	6,6431	6,58833	1,68876	1,67522	16,6803	0,000117724	0,0550747	0,000470895	18,5168	0,390879	0,390879
	100,237	66,3173	5,57388	5,52407	1,41577	1,40423	13,9813	0,00011907	0,109488	0,00047628	36,5396	0,395331	0,395331
	200	40,9796	3,44336	3,40445	0,872338	0,865032	8,61245	0,000119766	0,217967	0,000479065	72,4657	0,397633	0,397633
	0,2	91,7194	7,74283	7,71378	1,98558	1,97797	19,739	5,62962E-05	0,00077874	0,000225185	0,402644	0,187302	0,187302
	0,399052	91,5604	7,72142	7,6847	1,97607	1,96647	19,6134	7,13806E-05	0,00144409	0,000285522	0,657834	0,23737	0,23737
	0,796214	91,2571	7,68811	7,644	1,96364	1,95215	19,4601	8,60691E-05	0,00273055	0,000344276	1,11637	0,286076	0,286076
	1,58866	90,6662	7,63181	7,58163	1,94597	1,93295	19,26	9,85046E-05	0,00525248	0,000394018	1,97802	0,327274	0,327274
	3,16979	89,4995	7,52891	7,47464	1,91732	1,90331	18,9584	0,000107578	0,0102425	0,000430312	3,6493	0,357312	0,357312
0,0416277	6,32456	87,181	7,33092	7,27474	1,8653	1,85093	18,4328	0,000113375	0,0201661	0,000453501	6,94741	0,376495	0,376495
	12,6191	82,5612	6,94076	6,88492	1,76493	1,75091	17,4346	0,000116729	0,0399436	0,000466915	13,5038	0,387588	0,387588
	25,1785	73,3481	6,16524	6,11257	1,5667	1,55402	15,473	0,000118548	0,0793875	0,000474191	26,57	0,393604	0,393604
	50,2377	54,9739	4,62001	4,57502	1,17244	1,16278	11,577	0,000119498	0,158053	0,000477993	52,6235	0,396747	0,396747
	100,237	18,4335	1,54778	1,51876	0,388934	0,385451	3,83751	0,000119985	0,314494	0,000479938	104,433	0,398355	0,398355
	200	0,389453	0,0307569	0,00970216	0,00209001	0,00167632	0,0165113	0,000120082	0,391746	0,000480328	130,017	0,398678	0,398678
	0,2	91,4604	7,70975	7,66993	1,97145	1,96106	19,555	7,75117E-05	0,00186687	0,000310047	0,811576	0,257706	0,257706
	0,399052	91,0342	7,66612	7,61901	1,95641	1,94416	19,3762	9,21573E-05	0,00368093	0,000368629	1,44418	0,30625	0,30625
	0,796214	90,1901	7,58918	7,53672	1,9338	1,92021	19,1297	0,000103415	0,00728797	0,000413661	2,66231	0,343533	0,343533
	1,58866	88,5107	7,44401	7,38849	1,89479	1,88052	18,7291	0,000110911	0,0144745	0,000443644	5,05757	0,368342	0,368342
	3,16979	85,1628	7,16019	7,10389	1,82124	1,80696	17,9935	0,000115371	0,0288059	0,000461483	9,81262	0,383096	0,383096
0,120112	6,32456	78,4852	6,5975	6,54291	1,67711	1,66365	16,565	0,000117832	0,0573941	0,000471326	19,2851	0,391235	0,391235
	12,6191	65,1651	5,47698	5,42765	1,39105	1,3797	13,737	0,00011913	0,114421	0,000476519	38,1733	0,395529	0,395529
	25,1785	38,6121	3,2443	3,20642	0,821572	0,814667	8,11099	0,000119798	0,228103	0,000479191	75,8226	0,397738	0,397738
	50,2377	0,596518	0,0481654	0,0270192	0,00652917	0,00608023	0,060358	0,000120081	0,39086	0,000480325	129,723	0,398675	0,398675
	100,237	0,347269	0,0272104	0,00617426	0,00118565	0,000779139	0,00757867	0,000120082	0,391927	0,000480329	130,077	0,398678	0,398678
	200	0,3245	0,0252961	0,00427005	0,000697515	0,000294879	0,00275722	0,000120082	0,392024	0,000480329	130,109	0,398679	0,398679
1	0,2	88,9148	7,47859	7,42346	1,90391	1,88971	18,8214	0,000109782	0,0127448	0,000439129	4,48245	0,364607	0,364607

	0,399052	85,4333	7,18304	7,12672	1,82712	1,81281	18,052	0,000115171	0,0276479	0,000460684	9,42874	0,382435	0,382435
	0,796214	78,448	6,59437	6,5398	1,67631	1,66285	16,5571	0,000117839	0,0575532	0,000471355	19,3378	0,391259	0,391259
	1,58866	64,4939	5,42054	5,37149	1,37665	1,36541	13,5947	0,000119162	0,117295	0,000476649	39,125	0,395636	0,395636
	3,16979	36,67	3,08102	3,04399	0,779931	0,773354	7,69965	0,000119822	0,236418	0,000479286	78,5763	0,397816	0,397816
	6,32456	0,533486	0,0428662	0,0217478	0,00517787	0,00473965	0,0470108	0,000120081	0,39113	0,000480326	129,813	0,398676	0,398676
	12,6191	0,34486	0,0270078	0,00597278	0,001134	0,000727899	0,0070685	0,000120082	0,391937	0,000480329	130,08	0,398678	0,398678
	25,1785	0,323851	0,0252416	0,00421583	0,000683614	0,000281089	0,00261992	0,000120082	0,392027	0,000480329	130,11	0,398679	0,398679
	50,2377	0,316963	0,0246625	0,00363979	0,00053595	0,000134598	0,0011614	0,000120082	0,392057	0,00048033	130,12	0,398679	0,398679
	100,237	0,314077	0,0244198	0,00339841	0,000474072	7,32116E-05	0,000550225	0,000120082	0,392069	0,00048033	130,124	0,398679	0,398679

L-Galactose 1-phosphate phosphatase

K_i (GGP)	Relative activity	D-Glc 6-P	D-Fru 6-P	D-Man 6-P	D-Man 1-P	GDP-D-Man	GDP-L-Gal	L-Gal 1-P	L-Gal	L-GalL	L-Asc	DHA	Breakdown
	0,2	89,2598	7,50824	7,45357	1,91179	1,89769	18,9018	0,00659832	0,0112486	0,000434262	3,98451	0,36058	0,36058
	0,399052	89,2624	7,50845	7,45379	1,91184	1,89775	18,9023	0,00298005	0,0112487	0,000434262	3,98451	0,36058	0,36058
	0,796214	89,2635	7,50855	7,45388	1,91187	1,89777	18,9025	0,00142305	0,0112487	0,000434262	3,98451	0,36058	0,36058
	1,58866	89,264	7,50859	7,45392	1,91188	1,89778	18,9026	0,00069673	0,0112487	0,000434262	3,98451	0,36058	0,36058
	3,16979	89,2642	7,50861	7,45394	1,91188	1,89779	18,9027	0,000345193	0,0112487	0,000434262	3,98451	0,36058	0,36058
0,014427	6,32456	89,2644	7,50862	7,45395	1,91189	1,89779	18,9027	0,000172019	0,0112487	0,000434262	3,98451	0,36058	0,36058
	12,6191	89,2644	7,50863	7,45396	1,91189	1,89779	18,9027	8,59679E-05	0,0112487	0,000434262	3,98451	0,36058	0,36058
	25,1785	89,2644	7,50863	7,45396	1,91189	1,89779	18,9027	4,30245E-05	0,0112487	0,000434262	3,98451	0,36058	0,36058
	50,2377	89,2645	7,50863	7,45396	1,91189	1,89779	18,9027	2,15479E-05	0,0112487	0,000434262	3,98451	0,36058	0,36058
	100,237	89,2645	7,50863	7,45396	1,91189	1,89779	18,9027	1,07957E-05	0,0112487	0,000434262	3,98451	0,36058	0,36058
	200	89,2645	7,50863	7,45396	1,91189	1,89779	18,9027	5,40968E-06	0,0112487	0,000434262	3,98451	0,36058	0,36058
	0,2	84,4782	7,1024	7,04618	1,80639	1,79216	17,8459	0,0071415	0,0317157	0,000463249	10,7772	0,384556	0,384556
	0,399052	84,481	7,10263	7,04641	1,80644	1,79222	17,8465	0,00319933	0,0317157	0,000463249	10,7772	0,384556	0,384556
	0,796214	84,4821	7,10273	7,04651	1,80647	1,79225	17,8468	0,00152248	0,0317157	0,000463249	10,7772	0,384556	0,384556
	1,58866	84,4827	7,10278	7,04656	1,80648	1,79226	17,8469	0,000744206	0,0317157	0,000463249	10,7772	0,384556	0,384556
	3,16979	84,4829	7,1028	7,04658	1,80649	1,79226	17,8469	0,000368428	0,0317157	0,000463249	10,7772	0,384556	0,384556
0,0416277	6,32456	84,4831	7,10281	7,04659	1,80649	1,79227	17,847	0,000183527	0,0317157	0,000463249	10,7772	0,384556	0,384556
	12,6191	84,4831	7,10282	7,04659	1,80649	1,79227	17,847	9,17016E-05	0,0317157	0,000463249	10,7772	0,384556	0,384556
	25,1785	84,4832	7,10282	7,0466	1,80649	1,79227	17,847	4,58897E-05	0,0317157	0,000463249	10,7772	0,384556	0,384556
	50,2377	84,4832	7,10282	7,0466	1,80649	1,79227	17,847	2,29818E-05	0,0317157	0,000463249	10,7772	0,384556	0,384556
	100,237	84,4832	7,10282	7,0466	1,80649	1,79227	17,847	1,15138E-05	0,0317157	0,000463249	10,7772	0,384556	0,384556
	200	84,4832	7,10282	7,0466	1,80649	1,79227	17,847	5,76945E-06	0,0317157	0,000463249	10,7772	0,384556	0,384556
	0,2	70,7018	5,94264	5,89103	1,50988	1,49762	14,9113	0,00736884	0,0906948	0,000475135	30,3152	0,394384	0,394384
	0,399052	70,7047	5,94288	5,89127	1,50994	1,49768	14,9119	0,00329006	0,0906949	0,000475135	30,3152	0,394384	0,394384
	0,796214	70,7059	5,94299	5,89137	1,50997	1,49771	14,9122	0,00156341	0,0906949	0,000475135	30,3152	0,394384	0,394384
	1,58866	70,7065	5,94303	5,89142	1,50998	1,49772	14,9123	0,000763709	0,0906949	0,000475135	30,3152	0,394384	0,394384
	3,16979	70,7068	5,94306	5,89144	1,50998	1,49773	14,9124	0,000377962	0,0906949	0,000475135	30,3152	0,394384	0,394384
0,120112	6,32456	70,7069	5,94307	5,89145	1,50999	1,49773	14,9124	0,000188247	0,0906949	0,000475135	30,3152	0,394384	0,394384
	12,6191	70,707	5,94307	5,89146	1,50999	1,49773	14,9124	9,40524E-05	0,0906949	0,000475135	30,3152	0,394384	0,394384
	25,1785	70,707	5,94308	5,89146	1,50999	1,49773	14,9124	4,70643E-05	0,0906949	0,000475135	30,3152	0,394384	0,394384
	50,2377	70,707	5,94308	5,89146	1,50999	1,49773	14,9124	2,35696E-05	0,0906949	0,000475135	30,3152	0,394384	0,394384
	100,237	70,707	5,94308	5,89146	1,50999	1,49773	14,9124	1,18081E-05	0,0906949	0,000475135	30,3152	0,394384	0,394384
	200	70,707	5,94308	5,89146	1,50999	1,49773	14,9124	5,91693E-06	0,0906949	0,000475135	30,3152	0,394384	0,394384

1	0,2	0,363158	0,0285462	0,00750428	0,00152659	0,00111738	0,0109463	0,00746904	0,391837	0,000480329	130,047	0,398678	0,398678
	0,399052	0,363154	0,0285459	0,00750329	0,00152634	0,00111713	0,0109438	0,00332986	0,391849	0,000480329	130,051	0,398678	0,398678
	0,796214	0,363153	0,0285457	0,00750288	0,00152624	0,00111702	0,0109427	0,00158133	0,391855	0,000480329	130,053	0,398678	0,398678
	1,58866	0,363152	0,0285457	0,00750269	0,00152619	0,00111697	0,0109422	0,000772239	0,391857	0,000480329	130,054	0,398678	0,398678
	3,16979	0,363151	0,0285457	0,00750259	0,00152616	0,00111695	0,010942	0,00038213	0,391858	0,000480329	130,054	0,398678	0,398678
	6,32456	0,363151	0,0285456	0,00750255	0,00152615	0,00111694	0,0109419	0,000190309	0,391859	0,000480329	130,054	0,398678	0,398678
	12,6191	0,363151	0,0285456	0,00750252	0,00152615	0,00111693	0,0109418	9,50797E-05	0,391859	0,000480329	130,054	0,398678	0,398678
	25,1785	0,363151	0,0285456	0,00750251	0,00152614	0,00111693	0,0109418	4,75775E-05	0,391859	0,000480329	130,054	0,398678	0,398678
	50,2377	0,363151	0,0285456	0,00750251	0,00152614	0,00111693	0,0109418	2,38264E-05	0,391859	0,000480329	130,054	0,398678	0,398678
	100,237	0,363151	0,0285456	0,0075025	0,00152614	0,00111692	0,0109418	1,19368E-05	0,391859	0,000480329	130,054	0,398678	0,398678

L-Galactose dehydrogenase

K_i (GGP)	Relative activity	D-Glc 6-P	D-Fru 6-P	D-Man 6-P	D-Man 1-P	GDP-D-Man	GDP-L-Gal	L-Gal 1-P	L-Gal	L-GalL	L-Asc	DHA	Breakdown
0,014427	0,2	88,7916	7,46885	7,41446	1,90176	1,88773	18,8025	0,000108566	0,68366	0,000434262	3,9845	0,36058	0,36058
	0,399052	89,0552	7,49103	7,43648	1,9074	1,89334	18,8584	0,000108566	0,308767	0,000434262	3,9845	0,36058	0,36058
	0,796214	89,1686	7,50057	7,44595	1,90983	1,89575	18,8824	0,000108566	0,147444	0,000434262	3,9845	0,36058	0,36058
	1,58866	89,2216	7,50502	7,45037	1,91097	1,89688	18,8936	0,000108566	0,0721892	0,000434262	3,98451	0,36058	0,36058
	3,16979	89,2472	7,50717	7,45251	1,91152	1,89742	18,8991	0,000108566	0,035766	0,000434262	3,98451	0,36058	0,36058
	6,32456	89,2598	7,50824	7,45357	1,91179	1,89769	18,9017	0,000108566	0,0178232	0,000434262	3,98451	0,36058	0,36058
	12,6191	89,266	7,50876	7,45409	1,91192	1,89782	18,9031	0,000108566	0,00890727	0,000434262	3,98451	0,36058	0,36058
	25,1785	89,2692	7,50903	7,45435	1,91199	1,89789	18,9037	0,000108566	0,00445784	0,000434262	3,98451	0,36058	0,36058
	50,2377	89,2707	7,50916	7,45448	1,91202	1,89792	18,9041	0,000108566	0,00223261	0,000434262	3,98451	0,36058	0,36058
	100,237	89,2715	7,50922	7,45455	1,91204	1,89794	18,9042	0,000108566	0,00111856	0,000434262	3,98451	0,36058	0,36058
	200	89,2719	7,50926	7,45458	1,91205	1,89795	18,9043	0,000108566	0,000560506	0,000434262	3,98451	0,36058	0,36058
0,0416277	0,2	83,1298	6,98901	6,93366	1,77753	1,76353	17,5608	0,000115812	1,95572	0,000463249	10,7771	0,384556	0,384556
	0,399052	83,8892	7,05287	6,99703	1,79378	1,77966	17,7214	0,000115812	0,876149	0,000463249	10,7771	0,384556	0,384556
	0,796214	84,2122	7,08003	7,02398	1,80069	1,78651	17,7897	0,000115812	0,416936	0,000463249	10,7771	0,384556	0,384556
	1,58866	84,3621	7,09264	7,03649	1,8039	1,7897	17,8214	0,000115812	0,203804	0,000463249	10,7772	0,384556	0,384556
	3,16979	84,4345	7,09872	7,04253	1,80545	1,79123	17,8367	0,000115812	0,100896	0,000463249	10,7772	0,384556	0,384556
	6,32456	84,4701	7,10172	7,0455	1,80621	1,79199	17,8442	0,000115812	0,0502597	0,000463249	10,7772	0,384556	0,384556
	12,6191	84,4878	7,10321	7,04698	1,80659	1,79237	17,848	0,000115812	0,0251129	0,000463249	10,7772	0,384556	0,384556
	25,1785	84,4966	7,10395	7,04772	1,80678	1,79255	17,8498	0,000115812	0,0125671	0,000463249	10,7772	0,384556	0,384556
	50,2377	84,501	7,10432	7,04808	1,80687	1,79265	17,8508	0,000115812	0,00629367	0,000463249	10,7772	0,384556	0,384556
	100,237	84,5032	7,10451	7,04827	1,80692	1,79269	17,8512	0,000115812	0,0031531	0,000463249	10,7772	0,384556	0,384556
	200	84,5043	7,1046	7,04836	1,80694	1,79272	17,8515	0,000115812	0,00157999	0,000463249	10,7772	0,384556	0,384556
0,120112	0,2	66,8133	5,6157	5,56666	1,42672	1,41512	14,0898	0,000118784	5,62611	0,000475135	30,314	0,394384	0,394384
	0,399052	69,0038	5,79987	5,74938	1,47356	1,46159	14,5526	0,000118784	2,51202	0,000475135	30,3147	0,394384	0,394384
	0,796214	69,9311	5,87784	5,82674	1,49339	1,48127	14,7485	0,000118784	1,1937	0,000475135	30,315	0,394384	0,394384
	1,58866	70,3606	5,91395	5,86256	1,50258	1,49038	14,8392	0,000118784	0,583113	0,000475135	30,3151	0,394384	0,394384
	3,16979	70,5677	5,93137	5,87985	1,50701	1,49478	14,883	0,000118784	0,288585	0,000475135	30,3151	0,394384	0,394384
	6,32456	70,6696	5,93993	5,88835	1,50919	1,49694	14,9045	0,000118784	0,143732	0,000475135	30,3152	0,394384	0,394384
	12,6191	70,7202	5,94419	5,89257	1,51027	1,49801	14,9152	0,000118784	0,0718118	0,000475135	30,3152	0,394384	0,394384
	25,1785	70,7455	5,94631	5,89467	1,51081	1,49855	14,9205	0,000118784	0,035935	0,000475135	30,3152	0,394384	0,394384
	50,2377	70,7581	5,94737	5,89572	1,51108	1,49882	14,9232	0,000118784	0,0179961	0,000475135	30,3152	0,394384	0,394384

	100,237	70,7644	5,9479	5,89625	1,51122	1,49895	14,9245	0,000118784	0,00901587	0,000475135	30,3152	0,394384	0,394384
	200	70,7676	5,94817	5,89651	1,51128	1,49902	14,9252	0,000118784	0,00451775	0,000475135	30,3152	0,394384	0,394384
	0,2	0,310327	0,0241059	0,00630688	0,00121989	0,000813357	0,00791948	0,000120009	20,5888	0,000480037	109,92	0,398437	0,398437
	0,399052	0,337313	0,026374	0,00688388	0,00136767	0,000959817	0,00937761	0,00012005	10,059	0,000480201	120,418	0,398573	0,398573
	0,796214	0,35075	0,0275033	0,00719706	0,00144789	0,00103935	0,0101694	0,000120068	4,97847	0,000480271	125,482	0,39863	0,39863
	1,58866	0,357472	0,0280683	0,00736065	0,0014898	0,00108089	0,010583	0,000120076	2,4796	0,000480303	127,973	0,398657	0,398657
	3,16979	0,36084	0,0283514	0,00744438	0,00151125	0,00110216	0,0107948	0,00012008	1,23887	0,000480318	129,21	0,39867	0,39867
1	6,32456	0,362528	0,0284932	0,00748679	0,00152211	0,00111293	0,010902	0,000120082	0,61994	0,000480326	129,827	0,398676	0,398676
	12,6191	0,363374	0,0285643	0,00750816	0,00152759	0,00111836	0,0109561	0,000120082	0,310463	0,00048033	130,135	0,398679	0,398679
	25,1785	0,363798	0,0286	0,0075189	0,00153034	0,00112109	0,0109832	0,000120083	0,155539	0,000480332	130,29	0,398681	0,398681
	50,2377	0,36401	0,0286178	0,00752429	0,00153172	0,00112246	0,0109969	0,000120083	0,0779391	0,000480333	130,367	0,398681	0,398681
	100,237	0,364117	0,0286268	0,00752699	0,00153241	0,00112315	0,0110037	0,000120083	0,0390583	0,000480333	130,406	0,398682	0,398682

L-Galactono-1,4-lactone dehydrogenase

K_i (GGP)	Relative activity	D-Glc 6-P	D-Fru 6-P	D-Man 6-P	D-Man 1-P	GDP-D-Man	GDP-L-Gal	L-Gal 1-P	L-Gal	L-GalL	L-Asc	DHA	Breakdown
	0,2	89,2442	7,50693	7,45227	1,91145	1,89736	18,8985	0,000108566	0,0139479	0,0263933	3,98451	0,36058	0,36058
	0,399052	89,2555	7,50787	7,45321	1,9117	1,8976	18,9008	0,000108566	0,012443	0,0119202	3,98451	0,36058	0,36058
	0,796214	89,2603	7,50828	7,45361	1,9118	1,8977	18,9019	0,000108566	0,0117954	0,0056922	3,98451	0,36058	0,36058
	1,58866	89,2626	7,50847	7,4538	1,91185	1,89775	18,9023	0,000108566	0,0114933	0,00278692	3,98451	0,36058	0,36058
	3,16979	89,2637	7,50856	7,45389	1,91187	1,89777	18,9026	0,000108566	0,0113471	0,00138077	3,98451	0,36058	0,36058
0,014427	6,32456	89,2642	7,50861	7,45394	1,91188	1,89778	18,9027	0,000108566	0,011275	0,000688076	3,98451	0,36058	0,36058
	12,6191	89,2645	7,50863	7,45396	1,91189	1,89779	18,9027	0,000108566	0,0112393	0,000343871	3,98451	0,36058	0,36058
	25,1785	89,2646	7,50864	7,45397	1,91189	1,89779	18,9028	0,000108566	0,0112214	0,000172098	3,98451	0,36058	0,36058
	50,2377	89,2647	7,50865	7,45398	1,91189	1,89779	18,9028	0,000108566	0,0112125	8,61917E-05	3,98451	0,36058	0,36058
	100,237	89,2647	7,50865	7,45398	1,91189	1,8978	18,9028	0,000108566	0,011208	4,31827E-05	3,98451	0,36058	0,36058
	200	89,2647	7,50865	7,45398	1,91189	1,8978	18,9028	0,000108566	0,0112057	2,16387E-05	3,98451	0,36058	0,36058
	0,2	84,4613	7,10098	7,04477	1,80602	1,7918	17,8424	0,000115812	0,0346453	0,028566	10,7772	0,384556	0,384556
	0,399052	84,4735	7,10201	7,04579	1,80629	1,79206	17,845	0,000115812	0,0330015	0,0127973	10,7772	0,384556	0,384556
	0,796214	84,4787	7,10245	7,04623	1,8064	1,79217	17,8461	0,000115812	0,0323023	0,0060899	10,7772	0,384556	0,384556
	1,58866	84,4812	7,10265	7,04643	1,80645	1,79223	17,8466	0,000115812	0,0319778	0,00297682	10,7772	0,384556	0,384556
	3,16979	84,4823	7,10275	7,04653	1,80647	1,79225	17,8468	0,000115812	0,0318211	0,00147371	10,7772	0,384556	0,384556
0,0416277	6,32456	84,4829	7,1028	7,04658	1,80649	1,79226	17,8469	0,000115812	0,031744	0,000734108	10,7772	0,384556	0,384556
	12,6191	84,4832	7,10282	7,0466	1,80649	1,79227	17,847	0,000115812	0,0317057	0,000366806	10,7772	0,384556	0,384556
	25,1785	84,4833	7,10283	7,04661	1,8065	1,79227	17,847	0,000115812	0,0316866	0,000183559	10,7772	0,384556	0,384556
	50,2377	84,4834	7,10284	7,04662	1,8065	1,79227	17,847	0,000115812	0,031677	9,19272E-05	10,7772	0,384556	0,384556
	100,237	84,4834	7,10284	7,04662	1,8065	1,79227	17,847	0,000115812	0,0316722	4,60551E-05	10,7772	0,384556	0,384556
	200	84,4835	7,10285	7,04662	1,8065	1,79227	17,8471	0,000115812	0,0316698	2,30778E-05	10,7772	0,384556	0,384556
	0,2	70,6844	5,94118	5,88958	1,50951	1,49725	14,9077	0,000118784	0,0937212	0,0294754	30,3152	0,394384	0,394384
	0,399052	70,6971	5,94224	5,89064	1,50978	1,49752	14,9103	0,000118784	0,0920186	0,0131602	30,3152	0,394384	0,394384
	0,796214	70,7025	5,94269	5,89108	1,50989	1,49764	14,9115	0,000118784	0,0912979	0,00625365	30,3152	0,394384	0,394384
0,120112	1,58866	70,7049	5,9429	5,89129	1,50994	1,49769	14,912	0,000118784	0,0909641	0,00305484	30,3152	0,394384	0,394384
	3,16979	70,7061	5,943	5,89139	1,50997	1,49771	14,9122	0,000118784	0,0908031	0,00151185	30,3152	0,394384	0,394384
	6,32456	70,7067	5,94305	5,89144	1,50998	1,49773	14,9124	0,000118784	0,0907239	0,000752987	30,3152	0,394384	0,394384
	12,6191	70,707	5,94308	5,89146	1,50999	1,49773	14,9124	0,000118784	0,0906846	0,00037621	30,3152	0,394384	0,394384

	25,1785	70,7072	5,94309	5,89148	1,50999	1,49774	14,9125	0,000118784	0,0906649	0,000188257	30,3152	0,394384	0,394384
	50,2377	70,7072	5,9431	5,89148	1,50999	1,49774	14,9125	0,000118784	0,0906551	9,42783E-05	30,3152	0,394384	0,394384
	100,237	70,7073	5,9431	5,89149	1,50999	1,49774	14,9125	0,000118784	0,0906502	4,72326E-05	30,3152	0,394384	0,394384
	200	70,7073	5,9431	5,89149	1,50999	1,49774	14,9125	0,000118784	0,0906478	2,36677E-05	30,3152	0,394384	0,394384
	0,2	0,363063	0,0285382	0,00750029	0,00152557	0,00111636	0,0109362	0,000120082	0,394831	0,0298762	130,022	0,398678	0,398678
	0,399052	0,363113	0,0285424	0,00750155	0,0015259	0,00111668	0,0109394	0,000120082	0,393157	0,0133194	130,04	0,398678	0,398678
	0,796214	0,363134	0,0285442	0,00750209	0,00152603	0,00111682	0,0109407	0,000120082	0,39245	0,00632533	130,048	0,398678	0,398678
	1,58866	0,363143	0,028545	0,00750233	0,0015261	0,00111688	0,0109413	0,000120082	0,392123	0,00308895	130,051	0,398678	0,398678
	3,16979	0,363148	0,0285454	0,00750245	0,00152613	0,00111691	0,0109416	0,000120082	0,391965	0,00152852	130,053	0,398678	0,398678
1	6,32456	0,36315	0,0285456	0,00750251	0,00152614	0,00111693	0,0109418	0,000120082	0,391887	0,000761237	130,054	0,398678	0,398678
	12,6191	0,363151	0,0285457	0,00750254	0,00152615	0,00111693	0,0109418	0,000120082	0,391849	0,000380319	130,054	0,398678	0,398678
	25,1785	0,363152	0,0285457	0,00750255	0,00152615	0,00111694	0,0109419	0,000120082	0,39183	0,00019031	130,055	0,398678	0,398678
	50,2377	0,363152	0,0285457	0,00750256	0,00152615	0,00111694	0,0109419	0,000120082	0,39182	9,53056E-05	130,055	0,398678	0,398678
	100,237	0,363153	0,0285457	0,00750256	0,00152616	0,00111694	0,0109419	0,000120082	0,391815	0,000047747	130,055	0,398678	0,398678

Appendix 8. Species used in the phylogenetic study of VTC2 and the conservation of its N-terminus (Figure 23). Taxonomic information was consulted in The Plant List (www.theplantlist.org) for vascular plants and in Algaebase (https://www.algaebase.org) for algae.

Abbr.	Species	Phylum	Class	Order	Family
Acchi	*Actinidia chinensis* Planch.	Tracheophyta	Magnoliopsida	Ericales	Actinidiacea
Amhyp	*Amaranthus hypochondriacus* L.	Tracheophyta	Magnoliopsida	Caryophyllales	Amaranthaceae
Amtri	*Amborella trichopoda* Baill.	Tracheophyta	Magnoliopsida	Amborellales	Amborellaceae
Aqcoe	*Aquilegia caerulea* E.James	Tracheophyta	Magnoliopsida	Ranunculales	Ranunculaceae
Artha	*Arabidopsis thaliana* (L.) Heynh.	Tracheophyta	Magnoliopsida	Brassicales	Brassicaceae
Brdis	*Brachypodium distachyon* (L.) P.Beauv.	Tracheophyta	Liliopsida	Poales	Poaceae
Caann	*Capsicum annuum* L.	Tracheophyta	Magnoliopsida	Solanales	Solanaceae
Capap	*Carica papaya* L.	Tracheophyta	Magnoliopsida	Violales	Caricaceae
Chrei	*Chlamydomonas reinhardtii* P.A.Dangeard	Chlorophyta	Chlorophyceae	Chlamydomonadales	Chlamydomonadaceae
Cocan	*Coffea canephora* Pierre ex A.Froehner	Tracheophyta	Magnoliopsida	Gentianales	Rubiaceae
Cosub	*Coccomyxa subellipsoidea* E.Acton	Chlorophyta	Trebouxiophyceae	Trebouxiophyceae ordo incertae sedis	Coccomyxaceae
Cusat	*Cucumis sativus* L.	Tracheophyta	Magnoliopsida	Violales	Cucurbitaceae
Frves	*Fragaria vesca L.*	Tracheophyta	Magnoliopsida	Rosales	Rosaceae
Glmax	*Glycine max* (L.) Merr.	Tracheophyta	Magnoliopsida	Fabales	Fabaceae
Gorai	*Gossypium raimondii* Ulbr.	Tracheophyta	Magnoliopsida	Malvales	Malvaceae
Kamar	*Kalanchoe marnieriana* H. Jacobsen	Tracheophyta	Magnoliopsida	Saxifragales	Crassulaceae
Liusi	*Linum usitatissimum* L.	Tracheophyta	Magnoliopsida	Linales	Linaceae
Maesc	*Manihot esculenta* Crantz	Tracheophyta	Magnoliopsida	Malpighiales	Euphorbiaceae
Magla	*Malpighia glabra* L.	Tracheophyta	Magnoliopsida	Malpighiales	Malpighiaceae
Migut	*Mimulus guttatus* DC.	Tracheophyta	Magnoliopsida	Lamiales	Phrymaceae
Mipus	*Micromonas pusilla* (Butcher) I.Manton & M.Parke	Chlorophyta	Mamiellophyceae	Mamiellales	Mamiellaceae
Mumus	*Mus musculus L.*	Chordata	Mammalia	Rodentia	Muridae
Orsat	*Oryza sativa* L.	Tracheophyta	Liliopsida	Cyperales	Poaceae
Phpat	*Physcomitrella patens* (Hedw.) Bruch & Schimp.	Bryophyta	Bryopsida	Funariales	Funariaceae
Seita	*Setaria italica* (L.) P.Beauv.	Tracheophyta	Liliopsida	Cyperales	Poaceae
Semoe	*Selaginella moellendorffii* Hieron.	Lycopodiophyta (pteridophyta)	Lycopodiopsida	Selaginellasles	Selaginellaceae
Solyc	*Solanum lycopersicum* L.	Tracheophyta	Magnoliopsida	Solanales	Solanaceae
Spfal	*Sphagnum fallax* H. Klinggr.	Bryophyta	Sphagnopsida	Sphagnales	Sphagnaceae
Sppol	*Spirodela polyrrhiza* (L.) Schleid.	Tracheophyta	Liliopsida	Alismatales	Lemnaceae
Thcac	*Theobroma cacao* L.	Tracheophyta	Magnoliopsida	Malvales	Malvaceae
Vivin	*Vitis vinifera* L.	Tracheophyta	Magnoliopsida	Rhamnales	Vitaceae
Vocar	*Volvox carteri* F.Stein	Chlorophyta	Chlorophyceae	Chlamydomonadales	Volvocaceae
Zemay	*Zea mays* L.	Tracheophyta	Liliopsida	Poales	Poaceae
Zomar	*Zostera marina* L.	Tracheophyta	Liliopsida	Alismatales	Zosteraceae

REFERENCES

Footnotes:

[1]http://www.fao.org/faostat/en/#data;
[2]https://ndb.nal.usda.gov/ndb/search/list

Cited literature:

Agathocleous, M., Meacham, C.E., Burgess, R.J., Piskounova, E., Zhao, Z., Crane, G.M., Cowin, B.L., Bruner, E., Murphy, M.M., Chen, W., Spangrude, G.J., Hu, Z., DeBerardinis, R.J., Morrison, S.J., 2017. Ascorbate regulates haematopoietic stem cell function and leukaemogenesis. Nature 549, 476–481. https://doi.org/10.1038/nature23876

Agius, F., González-Lamothe, R., Caballero, J.L., Muñoz-Blanco, J., Botella, M.A., Valpuesta, V., 2003. Engineering increased vitamin C levels in plants by overexpression of a D-galacturonic acid reductase. Nat. Biotechnol. https://doi.org/10.1038/nbt777

Akhatou, I., Fernández-Recamales, Á., 2014. Nutritional and nutraceutical quality of strawberries in relation to harvest time and crop conditions. J. Agric. Food Chem. 62, 5749–5760. https://doi.org/10.1021/jf500769x

Akram, N.A., Shafiq, F., Ashraf, M., 2017. Ascorbic acid-a potential oxidant scavenger and its role in plant development and abiotic stress tolerance. Front. Plant Sci. https://doi.org/10.3389/fpls.2017.00613

Ali, B., Pantha, S., Acharya, R., Ueda, Y., Wu, L.B., Ashrafuzzaman, M., Ishizaki, T., Wissuwa, M., Bulley, S., Frei, M., 2019. Enhanced ascorbate level improves multi-stress tolerance in a widely grown indica rice variety without compromising its agronomic characteristics. J. Plant Physiol. https://doi.org/10.1016/j.jplph.2019.152998

Altschul, S.F., Madden, T.L., Schäffer, A.A., Zhang, J., Zhang, Z., Miller, W., Lipman, D.J., 1997. Gapped BLAST and PSI-BLAST: A new generation of protein database search programs. Nucleic Acids Res. https://doi.org/10.1093/nar/25.17.3389

Amaya, I., Osorio, S., Martinez-Ferri, E., Lima-Silva, V., Doblas, V.G., Fernández-Muñoz, R., Fernie, A.R., Botella, M.A., Valpuesta, V., 2015. Increased antioxidant capacity in tomato by ectopic expression of the strawberry D - *galacturonate reductase* gene. Biotechnol. J. 10, 490–500. https://doi.org/10.1002/biot.201400279

Amaya, I., Pillet, J., Folta, K.M., 2016. Identification of Genes Responsible for Natural Variation in Volatile Content Using Next-Generation Sequencing Technology, in: J., B., M., B. (Eds.), Plant Signal Transduction. Methods in Molecular Biology, Vol 1363. Humana Press, New York, NY, pp. 37–45. https://doi.org/10.1007/978-1-4939-3115-6_4

Amorim-Silva, V., García-Moreno, Á., Castillo, A.G., Lakhssassi, N., Del Valle, A.E., Pérez-Sancho, J., Li, Y., Posé, D., Pérez-Rodriguez, J., Lin, J., Valpuesta, V., Borsani, O., Zipfel, C., Macho, A.P., Botella, M.A., 2019. TTL proteins scaffold brassinosteroid signaling components at the plasma membrane to optimize signal transduction in arabidopsis. Plant Cell. https://doi.org/10.1105/tpc.19.00150

Antunes, M.D.C., Rodrigues, D., Pantazis, V., Cavaco, A.M., Siomos, A.S., Miguel, G., 2013. Nutritional quality changes of fresh-cut tomato during shelf life. Food Sci. Biotechnol. https://doi.org/10.1007/s10068-013-0206-6

Asada, K., 1999. THE WATER-WATER CYCLE IN CHLOROPLASTS: Scavenging of Active Oxygens and Dissipation of Excess Photons. Annu. Rev. Plant Physiol. Plant Mol. Biol. 50, 601–639. https://doi.org/10.1146/annurev.arplant.50.1.601

Asard, H., Barbaro, R., Trost, P., Bérczi, A., 2013. Cytochromes b561: Ascorbate-Mediated Trans-Membrane Electron Transport. Antioxid. Redox Signal. 19, 1026–1035. https://doi.org/10.1089/ars.2012.5065

Atherton, J.G., Rudich, J., 1986. The Tomato Crop. Springer Netherlands, Dordrecht. https://doi.org/10.1007/978-94-009-3137-4

Awad, J., Stotz, H.U., Fekete, A., Krischke, M., Engert, C., Havaux, M., Berger, S., Mueller, M.J., 2015. 2-Cysteine Peroxiredoxins and Thylakoid Ascorbate Peroxidase Create a Water-Water Cycle That Is Essential to Protect the Photosynthetic Apparatus under High Light Stress Conditions. Plant Physiol. 167, 1592–1603. https://doi.org/10.1104/pp.114.255356

Badejo, A.A., Fujikawa, Y., Esaka, M., 2009. Gene expression of ascorbic acid biosynthesis related enzymes of the Smirnoff-Wheeler pathway in acerola (Malpighia glabra). J. Plant Physiol. 166, 652–660. https://doi.org/10.1016/j.jplph.2008.09.004

Badejo, A.A., Jeong, S.T., Goto-Yamamoto, N., Esaka, M., 2007. Cloning and expression of GDP-d-mannose pyrophosphorylase gene and ascorbic acid content of acerola (Malpighia glabra L.) fruit at ripening stages. Plant Physiol. Biochem. https://doi.org/10.1016/j.plaphy.2007.07.003

Badejo, A.A., Tanaka, N., Esaka, M., 2008. Analysis of GDP-D-Mannose Pyrophosphorylase Gene Promoter from Acerola (Malpighia glabra) and Increase in Ascorbate Content of Transgenic Tobacco Expressing the Acerola Gene. Plant Cell Physiol. 49, 126–132. https://doi.org/10.1093/pcp/pcm164

Badejo, A.A., Wada, K., Gao, Y., Maruta, T., Sawa, Y., Shigeoka, S., Ishikawa, T., 2012. Translocation and the alternative D-galacturonate pathway contribute to increasing the ascorbate level in ripening tomato fruits together with the D-mannose/L-galactose pathway. J. Exp. Bot. 63, 229–239. https://doi.org/10.1093/jxb/err275

Baier, M., Dietz, K.J., 1997. The plant 2-Cys peroxiredoxin BAS1 is a nuclear-encoded chloroplast protein: its expressional regulation, phylogenetic origin, and implications for its specific physiological function in plants. Plant J. 12, 179–90.

Baker, E.M., Hodges, R.E., Hood, J., Sauberlich, H.E., March, S.C., 1969. Metabolism of ascorbic-1-14C acid in experimental human scurvy. Am. J. Clin. Nutr. 22, 549–58.

Baker, E.M., Hodges, R.E., Hood, J., Sauberlich, H.E., March, S.C., Canham, J.E., 1971. Metabolism of 14C- and 3H-labeled L-ascorbic acid in human scurvy. Am. J. Clin. Nutr. 24, 444–54.

Baron, J.H., 2009. Sailors' scurvy before and after James Lind - A reassessment. Nutr. Rev. 67, 315–332. https://doi.org/10.1111/j.1753-4887.2009.00205.x

Bartel, P., Chien, C.T., Sternglanz, R., Fields, S., 1993. Elimination of false positives that arise in using the two-hybrid system. Biotechniques 14, 920–924.

Bartoli, C.G., 2006. Inter-relationships between light and respiration in the control of ascorbic acid synthesis and accumulation in Arabidopsis thaliana leaves. J. Exp. Bot. 57, 1621–1631. https://doi.org/10.1093/jxb/erl005

Binder, J.X., Pletscher-Frankild, S., Tsafou, K., Stolte, C., O'Donoghue, S.I., Schneider, R., Jensen, L.J., 2014. COMPARTMENTS: unification and visualization of protein subcellular localization evidence. Database 2014, bau012–bau012. https://doi.org/10.1093/database/bau012

Blaschke, K., Ebata, K.T., Karimi, M.M., Zepeda-Martínez, J.A., Goyal, P., Mahapatra, S., Tam, A., Laird, D.J., Hirst, M., Rao, A., Lorincz, M.C., Ramalho-Santos, M., 2013. Vitamin C induces Tet-dependent DNA demethylation and a blastocyst-like state in ES cells. Nature 500, 222–226. https://doi.org/10.1038/nature12362

Bonin, C.P., Freshour, G., Hahn, M.G., Vanzin, G.F., Reiter, W.-D., 2003. The GMD1 and GMD2 genes of Arabidopsis encode isoforms of GDP-D-mannose 4,6-dehydratase with cell type-specific expression patterns. Plant Physiol. 132, 883–92. https://doi.org/10.1104/pp.103.022368

Bonin, C.P., Potter, I., Vanzin, G.F., Reiter, W.-D., 1997. The MUR1 gene of Arabidopsis thaliana encodes an isoform of GDP-D-mannose-4,6-dehydratase, catalyzing the first step in the de novo synthesis of GDP-L-fucose. Plant Biol. 94, 2085–2090. https://doi.org/10.1073/pnas.94.5.2085

Bonin, C.P., Reiter, W.D., 2000. A bifunctional epimerase-reductase acts downstream of the MUR1 gene product and completes the de novo synthesis of GDP-L-fucose in Arabidopsis. Plant J. 21, 445–454. https://doi.org/10.1046/j.1365-313X.2000.00698.x

Booker, F.L., Burkey, K.O., Jones, A.M., 2012. Re-evaluating the role of ascorbic acid and phenolic glycosides in ozone scavenging in the leaf apoplast of Arabidopsis thaliana L. Plant. Cell Environ. 35, 1456–1466. https://doi.org/10.1111/j.1365-3040.2012.02502.x

Boukouris, A.E., Zervopoulos, S.D., Michelakis, E.D., 2016. Metabolic Enzymes Moonlighting in the Nucleus: Metabolic Regulation of Gene Transcription. Trends Biochem. Sci. 41, 712–730. https://doi.org/10.1016/j.tibs.2016.05.013

Branduardi, P., Fossati, T., Sauer, M., Pagani, R., Mattanovich, D., Porro, D., 2007. Biosynthesis of Vitamin C by Yeast Leads to Increased Stress Resistance. PLoS One 2, e1092. https://doi.org/10.1371/journal.pone.0001092

Brennan, T., Frenkel, C., 1977. Involvement of hydrogen peroxide in the regulation of senescence in pear. Plant Physiol. 59, 411–6.

Bulley, S., Laing, W., 2016. The regulation of ascorbate biosynthesis. Curr. Opin. Plant Biol. 33, 15–22. https://doi.org/10.1016/j.pbi.2016.04.010

Bulley, S., Wright, M., Rommens, C., Yan, H., Rassam, M., Lin-Wang, K., Andre, C., Brewster, D., Karunairetnam, S., Allan, A.C., Laing, W.A., 2012. Enhancing ascorbate in fruits and tubers through over-expression of the L-galactose pathway gene GDP-L-galactose phosphorylase. Plant Biotechnol. J. 10, 390–397. https://doi.org/10.1111/j.1467-7652.2011.00668.x

Bulley, S.M., Rassam, M., Hoser, D., Otto, W., Schünemann, N., Wright, M., MacRae, E., Gleave, A., Laing, W., 2009. Gene expression studies in kiwifruit and gene over-expression in Arabidopsis indicates that GDP-L-galactose guanyltransferase is a major control point of vitamin C biosynthesis. J. Exp. Bot. 60, 765–778. https://doi.org/10.1093/jxb/ern327

Cai, X., Zhang, C., Shu, W., Ye, Z., Li, H., Zhang, Y., 2016. The transcription factor SlDof22 involved in ascorbate accumulation and salinity stress in tomato. Biochem. Biophys. Res. Commun. 474, 736–741. https://doi.org/10.1016/J.BBRC.2016.04.148

Cai, X., Zhang, C., Ye, J., Hu, T., Ye, Z., Li, H., Zhang, Y., 2015. Ectopic expression of FaGalUR leads to ascorbate accumulation with enhanced oxidative stress, cold, and salt tolerance in tomato. Plant Growth Regul. 76, 187–197. https://doi.org/10.1007/s10725-014-9988-7

Capel, C., Fernández del Carmen, A., Alba, J.M., Lima-Silva, V., Hernández-Gras, F., Salinas, M., Boronat, A., Angosto, T., Botella, M.A., Fernández-Muñoz, R., Granell, A., Capel, J., Lozano, R., 2015. Wide-genome QTL mapping of fruit quality traits in a tomato RIL population derived from the wild-relative species Solanum pimpinellifolium L. Theor. Appl. Genet. 128, 2019–2035. https://doi.org/10.1007/s00122-015-2563-4

Carr, A.C., Maggini, S., 2017. Vitamin C and Immune Function. Nutrients 9. https://doi.org/10.3390/nu9111211

Carr, A.C., Vissers, M.C.M., 2013. Synthetic or food-derived vitamin C. Are they equally bioavailable? Nutrients 5, 4284–304. https://doi.org/10.3390/nu5114284

Castro, J.C., Maddox, J.D., Cobos, M., Requena, D., Zimic, M., Bombarely, A., Imán, S.A., Cerdeira, L.A., Medina, A.E., 2015. De novo assembly and functional annotation of Myrciaria dubia fruit transcriptome reveals multiple metabolic pathways for L-ascorbic acid biosynthesis. BMC Genomics 16, 997. https://doi.org/10.1186/s12864-015-2225-6

Chatterjee, I.B., 1973. Evolution and the Biosynthesis of Ascorbic Acid. Science, 182, 1271–1272. https://doi.org/10.1126/science.182.4118.1271

Chen, Z., Gallie, D.R., 2004. The Ascorbic Acid Redox State Controls Guard Cell Signaling and Stomatal Movement. Plant Cell 16, 1143–1162. https://doi.org/10.1105/tpc.021584

Cho, K.M., Nguyen, H.T.K., Kim, S.Y., Shin, J.S.J.S., Cho, D.H., Hong, S.B., Shin, J.S.J.S., Ok, S.H., 2016. CML10, a variant of calmodulin, modulates ascorbic acid synthesis. New Phytol. 209, 664–678. https://doi.org/10.1111/nph.13612

Cimmino, L., Dolgalev, I., Wang, Y., Yoshimi, A., Martin, G.H., Wang, J., Ng, V., Xia, B., Witkowski, M.T., Mitchell-Flack, M., Grillo, I., Bakogianni, S., Ndiaye-Lobry, D., Martín, M.T., Guillamot, M., Banh, R.S., Xu, M., Figueroa, M.E., Dickins, R.A., Abdel-Wahab, O., Park, C.Y., Tsirigos, A., Neel, B.G., Aifantis, I., 2017. Restoration of TET2 Function Blocks Aberrant Self-Renewal and Leukemia Progression. Cell 170, 1079-1095.e20. https://doi.org/10.1016/j.cell.2017.07.032

Clough, S.J., Bent, A.F., 1998. Floral dip: a simplified method forAgrobacterium-mediated transformation ofArabidopsis thaliana. Plant J. 16, 735–743. https://doi.org/10.1046/j.1365-313x.1998.00343.x

Conklin, P.L., Depaolo, D., Wintle, B., Schatz, C., Buckenmeyer, G., 2013. Identification of Arabidopsis VTC3 as a putative and unique dual function protein kinase:: Protein phosphatase involved in the regulation of the ascorbic acid pool in plants. J. Exp. Bot. https://doi.org/10.1093/jxb/ert140

Conklin, P.L., Gatzek, S., Wheeler, G.L., Dowdle, J., Raymond, M.J., Rolinski, S., Isupov, M., Littlechild, J.A., Smirnoff, N., 2006. Arabidopsis thaliana VTC4 encodes L-galactose-1-P phosphatase, a plant ascorbic acid biosynthetic enzyme. J. Biol. Chem. 281, 15662–15670. https://doi.org/10.1074/jbc.M601409200

Conklin, P.L., Norris, S.R., Wheeler, G.L., Williams, E.H., Smirnoff, N., Last, R.L., 1999. Genetic evidence for the role of GDP-mannose in plant ascorbic acid (vitamin C) biosynthesis. Proc. Natl. Acad. Sci. 96, 4198–4203. https://doi.org/10.1073/pnas.96.7.4198

Conklin, P.L., Pallanca, J.E., Last, R.L., Smirnoff, N., 1997. L-ascorbic acid metabolism in the ascorbate-deficient arabidopsis mutant vtc1. Plant Physiol. 115, 1277–85. https://doi.org/10.1016/s0168-9452(03)00277-2

Conklin, P.L., Saracco, S.A., Norris, S.R., Last, R.L., 2000. Identification of ascorbic acid-deficient Arabidopsis thaliana mutants. Genetics 154, 847–56.

Conklin, P.L., Willlams, E.H., Last, R.L., 1996. Environmental stress sensitivity of an ascorbic acid-deficient Arabidopsis mutant. Proc. Natl. Acad. Sci. 93, 9970–9974.

Covington, M.F., Harmer, S.L., 2007. The Circadian Clock Regulates Auxin Signaling and Responses in Arabidopsis. PLoS Biol. 5, e222. https://doi.org/10.1371/journal.pbio.0050222

Cronje, C., George, G.M., Fernie, A.R., Bekker, J., Kossmann, J., Bauer, R., 2012. Manipulation of L-ascorbic acid biosynthesis pathways in Solanum lycopersicum: elevated GDP-mannose pyrophosphorylase activity enhances L-ascorbate levels in red fruit. Planta 235, 553–564. https://doi.org/10.1007/s00425-011-1525-6

Crossa, J., Pérez-Rodríguez, P., Cuevas, J., Montesinos-López, O., Jarquín, D., de los Campos, G., Burgueño, J., González-Camacho, J.M., Pérez-Elizalde, S., Beyene, Y., Dreisigacker, S., Singh, R., Zhang, X., Gowda, M., Roorkiwal, M., Rutkoski, J., Varshney, R.K., 2017. Genomic Selection in Plant Breeding: Methods, Models, and Perspectives. Trends Plant Sci. 22, 961–975. https://doi.org/10.1016/j.tplants.2017.08.011

Cruz-Rus, E., Amaya, I., Sánchez-Sevilla, J.F., Botella, M.A., Valpuesta, V., 2011. Regulation of L-ascorbic acid content in strawberry fruits. J. Exp. Bot. 62, 4191–4201. https://doi.org/10.1093/jxb/err122

Cruz-Rus, E., Botella, M.A., Valpuesta, V., Gomez-Jimenez, M.C., 2010. Analysis of genes involved in l-ascorbic acid biosynthesis during growth and ripening of grape berries. J. Plant Physiol. https://doi.org/10.1016/j.jplph.2009.12.017

Davey, M.W., Auwerkerken, A., Keulemans, J., 2007. Relationship of apple vitamin C and antioxidant contents to harvest date and postharvest pathogen infection. J. Sci. Food Agric. 87, 802–813. https://doi.org/10.1002/jsfa.2777

Davey, M.W., Gilot, C., Persiau, G., Ostergaard, J., Han, Y., Bauw, G.C., Van Montagu, M.C., 1999. Ascorbate biosynthesis in Arabidopsis cell suspension culture. Plant Physiol. 121, 535–43.

Davey, M.W., Kenis, K., Keulemans, J., 2006. Genetic control of fruit vitamin C contents. Plant Physiol. https://doi.org/10.1104/pp.106.083279

Davey, M.W., Van Montagu, M., Inzé, D., Sanmartin, M., Kanellis, A., Smirnoff, N., Benzie, I.J.J.F.F., Strain, J.J., Favell, D., Fletcher, J., Davey, M.W., Montagu, M. Van, Inze, D., Kanellis, A., Smirnoff, N., Benzie, I.J.J.F.F., Strain, J.J., Favell, D., Fletcher, J., 2000. Plant L-ascorbic acid: chemistry, function, metabolism, bioavailability and effects of processing. J. Sci. Food Agric. 80, 825–860. https://doi.org/10.1002/(sici)1097-0010(20000515)80:7<825::aid-jsfa598>3.0.co;2-6

Davies, J.N., Hobson, G.E., 1981. The influence of environment, nutrition and genotype. Crit. Rev. Food Sci. Nutr. 15, 205–280.

de Jong, L., Albracht, S.P., Kemp, A., 1982. Prolyl 4-hydroxylase activity in relation to the oxidation state of enzyme-bound iron. The role of ascorbate in peptidyl proline hydroxylation. Biochim. Biophys. Acta 704, 326–32.

de Pinto, M.C., Locato, V., Paradiso, A., De Gara, L., 2015. Role of redox homeostasis in thermo-tolerance under a climate change scenario: Fig. 1. Ann. Bot. 116, 487–496. https://doi.org/10.1093/aob/mcv071

DeBolt, S., Cook, D.R., Ford, C.M., 2006. L-Tartaric acid synthesis from vitamin C in higher plants. Proc. Natl. Acad. Sci. 103, 5608–5613. https://doi.org/10.1073/pnas.0510864103

Debolt, S., Melino, V., Ford, C.M., 2007. Ascorbate as a Biosynthetic Precursor in Plants. Ann. Bot. 99, 3–8. https://doi.org/10.1093/aob/mcl236

Dewhirst, R.A., Clarkson, G.J.J., Rothwell, S.D., Fry, S.C., 2017. Novel insights into ascorbate retention and degradation during the washing and post-harvest storage of spinach and other salad leaves. Food Chem. https://doi.org/10.1016/j.foodchem.2017.04.082

Dewhirst, R.A., Fry, S.C., 2018. The oxidation of dehydroascorbic acid and 2,3-diketogulonate by distinct reactive oxygen species. Biochem. J. https://doi.org/10.1042/BCJ20180688

Dewhirst, R.A., Murray, L., Mackay, C.L., Sadler, I.H., Fry, S.C., 2020. Characterisation of the non-oxidative degradation pathway of dehydroascorbic acid in slightly acidic aqueous solution. Arch. Biochem. Biophys. 681, 108240. https://doi.org/10.1016/j.abb.2019.108240

Di Matteo, A., Sacco, A., Anacleria, M., Pezzotti, M., Delledonne, M., Ferrarini, A., Frusciante, L., Barone, A., 2010. The ascorbic acid content of tomato fruits is associated with the expression of genes involved in pectin degradation. BMC Plant Biol. 10, 163. https://doi.org/10.1186/1471-2229-10-163

Doudna, J.A., Charpentier, E., 2014. The new frontier of genome engineering with CRISPR-Cas9. Science,. 346, 1258096–1258096. https://doi.org/10.1126/science.1258096

Dowdle, J., Ishikawa, T., Gatzek, S., Rolinski, S., Smirnoff, N., 2007. Two genes in Arabidopsis thaliana encoding GDP-L-galactose phosphorylase are required for ascorbate biosynthesis and seedling viability. Plant J. https://doi.org/10.1111/j.1365-313X.2007.03266.x

Drouin, G., Godin, J.-R., Page, B., 2011. The Genetics of Vitamin C Loss in Vertebrates. Curr. Genomics 12, 371–378. https://doi.org/10.2174/138920211796429736

Dumas, Y., Dadomo, M., Di Lucca, G., Grolier, P., 2003. Effects of environmental factors and agricultural techniques on antioxidant content of tomatoes. J. Sci. Food Agric. 83, 369–382. https://doi.org/10.1002/jsfa.1370

Dumville, J.C., Fry, S.C., 2003. Solubilisation of tomato fruit pectins by ascorbate: A possible non-enzymic mechanism of fruit softening. Planta 217, 951–961. https://doi.org/10.1007/s00425-003-1061-0

Dunkley, T.P.J., Hester, S., Shadforth, I.P., Runions, J., Weimar, T., Hanton, S.L., Griffin, J.L., Bessant, C., Brandizzi, F., Hawes, C., Watson, R.B., Dupree, P., Lilley, K.S., 2006. Mapping the Arabidopsis organelle proteome. Proc. Natl. Acad. Sci. 103, 6518–6523. https://doi.org/10.1073/pnas.0506958103

EFSA Panel on Dietetic Products and Nutrition Allergies, 2013. Scientific Opinion on Dietary Reference Values for vitamin C. EFSA J. 11, 1–68. https://doi.org/10.2903/j.efsa.2013.3418

Egelund, J., Petersen, B.L., Motawia, M.S., Damager, I., Faik, A., Olsen, C.E., Ishii, T., Clausen, H., Ulvskov, P., Geshi, N., 2006. Arabidopsis thaliana RGXT1 and RGXT2 Encode Golgi-Localized (1,3)-α-D-Xylosyltransferases Involved in the Synthesis of Pectic Rhamnogalacturonan-II. Plant Cell 18, 2593–2607. https://doi.org/10.1105/tpc.105.036566

Endres, S., Tenhaken, R., 2011. Down-regulation of the myo-inositol oxygenase gene family has no effect on cell wall composition in Arabidopsis. Planta 234, 157–169. https://doi.org/10.1007/s00425-011-1394-z

Endres, S., Tenhaken, R., 2009. Myoinositol Oxygenase Controls the Level of Myoinositol in Arabidopsis, But Does Not Increase Ascorbic Acid. Plant Physiol. 149, 1042–1049. https://doi.org/10.1104/pp.108.130948

Esquinas-Alcazar, J.T., 1981. Genetic Resources of Tomatoes and Wild Relatives, International Board for Plant Genetic Resources. IBPGR Secretariat.

Eurostat, 2017. Agriculture, forestry and fishery statistics. https://doi.org/10.2785/570022

Exposito-rodriguez, M., Laissue, P.P., Littlejohn, G.R., Smirnoff, N., Mullineaux, P.M., 2013. The Use of HyPer to Examine Spatial and Temporal Changes in H2O2 in High Light-Exposed Plants, 1st ed, Hydrogen Peroxide and cell signaling, Part B. Elsevier Inc. https://doi.org/10.1016/B978-0-12-405882-8.00010-6

Exposito-Rodriguez, M., Laissue, P.P., Yvon-Durocher, G., Smirnoff, N., Mullineaux, P.M., 2017. Photosynthesis-dependent H2O2transfer from chloroplasts to nuclei provides a high-light signalling mechanism. Nat. Commun. 8. https://doi.org/10.1038/s41467-017-00074-w

Fell, D.A., 1992. Metabolic control analysis: a survey of its theoretical and experimental development. Biochem. J. 286, 313–330. https://doi.org/10.1042/bj2860313

Fenech, M., Amaya, I., Valpuesta, V., Botella, M.A., 2019. Vitamin C content in fruits: Biosynthesis and regulation. Front. Plant Sci. 9, 1–21. https://doi.org/10.3389/fpls.2018.02006

Fields, S., Song, O., 1989. A novel genetic system to detect protein–protein interactions. Nature 340, 245–246. https://doi.org/10.1038/340245a0

Food and Nutrition Board; Institute of Medicine; National Academies, 2000. Dietary Reference Intakes for Vitamin C, Vitamin E, Selenium, and Carotenoids, Food and Nutrition Board; Institute of Medicine; National Academies. National Academies Press, Washington, D.C. https://doi.org/10.17226/9810

Fossati, T., Solinas, N., Porro, D., Branduardi, P., 2011. L-ascorbic acid producing yeasts learn from plants how to recycle it. Metab. Eng. 13, 177–185. https://doi.org/10.1016/j.ymben.2010.12.007

Foyer, C.H., Halliwell, B., 1976. The presence of glutathione and glutathione reductase in chloroplasts: A proposed role in ascorbic acid metabolism. Planta 133, 21–25. https://doi.org/10.1007/BF00386001

Foyer, C.H., Lelandais, M., 1996. A Comparison of the Relative Rates of Transport of Ascorbate and Glucose Across the Thylakoid, Chloroplast and Plasmalemma Membranes of Pea Leaf Mesophyll Cells. J. Plant Physiol. 148, 391–398. https://doi.org/10.1016/S0176-1617(96)80271-9

Foyer, C.H., Noctor, G., 2011. Ascorbate and Glutathione: The Heart of the Redox Hub. Plant Physiol. 155, 2–18. https://doi.org/10.1104/pp.110.167569

Franceschi, V.R., Tarlyn, N.M., 2002. L-Ascorbic Acid Is Accumulated in Source Leaf Phloem and Transported to Sink Tissues in Plants. Plant Physiol. 130, 649–656. https://doi.org/10.1104/pp.007062

Gao, Y., Badejo, A.A., Shibata, H., Sawa, Y., Maruta, T., Shigeoka, S., Page, M., Smirnoff, N., Ishikawa, T., 2011. Expression Analysis of the VTC2 and VTC5 Genes Encoding GDP-L-Galactose Phosphorylase, an Enzyme Involved in Ascorbate Biosynthesis, in Arabidopsis thaliana. Biosci. Biotechnol. Biochem. 75, 1783–1788. https://doi.org/10.1271/bbb.110320

Gatzek, S., Wheeler, G.L., Smirnoff, N., 2002. Antisense suppression of L-galactose dehydrogenase in Arabidopsis thaliana provides evidence for its role in ascorbate synthesis and reveals light modulated L-galactose synthesis. Plant J. https://doi.org/10.1046/j.1365-313X.2002.01315.x

Gautier, H., Diakou-Verdin, V., Bénard, C., Reich, M., Buret, M., Bourgaud, F., Poëssel, J.L., Caris-Veyrat, C., Génard, M., 2008. How does tomato quality (sugar, acid, and nutritional quality) vary with ripening stage, temperature, and irradiance? J. Agric. Food Chem. 56, 1241–1250. https://doi.org/10.1021/jf072196t

Giacomelli, L., Masi, A., Ripoll, D.R., Lee, M.J., van Wijk, K.J., 2007. Arabidopsis thaliana deficient in two chloroplast ascorbate peroxidases shows accelerated light-induced necrosis when levels of cellular ascorbate are low. Plant Mol. Biol. 65, 627–644. https://doi.org/10.1007/s11103-007-9227-y

Gietz, R.D., Schiestl, R.H., 1995. Transforming yeast with DNA. Methods Mol. Cell. Biol. 5, 255–269.

Gilbert, L., Alhagdow, M., Nunes-Nesi, A., Quemener, B., Guillon, F., Bouchet, B., Faurobert, M., Gouble, B., Page, D., Garcia, V., Petit, J., Stevens, R., Causse, M., Fernie, A.R., Lahaye, M., Rothan, C., Baldet, P., 2009. GDP-d-mannose 3,5-epimerase (GME) plays a key role at the intersection of ascorbate and non-cellulosic cell-wall biosynthesis in tomato. Plant J. 60, 499–508. https://doi.org/10.1111/j.1365-313X.2009.03972.x

Gorres, K.L., Raines, R.T., 2010. Prolyl 4-hydroxylase. Crit. Rev. Biochem. Mol. Biol. 45, 106–24. https://doi.org/10.3109/10409231003627991

Green, M.A., Fry, S.C., 2005. Vitamin C degradation in plant cells via enzymatic hydrolysis of 4-O-oxalyl-l-threonate. Nature 433, 83–87. https://doi.org/10.1038/nature03172

Griesen, D., Su, D., Bérczi, A., Asard, H., 2004. Localization of an Ascorbate-Reducible Cytochrome b561 in the Plant Tonoplast. Plant Physiol. 134, 726–734. https://doi.org/10.1104/pp.103.032359

Guo, B., Irigoyen, S., Fowler, T.B., Versaw, W.K., 2008. Differential expression and phylogenetic analysis suggest specialization of plastid-localized members of the PHT4 phosphate transporter family for photosynthetic and heterotrophic tissues. Plant Signal. Behav. 3, 784–90.

Hallberg, L., Brune, M., Rossander-Hulthén, L., 1987. Is there a physiological role of vitamin C in iron absorption? Ann. N. Y. Acad. Sci. 498, 324–32.

Hallberg, L., Brune, M., Rossander, L., 1989. The role of vitamin C in iron absorption. Int. J. Vitam. Nutr. Res. Suppl. 30, 103–8.

Hallberg, L., Rossander, L., Persson, H., Svahn, E., 1982. Deleterious effects of prolonged warming of meals on ascorbic acid content and iron absorption. Am. J. Clin. Nutr. 36, 846–50.

Hampl, J.S., Taylor, C.A., Johnston, C.S., 2004. Vitamin C deficiency and depletion in the United States: the Third National Health and Nutrition Examination Survey, 1988 to 1994. Am. J. Public Health 94, 870–5.

Hantus, S., Pauly, M., Darvill, A.G., Albersheim, P., York, W.S., 1997. Structural characterization of novel L-galactose-containing oligosaccharide subunits of jojoba seed xyloglucans. Carbohydr. Res. https://doi.org/10.1016/S0008-6215(97)00200-0

Harapanhalli, R.S., Howell, R.W., Rao, D. V., 1993. Testicular and plasma ascorbic acid levels in mice following dietary intake: a high-performance liquid chromatographic analysis. J. Chromatogr. B Biomed. Sci. Appl. https://doi.org/10.1016/0378-4347(93)80314-T

Hausen, S. v., 1935. Effect of Vitamin C (Ascorbic Acid) on the Growth of Plants. Nature 136, 516–516. https://doi.org/10.1038/136516b0

Havas, L., 1935. Ascorbic Acid (Vitamin C) and the Germination and Growth of Seedlings. Nature 136, 435–435. https://doi.org/10.1038/136435a0

Heazlewood, J.L., Tonti-Filippini, J.S., Gout, A.M., Day, D.A., Whelan, J., Millar, A.H., 2004. Experimental Analysis of the Arabidopsis Mitochondrial Proteome Highlights Signaling and Regulatory Components, Provides Assessment of Targeting Prediction Programs, and Indicates Plant-Specific Mitochondrial Proteins. Plant Cell 16, 241–256. https://doi.org/10.1105/tpc.016055

Hieber, A.D., Bugos, R.C., Yamamoto, H.Y., 2000. Plant lipocalins: violaxanthin de-epoxidase and zeaxanthin epoxidase. Biochim. Biophys. Acta - Protein Struct. Mol. Enzymol. 1482, 84–91. https://doi.org/10.1016/S0167-4838(00)00141-2

Hijazi, M., Velasquez, S.M., Jamet, E., Estevez, J.M., Albenne, C., 2014. An update on post-translational modifications of hydroxyproline-rich glycoproteins: toward a model highlighting their contribution to plant cell wall architecture. Front. Plant Sci. 5, 395. https://doi.org/10.3389/fpls.2014.00395

Hodges, R.E., Baker, E.M., Hood, J., Sauberlich, H.E., March, S.C., 1969. Experimental scurvy in man. Am. J. Clin. Nutr. 22, 535–48.

Hodges, R.E., Hood, J., Canham, J.E., Sauberlich, H.E., Baker, E.M., 1971. Clinical manifestations of ascorbic acid deficiency in man. Am. J. Clin. Nutr. 24, 432–43.

Hoeberichts, F.A., Vaeck, E., Kiddle, G., Coppens, E., Van De Cotte, B., Adamantidis, A., Ormenese, S., Foyer, C.H., Zabeau, M., Inzé, D., Périlleux, C., Van Breusegem, F., Vuylsteke, M., 2008. A temperature-sensitive mutation in the Arabidopsis thaliana phosphomannomutase gene disrupts protein glycosylation and triggers cell death. J. Biol. Chem. 283, 5708–5718. https://doi.org/10.1074/jbc.M704991200

Hoops, S., Gauges, R., Lee, C., Pahle, J., Simus, N., Singhal, M., Xu, L., Mendes, P., Kummer, U., 2006. COPASI - A COmplex PAthway SImulator. Bioinformatics. https://doi.org/10.1093/bioinformatics/btl485

Horemans, N., Asard, H., Caubergs, R.J., 1997. The Ascorbate Carrier of Higher Plant Plasma Membranes Preferentially Translocates the Fully Oxidized (Dehydroascorbate) Molecule. Plant Physiol. 114, 1247–1253.

Horemans, N., Asard, H., Caubergs, R.J., 1996. Transport of ascorbate into plasma membrane vesicles of Phaseolus vulgaris L. Protoplasma 194, 177–185. https://doi.org/10.1007/BF01882025

Horemans, N., Asard, H., Caubergs, R.J., 1994. The Role of Ascorbate Free Radical as an Electron Acceptor to Cytochrome b-Mediated Trans-Plasma Membrane Electron Transport in Higher Plants. Plant Physiol. 104, 1455–1458.

Horemans, N., Asard, H., Van Gestelen, P., Caubergs, R.J., 1998. Facilitated diffusion drives transport of oxidised ascorbate molecules into purified plasma membrane vesicles of Phaseolus vulgaris. Physiol. Plant. 104, 783–789.

Horemans, N., Foyer, C.H., Asard, H., 2000. Transport and action of ascorbate at the plant plasma membrane. Trends Plant Sci. https://doi.org/10.1016/S1360-1385(00)01649-6

Hu, L., Lu, J., Cheng, J., Rao, Q., Li, Z., Hou, H., Lou, Z., Zhang, L., Li, W., Gong, W., Liu, M.,

Sun, C., Yin, X., Li, J., Tan, X., Wang, P., Wang, Y., Fang, D., Cui, Q., Yang, P., He, C., Jiang, H., Luo, C., Xu, Y., 2015. Structural insight into substrate preference for TET-mediated oxidation. Nature 527, 118–122. https://doi.org/10.1038/nature15713

Hu, T., Ye, J., Tao, P., Li, H., Zhang, J., Zhang, Y., Ye, Z., 2016. The tomato HD-Zip I transcription factor SlHZ24 modulates ascorbate accumulation through positive regulation of the <scp>d</scp> -mannose/ <scp>l</scp> -galactose pathway. Plant J. 85, 16–29. https://doi.org/10.1111/tpj.13085

Huan, C., Jiang, L., An, X., Yu, M., Xu, Y., Ma, R., Yu, Z., 2016. Potential role of reactive oxygen species and antioxidant genes in the regulation of peach fruit development and ripening. Plant Physiol. Biochem. 104, 294–303. https://doi.org/10.1016/j.plaphy.2016.05.013

Huang, S., Weigel, D., Beachy, R.N., Li, J., 2016. A proposed regulatory framework for genome-edited crops. Nat. Genet. 48, 109–111. https://doi.org/10.1038/ng.3484

Imai, T., Ban, Y., Terakami, S., Yamamoto, T., Moriguchi, T., 2009. L-Ascorbate biosynthesis in peach: Cloning of six l-galactose pathway-related genes and their expression during peach fruit development. Physiol. Plant. 136, 139–149. https://doi.org/10.1111/j.1399-3054.2009.01213.x

Imai, T., Karita, S., Shiratori ', G.-I., Hattori, M., Nunome ', T., Oba, K., Hirai, M., 1998. L-Galactono-1,4-lactone Dehydrogenase from Sweet Potato: Purification and cDNA Sequence Analysis. Plant Cell Physiol. 39, 1350–1358.

Ioannidi, E., Kalamaki, M.S., Engineer, C., Pateraki, I., Alexandrou, D., Mellidou, I., Giovannonni, J., Kanellis, A.K., 2009. Expression profiling of ascorbic acid-related genes during tomato fruit development and ripening and in response to stress conditions. J. Exp. Bot. 60, 663–678. https://doi.org/10.1093/jxb/ern322

Ivanov Kavkova, E., Blöchl, C., Tenhaken, R., 2018. The *Myo* -inositol pathway does not contribute to ascorbic acid synthesis. Plant Biol. 21, 95–102. https://doi.org/10.1111/plb.12898

Iwabuchi, K., Li, B., Bartel, P., Fields, S., 1993. Use of the two-hybrid system to identify the domain of p53 involved in oligomerization. Oncogene 8, 1693–6.

Jain, A.K., Nessler, C.L., 2000. Metabolic engineering of an alternative pathway for ascorbic acid biosynthesis in plants. Mol. Breed. 6, 73–78. https://doi.org/10.1023/A:1009680818138

Jamil, H., 2018. The Effect of the KONJAC1 and KONJAC2 Proteins on GDP-Glucose Pyrophosphorylase Activity of VTC1. Eastern Michigan University.

Jimenez, A., Creissen, G., Kular, B., Firmin, J., Robinson, S., Verhoeyen, M., Mullineaux, P., 2002. Changes in oxidative processes and components of the antioxidant system during tomato fruit ripening. Planta 214, 751–758. https://doi.org/10.1007/s004250100667

Johnstone, W.M., Drake, T.G., Tisdall, F.F., Harvie, F.H., 1946. Ascorbic Acid metabolism of healthy young canadians. Can. Med. Assoc. J. 55, 581–5.

Jones, D.T., Taylor, W.R., Thornton, J.M., 1992. The rapid generation of mutation data matrices from protein sequences. Bioinformatics 8, 275–282. https://doi.org/10.1093/bioinformatics/8.3.275

Kallner, A., Hartmann, D., Hornig, D., 1979. Steady-state turnover and body pool of ascorbic acid in man. Am. J. Clin. Nutr. 32, 530–9.

Karpinska, B., Zhang, K., Rasool, B., Pastok, D., Morris, J., Verrall, S.R., Hedley, P.E., Hancock, R.D., Foyer, C.H., 2018. The redox state of the apoplast influences the acclimation of photosynthesis and leaf metabolism to changing irradiance. Plant Cell Environ. 41, 1083–1097. https://doi.org/10.1111/pce.12960

Katoh, S., San Pietro, A., 1967. Ascorbate-supported NADP photoreduction by heated Euglena

chloroplasts. Arch. Biochem. Biophys. 122, 144–152. https://doi.org/10.1016/0003-9861(67)90133-6

Kevers, C., Pincemail, J., Tabart, J., Defraigne, J.-O., Dommes, J., 2011. Influence of Cultivar, Harvest Time, Storage Conditions, and Peeling on the Antioxidant Capacity and Phenolic and Ascorbic Acid Contents of Apples and Pears. J. Agric. Food Chem. 59, 6165–6171. https://doi.org/10.1021/jf201013k

Kishor, P.B.K., Hima Kumari, P., Sunita, M.S.L., Sreenivasulu, N., 2015. Role of proline in cell wall synthesis and plant development and its implications in plant ontogeny. Front. Plant Sci. 6, 544. https://doi.org/10.3389/fpls.2015.00544

Klepikova, A. V., Kasianov, A.S., Gerasimov, E.S., Logacheva, M.D., Penin, A.A., 2016. A high resolution map of the Arabidopsis thaliana developmental transcriptome based on RNA-seq profiling. Plant J. 88, 1058–1070. https://doi.org/10.1111/tpj.13312

Ko, M., An, J., Pastor, W.A., Koralov, S.B., Rajewsky, K., Rao, A., 2015. TET proteins and 5-methylcytosine oxidation in hematological cancers. Immunol. Rev. 263, 6–21. https://doi.org/10.1111/imr.12239

Koide, T., Nagata, K., 2005. Collagen biosynthesis. Top. Curr. Chem. 247, 85–114. https://doi.org/10.1007/b103820

Kumar, S., Stecher, G., Li, M., Knyaz, C., Tamura, K., 2018. MEGA X: Molecular evolutionary genetics analysis across computing platforms. Mol. Biol. Evol. https://doi.org/10.1093/molbev/msy096

Laing, W., Norling, C., Brewster, D., Wright, M., Bulley, S., 2017. Ascorbate concentration in Arabidopsis thaliana and expression of ascorbate related genes using RNAseq in response to light and the diurnal cycle. bioRxiv 138008. https://doi.org/10.1101/138008

Laing, W. A., Bulley, S., Wright, M., Cooney, J., Jensen, D., Barraclough, D., MacRae, E., 2004. A highly specific L-galactose-1-phosphate phosphatase on the path to ascorbate biosynthesis. Proc. Natl. Acad. Sci. 101, 16976–16981. https://doi.org/10.1073/pnas.0407453101

Laing, William A, Frearson, N., Bulley, S., MacRae, E., 2004. Kiwifruit L-galactose dehydrogenase: molecular, biochemical and physiological aspects of the enzyme. Funct. Plant Biol. 31, 1015–1025. https://doi.org/10.1071/FP04090

Laing, W.A., Martínez-Sánchez, M., Wright, M.A., Bulley, S.M., Brewster, D., Dare, A.P., Rassam, M., Wang, D., Storey, R., Macknight, R.C., Hellens, R.P., 2015. An Upstream Open Reading Frame Is Essential for Feedback Regulation of Ascorbate Biosynthesis in Arabidopsis. Plant Cell. https://doi.org/10.1105/tpc.114.133777

Laing, W.A., Wright, M.A., Cooney, J., Bulley, S.M., 2007. The missing step of the L-galactose pathway of ascorbate biosynthesis in plants, an L-galactose guanyltransferase, increases leaf ascorbate content. Proc. Natl. Acad. Sci. 104, 9534–9539.

Lamport, D.T.A., Kieliszewski, M.J., Showalter, A.M., 2006. Salt stress upregulates periplasmic arabinogalactan proteins: using salt stress to analyse AGP function*. New Phytol. 169, 479–492. https://doi.org/10.1111/j.1469-8137.2005.01591.x

Laur, L.M., Tian, L., 2011. Provitamin A and vitamin C contents in selected California-grown cantaloupe and honeydew melons and imported melons. J. Food Compos. Anal. 24, 194–201. https://doi.org/10.1016/J.JFCA.2010.07.009

Leferink, N.G.H., Van Duijn, E., Barendregt, A., Heck, A.J.R., Van Berkel, W.J.H., 2009. Galactonolactone Dehydrogenase Requires a Redox-Sensitive Thiol for Optimal Production of Vitamin C. Plant Physiol. 150, 596–605. https://doi.org/10.1104/pp.109.136929

Li, B., Fields, S., 1993. Identification of mutations in p53 that affect its binding to SV40 large T antigen by using the yeast two-hybrid system. FASEB J.

https://doi.org/10.1096/fasebj.7.10.8344494

Li, J., Liang, D., Li, M., Ma, F., 2013. Light and abiotic stresses regulate the expression of GDP-L-galactose phosphorylase and levels of ascorbic acid in two kiwifruit genotypes via light-responsive and stress-inducible cis-elements in their promoters. Planta 238, 535–547. https://doi.org/10.1007/s00425-013-1915-z

Li, M., Ma, F., Liang, D., Li, J., Wang, Y., 2010. Ascorbate biosynthesis during early fruit development is the main reason for its accumulation in kiwi. PLoS One 5. https://doi.org/10.1371/journal.pone.0014281

Li, Q., Li, Y., Li, C., Yu, X., 2012. Enhanced ascorbic acid accumulation through overexpression of dehydroascorbate reductase confers tolerance to methyl viologen and salt stresses in tomato. Czech J. Genet. Plant Breed. 48, 74–86. https://doi.org/10.17221/100/2011-CJGPB

Li, S., Wang, J., Yu, Y., Wang, F., Dong, J., Huang, R., 2016. D27E mutation of VTC1 impairs the interaction with CSN5B and enhances ascorbic acid biosynthesis and seedling growth in Arabidopsis. Plant Mol. Biol. 92, 473–482. https://doi.org/10.1007/s11103-016-0525-0

Li, T., Yang, X., Yu, Y., Si, X., Zhai, X., Zhang, H., Dong, W., Gao, C., Xu, C., 2018. Domestication of wild tomato is accelerated by genome editing. Nat. Biotechnol. https://doi.org/10.1038/nbt.4273

Li, X., Ye, J., Munir, S., Yang, T., Chen, W., Liu, G., Zheng, W., Zhang, Y., 2019. Biosynthetic Gene Pyramiding Leads to Ascorbate Accumulation with Enhanced Oxidative Stress Tolerance in Tomato. Int. J. Mol. Sci. 20, 1558. https://doi.org/10.3390/ijms20071558

Liepman, A.H., Wilkerson, C.G., Keegstra, K., 2005. Expression of cellulose synthase-like (Csl) genes in insect cells reveals that CslA family members encode mannan synthases. Proc. Natl. Acad. Sci. 102, 2221–2226. https://doi.org/10.1073/pnas.0409179102

Lieu, P.T., Heiskala, M., Peterson, P.A., Yang, Y., 2001. The roles of iron in health and disease. Mol. Aspects Med. 22, 1–87.

Lim, B., Smirnoff, N., Cobbett, C.S., Golz, J.F., 2016. Ascorbate-Deficient vtc2 Mutants in Arabidopsis Do Not Exhibit Decreased Growth. Front. Plant Sci. 7, 1–9. https://doi.org/10.3389/fpls.2016.01025

Lim, M.Y., Jeong, B.R., Jung, M., Harn, C.H., 2016. Transgenic tomato plants expressing strawberry d-galacturonic acid reductase gene display enhanced tolerance to abiotic stresses. Plant Biotechnol. Rep. 10, 105–116. https://doi.org/10.1007/s11816-016-0392-9

Lima-Silva, V., Rosado, A., Amorim-Silva, V., Muñoz-Mérida, A., Pons, C., Bombarely, A., Trelles, O., Fernández-Muñoz, R., Granell, A., Valpuesta, V., Botella, M.T., 2012. Genetic and genome-wide transcriptomic analyses identify co-regulation of oxidative response and hormone transcript abundance with vitamin C content in tomato fruit. BMC Genomics. https://doi.org/10.1186/1471-2164-13-187

Lind, J., 1753. A treatise of the scurvy : in three parts, containing an inquiry into the nature, causes, and cure, of that disease, together with a critical and chronological view of what has been published on the subject. Bull. World Heal. Organ. Int. J. Public Heal. 2004; 82(10) 793-796.

Lindblad, B., Lindstedt, G., Lindstedt, S., 1970. The mechanism of enzymic formation of homogentisate from p-hydroxyphenylpyruvate. J. Am. Chem. Soc. 92, 7446–9.

Linster, C.L., Gomez, T.A., Christensen, K.C., Adler, L.N., Young, B.D., Brenner, C., Clarke, S.G., 2007. Arabidopsis VTC2 encodes a GDP-L-galactose phosphorylase, the last unknown enzyme in the smirnoff-wheeler pathway to ascorbic acid in plants. J. Biol. Chem. https://doi.org/10.1074/jbc.M702094200

Loewus, F.A., 1999. Biosynthesis and metabolism of ascorbic acid in plants and of analogs of ascorbic acid in fungi. Phytochemistry 52, 193–210. https://doi.org/10.1016/S0031-9422(99)00145-4

Loewus, F.A., 1963. Tracer studies on ascorbic acid formation in plants. Phytochemistry 2, 109–128. https://doi.org/10.1016/S0031-9422(00)82971-4

Lorence, A., Chevone, B.I., Mendes, P., Nessler, C.L., 2004. myo-Inositol Oxygenase Offers a Possible Entry Point into Plant Ascorbate Biosynthesis. Plant Physiol. 134, 1200–1205. https://doi.org/10.1104/pp.103.033936

Lu, Y.X., Wu, Q.N., Chen, D.L., Chen, L.Z., Wang, Z.X., Ren, C., Mo, H.Y., Chen, Y., Sheng, H., Wang, Y.N., Wang, Y., Lu, J.H., Wang, D.S., Zeng, Z.L., Wang, F., Wang, F.H., Li, Y.H., Ju, H.Q., Xu, R.H., 2018. Pharmacological ascorbate suppresses growth of gastric cancer cells with GLUT1 overexpression and enhances the efficacy of oxaliplatin through redox modulation. Theranostics 8, 1312–1326. https://doi.org/10.7150/thno.21745

Lukowitz, W., Nickle, T.C., Meinke, D.W., Last, R.L., Conklin, P.L., Somerville, C.R., 2001. Arabidopsis cyt1 mutants are deficient in a mannose-1-phosphate guanylyltransferase and point to a requirement of N-linked glycosylation for cellulose biosynthesis. Proc. Natl. Acad. Sci. 98, 2262–2267. https://doi.org/10.1073/pnas.051625798

Mackay, T.F.C., Stone, E.A., Ayroles, J.F., 2009. The genetics of quantitative traits: challenges and prospects. Nat. Rev. Genet. 10, 565–577. https://doi.org/10.1038/nrg2612

Macknight, R.C., Laing, W.A., Bulley, S.M., Broad, R.C., Johnson, A.A., Hellens, R.P., 2017. Increasing ascorbate levels in crops to enhance human nutrition and plant abiotic stress tolerance. Curr. Opin. Biotechnol. 44, 153–160. https://doi.org/10.1016/j.copbio.2017.01.011

Major, L.L., Wolucka, B.A., Naismith, J.H., 2005. Structure and function of GDP-mannose-3′,5′-epimerase: An enzyme which performs three chemical reactions at the same active site. J. Am. Chem. Soc. 127, 18309–18320. https://doi.org/10.1021/ja056490i

Mano, J., Ushimaru, T., Asada, K., 1997. Ascorbate in thylakoid lumen as an endogenous electron donor to Photosystem II: Protection of thylakoids from photoinhibition and regeneration of ascorbate in stroma by dehydroascorbate reductase. Photosynth. Res. 53, 197–204. https://doi.org/10.1023/A:1005832022204

Mapson, L.W., Breslow, E., 1958. Biological synthesis of ascorbic acid: L-galactono-gamma-lactone dehydrogenase. Biochem. J. 68, 395–406.

Mapson, L.W., Isherwood, F.A., 1956. Biological synthesis of ascorbic acid: the conversion of derivatives of D-galacturonic acid into L-ascorbic acid by plant extracts. Biochem. J. 64, 13–22.

Marchler-Bauer, A., Bo, Y., Han, L., He, J., Lanczycki, C.J., Lu, S., Chitsaz, F., Derbyshire, M.K., Geer, R.C., Gonzales, N.R., Gwadz, M., Hurwitz, D.I., Lu, F., Marchler, G.H., Song, J.S., Thanki, N., Wang, Z., Yamashita, R.A., Zhang, D., Zheng, C., Geer, L.Y., Bryant, S.H., 2017. CDD/SPARCLE: functional classification of proteins via subfamily domain architectures. Nucleic Acids Res. 45, D200–D203. https://doi.org/10.1093/nar/gkw1129

Marchler-Bauer, A., Bryant, S.H., 2004. CD-Search: protein domain annotations on the fly. Nucleic Acids Res. 32, W327–W331. https://doi.org/10.1093/nar/gkh454

Marchler-Bauer, A., Derbyshire, M.K., Gonzales, N.R., Lu, S., Chitsaz, F., Geer, L.Y., Geer, R.C., He, J., Gwadz, M., Hurwitz, D.I., Lanczycki, C.J., Lu, F., Marchler, G.H., Song, J.S., Thanki, N., Wang, Z., Yamashita, R.A., Zhang, D., Zheng, C., Bryant, S.H., 2015. CDD: NCBI's conserved domain database. Nucleic Acids Res. https://doi.org/10.1093/nar/gku1221

Marchler-Bauer, A., Lu, S., Anderson, J.B., Chitsaz, F., Derbyshire, M.K., DeWeese-Scott, C., Fong, J.H., Geer, L.Y., Geer, R.C., Gonzales, N.R., Gwadz, M., Hurwitz, D.I., Jackson, J.D., Ke, Z., Lanczycki, C.J., Lu, F., Marchler, G.H., Mullokandov, M., Omelchenko, M. V., Robertson, C.L., Song, J.S., Thanki, N., Yamashita, R.A., Zhang, D., Zhang, N., Zheng, C., Bryant, S.H., 2011. CDD: a Conserved Domain Database for the functional annotation of proteins. Nucleic Acids Res. 39, D225–D229. https://doi.org/10.1093/nar/gkq1189

Marrè, E., Arrigoni, O., Rossi, G., 1959. Ascobic acid and photosynthesis: II. Anaerobic photo-

oxidation of ascorbic acid by chloroplast fragments and by whole chloroplasts. Biochim. Biophys. Acta 36, 56–64. https://doi.org/10.1016/0006-3002(59)90069-1

Maruta, T., Ichikawa, Y., Mieda, T., Takeda, T., Tamoi, M., Yabuta, Y., Ishikawa, T., Shigeoka, S., 2010. The Contribution of Arabidopsis Homologs of L-Gulono-1,4-Lactone Oxidase to the Biosynthesis of Ascorbic Acid. Biosci. Biotechnol. Biochem. 74, 1494–1497. https://doi.org/10.1271/bbb.100157

Maruta, T., Yonemitsu, M., Yabuta, Y., Tamoi, M., Ishikawa, T., Shigeoka, S., 2008. Arabidopsis phosphomannose isomerase 1, but not phosphomannose isomerase 2, is essential for ascorbic acid biosynthesis. J. Biol. Chem. 283, 28842–28851. https://doi.org/10.1074/jbc.M805538200

Marzol, E., Borassi, C., Bringas, M., Sede, A., Rodríguez Garcia, D.R., Capece, L., Estevez, J.M., 2018. Filling the Gaps to Solve the Extensin Puzzle. Mol. Plant. https://doi.org/10.1016/j.molp.2018.03.003

Más, P., Kim, W.Y., Somers, D.E., Kay, S.A., 2003. Targeted degradation of TOC1 by ZTL modulates circadian function in Arabidopsis thaliana. Nature. https://doi.org/10.1038/nature02163

Massot, C., Bancel, D., Lopez Lauri, F., Truffault, V., Baldet, P., Stevens, R., Gautier, H., 2013. High Temperature Inhibits Ascorbate Recycling and Light Stimulation of the Ascorbate Pool in Tomato despite Increased Expression of Biosynthesis Genes. PLoS One 8, e84474. https://doi.org/10.1371/journal.pone.0084474

Mellidou, I., Buts, K., Hatoum, D., Ho, Q.T., Johnston, J.W., Watkins, C.B., Schaffer, R.J., Gapper, N.E., Giovannoni, J.J., Rudell, D.R., Hertog, M.L.A.T.M., Nicolai, B.M., 2014. Transcriptomic events associated with internal browning of apple during postharvest storage. BMC Plant Biol. 14, 328. https://doi.org/10.1186/s12870-014-0328-x

Mellidou, I., Chagne, D., Laing, W.A., Keulemans, J., Davey, M.W., 2012a. Allelic Variation in Paralogs of GDP-l-Galactose Phosphorylase Is a Major Determinant of Vitamin C Concentrations in Apple Fruit. Plant Physiol. 160, 1613–1629. https://doi.org/10.1104/pp.112.203786

Mellidou, I., Kanellis, A.K., 2017. Genetic Control of Ascorbic Acid Biosynthesis and Recycling in Horticultural Crops. Front. Chem. 5, 1–8. https://doi.org/10.3389/fchem.2017.00050

Mellidou, I., Keulemans, J., Kanellis, A.K., Davey, M.W., 2012b. Regulation of fruit ascorbic acid concentrations during ripening in high and low vitamin C tomato cultivars. BMC Plant Biol. 12. https://doi.org/10.1186/1471-2229-12-239

Mergner, J., Frejno, M., List, M., Papacek, M., Chen, X., Chaudhary, A., Samaras, P., Richter, S., Shikata, H., Messerer, M., Lang, D., Altmann, S., Cyprys, P., Zolg, D.P., Mathieson, T., Bantscheff, M., Hazarika, R.R., Schmidt, T., Dawid, C., Dunkel, A., Hofmann, T., Sprunck, S., Falter-Braun, P., Johannes, F., Mayer, K.F.X., Jürgens, G., Wilhelm, M., Baumbach, J., Grill, E., Schneitz, K., Schwechheimer, C., Kuster, B., 2020. Mass-spectrometry-based draft of the Arabidopsis proteome. Nature. https://doi.org/10.1038/s41586-020-2094-2

Mezzetti, B., Balducci, F., Capocasa, F., Zhong, C.F., Cappelletti, R., Di Vittori, L., Mazzoni, L., Giampieri, F., Battino, M., 2016. Breeding Strawberry for Higher Phytochemicals Content and Claim It: Is It Possible? Int. J. Fruit Sci. 16, 194–206. https://doi.org/10.1080/15538362.2016.1250695

Mhamdi, A., Noctor, G., Baker, A., 2012. Plant catalases: Peroxisomal redox guardians. Arch. Biochem. Biophys. 525, 181–194. https://doi.org/10.1016/j.abb.2012.04.015

Mhamdi, A., Queval, G., Chaouch, S., Vanderauwera, S., Van Breusegem, F., Noctor, G., 2010. Catalase function in plants: a focus on Arabidopsis mutants as stress-mimic models. J. Exp. Bot. 61, 4197–4220. https://doi.org/10.1093/jxb/erq282

Michael, T.P., Mockler, T.C., Breton, G., McEntee, C., Byer, A., Trout, J.D., Hazen, S.P., Shen, R., Priest, H.D., Sullivan, C.M., Givan, S.A., Yanovsky, M., Hong, F., Kay, S.A., Chory, J., 2008. Network discovery pipeline elucidates conserved time-of-day-specific cis-regulatory

modules. PLoS Genet. https://doi.org/10.1371/journal.pgen.0040014

Mieda, T., Yabuta, Y., Rapolu, M., Motoki, T., Takeda, T., Yoshimura, K., Ishikawa, T., Shigeoka, S., 2004. Feedback inhibition of spinach L-galactose dehydrogenase by L-ascorbate. Plant Cell Physiol. 45, 1271–1279. https://doi.org/10.1093/pcp/pch152

Miki, D., Zhang, W., Zeng, W., Feng, Z., Zhu, J.-K., 2018. CRISPR/Cas9-mediated gene targeting in Arabidopsis using sequential transformation. Nat. Commun. 9, 1967. https://doi.org/10.1038/s41467-018-04416-0

Minor, E.A., Court, B.L., Young, J.I., Wang, G., 2013. Ascorbate induces ten-eleven translocation (Tet) methylcytosine dioxygenase-mediated generation of 5-hydroxymethylcytosine. J. Biol. Chem. 288, 13669–13674. https://doi.org/10.1074/jbc.C113.464800

Mittler, R., 2017. ROS Are Good. Trends Plant Sci. 22, 11–19. https://doi.org/10.1016/j.tplants.2016.08.002

Miura, K., Haraguchi, M., Ito, H., Tai, A., 2018. Potential Antitumor Activity of 2-O-α-d-Glucopyranosyl-6-O-(2-Pentylheptanoyl)-l-Ascorbic Acid. Int. J. Mol. Sci. 19, 535. https://doi.org/10.3390/ijms19020535

Miyaji, T., Kuromori, T., Takeuchi, Y., Yamaji, N., Yokosho, K., Shimazawa, A., Sugimoto, E., Omote, H., Ma, J.F., Shinozaki, K., Moriyama, Y., 2015. AtPHT4;4 is a chloroplast-localized ascorbate transporter in Arabidopsis. Nat. Commun. https://doi.org/10.1038/ncomms6928

Mounet-Gilbert, L., Dumont, M., Ferrand, C., Bournonville, C., Monier, A., Jorly, J., Lemaire-Chamley, M., Mori, K., Atienza, I., Hernould, M., Stevens, R., Lehner, A., Mollet, J.C., Rothan, C., Lerouge, P., Baldet, P., 2016. Two tomato GDP-D-mannose epimerase isoforms involved in ascorbate biosynthesis play specific roles in cell wall biosynthesis and development. J. Exp. Bot. 67, 4767–4777. https://doi.org/10.1093/jxb/erw260

Muckenthaler, M.U., Galy, B., Hentze, M.W., 2008. Systemic Iron Homeostasis and the Iron-Responsive Element/Iron-Regulatory Protein (IRE/IRP) Regulatory Network. Annu. Rev. Nutr. 28, 197–213. https://doi.org/10.1146/annurev.nutr.28.061807.155521

Müller-Moulé, P., 2008. An expression analysis of the ascorbate biosynthesis enzyme VTC2. Plant Mol. Biol. 68, 31–41. https://doi.org/10.1007/s11103-008-9350-4

Müller-Moulé, P., Conklin, P.L., Niyogi, K.K., 2002. Ascorbate Deficiency Can Limit Violaxanthin De-Epoxidase Activity in Vivo. Plant Physiol. 128, 970–977. https://doi.org/10.1104/pp.010924

Mullineaux, P.M., Exposito-Rodriguez, M., Laissue, P.P., Smirnoff, N., 2018. ROS-dependent signalling pathways in plants and algae exposed to high light: Comparisons with other eukaryotes. Free Radic. Biol. Med. https://doi.org/10.1016/j.freeradbiomed.2018.01.033

Myllylä, R., Majamaa, K., Günzler, V., Hanauske-Abel, H.M., Kivirikko, K.I., 1984. Ascorbate is consumed stoichiometrically in the uncoupled reactions catalyzed by prolyl 4-hydroxylase and lysyl hydroxylase. J. Biol. Chem. 259, 5403–5.

Nakagawa, T., Kurose, T., Hino, T., Tanaka, K., Kawamukai, M., Niwa, Y., Toyooka, K., Matsuoka, K., Jinbo, T., Kimura, T., 2007. Development of series of gateway binary vectors, pGWBs, for realizing efficient construction of fusion genes for plant transformation. J. Biosci. Bioeng. https://doi.org/10.1263/jbb.104.34

Nakayama, K., Maeda, Y., Jigami, Y., 2003. Interaction of GDP-4-keto-6-deoxymannose-3,5-epimerase-4-reductase with GDP-mannose-4,6-dehydratase stabilizes the enzyme activity for formation of GDP-fucose from GDP-mannose. Glycobiology 13, 673–80. https://doi.org/10.1093/glycob/cwg099

Nishikimi, M., Fukuyama, R., Minoshima, S., Shimizu, N., Yagi, K., 1994. Cloning and chromosomal mapping of the human nonfunctional gene for L-gulono-gamma-lactone oxidase, the enzyme for L-ascorbic acid biosynthesis missing in man. J. Biol. Chem. 269,

13685–13688. https://doi.org/10.1007/978-4-431-54011-3_4

Norris, S.R., Shen, X., DellaPenna, D., 1998. Complementation of the Arabidopsis pds1 mutation with the gene encoding p-hydroxyphenylpyruvate dioxygenase. Plant Physiol. 117, 1317–23.

Nourbakhsh, A., Collakova, E., Gillaspy, G.E., 2015. Characterization of the inositol monophosphatase gene family in Arabidopsis. Front. Plant Sci. 5, 1–14. https://doi.org/10.3389/fpls.2014.00725

O'Neill, M.A., Eberhard, S., Albersheim, P., Darvill, A.G., 2001. Requirement of borate cross-linking of cell wall rhamnogalacturonan II for Arabidopsis growth. Science,. 294, 846–849. https://doi.org/10.1126/science.1062319

Oba, K., Ishikawa, S., Nishikawa, M., Mizuno, H., Yamamoto, T., 1995. Purification and properties of L-galactono-gamma-lactone dehydrogenase, a key enzyme for ascorbic acid biosynthesis, from sweet potato roots. J. Biochem. 117, 120–4.

Ogura, Y., Komatsu, A., Zikihara, K., Nanjo, T., Tokutomi, S., Wada, M., Kiyosue, T., 2008. Blue light diminishes interaction of PAS/LOV proteins, putative blue light receptors in Arabidopsis thaliana, with their interacting partners. J. Plant Res. 121, 97–105. https://doi.org/10.1007/s10265-007-0118-8

Oms-Oliu, G., Hertog, M.L.A.T.M., Van de Poel, B., Ampofo-Asiama, J., Geeraerd, A.H., Nicolai, B.M., 2011. Metabolic characterization of tomato fruit during preharvest development, ripening, and postharvest shelf-life. Postharvest Biol. Technol. 62, 7–16. https://doi.org/10.1016/j.postharvbio.2011.04.010

Østergaard, J., Persiau, G., Davey, M.W., Bauw, G., Van Montagu, M., 1997. Isolation of a cDNA coding for L-galactono-gamma-lactone dehydrogenase, an enzyme involved in the biosynthesis of ascorbic acid in plants. Purification, characterization, cDNA cloning, and expression in yeast. J. Biol. Chem. 272, 30009–16.

Packer, J.E., Slater, T.F., Willson, R.L., 1979. Direct observation of a free radical interaction between vitamin E and vitamin C. Nature 278, 737–8.

Padayatty, S.J., Levine, M., 2016. Vitamin C: the known and the unknown and Goldilocks. Oral Dis. 22, 463–493. https://doi.org/10.1111/odi.12446

Page, M., Sultana, N., Paszkiewicz, K., Florance, H., Smirnoff, N., 2012. The influence of ascorbate on anthocyanin accumulation during high light acclimation in Arabidopsis thaliana: further evidence for redox control of anthocyanin synthesis. Plant. Cell Environ. 35, 388–404. https://doi.org/10.1111/j.1365-3040.2011.02369.x

Pallanca, J.E., Smirnoff, N., 2000. The control of ascorbic acid synthesis and turnover in pea seedlings. J. Exp. Bot. 51, 669–674. https://doi.org/10.1093/jexbot/51.345.669

Park, S.O., Hwang, H.Y., Crosby, K.M., 2009. A Genetic Linkage Map including Loci for Male Sterility, Sugars, and Ascorbic Acid in Melon. J. Am. Soc. Hortic. Sci. 134, 67–76.

Parsons, H.T., Yasmin, T., Fry, S.C., 2011. Alternative pathways of dehydroascorbic acid degradation *in vitro* and in plant cell cultures: novel insights into vitamin C catabolism. Biochem. J. 440, 375–385. https://doi.org/10.1042/BJ20110939

Pateraki, I., Sanmartin, M., Kalamaki, M.S., Gerasopoulos, D., Kanellis, A.K., 2004. Molecular characterization and expression studies during melon fruit development and ripening of L-galactono-1,4-lactone dehydrogenase. J. Exp. Bot. 55, 1623–1633. https://doi.org/10.1093/jxb/erh186

Pauly, M., Keegstra, K., 2016. Biosynthesis of the Plant Cell Wall Matrix Polysaccharide Xyloglucan. Annu. Rev. Plant Biol. https://doi.org/10.1146/annurev-arplant-043015-112222

Pavón, L.R., Lundh, F., Lundin, B., Mishra, A., Persson, B.L., Spetea, C., 2008. *Arabidopsis* ANTR1 Is a Thylakoid Na $^{+}$ -dependent Phosphate Transporter. J. Biol. Chem. 283, 13520–13527. https://doi.org/10.1074/jbc.M709371200

Pekkala, M., Hieta, R., Kursula, P., Kivirikko, K.I., Wierenga, R.K., Myllyharju, J., 2003. Crystallization of the proline-rich-peptide binding domain of human type I collagen prolyl 4-hydroxylase. Acta Crystallogr. D. Biol. Crystallogr. 59, 940–2.

Pérez-Ruiz, J.M., Naranjo, B., Ojeda, V., Guinea, M., Cejudo, F.J., 2017. NTRC-dependent redox balance of 2-Cys peroxiredoxins is needed for optimal function of the photosynthetic apparatus. Proc. Natl. Acad. Sci. U. S. A. 114, 12069–12074. https://doi.org/10.1073/pnas.1706003114

Perrin, R.M., DeRocher, A.E., Bar-Peled, M., Zeng, W., Norambuena, L., Orellana, A., Raikhel, N. V, Keegstra, K., 1999. Xyloglucan fucosyltransferase, an enzyme involved in plant cell wall biosynthesis. Science,. 284, 1976–9.

Peterkofsky, B., 1991. Ascorbate requirement for hydroxylation and secretion of procollagen: relationship to inhibition of collagen synthesis in scurvy. Am. J. Clin. Nutr. 54, 1135S-1140S. https://doi.org/10.1093/ajcn/54.6.1135s

Pineau, B., Layoune, O., Danon, A., De Paepe, R., 2008. L-galactono-1,4-lactone dehydrogenase is required for the accumulation of plant respiratory complex I. J. Biol. Chem. 283, 32500–32505. https://doi.org/10.1074/jbc.M805320200

Plumb, W., Townsend, A.J., Rasool, B., Alomrani, S., Razak, N., Karpinska, B., Ruban, A. V., Foyer, C.H., 2018. Ascorbate-mediated regulation of growth, photoprotection, and photoinhibition in Arabidopsis thaliana. J. Exp. Bot. https://doi.org/10.1093/jxb/ery170

Prigge, S.T., Kolhekar, A.S., Eipper, B.A., Mains, R.E., Mario Amzel, L., 1999. Substrate-mediated electron transfer in peptidylglycine α-hydroxylating monooxygenase. Nat. Struct. Biol. 6, 976–983. https://doi.org/10.1038/13351

Qi, T., Liu, Z., Fan, M., Chen, Y., Tian, H., Wu, D., Gao, H., Ren, C., Song, S., Xie, D., 2017. GDP-D-mannose epimerase regulates male gametophyte development, plant growth and leaf senescence in Arabidopsis. Sci. Rep. 7, 10309. https://doi.org/10.1038/s41598-017-10765-5

Qian, W., Yu, C., Qin, H., Liu, X., Zhang, A., Johansen, I.E., Wang, D., 2007. Molecular and functional analysis of phosphomannomutase (PMM) from higher plants and genetic evidence for the involvement of PMM in ascorbic acid biosynthesis in Arabidopsis and Nicotiana benthamiana. Plant J. 49, 399–413. https://doi.org/10.1111/j.1365-313X.2006.02967.x

Radzio, J.A., Lorence, A., Chevone, B.I., Nessler, C.L., 2003. L-Gulono-1,4-lactone oxidase expression rescues vitamin C-deficient Arabidopsis (vtc) mutants. Plant Mol. Biol. https://doi.org/10.1023/B:PLAN.0000023671.99451.1d

Rebouche, C.J., 1991. Ascorbic acid and carnitine biosynthesis. Am. J. Clin. Nutr. 54, 1147S-1152S. https://doi.org/10.1093/ajcn/54.6.1147s

Reczek, C.R., Chandel, N.S., 2015. Revisiting vitamin C and cancer. Science,. 350, 1317–1318. https://doi.org/10.1126/science.aad8671

Reiter, W.-D., Chapple, C.C.S., Somerville, C.R., 1993. Altered Growth and Cell Walls in a Fucose-Deficient Mutant of Arabidopsis. Science,. 261, 1032–1035. https://doi.org/10.1126/science.261.5124.1032

Reiter, W.D., Vanzin, G.F., 2001. Molecular genetics of nucleotide sugar interconversion pathways in plants. Plant Mol. Biol. 47, 95–113.

Rigano, M.M., Raiola, A., Tenore, G.C., Monti, D.M., Giudice, R. Del, Frusciante, L., Barone, A., 2014. Quantitative Trait Loci Pyramiding Can Improve the Nutritional Potential of Tomato (Solanum lycopersicum) Fruits. J. Agric. Food Chem. 62, 11519–11527. https://doi.org/10.1021/jf502573n

Rodríguez-Leal, D., Lemmon, Z.H., Man, J., Bartlett, M.E., Lippman, Z.B., 2017. Engineering Quantitative Trait Variation for Crop Improvement by Genome Editing. Cell 171, 470-480.e8. https://doi.org/10.1016/j.cell.2017.08.030

Rodríguez-Negrete, E., Bejarano, E.R., Castillo, A.G., 2014. Using the Yeast Two-Hybrid System to Identify Protein–Protein Interactions, in: Jorrin-Novo, J. V., Komatsu, S., Weckwerth, W., Wienkoop, S. (Eds.), Plant Proteomics: Methods and Protocols, Methods in Molecular Biology. Humana Press, Totowa, NJ, pp. 241–258. https://doi.org/10.1007/978-1-62703-631-3_18

Rodríguez-Ruiz, M., Mateos, R.M., Codesido, V., Corpas, F.J., Palma, J.M., 2017. Characterization of the galactono-1,4-lactone dehydrogenase from pepper fruits and its modulation in the ascorbate biosynthesis. Role of nitric oxide. Redox Biol. 12, 171–181. https://doi.org/10.1016/j.redox.2017.02.009

Rogiers, S.Y., Kumar, G.N.M., Knowles, N.R., 1998. Maturation and Ripening of Fruit of Amelanchier alnifolia Nutt. are Accompanied by Increasing Oxidative Stress. Ann. Bot. 81, 203–211. https://doi.org/10.1006/ANBO.1997.0543

Ruggieri, V., Sacco, A., Calafiore, R., Frusciante, L., Barone, A., 2015. Dissecting a QTL into Candidate Genes Highlighted the Key Role of Pectinesterases in Regulating the Ascorbic Acid Content in Tomato Fruit. Plant Genome 8. https://doi.org/10.3835/plantgenome2014.08.0038

Rush, R.A., Geffen, L.B., 1980. Dopamine β-Hydroxylase in Health and Disease. CRC Crit. Rev. Clin. Lab. Sci. 12, 241–277. https://doi.org/10.3109/10408368009108731

Sacco, A., Di Matteo, A., Lombardi, N., Trotta, N., Punzo, B., Mari, A., Barone, A., 2013. Quantitative trait loci pyramiding for fruit quality traits in tomato. Mol. Breed. 31, 217–222. https://doi.org/10.1007/s11032-012-9763-2

Saga, G., Giorgetti, A., Fufezan, C., Giacometti, G.M., Bassi, R., Morosinotto, T., 2010. Mutation Analysis of Violaxanthin De-epoxidase Identifies Substrate-binding Sites and Residues Involved in Catalysis. J. Biol. Chem. 285, 23763–23770. https://doi.org/10.1074/jbc.M110.115097

Sauvage, C., Segura, V., Bauchet, G., Stevens, R., Do, P.T., Nikoloski, Z., Fernie, A.R., Causse, M., 2014. Genome-Wide Association in Tomato Reveals 44 Candidate Loci for Fruit Metabolic Traits. Plant Physiol. 165, 1120–1132. https://doi.org/10.1104/pp.114.241521

Sawake, S., Tajima, N., Mortimer, J.C., Lao, J., Ishikawa, T., Yu, X., Yamanashi, Y., Yoshimi, Y., Kawai-Yamada, M., Dupree, P., Tsumuraya, Y., Kotake, T., 2015. KONJAC1 and 2 Are Key Factors for GDP-Mannose Generation and Affect l-Ascorbic Acid and Glucomannan Biosynthesis in Arabidopsis. Plant Cell. https://doi.org/10.1105/tpc.15.00379

Schertl, P., Sunderhaus, S., Klodmann, J., Grozeff, G.E.G., Bartoli, C.G., Braun, H.-P., 2012. L-galactono-1,4-lactone dehydrogenase (GLDH) forms part of three subcomplexes of mitochondrial complex I in Arabidopsis thaliana. J. Biol. Chem. 287, 14412–9. https://doi.org/10.1074/jbc.M111.305144

Schimmeyer, J., Bock, R., Meyer, E.H., 2016. L-Galactono-1,4-lactone dehydrogenase is an assembly factor of the membrane arm of mitochondrial complex I in Arabidopsis. Plant Mol. Biol. 90, 117–126. https://doi.org/10.1007/s11103-015-0400-4

Schindelin, J., Arganda-Carreras, I., Frise, E., Kaynig, V., Longair, M., Pietzsch, T., Preibisch, S., Rueden, C., Saalfeld, S., Schmid, B., Tinevez, J.-Y., White, D.J., Hartenstein, V., Eliceiri, K., Tomancak, P., Cardona, A., 2012. Fiji: an open-source platform for biological-image analysis. Nat. Methods 9, 676–682. https://doi.org/10.1038/nmeth.2019

Schleicher, R.L., Carroll, M.D., Ford, E.S., Lacher, D.A., 2009. Serum vitamin C and the prevalence of vitamin C deficiency in the United States: 2003–2004 National Health and Nutrition Examination Survey (NHANES). Am. J. Clin. Nutr. 90, 1252–1263. https://doi.org/10.3945/ajcn.2008.27016

Schneider, C.A., Rasband, W.S., Eliceiri, K.W., 2012. NIH Image to ImageJ: 25 years of image analysis. Nat. Methods 9, 671–675. https://doi.org/10.1038/nmeth.2089

Schwechheimer, C., Isono, E., 2010. The COP9 signalosome and its role in plant development.

Eur. J. Cell Biol. https://doi.org/10.1016/j.ejcb.2009.11.021

Semchuk, N.M., Lushchak, O. V., Falk, J., Krupinska, K., Lushchak, V.I., 2009. Inactivation of genes, encoding tocopherol biosynthetic pathway enzymes, results in oxidative stress in outdoor grown Arabidopsis thaliana. Plant Physiol. Biochem. 47, 384–390. https://doi.org/10.1016/j.plaphy.2009.01.009

Shenoy, N., Bhagat, T., Nieves, E., Stenson, M., Lawson, J., Choudhary, G.S., Habermann, T., Nowakowski, G., Singh, R., Wu, X., Verma, A., Witzig, T.E., 2017. Upregulation of TET activity with ascorbic acid induces epigenetic modulation of lymphoma cells. Blood Cancer J. 7, e587. https://doi.org/10.1038/bcj.2017.65

Shigeoka, S., Nakano, Y., Kitaoka, S., 1979. The biosynthetic pathway of L-ascorbic acid in Euglena gracilis Z. J. Nutr. Sci. Vitaminol. (Tokyo). 25, 299–307.

Showalter, A.M., Basu, D., 2016. Extensin and Arabinogalactan-Protein Biosynthesis: Glycosyltransferases, Research Challenges, and Biosensors. Front. Plant Sci. 7, 814. https://doi.org/10.3389/fpls.2016.00814

Sinclair, J.W., Park, S.O., Lester, G.E., Yoo, K.S., Crosby, K.M., 2006. Identification and confirmation of RAPD markers and andromonoecious associated with quantitative trait loci for sugars in melon, Journal of the American Society for Horticultural Science. [American Society for Horticultural Science].

Singh, B.D., Singh, A.K., 2015. Marker-Assisted Plant Breeding: Principles and Practices. Springer India, New Delhi. https://doi.org/10.1007/978-81-322-2316-0

Smirnoff, N., 2019. Engineering of metabolic pathways using synthetic enzyme complexes. Plant Physiol. https://doi.org/10.1104/pp.18.01280

Smirnoff, N., 2018. Ascorbic acid metabolism and functions: A comparison of plants and mammals. Free Radic. Biol. Med. 0–1. https://doi.org/10.1016/j.freeradbiomed.2018.03.033

Smirnoff, N., 2000. Ascorbate biosynthesis and function in photoprotection. Philos. Trans. R. Soc. Lond. B. Biol. Sci. 355, 1455–1464. https://doi.org/10.1098/rstb.2000.0706

Sperschneider, J., Catanzariti, A.M., Deboer, K., Petre, B., Gardiner, D.M., Singh, K.B., Dodds, P.N., Taylor, J.M., 2017. LOCALIZER: Subcellular localization prediction of both plant and effector proteins in the plant cell. Sci. Rep. https://doi.org/10.1038/srep44598

Stevens, R., Buret, M., Duffé, P., Garchery, C., Baldet, P., Rothan, C., Causse, M., 2007. Candidate Genes and Quantitative Trait Loci Affecting Fruit Ascorbic Acid Content in Three Tomato Populations. Plant Physiol. 143, 1943–1953. https://doi.org/10.1104/pp.106.091413

Stevens, R., Page, D., Gouble, B., Garchery, C., Zamir, D., Causse, M., 2008. Tomato fruit ascorbic acid content is linked with monodehydroascorbate reductase activity and tolerance to chilling stress. Plant, Cell Environ. 31, 1086–1096. https://doi.org/10.1111/j.1365-3040.2008.01824.x

Stork, T., Michel, K.-P., Pistorius, E.K., Dietz, K.-J., 2005. Bioinformatic analysis of the genomes of the cyanobacteria Synechocystis sp. PCC 6803 and Synechococcus elongatus PCC 7942 for the presence of peroxiredoxins and their transcript regulation under stress. J. Exp. Bot. 56, 3193–3206. https://doi.org/10.1093/jxb/eri316

Sullivan, A., Purohit, P.K., Freese, N.H., Pasha, A., Esteban, E., Waese, J., Wu, A., Chen, M., Chin, C.Y., Song, R., Watharkar, S.R., Chan, A.P., Krishnakumar, V., Vaughn, M.W., Town, C., Loraine, A.E., Provart, N.J., 2019. An '<scp>eFP</scp> -Seq Browser' for visualizing and exploring <scp>RNA</scp> sequencing data. Plant J. 100, 641–654. https://doi.org/10.1111/tpj.14468

Sun, R., Li, H., Zhang, Q., Chen, D., Yang, F., Zhao, Y., Wang, Y., Han, Y., Zhang, X., Han, Z., 2014. Mapping for Quantitative Trait Loci and Major Genes Associated with Fresh-cut Browning in Apple. HortScience 49, 25–30.

Suzuki, N., Rivero, R.M., Shulaev, V., Blumwald, E., Mittler, R., 2014. Abiotic and biotic stress combinations. New Phytol. 203, 32–43. https://doi.org/10.1111/nph.12797

Sweetlove, L.J., Fernie, A.R., 2018. The role of dynamic enzyme assemblies and substrate channelling in metabolic regulation. Nat. Commun. 9, 2136. https://doi.org/10.1038/s41467-018-04543-8

Takagi, H., Abe, A., Yoshida, K., Kosugi, S., Natsume, S., Mitsuoka, C., Uemura, A., Utsushi, H., Tamiru, M., Takuno, S., Innan, H., Cano, L.M., Kamoun, S., Terauchi, R., 2013. QTL-seq: rapid mapping of quantitative trait loci in rice by whole genome resequencing of DNA from two bulked populations. Plant J. 74, 174–183. https://doi.org/10.1111/tpj.12105

Takahama, U., 2004. Oxidation of vacuolar and apoplastic phenolic substrates by peroxidase: Physiological significance of the oxidation reactions. Phytochem. Rev. https://doi.org/10.1023/B:PHYT.0000047805.08470.e3

Tan, L., Eberhard, S., Pattathil, S., Warder, C., Glushka, J., Yuan, C., Hao, Z., Zhu, X., Avci, U., Miller, J.S., Baldwin, D., Pham, C., Orlando, R., Darvill, A., Hahn, M.G., Kieliszewski, M.J., Mohnen, D., 2013. An Arabidopsis cell wall proteoglycan consists of pectin and arabinoxylan covalently linked to an arabinogalactan protein. Plant Cell 25, 270–87. https://doi.org/10.1105/tpc.112.107334

Tanaka, K., Hashimoto, T., Tokumaru, S., Iguchi, H., Kojo, S., 1997. Interactions between vitamin C and vitamin E are observed in tissues of inherently scorbutic rats. J. Nutr. 127, 2060–4. https://doi.org/10.1093/jn/127.10.2060

Terai, Y., Ueno, H., Ogawa, T., Sawa, Y., Miyagi, A., Kawai-Yamada, M., Ishikawa, T., Maruta, T., 2020. Dehydroascorbate Reductases and Glutathione Set a Threshold for High-Light-Induced Ascorbate Accumulation. Plant Physiol. https://doi.org/10.1104/pp.19.01556

Top, O., Bar, C., Ökmen, B., Özer, D.Y., Rusçuklu, D., Tamer, N., Frary, A., Doğanlar, S., 2014. Exploration of three Solanum species for improvement of antioxidant traits in tomato. HortScience 49, 1003–1009.

Torabinejad, J., Donahue, J.L., Gunesekera, B.N., Allen-Daniels, M.J., Gillaspy, G.E., 2009. VTC4 Is a Bifunctional Enzyme That Affects Myoinositol and Ascorbate Biosynthesis in Plants. Plant Physiol. 150, 951–961. https://doi.org/10.1104/pp.108.135129

Tóth, S.Z., Puthur, J.T., Nagy, V., Garab, G., 2009. Experimental evidence for ascorbate-dependent electron transport in leaves with inactive oxygen-evolving complexes. Plant Physiol. 149, 1568–78. https://doi.org/10.1104/pp.108.132621

Tóth, S.Z., Schansker, G., Garab, G., 2013. The physiological roles and metabolism of ascorbate in chloroplasts. Physiol. Plant. 148, 161–175. https://doi.org/10.1111/ppl.12006

Truffault, V., Fry, S.C., Stevens, R.G., Edinburgh, T., Wall, C., Building, D.R., Gautier, H., Edinburgh, T., Wall, C., Building, D.R., 2017. Ascorbate degradation in tomato leads to accumulation of oxalate , threonate and oxalyl threonate. Plant J. 89, 996–1008. https://doi.org/10.1111/tpj.13439

Turbant, A., Fournet, F., Lequart, M., Zabijak, L., Pageau, K., Bouton, S., Van Wuytswinkel, O., 2016. PME58 plays a role in pectin distribution during seed coat mucilage extrusion through homogalacturonan modification. J. Exp. Bot. 67, 2177–90. https://doi.org/10.1093/jxb/erw025

Tyystjärvi, E., 2008. Photoinhibition of Photosystem II and photodamage of the oxygen evolving manganese cluster. Coord. Chem. Rev. 252, 361–376. https://doi.org/10.1016/J.CCR.2007.08.021

Urzica, E.I., Adler, L.N., Page, M.D., Linster, C.L., Arbing, M.A., Casero, D., Pellegrini, M., Merchant, S.S., Clarke, S.G., 2012. Impact of oxidative stress on ascorbate biosynthesis in Chlamydomonas via regulation of the VTC2 gene encoding a GDP-L-galactose phosphorylase. J. Biol. Chem. 287, 14234–14245. https://doi.org/10.1074/jbc.M112.341982

Vallarino, J.G., Pott, D.M., Cruz-Rus, E., Miranda, L., Medina-Minguez, J.J., Valpuesta, V., Fernie, A.R., Sánchez-Sevilla, J.F., Osorio, S., Amaya, I., 2019. Identification of quantitative trait loci and candidate genes for primary metabolite content in strawberry fruit. Hortic. Res. https://doi.org/10.1038/s41438-018-0077-3

Valpuesta, V., Botella, M.A., 2004. Biosynthesis of L-ascorbic acid in plants: New pathways for an old antioxidant. Trends Plant Sci. https://doi.org/10.1016/j.tplants.2004.10.002

van Gorkom, G., Klein Wolterink, R., Van Elssen, C., Wieten, L., Germeraad, W., Bos, G., 2018. Influence of Vitamin C on Lymphocytes: An Overview. Antioxidants 7, 41. https://doi.org/10.3390/antiox7030041

Vanzin, G.F., Madson, M., Carpita, N.C., Raikhel, N. V., Keegstra, K., Reiter, W.-D.W.-D., 2002. The mur2 mutant of Arabidopsis thaliana lacks fucosylated xyloglucan because of a lesion in fucosyltransferase AtFUT1. Proc. Natl. Acad. Sci. U. S. A. 99, 3340–3345. https://doi.org/10.1073/pnas.052450699

von Schaewen, A., Sturm, A., O'Neill, J., Chrispeels, M.J., 1993. Isolation of a mutant Arabidopsis plant that lacks N-acetyl glucosaminyl transferase I and is unable to synthesize Golgi-modified complex N-linked glycans. Plant Physiol. 102, 1109–18. https://doi.org/10.1104/PP.102.4.1109

Voxeur, A., Gilbert, L., Rihouey, C., Driouich, A., Rothan, C., Baldet, P., Lerouge, P., 2011. Silencing of the GDP-D-mannose 3,5-epimerase affects the structure and cross-linking of the pectic polysaccharide rhamnogalacturonan II and plant growth in tomato. J. Biol. Chem. 286, 8014–8020. https://doi.org/10.1074/jbc.M110.198614

Wang, J., Yu, Y., Zhang, Z., Quan, R., Zhang, H., Ma, L., Deng, X.W., Huang, R., 2013. Arabidopsis CSN5B Interacts with VTC1 and Modulates Ascorbic Acid Synthesis. Plant Cell. https://doi.org/10.1105/tpc.112.106880

Wang, H. Sen, Yu, C., Zhu, Z.J., Yu, X.C., 2011. Overexpression in tobacco of a tomato GMPase gene improves tolerance to both low and high temperature stress by enhancing antioxidation capacity. Plant Cell Rep. 30, 1029–1040. https://doi.org/10.1007/s00299-011-1009-y

Waszczak, C., Carmody, M., Kangasjärvi, J., 2018. Reactive Oxygen Species in Plant Signaling. Annu. Rev. Plant Biol. 69, 209–236. https://doi.org/10.1007/978-3-642-00390-5

Wheeler, G., Ishikawa, T., Pornsaksit, V., Smirnoff, N., 2015. Evolution of alternative biosynthetic pathways for vitamin C following plastid acquisition in photosynthetic eukaryotes. Elife 2015, 1–14. https://doi.org/10.7554/eLife.06369

Wheeler, G.L., Jones, M.A., Smirnoff, N., 1998. The biosynthetic pathway of vitamin C in higher plants. Nature 393, 365–369. https://doi.org/10.1038/30728

Wintergerst, E.S., Maggini, S., Hornig, D.H., 2006. Immune-Enhancing Role of Vitamin C and Zinc and Effect on Clinical Conditions. Ann. Nutr. Metab. 50, 85–94. https://doi.org/10.1159/000090495

Wolucka, B.A., Persiau, G., Doorsselaere, J. Van, Davey, M.W., Demol, H., Vandekerckhove, J.L., Montagu, M. Van, Zabeau, M., Boerjan, W., 2001. Partial purification and identification of GDP-mannose 3',5'-epimerase of Arabidopsis thaliana, a key enzyme of the plant vitamin C pathway. Proc. Natl. Acad. Sci. 98, 14843–14848.

Wolucka, B.A., Van Montagu, M., 2003. GDP-Mannose 3′,5′-Epimerase Forms GDP-L-gulose, a Putative Intermediate for the de Novo Biosynthesis of Vitamin C in Plants. J. Biol. Chem. 278, 47483–47490. https://doi.org/10.1074/jbc.M309135200

Yabuta, Y., Mieda, T., Rapolu, M., Nakamura, A., Motoki, T., Maruta, T., Yoshimura, K., Ishikawa, T., Shigeoka, S., 2007. Light regulation of ascorbate biosynthesis is dependent on the photosynthetic electron transport chain but independent of sugars in Arabidopsis. J. Exp. Bot. 58, 2661–2671. https://doi.org/10.1093/jxb/erm124

Yamamoto, H.Y., Kamite, L., Wang, Y.Y., 1972. An Ascorbate-induced Absorbance Change in

Chloroplasts from Violaxanthin De-epoxidation. Plant Physiol. 49, 224–8. https://doi.org/10.1104/PP.49.2.224

Ye, Q., Worman, H.J., 1995. Protein-protein interactions between human nuclear lamins expressed in yeast. Exp. Cell Res. https://doi.org/10.1006/excr.1995.1230

Yoshimura, K., Nakane, T., Kume, S., Shiomi, Y., Maruta, T., Ishikawa, T., Shigeoka, S., 2014. Transient expression analysis revealed the importance of VTC2 expression level in light/dark regulation of ascorbate biosynthesis in Arabidopsis 78, 60–6. https://doi.org/10.1080/09168451.2014.877831

Young, J.I., Züchner, S., Wang, G., 2015. Regulation of the Epigenome by Vitamin C. Annu. Rev. Nutr. https://doi.org/10.1146/annurev-nutr-071714-034228

Yun, J., Mullarky, E., Lu, C., Bosch, K.N., Kavalier, A., Rivera, K., Roper, J., Chio, I.I.C., Giannopoulou, E.G., Rago, C., Muley, A., Asara, J.M., Paik, J., Elemento, O., Chen, Z., Pappin, D.J., Dow, L.E., Papadopoulos, N., Gross, S.S., Cantley, L.C., 2015. Vitamin C selectively kills KRAS and BRAF mutant colorectal cancer cells by targeting GAPDH. Science,. 350, 1391–1396. https://doi.org/10.1126/science.aaa5004

Zablackis, E., York, W.S., Pauly, M., Hantus, S., Reiter, W.-D., Chapple, C.C.S., Albersheim, P., Darvill, A., 1996. Substitution of L-Fucose by L-Galactose in Cell Walls of Arabidopsis mur1. Science,. 272, 1808–1810. https://doi.org/10.1126/science.272.5269.1808

Zechmann, B., 2011. Subcellular distribution of ascorbate in plants. Plant Signal. Behav. 6, 360–363. https://doi.org/10.4161/psb.6.3.14342

Zechmann, B., Stumpe, · M, Mauch, F., 2011. Immunocytochemical determination of the subcellular distribution of ascorbate in plants. Planta 233, 1–12. https://doi.org/10.1007/s00425-010-1275-x

Zhang, C., Liu, J., Zhang, Y., Cai, X., Gong, P., Zhang, J., Wang, T., Li, H., Ye, Z., 2011. Overexpression of SlGMEs leads to ascorbate accumulation with enhanced oxidative stress, cold, and salt tolerance in tomato. Plant Cell Rep. 30, 389–398. https://doi.org/10.1007/s00299-010-0939-0

Zhang, G.Y., Liu, R.R., Zhang, C.Q., Tang, K.X., Sun, M.F., Yan, G.H., Liu, Q.Q., 2015. Manipulation of the rice L-galactose pathway: Evaluation of the effects of transgene overexpression on ascorbate accumulation and abiotic stress tolerance. PLoS One. https://doi.org/10.1371/journal.pone.0125870

Zhang, H., Si, X., Ji, X., Fan, R., Liu, J., Chen, K., Wang, D., Gao, C., 2018. Genome editing of upstream open reading frames enables translational control in plants. Nat. Biotechnol. 36, 894–898. https://doi.org/10.1038/nbt.4202

Zhang, J.Y., Pan, D.L., Jia, Z.H., Wang, T., Wang, G., Guo, Z.R., 2018. Chlorophyll, carotenoid and Vitamin C metabolism regulation in Actinidia chinensis “Hongyang” outer pericarp during fruit development. PLoS One. https://doi.org/10.1371/journal.pone.0194835

Zhang, W., Lorence, A., Gruszewski, H.A., Chevone, B.I., Nessler, C.L., 2009. AMR1, an Arabidopsis Gene That Coordinately and Negatively Regulates the Mannose/L-Galactose Ascorbic Acid Biosynthetic Pathway. Plant Physiol. 150, 942–950. https://doi.org/10.1104/pp.109.138453

Zhang, Y., Beard, K.F.M., Swart, C., Bergmann, S., Krahnert, I., Nikoloski, Z., Graf, A., George Ratcliffe, R., Sweetlove, L.J., Fernie, A.R., Obata, T., 2017. Protein-protein interactions and metabolite channelling in the plant tricarboxylic acid cycle. Nat. Commun. 8. https://doi.org/10.1038/ncomms15212

Zhang, Y., Butelli, E., Martin, C., 2014. Engineering anthocyanin biosynthesis in plants. Curr. Opin. Plant Biol. https://doi.org/10.1016/j.pbi.2014.05.011

Zhang, Z., Wang, J., Zhang, R., Huang, R., 2012. The ethylene response factor AtERF98 enhances tolerance to salt through the transcriptional activation of ascorbic acid synthesis in Arabidopsis. Plant J. 71, 273–87. https://doi.org/10.1111/j.1365-313X.2012.04996.x

Zhou, Y., Tao, Q.C., Wang, Z.N., Fan, R., Li, Y., Sun, X.F., Tang, K.X., 2012. Engineering ascorbic acid biosynthetic pathway in Arabidopsis leaves by single and double gene transformation. Biol. Plant. 56, 451–457.

Zhou, Z., Wang, Y., Cai, G., He, Q., 2012. Neurospora COP9 signalosome integrity plays major roles for hyphal growth, conidial development, and circadian function. PLoS Genet. https://doi.org/10.1371/journal.pgen.1002712

Zhu, J.-K., 2002. Salt and drought stress signal transduction in plants. Annu. Rev. Plant Biol. 53, 247–273. https://doi.org/10.1146/annurev.arplant.53.091401.143329

Zimmermann, P., Hirsch-Hoffmann, M., Hennig, L., Gruissem, W., 2004. GENEVESTIGATOR. Arabidopsis Microarray Database and Analysis Toolbox. Plant Physiol. 136, 2621–2632. https://doi.org/10.1104/pp.104.046367

Zorrilla-Fontanesi, Y., Cabeza, A., Domínguez, P., Medina, J.J., Valpuesta, V., Denoyes-Rothan, B., Sánchez-Sevilla, J.F., Amaya, I., 2011. Quantitative trait loci and underlying candidate genes controlling agronomical and fruit quality traits in octoploid strawberry (Fragaria × ananassa). Theor. Appl. Genet. 123, 755–778. https://doi.org/10.1007/s00122-011-1624-6

PUBLICATION

frontiers in Plant Science

REVIEW
published: 24 January 2019
doi: 10.3389/fpls.2018.02006

Vitamin C Content in Fruits: Biosynthesis and Regulation

*Mario Fenech[1], Iraida Amaya[2], Victoriano Valpuesta[1] and Miguel A. Botella[1]**

[1] Departamento de Biología Molecular y Bioquímica, Instituto de Hortofruticultura Subtropical y Mediterránea (IHSM), Consejo Superior de Investigaciones Científicas, Universidad de Málaga, Málaga, Spain, [2] Instituto Andaluz de Investigación y Formación Agraria y Pesquera, Area de Genómica y Biotecnología, Centro de Málaga, Spain

Throughout evolution, a number of animals including humans have lost the ability to synthesize ascorbic acid (ascorbate, vitamin C), an essential molecule in the physiology of animals and plants. In addition to its main role as an antioxidant and cofactor in redox reactions, recent reports have shown an important role of ascorbate in the activation of epigenetic mechanisms controlling cell differentiation, dysregulation of which can lead to the development of certain types of cancer. Although fruits and vegetables constitute the main source of ascorbate in the human diet, rising its content has not been a major breeding goal, despite the large inter- and intraspecific variation in ascorbate content in fruit crops. Nowadays, there is an increasing interest to boost ascorbate content, not only to improve fruit quality but also to generate crops with elevated stress tolerance. Several attempts to increase ascorbate in fruits have achieved fairly good results but, in some cases, detrimental effects in fruit development also occur, likely due to the interaction between the biosynthesis of ascorbate and components of the cell wall. Plants synthesize ascorbate *de novo* mainly through the Smirnoff-Wheeler pathway, the dominant pathway in photosynthetic tissues. Two intermediates of the Smirnoff-Wheeler pathway, GDP-D-mannose and GDP-L-galactose, are also precursors of the non-cellulosic components of the plant cell wall. Therefore, a better understanding of ascorbate biosynthesis and regulation is essential for generation of improved fruits without developmental side effects. This is likely to involve a yet unknown tight regulation enabling plant growth and development, without impairing the cell redox state modulated by ascorbate pool. In certain fruits and developmental conditions, an alternative pathway from D-galacturonate might be also relevant. We here review the regulation of ascorbate synthesis, its close connection with the cell wall, as well as different strategies to increase its content in plants, with a special focus on fruits.

Keywords: ascorbic acid, vitamin C, cell wall, biosynthesis, fruit, regulation

Edited by:
Wim Van den Ende, KU Leuven, Belgium

Reviewed by:
William Laing, The New Zealand Institute for Plant & Food Research Ltd., New Zealand
Mark Davey, BASF Agricultural Solutions Belgium NV, Belgium

****Correspondence:***
Miguel A. Botella
mabotella@uma.es

Specialty section:
This article was submitted to Plant Physiology, a section of the journal Frontiers in Plant Science

Received: *12 July 2018*
Accepted: *31 December 2018*
Published: *24 January 2019*

Citation:
Fenech M, Amaya I, Valpuesta V and Botella MA (2019) Vitamin C Content in Fruits: Biosynthesis and Regulation. Front. Plant Sci. 9:2006. doi: 10.3389/fpls.2018.02006

MULTIPLE ROLES OF VITAMIN C IN HUMANS

L-Ascorbic Acid (L-threo-hex-2-enono-1,4-lactone, ascorbate), also called vitamin C, is an essential antioxidant molecule in plant and animal metabolism and also functioning as a cofactor in many enzymes. While many animals are able to synthesize ascorbate in the liver or in the kidney, others, such as humans, non-human primates, guinea pigs, and certain groups of bats and birds have lost this ability due to the accumulation of mutations in the coding sequence of the last committed